NATÁLIA KARLA BELLINI

Diversity of free-living amoebas in the Monjolinho River in São Paulo state – morphological and molecular approaches

SÃO CARLOS/SAN CRISTÓBAL DE LA LAGUNA

2020

NATÁLIA KARLA BELLINI

Diversity of free-living amoebas in the Monjolinho River in São Paulo state – morphological and molecular approaches

Thesis presented to the Graduate Program in Physics, in the Instituto de Fisica de São Carlos/ Universidade de São Paulo – Brazil and to the Program in Medical and Pharmaceutical Sciences, Development and Quality of Life in the University Institute of Tropical Diseases and Public Health of the Canary Islands/University of La Laguna – Spain to obtain the Double Degree of Doctor in Science.

Concentration area: Applied Physics
Option: Biomolecular Physics

Advisors:
Prof. Dr. Otavio Henrique Thiemann
Prof. Dr. Jacob Lorenzo-Morales

Corrected version

(Original version available on the Program Unit)

SÃO CARLOS/SAN CRISTÓBAL DE LA LAGUNA

2020

Cataloguing data reviewed by the Library and Information Service of the IFSC, information supplied by the author.

Bellini, Natália Karla
Diversity of free-living amoebas in the Monjolinho River in São Paulo state - morphological and molecular approaches / Natália Karla Bellini; advisor Otavio Henrique Thiemann; Jacob Lorenzo-Morales - corrected version -- São Carlos/San Cristóbal de La Laguna 2020.
222 p.

Thesis (Doctorate with double degree - Graduate Program in Biomolecular Physics) -- Instituto de Física de São Carlos, Universidade de São Paulo - Brasil and Institute of Tropical Diseases and Public Health of the Canary Islands,,University of La Laguna - San Cristóbal de La Laguna, 2020.

1. Free-living amoeba. 2. Waterborne protozoan. 3. Amoeba resistant microorganisms. I. Thiemann, Otavio Henrique, II. Lorenzo-Morales, Jacob , advisor. III. Title.

NATÁLIA KARLA BELLINI

Diversidade de amebas de vida livre no Rio Monjolinho no estado de São Paulo – abordagem morfológica e molecular

Tese apresentada ao Programa de Pós-Graduação em Física, Instituto de Física de São Carlos da Universidade de São Paulo, Brasil, e ao Programa de Ciências Médicas e Farmacêuticas, Desenvolvimento e Qualidade de Vida do Instituto Universitário de Enfermidades Tropicais e Saúde Pública das Ilhas Canárias, da Universidade de La Laguna, Espanha, para obtenção do título de Doutora em Ciências.

Área de concentração: Física aplicada
Opção: Física biomolecular

Orientadores:
Prof. Dr. Otavio Henrique Thiemann
Prof. Dr. Jacob Lorenzo-Morales

Versão Corrigida

(versão original disponível na Unidade que aloja o Programa)

SÃO CARLOS/SAN CRISTÓBAL DE LA LAGUNA

2020

Ficha catalográfica revisada pelo Serviço de Biblioteca e Informação do IFSC, com os dados fornecidos pelo(a) autor(a)

Bellini, Natália Karla
Diversidade de amebas de vida livre no Rio Monjolinho no estado de São Paulo - abordagem morfológica e molecular / Natália Karla Bellini; advisor Otavio Henrique Thiemann; Jacob Lorenzo-Morales - corrected version -- São Carlos/San Cristóbal de La Laguna 2020.
222 p.

Thesis (Doctorate with double degree - Graduate Program in Biomolecular Physics) -- Instituto de Física de São Carlos, Universidade de São Paulo - Brasil and Instituto Universitário de Doenças Tropicais e Saúde Pública das Ilhas Canárias - San Cristóbal de La Laguna, 2020.

1. Amebas de vida-livre. 2. Protozoários transmitidos pela água. 3. Microrganismos resistentes a amebas. I. Thiemann, Otavio Henrique, II. Lorenzo-Morales, Jacob , advisor. III. Title.

This work is dedicated to my family.

ACKNOWLEDGEMENTS

This PhD study could be concluded thanks to many people who assisted directly or indirectly in my steps so far. I kindly thank each one and I would like to let them know that I am very grateful for having the opportunity to learn with them.

My supervisors: I kindly thank my Brazilian advisor **Prof. Otavio Henrique Thiemann**, his knowledge and all advisements that contributed to the development of the present PhD study. I thanks for the many years of guidance that enriched my concept of making science and I thank the opportunity he gave to me of conducting the research in my ways. I deeply thank my Spanish advisor **Prof. Jacob Lorenzo-Morales**, whose support, suggestions, and expertise to guide my scientific steps were invaluable. I thanks for the enthusiasm to discuss science, for his availability to receive me at his laboratory, and all opportunities he provided to me enabling the enrichment of my PhD research. I sincerely thank both supervisors for having settled the cotutelle agreement, the origin of the present Double Degree PhD. I thank you both for all assistance, professional instructions, and encouragement along my PhD journey.

The laboratory members: I thank all members of the **Structural Biology Laboratory (USP)**. You all have helped in different manners, sharing the daily lab journey and motivating to go further. I thank you for each scientific discussion, exchange of knowledge, and opportunity to enhance scientific abilities. I thanks to Ivan, Marco Túlio, Tatiana, Evandro, Diego, Murilo, Vitor, Witer, and Fernanda. Special thanks go to Ana Letícia and Matheus Issa, undergraduate students who have been working with me. It has been an exciting challenge and a great opportunity to develop manners to teach scientific skills. I have also learned a lot with you both, thank you! I thank Dra. Susana Sculaccio, for her extensive support and technical expertise, shared with me during my scientific development. I also thank her for years of friendship. As well for Dr. Humberto, I thank his support in the laboratory routine. Also, a special thank to the Biophysics Laboratory at IFSC/USP assistance, in persons of Bel, Andressa, Rafael! My gratitude to all members of the **Free Living Amoeba Laboratory (ULL)**: Aitor, Atteneri, Carlo, Desiree, Edyta, Ely, Ines, Iñigo, Ikrame, Jona, Maria, Olfa, Ruben, Ursula, and Prof. José Piñero. Lovely people who have assisted my training time at ULL. I want to let them know that I felt supported during the lab daily routine, as well I felt well acclimated in the local culture of Tenerife accompanied by them. Particularly, I thank Dr. Maria Reyes-Battle, an enthusiastic researcher, that carefully guided me during six months internship at the University of La Laguna. I kindly thank her for each advisement and scientific knowledge I could gain with her, experience that will carry with me to my entire career.

Collaborators and persons who helped particular assays during this PhD research: I gratefully acknowledge Prof. Odete who kindly assisted in developing the framework to perform water collection as well by providing the know-how to conduct the abiotic characterization of water. I thank all discussions and knowledge I have gained with her. I also thank Dr. José Valdecir de Lucca who assisted in situ both

samplings, as well as Dr. Mariana Miguel. I would like to thank Prof. Douglas Dedrim who directly assisted with the computational approach regarding cyst characterization embraced in this PhD research. I thanks for all the scientific ideas we have shared and the learning I have gained with him. I thank to the Center of Scientific and Cultural Diffusion (CDCC/USP) for providing the Monjolinho River basin map. I also thank the assistance of Prof. Claudio Bielenke with Monjolinho River cartography, his book "Geoprocessamento e recursos hídricos" greatly contributed to perform the sampling sites mapping in the Monjolinho Basin hydrography. I deeply thank Prof. Iva Dikova who kindly provided a copy of her guide to perform FLA microscopy analysis: "Illustrated guide to culture collection of free-living amoebae". I am very gratified for gained access to such instructive literature.

Evaluation committees: I am grateful for the evaluation committee that acted on the qualifying examination, who gave their evaluation on my PhD and contributed a lot with advice that I adopted during my study. Likewise, I kindly thank the evaluation committee that is acting in the present PhD defense, for dedicating their time to give contributions on this work.

Friends: I thank all my friends that have been patient hearing so many times about amoeba. My life is much more pleasant and happy surrounded by each one of you: Renata, Malú, Paty, Fer, Thomas, Ana Laura, Hilde, Nádia, João, Amélia, Lucilly, Ana Elisa, Laure, Winnie, Paty Villar and Tati Massaro. My gratitude for having been watched not only my PhD journey but also my personal development.

Familly: Finally, I immensely thank my family for being always on my side, the basis of every conquer in my life. My mother, Deise, and my father, Luiz, for the extensive encouragement, patience, and support dedicated to me. My brother Luiz, and my sister in law, Camila, I thank you for all assistance and friendship. I am very grateful to have been under your eyes. You all will always be my mirrors. My gratitude to all my relatives, who gave support to me with care and close contact.

Scholarships and Universities: I express my great recognition to funding agencies that assisted my research, essential help to the accomplishment of my PhD study. This study was financed in part by the Coordenação de Aperfeiçoamento de Pessoal de Nível Superior - Brasil (Capes) - Finance Code 001. I am very grateful to the University of São Paulo, especially the Physics Institute of São Carlos, as well the University of La Laguna, espeacially the University Institute of Tropical Diseases and Public Health of the Canary Islands. From USP, I kindly thank to Cris Dziabas and Neusa Azevedo from USP, experts on formatting scientific documents and managing references. I am deeply thankful for all assistance in formating this thesis manuscript. Special thanks to Ana Paula Plazza, Silvio Atahyde, Ricardo Vital and Prof. Luiz Victor, from USP, and dears Elizabeth Carrillo and Paloma Bernal, from ULL, for all assistance with the cotutell agreement and continuous assistance with remaining process related to the management of this PhD. Overall, I express my gratitude to all research, faculty and administrative staff, in persons of Rejane, Cláudia and Lhais, at USP, and Ana Rosellón, Emma and Gabriel, at ULL.

“Where your fair is, there is your task.”

(C. G. Jung)

ABSTRACT

BELLINI, N.K. *Diversity of free-living amoebas in the Monjolinho River in São Paulo state – morphological and molecular approaches.* 2020.222p. Thesis (Doctor in Science). Instituto de Física de São Carlos, Universidade de São Paulo, São Carlos, and University Institute of Tropical Diseases and Public Health of the Canary Islands, University of La Laguna, San Cristóbal de La Laguna, Tenerife, 2020.

Free Living Amoeba (FLA) has gained increasing visibility due to human health concerns. They are unicellular heterotrophic protozoans, widely spread in nature. Water is the main source of amoebic contaminations that may result in encephalitis, keratitis, and skin infections. Pathogenic species belong to the *Naegleria, Acanthamoeba, Sappinia, Balamuthia*, and *Hartmannella* genera. To date, there is a lack of effective treatment and accurate diagnosis for amoebic infections, which has motivated the environmental characterization of FLA as a human health risk assessment strategy. However, FLA epidemiology in Brazil is scarce, contrasting with the country's freshwater abundance. To address this gap, the present research aimed at the FLA characterization along the Monjolinho River, São Carlos, Brazil. The water abiotic evaluation as well as the morphological, and molecular investigation of FLA encompasses the central methodology. Dissolved oxygen and electrical conductivity were measured as the most informative features to inspect anthropogenic driving forces acting upon the hydric ecosystem. Eutrophic sites, downstream of the urban areas, were revealed as hotspots to a diversity of FLA. Non-nutrient agar (NNA) plates seeding confirmed the amoeba growth by light and electron microscopy characterization. Based on these results, relevant taxonomic details (e.g.: flagella, cyst walls, and pseudopodia branching patterns) were described to all FLA life cycle stages. Axenization attempts revealed the persistence of bacteria contamination, suggestive of the presence of amoebic resistant microorganisms, enhancing its threat to humans. Molecular characterization enabled us to detect the potentially pathogenic genera *Naegleria* (*N. australiensis and N. phillipinensis*), *Acanthamoeba* (*A. genotype T4* and *A. hatchetti*), and *Hartmanella* (*V. vermiforms*); besides the non-pathogenic *Vannela* sp, *Stenamoeba*, *Filamoeba*, and *Naegleria* (*N. canariensisi, N.gruberi,* and *N. dobsoni*). In this work, the knowledge of FLA distribution allowed the recognition of Brazilian freshwaters as suitable ecological niches to FLA spread, as well as the development of the methodology necessary for the future identification and characterization of FLA in the environment. Although conducted to a local extend, this research

suggests that other FLA genus can be equally isolated in Brazilian freshwater systems that can finally booster later expansion to other water streams.
Key-words: Free-living amoeba. Waterborne protozoan. Amoeba resistant microorganisms.

RESUMO

BELLINI, N.K. *Diversidade de amebas de vida livre no Rio Monjolinho no estado de São Paulo – abordagens morfológicas e moleculares.* 2020. 222p. Tese (Doutor em Ciências). Instituto de Física de São Carlos, Universidade de São Paulo, São Carlos, e Instituto Universitário de Enfermidades Tropicais e Saúde Pública das Ilhas Canárias, Universidade de La Laguna, San Cristóbal de La Laguna, Tenerife, 2020.

Amebas de vida livre (AVL) tem ganhado visibilidade devido à preocupação que provocam à saúde humana. São protozoários unicelulalres heterotróficos amplamente distribuídos na natureza, importantes para a saúde humana. A água é a principal fonte de contaminação por amebas, causando encefalites, ceratites, e infecções de pele. Espécies patogênicas pertencem aos gêneros *Naegleria, Acanthamoeba, Sappinia, Balamuthia*, e *Hartmanella.* Atualmente, os tratamentos e diagnósticos são pouco efetivos, o que impulsiona a caracterização ambiental de AVL como estratégia para monitoramento do risco de contaminação ao homem. Entretanto a epidemiologia de AVL no Brasil é pouco explorada, contrastando com a abundância do país em fontes de água doce. Para abordar esta lacuna, a presente pesquisa teve como objetivo a identificação de AVL no Rio Monjolinho, São Carlos, Brasil. A avaliação dos parâmetros abióticos da água, assim como investigação morfológica e molecular de AVL compuseram a metodologia central deste trabalho. Oxigênio dissolvido e condutividade elétrica foram os parâmetros limnologicos mais informativos para caracterizar as ações antropogênicas atuando sobre o ecossistema aquático. Sítios eutrofizados, à jusante da área urbana, revelaram ser foco para uma diversidade de AVL. As caracterizações por microscopia de luz e microscopia eletrônica confirmaram o crescimento de amebas em placas de ágar não nutritivo. Baseado nestes resultados, relevantes detalhes taxonômicos típicos dos estágios trofozoito, cisto, e flagelar (ex: flagelos, parede dos cistos e padrão de ramificação dos pseudopodes) foram evidenciados. Ensaios de axenização indicaram persistente contaminação bacteriana, possível consequência das AVLs atuando como reservatório para microrganismos resistentes à AVL, aumentando sua ameaça ao homem. A caracterização molecular permitiu a detecção de gêneros potencialmente patogênicos: *Naegleria* (*N. australiensis and N. phillipinensis*), *Acanthamoeba* (*A. genotype T4* e *A. hatchetti*) e *Hartmanella* (*V. vermiformis*); além de não patogênicos *Vannela, Stenamoeba, Filamoeba* e *Naegleria (N. canariensisi, N.gruberi,* e *N. dobsoni*). No presente trabalho, o conhecimento da distribuição de AVLs permitiu o reconhecimento de corpos de água doce no Brasil como nichos ecológicos apropriados para a dispersão de AVL, assim como o

desenvolvimento da metodologia necessária para a identificação e caracterização de AVL no ambiente em trabalhos futuros. Embora realizada em uma escala local, esta pesquisa sugere que outros gêneros de AVL podem ser igualmente isolados em sistemas de água doce do Brasil e, consequentemente impulsionar a expansão das investigações de AVL para outros sistemas aquáticos.

Palavras-chave: Amebas de vida-livre. Protozoários transmitidos pela água. Microrganismos resistentes a amebas.

LIST OF FIGURES

LIST OF TABLES

TERMS AND ABBREVIATIONS

AK	Amoebic Keratitis
ANA	Brazil´s National water Agency
APMV	*Acanthamoeba polyphaga* mimivirus
ARM	Amoeba-Resistant Microorganisms
ATCC	American Type Culture Collection
BAE	*Balamuthia* Amoebic Encephalitis
BLASTn	Basic Local Alignment Search Tool nucleotide
CDC	Center for Disease Control and prevention
CDP	Critical Point Drying
CNS	Central Nervous System
CSF	Cerebrospinal Fluid
DMSO	Dimethyl Sulfoxide
DWDS	Drinking Water Distribution Systems
FAO	Food and Agriculture Organization
FBS	Fetal Bovine Serum
FLA	Free-Living Amoeba
GAE	Granulomatous Amoebic Encephalitis
GIS	Geographic Information System
HIV/AIDS	Human Immunodeficiency Virus/ Acquired Immunodeficiency Syndrome
HMDS	Hexamethyldisilazane
INPE	National Institute for Space Research
ITS	Internal Transcribed Spacer
MEGA	Molecular Evolutionary Genetics Analysis
NCBI	National Center for Biotechnology Information
NNA	Non-Nutrient Agar
PAM	Primary Amoebic Meningoencephalitis
PCR	Polymerase Chain Reaction
PHMB	Polyhexamethylene Biguanide
PYG	Peptone Yeast-extract Glucose
RT	Room Temperature
SAE	*Sappinia* Amoebic Encephalitis
SPRING	Georeferenced Information Processing System
SSU rRNA	Small Subunit ribosomal Ribonucleic acid
TE	Tris-EDTA buffer
Tm	Melting Temperature
UTM	Universal Transverse Mercator

THESIS OUTLINE

The present thesis has been written in four chapters containing:

Chapter 1: conceptualization based on relevant literature discussing Free-Living Amoeba (FLA) issues, the Brazilian background on FLA investigations, and corresponding literature gaps that motivated our work;

Chapter 2: devoted to the description of the methodology employed in the limnological characterization of the Monjolinho River, and the corresponding morphological and molecular approaches were undertaken to characterize FLA diversity. Additionally, this chapter presents a brief mention of institutions and researchers involved in the experimental work.

Chapter 3: presents the findings of this research. It is concerned with detailing achievements in physicochemical water quality assessment (3.1), morphological (3.2), and molecular (3.3) screening of environmental samples. An integrated discussion section can be found at the end of each topic from 3.1 to 3.3 to debate the data obtained with the current literature. Moreover, this chapter names suggestions for further initiatives towards the expansion of this study.

Chapter 4: contains concluding remarks and reveals the potential of the thesis on shedding light on FLA epidemiology by highlighting the major contributions to the scientific community.

Finally, two appendices had been included to complement the information discussed in this document in which the first (APPENDIX I) consists of a review on Primary Amoebic Meningoencephalitis (PAM) caused by *Naegleria fowleri* and the second (APPENDIX II), a report of *Naegleria* diversity in Monjolinho river, both authored by the student, and collaborators, during her PhD study.

SUMMARY

Chapter 1 Introduction

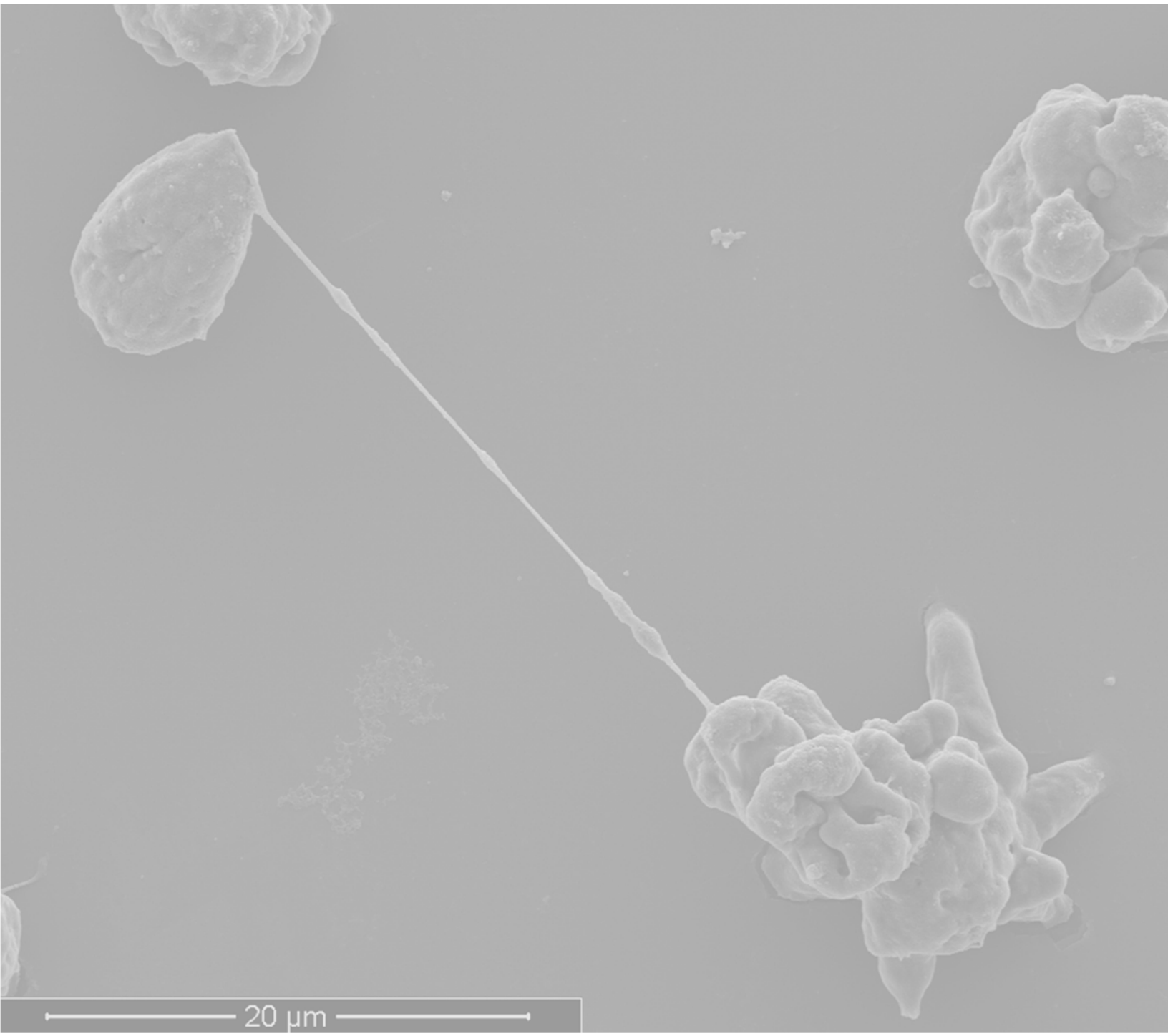

Scanning electron microscopy of *Naegleria gruberi* trophozoites. Emphasis on the cell division process.

Source: By the author.

1.1 Free-Living Amoeba (FLA)

Amoebas are unicellular eukaryotic organisms whose species diversity share the presence of pseudopods, as a motility strategy promoted by cytoplasmic projections, and for phagocytosis as a feeding strategy. Ancient morphology-based phylogeny classified amoeba in the Sarcodina subphylum, within the kingdom Protist, a model adopted for more than a century (Figure 1.1. part A). Basically, the presence of pseudopodia was the synapomorphy clustering the Sarcodina. (1-2) The kingdom Protist, positioned in the base of the tree of life, in the ancient phylogeny proposed by Whittaker in 1969, was defined based on photosynthesis and carbon intake strategies adopted by the organisms (photosynthesis, ingestion, and adsorption).(3) Then, during the 70s, Carl Woese proposed a tree of life containing the Eukarya, Bacteria, and Archaea domains, based upon ribosomal DNA data.(4-5)

In regard to Protists, based on continuous revisions towards resolving the tree of life, it is no longer recognized as a kingdom. Likewise, the subphylum Sarcodina has been reviewed and its members distributed into other lineages due to novel methods used to comprehend relatedness among eukaryotes. These approaches relied upon complementary molecular and biochemical information that enabled new proposals to the eukaryotic clustering and allowed to reposition the Protist groups. Pioneering studies reported between 2004 (6) and 2005 (7) gathering phylogenetic examinations of all eukaryotic organisms, argued for the first time the division of eukaryotes into six major groups: Amoebozoa, Opisthokonta, Rhizaria, Archeoplastida, Chromalveolata, and Excavata. Among them, all amoeba organisms are placed in four groups: Amoebozoa, Rhizaria, Chromalveolata, and Excavata highlighting the polyphyletic relationship, (7) as illustrated in Figure 1.1, part B.

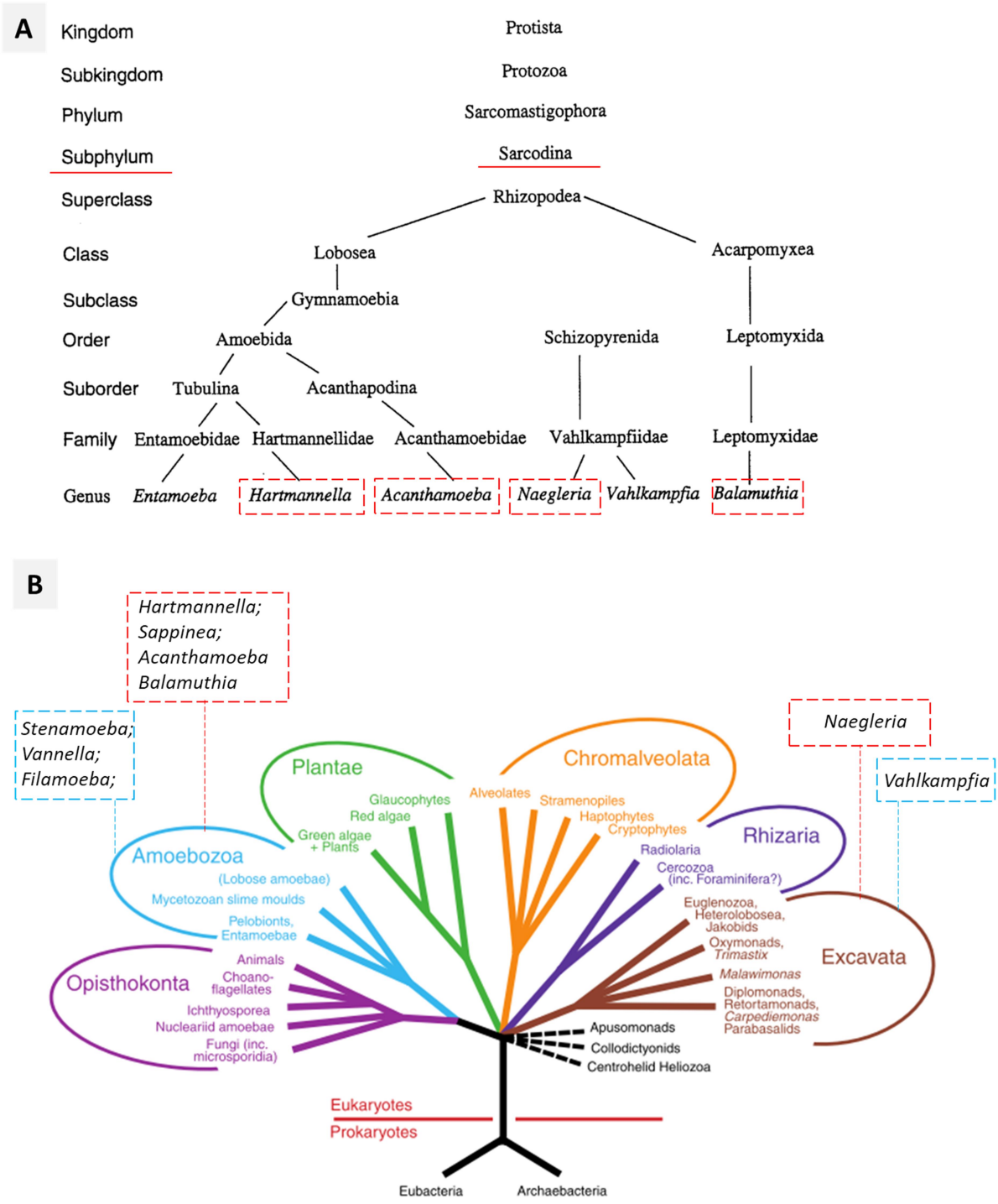

Figure 1.1 - Phylogeny of FLA, the ancient and modern points of view. A and B representations gather examples of FLA discriminated as potentially pathogenic (red rectangles). B contains additional examples of non-pathogenic genera (blue rectangles).

Source: Adapted from MARTINEZ *et al.*[2]; AD *et al.*[7]; SIMPSON *et al.*[6]

Figure 1.1. is illustrative of the evolutionary history of life that comprises potentially pathogenic FLA genera grouped in the supergroups Excavata and Amoebozoa (Fig. 1.1, part B).(7) Additional free-living amoeba groups non-presenting clinical health concerns (blue rectangles, Fig 1.1 B) have also been clustered within both Excavata and Amoebozoa. The former is a clade that comprises Heterolobosoea (e.g.: *Naegleria* and *Vahlkampfia*) and the latter gathers the genera *Acanthamoeba*, *Sappinia*, *Balamuthia*, *Hartmannella*, *Filamoeba*, and *Stenamoeba.* (7)

Heterolobosea, grouping the amoeboflagellates, was previously presented as the sister taxa of Euglenozoa, based on protein analysis (e.g. α- and β-tubulin),(8,9) however, gene-based studies (e.g. SSU rRNA) have further positioned it as the sister taxa of Jakobids. (1,10) Nowadays, Excavata has been dissolved into Discobids and Metamonads. (11) Among protozoologists, there is still disagreement on the phylogenetic positioning of the different groups of amoebas and new propositions have been put forward to arrange the FLA clades. Even the latest phylogenetic study concerned with resolving the phylogeny of all living eukaryotes resulted in a polytomy of those taxa formerly grouped as Excavata. (12) Due to be a robust phylogenomic study, (12) the uncertainness related to ancient groups reinforced that the evolutionary reconstruction of the protists remain a concern regularly updated and reviewed. Thus, at the present research, we are following the revised classification proposed in 2005 (Fig1.1. B).

Presently, several environmental and clinical reports concerned with isolating FLA have proposed the phylogenetic characterization based mostly on SSU rRNA gene sequencing. (13–15) Specifically of *Naegleria* phylogeny, studies highlighted that instead of the 18S rRNA sequences, the ITS1-5.8S and ITS2 regions are more suitable for molecular detection due to its potential to detect species heterogeneity and on revealing biological phenomena, as speciation. (16) Meanwhile, advances on FLA phylogeny have been focused on those species well recognized due to its human health interest. FLA pathogenic genera call attention due to three major disorders in humans and other animals: granulomatous amoebic encephalitis (GAE), primary amoebic meningoencephalitis (PAM) and amoebic keratitis (AK). (17-18) Aetiological agents of FLA related diseases are distributed in five genera: *Acanthamoeba*, *Balamuthia*, *Naegleria*, *Sappinea* (19) and the latest recognized *Vermamoeba* (formerly *Hartmannella*). (20-21) These genera are ubiquitously spread in nature in which water is its main environment, and as

a consequence, the main path they take to reach its hosts. The dual life cycle behavior, free-living and pathogenic, gives to this FLA groups the attribution of amphizoic amoebas. (22)

These aforementioned free-living amoeba genera are morphologically diverse, and in whatsoever class they belong, there are two lifecycle features shared by them: the presence of trophozoites and cyst stages as the vegetative and dormant forms, respectively. Particularly the *Naegleria* genera present a third, the flagellate stage. (22) Several studies employ the morphological characterization as a pre-classification step to group an amoeba into its respective genus, a task commonly guided by a morphological manual proposed by F. C. Page, named "A new key to freshwater and soil gymnamoebae". (23) Particular features distinguishing trophozoites, cyst and flagellate forms can be compared as illustrated in Figure 1.2.

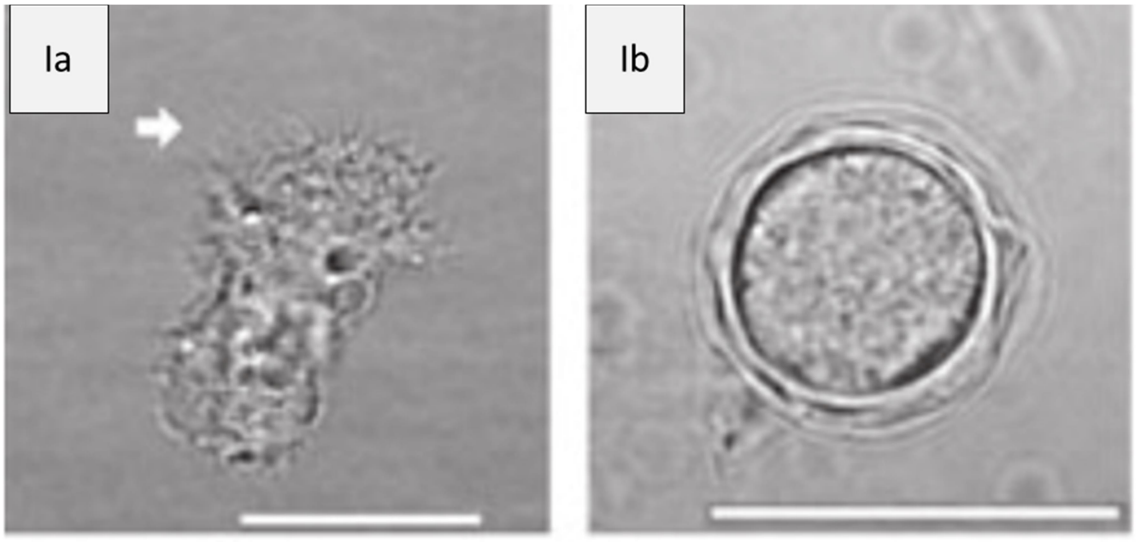

(to be continue)

(continuation)

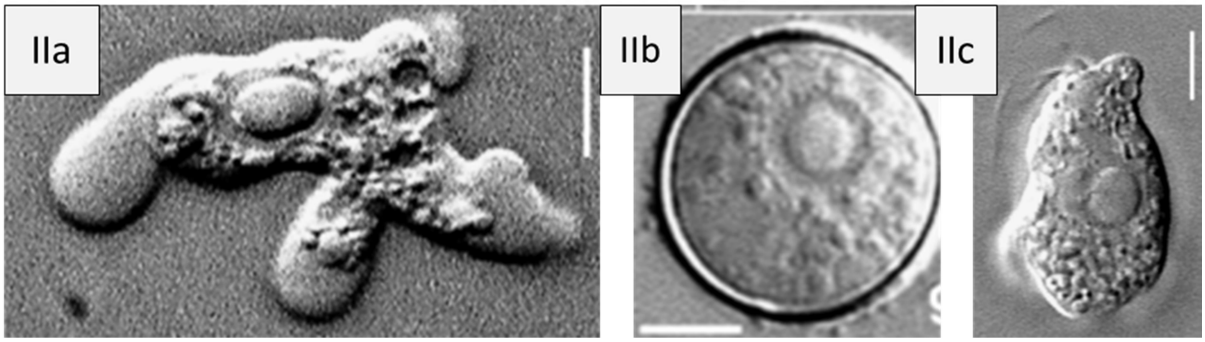

Figure 1.2 - Photomicrographs of *Acanthamoeba* (I) and *Naegleria* (II) isolates. Trophozoite (a), cyst (b) and flagellate (c) stages. Scale bars represent 10 µm (Ia and Ib), 5 µm (IIa and IIb), and 4 µm (IIc). Ia and Ib were isolated from rice field samples (24) and IIa-c isolated from a water sample. (25)
Source: Adapted from LIANG *et al.*[24]; VISVESVARA *et al.*[25]

Figure 1.2, Ia and IIa, depicts trophozoite forms, the stage in which the amoeba spends most of its life, and a characteristic stage in which the amoeba can move, feed mainly on bacteria, and divide by binary fission. (19,26) Trophozoites usually feature phagocytic related structures named food-cups. (27) The food-cups have also been associated with "trogocytosis", a process used by the amoeba to promote injuries on target host cells. (28)

Trophozoites commonly move through constrictions of the body that promotes hyaloplasmic projections (pseudopodia), whose terminal end diverges from the lobopodia zone with the presence of eruptive hemispheric bulges (Fig1.2-IIa) or spine-like projections emerging from the hyaline zones, the so-called acanthopodia (Fig 1.2– Ia). (26) Pseudopods and adhesion-like protuberances function to allow cell movement and its change in direction. Trophozoites are generally distinguished as flattened or cylindrical, whose corresponding pseudopodia types range from monotactic hyaloplasmic projections, typical of *Vermamoeba*, to extremely branched subpseudopodia similar to acanthopodia, typical of *Stenamoeba*. (29) Regarding subpseudopodium, in water, some trophozoites can be found as floating forms, in which subpseudopodium turns to a tapering form, typically stellate or star-shaped, mainly found in the Amoebozoa genera belonging to the Vannellidae family. (28,31-32)

The morphotypic characterization of trophozoites is often observed in the cytoplasmic portion in which, to most trophozoites, the hyaloplasm can be easily distinguished from the granuloplasma, as shown in the trophozoite illustrated in Fig. 1.2- part IIa. Hyaloplasm commonly harbors the nucleus, a large number of mitochondria, ribosomes, and food and contractile vacuoles. (26) Most FLA is uninucleate, (26) although binucleate amoeba has been

reported mainly in *Sappinia* isolates. (32) Additionally, the overall outline of a trophozoite is irregular and its greatest dimension range from about 6 to 37 µm in *Vermamoeba* isolates, (23,33) 12 to 35 µm in *Acanthamoeba*, (34) 7 to 25 µm in *Naegleria* (26,35), 12 to 60 µm to *Balamuthia* (26) and 40 to 80 µm to *Sappinea*. (26)

Taking into account the environmental diversity in which free-living amoeba inhabits, they have to have adaptive mechanisms of cell protection against stress factors in water, a role exerted by the cyst stage (Figure 1.2, Ib and IIb). Cysts present a high resistance against extreme physical and chemical conditions. (19) The overall outline of a resistant cell is oval or spherical with a double or single wall, usually containing pores for further amoeba excystment. (26) The overall cyst size ranges from 5-20 µm of diameter in *Acanthamoeba* (34) and can present wrinkled inner and out layers (Fig. 1.2, Ib). The endocyst usually assumes a characteristic stellate form. (36) Otherwise, typically rounded cysts (Fig.1.2, part II b) range from 5-14 µm in *Naegleria*, (24,26) 10 – 30 µm in *Balamuthia*, (37) 15 – 30 µm in *Sappinea* (26) and about 4 - 9 µm in *Vermamoeba*. (33)

Finally, a non-diving, non-feeding flagellate form (Fig 1.2, II c) is characteristic of the *Naegleria* genus and, in the initial stage of the differentiation, flagellates are spherical and called a pre-mature (pm) stage, whereas the mature (m) stage is elongated with unidirectional moving flagella, normally biflagellate. (20,42-43) Both, pre-mature and mature flagellates can be seen in Figure 1.3-F. Cell dimensions of the flagellate form commonly ranges from 10 – 16 µm. (26)

Alternatively, FLA shapes were represented here in an integrated life cycle to name the transitions adopted by these cells to change from one shape to the other (Figure 1.3).

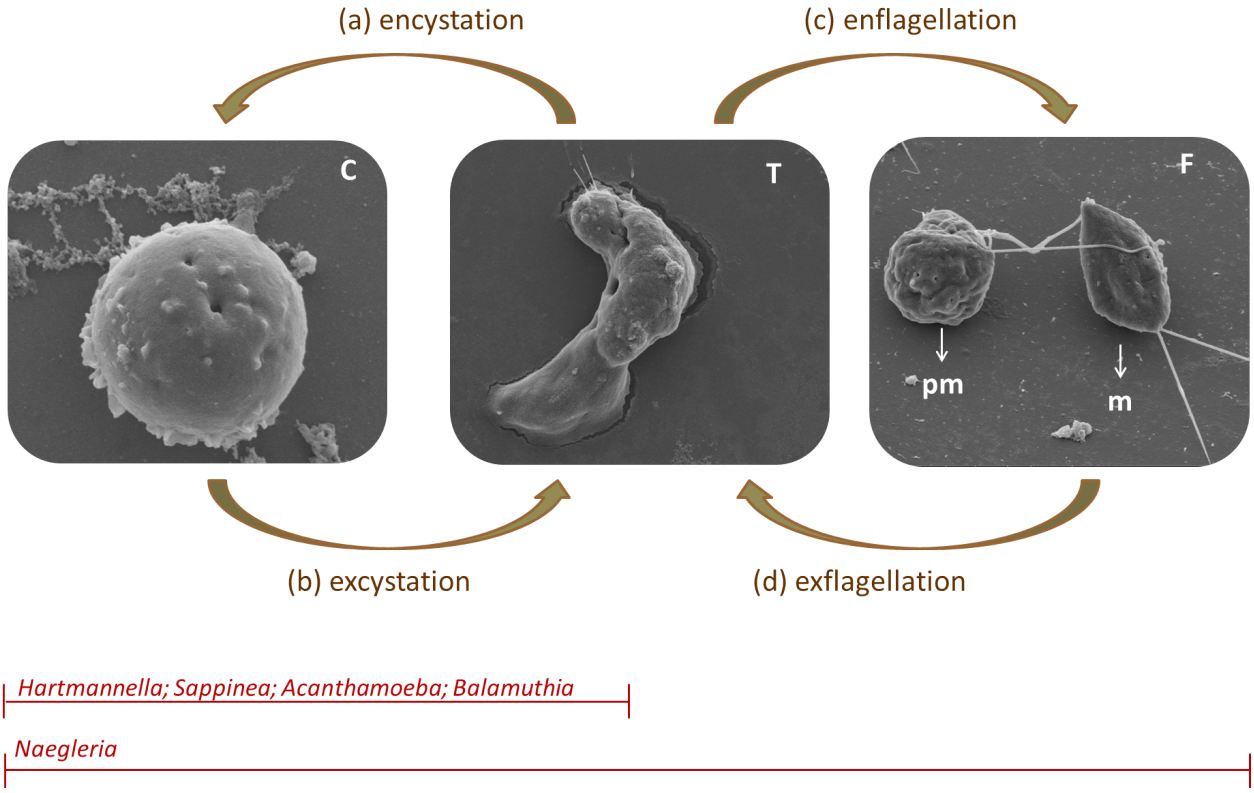

Figure 1.3 – The FLA life cycle. Cyst (C), trophozoite (T), and flagellate (F) stages. Annotations "pm" and "m" refer to pre-mature and mature flagellates. The red lines indicate those FLA genera capable of performing encystation and excystation (*Hartmanella*, *Sappinia*, *Acanthamoeba* and *Balamuthia*) and the genus capable of transforming into both, cysts and flagellate stages (*Naegleria*).
Source: By the author.

Briefly, as represented in Figure 1.3, a vegetative form (T), whether faces stress by starvation, environmental dryness, or physicochemical unbalance in the water environment can develop into the dormant stage (C) through the process of encystation (a). (17,40,41) In favorable conditions of nutrient availability and suitable humidity levels, a viable cyst can recover the trophozoite stage commonly through pseudopod projections outside from a pore in the process of excystation (Fig. 1.3, b). (9,40,42) As represented in Figure 1.3., *Acanthamoeba*, *Sappinia*, *Balamuthia*, and *Vermamoeba* experience "a" and "b" processes in their life cycles whereas *Naegleria* presents the additional enflagellation capability (c). The enflagellation process allows the cells to quickly move toward a better environment avoiding the ones under ionic unbalance, high hydrostatic pressure, extreme temperatures, or nutrient scarcity. (9) At the time that the amoeboflagellate (F) escaped from such adverse habitats, it can recover the trophozoite form (T) through exflagellation process (Fig. 1.3, d). Regarding the molecular machinery involved in the transition from one stage to the other, comprehensive surveys have

contributed to elucidating these differentiations from trophozoites to cysts (42-43) and from trophozoite to flagellate form elucidating the flagella apparatus maturation and other details. (9,44) The investigation of amoeboid cells, as well as cysts and flagellar stages, are commonly seen as a study model to elucidate canonical cell processes as motility, phagocytosis, cell division, encystation elicitors, flagella maturation among others. (9,40)

However, although knowing the morphologic outline of each stage, their fine-structures and biochemical elucidation remain under continuous investigation, mainly regarding the pathogenic FLA species. This gap encourages a continuous scientific effort in the field.

1.2 Clinical importance

In nature, the trophozoite stage feeds mostly upon bacteria, algae, fungi, amoeba, and other protozoans.(45,46) However, infecting the human host it can affect at least one of four different tissues: corneal tissue, causing amoeba keratitis (AK); nervous system cells, causing amoebic encephalitis; skin or lung cells causing skin abscesses and pulmonary infections, respectively. (47) Its capacity of infecting humans was the milestone to the striking recognition of the FLA group. Although *Naegleria* cysts and flagellate stages have been reported to enter into the human body, only the trophozoite stage is capable of establishing an infection. (37,48–50) Thus, cyst, trophozoite, and flagellate stages can reach the host, in an opportune human-protozoan contact, through three main routes, as summarized in the following life cycle (Figure 1.4).

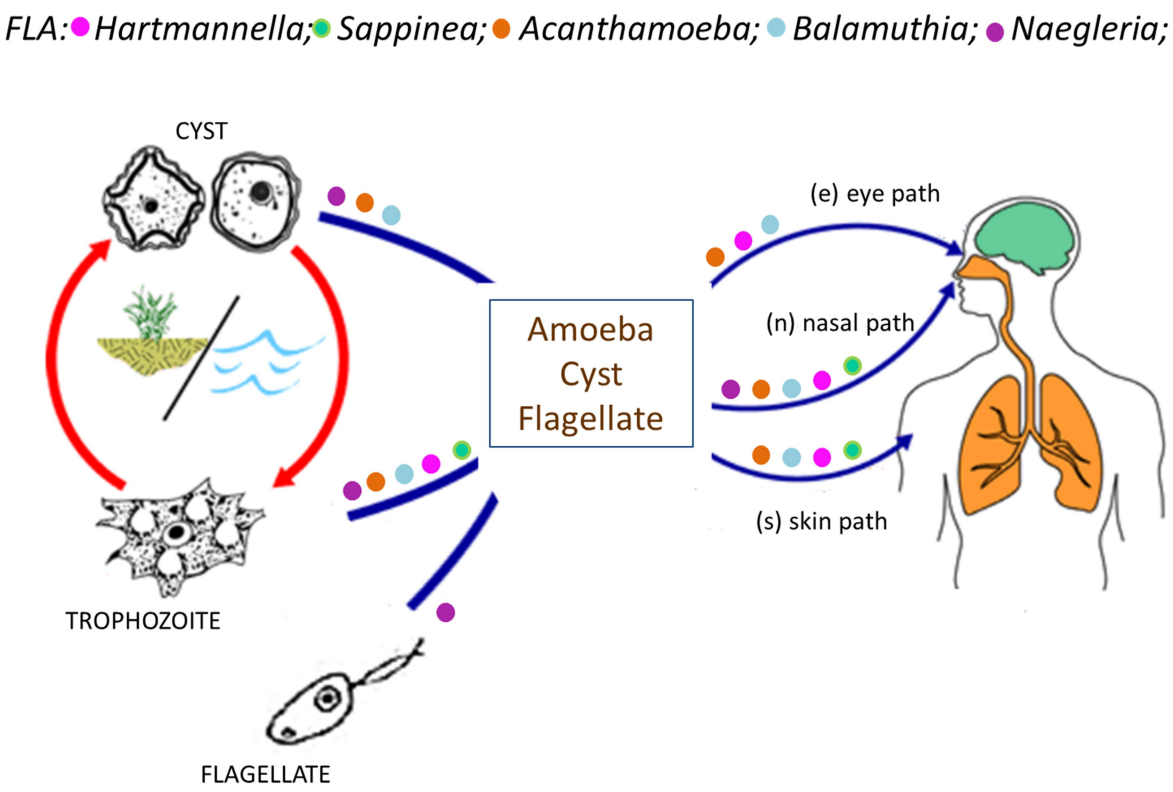

Figure 1.4 - *FLA* related infections - life cycle. Trophozoites, cysts and even flagellates can get access into the human body through either eyes (a), nostrils (b) or skin lesions (c) causing respectively keratitis, encephalitis or respiratory illness and skin ulcers. Adapted from the Center for Disease Control and Prevention (CDC) life cycles to FLA pathogenic genera and adapted from literature references (37), (51) and (47).
Source: Adapted from LORENZO-MORALES *et al.*[37] ; KRÓL-TURMIŃSKA *et al.*[47]; LORENZO-MORALES *et al.*[51]

As shown in Figure 1.4., the pathogenic FLA genera may cause human maladies whether contacting the host by the eyes (e), nasal (n), and skin (s) entries. In regard of skin maladies (s), trophozoites and cysts enter its hosts through cuts or wounds, and the respective reported symptoms can range from ulcers, abscesses, and reddish nodules, as shown it Figure 1.5:

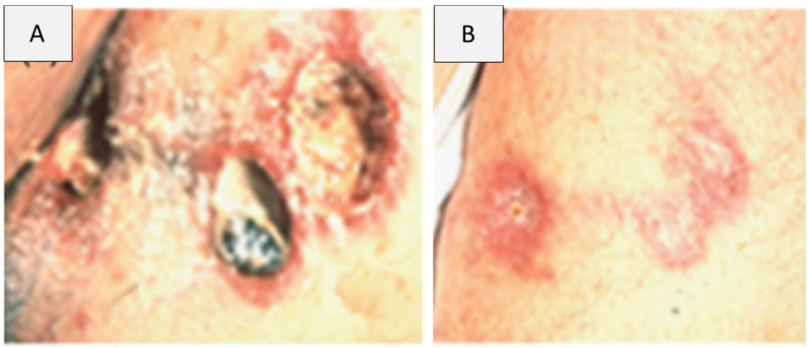

(to be continued)

(continuation)

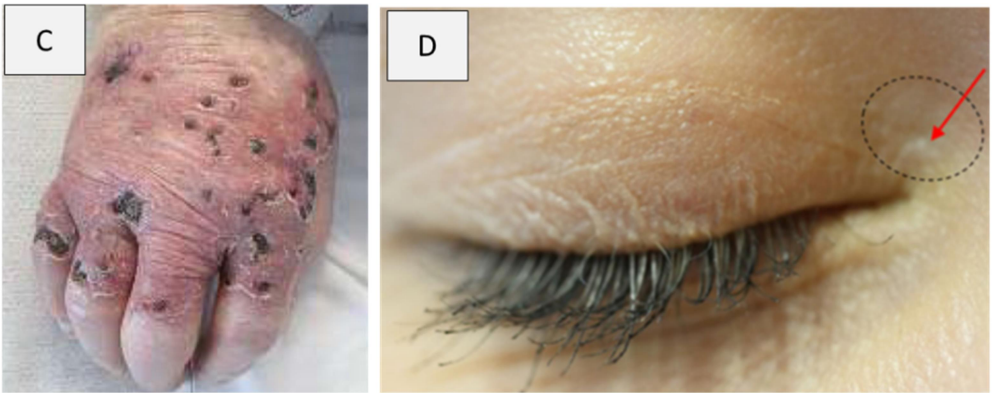

Figure 1.5 - Skin injuries caused by pathogenic FLA strains. *Acanthamoeba* ulcers (A, B), (19) *Balamuthia mandrillaris* disseminated infection (C) (52) and a *Vermamoeba vermiformis* skin ulcer next to the eye (D). (53)

Source: Adapted from VISVESVARA *et al.*[20]; SCHAFER *et al.*[53]; SCHEID *et al.*[54]

Vermamoeba vermiformis, *Acanthamoeba spp*, and *Balamuthia mandrillaris* have been commonly reported as etiological agents of skin infections, as illustrated in Figure 1.5. Although not illustrated above, *Sappinia pedata* is also capable of causing tissue lesions. (47)

Overall, the number of patients afflicted by amoebic skin lesions is not well known; however, it has been often easily treated. Successful treatments relied on using ketoconazole, (54) chlorhexidine gluconate, (47,54) pentamidine isethionate, flucytosine or fluconazole and zinc paste. (53) Unlike local infections (e.g. AK and GAE), *Acanthamoeba* and *Balamuthia* have the ability to causing disseminated infections (47) afflicting lungs, kidneys, and bones (47) in which the trophozoites enter through skin lesions and gain access to the circulatory system. (19)

Resuming the FLA life cycle illustration (Figure 1.4), trophozoites and cysts reaching the host through the eyes (e) can elicit an amoeba keratitis onset. The first symptoms usually include eye pain, blurred vision, abnormal tearing, eye redness and light sensitivity. (50,55) The infection course spans corneal ulcers that typically evolve to tissue necrosis and ultimately blindness, (56) as shown in Figure 1.6.

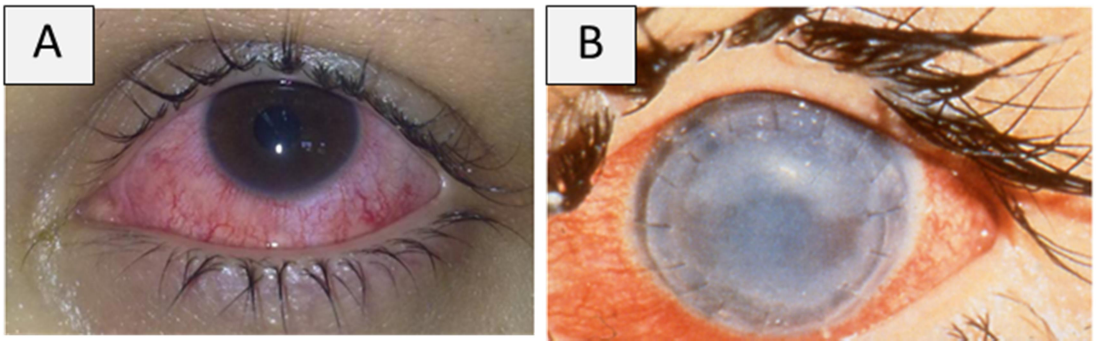

Figure 1.6 – Clinical symptoms of amoebic keratitis. Eye clinical photographs highlighting eye redness (A) and the stage pre receiving corneal transplantation (B). A- *Hartmmannela* keratitis; (57) B – *Acanthamoeba* infected eye. (58)
Source: Adapted from ABEDKHOJASTEH *et al.*[58]; SIDDIQUI *et al.*[59]

Amoebic keratitis often affects contact lens wearers and persons previously presenting corneal abrasions or corneal transplantation. (38,51) It is usually caused by *Acanthamoeba spp.* with more than 3000 reported cases, (47) although some cases of *Vermamoeba vermiformis* and *Balamuthia mandrillaris* corneal infections have been reported. (56-57,59-60) The aforementioned genera have been isolated from corneal biopsy separately and even mixed, coexisting in the same patient as the example of *Acanthamoeba* and *Hartmanella* mixed infection. (38,61) Poor hygiene on storing and handling contact lenses, as well as swimming or showering wearing contact lenses, are some of the leading behaviors to be avoided to prevent keratitis. (47)

A 2016 review on *Acanthamoeba* keratitis emphasized the high incidence of cases globally reported, greatly leveraged by the spreading of using contact lenses in the latest 20 years. Once diagnosed on time, the commonest chemotherapy approach is based on a combination of propamidine isethionate and polyhexamethylene biguanide or chlorhexidine. (62) However, after the completion of the treatment, viable cysts able to differentiating into trophozoites are often prevalent, explaining the number of cases evolving into blindness. (51) Thus, concerned about the urgency to develop new chemotherapies, recent findings revealed caffeine and maslinic acid as potential agents against cysts´ prevalence. (63) Likewise, other attempts have aimed at blocking the amoebae entrance in human tissues through interfering with several amoebic pathways and enzymes. One example is the recent RNAi serine proteases genes knockdown attempts. (64) Moreover, therapeutic strategies against *Acanthamoeba* keratitis have emerged toward mixtures of synthetic and natural products as examples of atorvastatine, (56) ursolic acid derivatives, (65) and staurosporine. (66) The latter has been suggested as a promising compound

to solve the cyst persistence bottleneck. (66) Figure 1.4. also illustrates the most common path usually taken by pathogenic FLA amoeba to reach the host, the nostril (n) contact, leading mainly to the onset of encephalitis. Central nervous system (CNS) infections caused by pathogenic FLA, species termed “brain-eating amoebas”, can be classified according to the aetiological agent. Thus, granulomatous amoebic encephalitis (GAE) is caused by *Acanthamoeba* spp.*;*(51) primary amoebic meningoencephalitis (PAM) caused by the emerging parasite *Naegleria fowleri*; (67) *Balamuthia* amoebic encephalitis (BAE) by *Balamuthia mandrillaris* (68) and *Sappinia* amoebic encephalitis (SAE) by *Sappinia pedata*. (69) SAE comprises a unique report, credited to a species formerly named *Sappinea diploidea* and, based on further molecular studies, the infection was considered to be caused by *Sappinea pedata*. (47,70) *Balamuthia mandrillaris* encephalitis, like the *Acanthamoeba* cases, has been reported infecting immunosuppressed hosts generally suffering from HIV/AIDS, cancer, diabetes, intravenous drug-addicted or patients of organ transplant. (18,37,45,75-76) PAM cases are commonly reported in summer months, considering the thermophilic potential of *N. fowleri*. GAE and AK infections have no seasonality prevalence (26) To date, a single case of *Sappinia* infection has been reported, in Texas USA (17,19,70) and, BAE are sporadic and therefore no sufficient information is available to reveal any pattern.

Overall, amoebic brain infections have major aggravating aspects that lead to death within a few weeks post the infection. (77-78) Thus, likewise AK, early diagnosis is essential to encephalitis treatment. However, the lack of specific symptoms leads to its common misdiagnosis as a bacterial infection. FLA encephalistis diagnosis is generally obtained post-mortem and there are few cases of amoebic encephalitis treatment success. (75–77) The symptom coincidence with bacterial meningitis and viral encephalitis is the first major aggravating issue hampering a prompt and accurate diagnose. (54,78–80) Fever, headache, vomiting, abnormal neurologic behavior, comprise the first symptoms faced by amoeba infection patients. Over a few weeks, the illness can develop to a chronic (GAE) or a rapidly progressive, fulminant (PAM) central nervous system (CNS) infection, features challenging to the treatment of the disease.(62,81) Literature reports have identifiied 300 cases of GAE and 440 cases of PAM worldwide.(47,80,82) An exceedingly low survival rate, of less than 10% and 5% is associated with GAE and PAM encephalitis, respectively.(81) BAE fatality rate ranges from 90-94%, considering about 200 *Balamuthia* encephalitis reported cases.(47) BAE has also been reported in non-human hosts as

gorillas, dogs, sheep, and horses.(19) *Sappinea* was also identified in a cerebral infection, nonetheless, it did not result in death.(83)

Overall, once suspecting about amoeba encephalitis, neuroimaging is used to confirm the investigation, as shown in Figure 1.7.

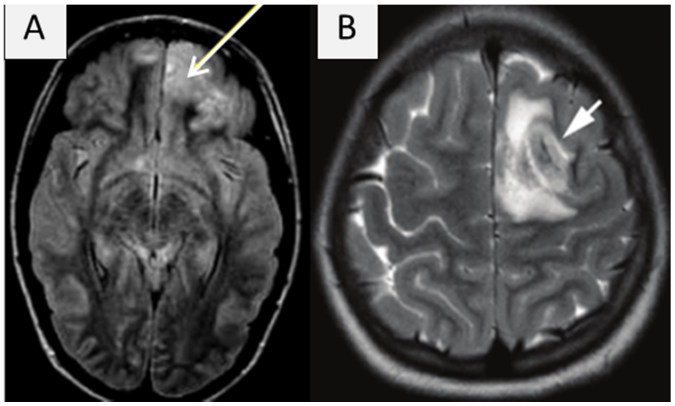

Figure 1.7 - Magnetic resonance imaging (MRI) revealing a focal PAM (A) (84) and *Balamuthia* encephalitis with a hemorrhagic lesion (B) (85), both in the superior left frontal lobe (white arrows).
Source: Adapted from LINAM *et al.*[84]; GRENINGER *et al.*[85]

However, radiological investigations may not be a definitive diagnostic method. Indeed, it has been reported that other nervous system impairments such as viral encephalitis, bacterial encephalitis, and even cysticercosis symptomatic edemas may result in similar radiological images.(86) Thus, neuroimaging is commonly followed by cerebrospinal fluid (CSF) biopsy, an invasive analysis, obtained for culturing, microscopic observation, and molecular identification.(71,87) The identification of pathogenic species on CSF has also been performed through immunological methods, as western blot and immunofluorescence.(75,80) Intracranial pressure, polymorphonuclear leucocytes count, and protein concentration are complementarily assessed in the diagnosis framework.(47)

Once diagnosed in an early stage, all available treatments are considered towards a successful outcome, although the therapeutic arsenal still lacks efficiency due to its high toxicity or, on the contrary, loss of concentration while penetrating the blood-brain barrier.(88–90) This is the third major issue related to amoebic encephalitis. The therapeutic first line of choice includes drugs commonly used to treat antifungal, antibacterial, anti leishmaniasis infections, and even anticancer compounds.(91) Among them amphotericin B, miltefosine, corifugin, metronidazole, fluconazole, rifampin are reported.(92-93) Amphotericin B has been also used associated with

voriconazole, ketoconazole, itraconazole, and sulfadiazine, for treating GAE (62). These compounds are commonly given through intravenously or by intrathecal injection.(94-95) Normally, amphotericin B is the most common drug used against *N. fowleri* infections and the latest cases have combined one or more of the following compounds: miltefosine (anti-leishmanial drug), rifampin (antibiotic), and azoles (antifungal) (39) (Appendix I, table 3). Auranofin, also a repurposing example, has demonstrated promising results on *Naegleria* encephalitis.(96-97) For *Balamuthia* infections, the ongoing drugs include miltefosine, pentamidine, azithromycin, fluconazole.(71,95,98–100) Aside from being a broad therapeutic arsenal, the combination of chemotherapy conjures a variety of side effects hampering the treatment.(19,62) A successful treatment reported to *Balamuthia* patients included a drug combination with amphotericin B, doxycycline and ceftriaxone. (77)

Overall, considering all FLA caused infections (Fig. 1.4.), the encephalitis cases are the most lethal ones. Moreover, there is another health issue promoted by pathogenic FLA, as well as non-pathogenic FLA species: the amoeba potential for hosting pathogenic microorganisms. (101) Typical intra-FLA bacteria examples include *Afipia spp., Bosea spp.* and *Parachlamydia spp.,* genera disclosing healthy interest due to nosocomial pneumonia caused by them.(102) Also *Aeromonas, Arcobacter, Mycobacterium, Pseudomonas*, and *Salmonella*, resistant to FLA, are related to a diversity of infectious onset to humans. (103-104) *Acinetobacter* and *Aeromonas*,(105) both *Acanthamoeba* spp. resistant bacteria (15) pose a threat to human health due to its multidrug resistance (e.g: sulphonamide, aminoglycoside, penicillin, and ampicillin resistance).(106-107)

Summarizing, FLA pathologies present several biological aspects not well-known, have been misdiagnosed, and can be the vehicle of secondary diseases elicited by intra amoebic microorganisms. Thus, it is urgent to search for effective therapies, to characterize in detail the diseases caused by each amoeba, as well as to conduct its environmental identification aiming to prevent new cases of accidental contact with the human host. Considering that most of the reported FLA patients have a history of water contact (e.g.: bathing in freshwater) before the FLA infection onsets, the scientific community has applied efforts to expand the amoebic identification in environmental sources as an attempt to prevent new cases and to characterize the habitat preferences for amoeba proliferation. (56,108–110) Molecular investigations become a worthwhile approach to broaden the knowledge about FLA geographic distribution and have

been used by the newest studies concerning pathogenic FLA to obtain a faster and more reliable detection of the aetiological agent in clinical samples.(70,111-112) Likewise, studies aiming at FLA environmental occurrence have combined the molecular strategies, with the morphological investigations.(113) Even though in the past 50 years, outbreaks have been related to PAM and GAE infections, (48,114) heightening the concern with water as an important path to new cases, FLA is considered as a neglected waterborne parasitic protozoan group. (114) Such lack of knowledge of the relevance of FLA increases the need for studies aiming to understand the FLA ecological presence through the world to define if the scarcity of reported cases are related to underreporting due to a deficiency of knowledge or indeed FLA infections are naturally rare. An updated overview of the environmental distribution of FLA, mainly in an aqueous system, is detailed ahead.

1.3 Epidemiology

The FLA group is ubiquitous in the world and its pathogenic genera (1.2. section) have been widely reported. Although there is a set of reports isolating FLA from the soil, air, and other habitats (e.g.: dental unit systems, conditioned air system, contact lenses solutions),(92) water sources comprise the most significant source to its spreading. For instance, literature reports have identified FLA pathogens in water samples isolated in Pakistan (*Acanthamoeba*),(115) Western Australia (*Naegleria fowleri* and *Vermamoeba*),(116) Southeast Asian countries (*Acanthamoeba sp., Naegleria* spp., *Vermamoeba* spp.),(38) Spain (*Naegleria* spp), (117) Northern Iran (*Naegleria* spp.), (118) and Venezuela (*Naegleria fowleri*). (119) Table 1.1 better clarify the huge diversity of water sources in which FLA has been detected.

Overall, table 1.1 content endorses the ubiquitous profile of FLA to be spread in water sources. Its capability of surviving in habitats under extreme environmental conditions (e.g.: wastewater, chlorinated swimming pools, and water treatment system) is likely due to its ability to transforming into the cyst stage.(120-121) Table 1.1 also suggests that *Acanthamoeba* is the most frequent FLA genus encountered in environmental samples, reinforced by the literature.(101) The impressive *Acanthamoeba* cyst resistance to chemical compounds used in water disinfection systems, its resistance to dissection and harshened environments justifies its abundance in the environment.(33)

Table 1.1 – The main aqueous matrices in which potentially pathogenic FLA have been isolated through five continents. The colors orange, pink, purple, blue and green indicate FLA genera, respectively, *Acanthamoeba*, *Vermamoeba*, *Naegleria*, *Sappinia* and *Balamuthia*. The numbers listed in the table refer to the literature used as references to amoeba identifications.

Aqueous Habitat	South America	North America	Europe	Australia	Asia
Emergency combined shower	*Acanthamoeba;* (113)				
Sewage water and wastewater			*Acanthamoeba; Vermamoeba; Balamuthia;* (122,123)		
Industrial wastewater	*Acanthamoeba; Vermamoeba; Naegleria;* (124)		*Acanthamoeba; Vermamoeba;*(125)		
Tap water					*Acanthamoeba; Vermamoeba; Naegleria;* (38,126)
Drinking water samples	*Acanthamoeba;* (127)	*Naegleria;* (128)	*Acanthamoeba; Vermamoeba; Balamuthia; Naegleria;* (15,123,129,130)	*Naegleria; Vermamoeba;* (131,132)	*Acanthamoeba; Naegleria;* (133,134)
Man-made recreational water	*Naegleria;* (135)	*Naegleria;* (136)			
Hospital related water			*Vermamoeba;*(20)		

(to be continued)

(continuation)					
Household water		*Acanthamoeba; Vermamoeba; Naegleria; Balamuthia;* (137,138)		*Naegleria;* (139)	
Water treatment system			*Acanthamoeba; Vermamoeba; Naegleria;*(13)		
Biofilm networks				*Vermamoeba; Naegleria;*(116,140)	
Swimming pool	*Acanthamoeba;* (141–144)				*Acanthamoeba; Naegleria;* (38,134,145)
Snow			*Vermamoeba;*(146)		
Lakes		*Naegleria;*(147)	*Acanthamoeba; Vermamoeba;*(33)		*Acanthamoeba ; Vermamoeba;* (38,148)
Surface river water	*Acanthamoeba; Vermamoeba ;Naegleria;* (13,149,150)	*Acanth; Vermamoeba; Naegleria;* (151)	*Acanthamoeba; Naegleria;*(15,33,152)		*Acanthamoeba; Vermamoeba; Naegleria;* (38,153,154)
Thermophilic water sources	*Acanthamoeba; Vermamoeba; Naegleria;*(155)		*Vermamoeba;*(156)		*Acanthamoeba; Vermamoeba; Naegleria;* (118,157,158)
Freshwater pounds			*Sappinia;* (14)		

Source: By the author.

Moreover, Table 1.1. depicts the scarcity of environmental data about *Sappinia* and *Balamuthia* in comparison to *Acanthamoeba*, *Naegleria*, and *Vermamoeba*. It can be a natural consequence of the low number of amoeba cells in the water or a consequence of the identification methods employed, based on microbiological culturing without a complementary molecular analysis, a practice that has been indicated as ineffective to reveal the whole environmental diversity, since several FLAs are unable to grow in vitro.(120-121) Thus, to overcome this issue, the molecular investigation complementing the culture methods are employed.(150) In this regard, surveys have combined polymerase chain reaction (PCR), real-time PCR, and even next-generation sequencing approaches to investigate human and waterborne pathogens, and to obtain a comprehensive insight into FLA microbiome presence in the water sources.(159) Recently, environmental FLA based studies detected *Vermamoeba*, *Naegleria*, and *Acanthamoeba* through 18S rDNA amplicon-based sequencing approach and through whole metagenomics sequencing on drinking water (160) and irrigation water,(152) respectively.

Many water sources inspected for FLA epidemiological purposes (Table 1.1.) present a link regarding protozoan detection and human pressures in the environment. For instance, it has been shown relationships between the use of the area in the surrounding of the river for agriculture practices, sewage disposal or water treatment plants, and cases of infection elicited by pathogenic amoeba. (121,161–163) Anthropogenic activities (e.g.: land usage) bring ecological disturbances in natural water quality that directly influence the microbiota community.(22) On the other hand, intense urbanization and human-nature close interactions favor human exposure to pathogenic FLA present in natural waters.(164) Important hydric habitats with a close relation to human exposure include drinking water systems, for example the Pakistan Drinking Water Distribution Systems (DWDS) samples that tested positive for *N. fowleri*. An interesting assay revealed that due to the delivery of contaminated water to the population through tap water, 50 cases have been reported between 2008-2015.(164) Particular attention should be given to thermal waters as a hotspot to thermophilic amoeba growth, such as *Vermamoeba*,(59) *Acanthamoeba* (157), and *Naegleria*.(158) For instance, thermal watercourses revealed *N. fowleri* (22) prominence and its proliferation in river water has been a concern in light of the climate change perspective of global warming. (165) The survey resulting from the present PhD research suggested that Brazil needs to be under periodic surveillance aiming to predict any evidence of water heating and pathogenic

thermophilic FLA concerning risks to humans (150) (Appendix II). In this respect, the next topic is devoted to offering an updated context of FLA in Brazil.

Regarding FLA ecological role, due to its niche (e.g.: Table 1.1), they share the habitat with a diversity of microorganisms such as bacteria and eukaryote, known as a food source to them. Distinct food preferences according to FLA genus can later influence water microbiota structure and availability of nutrients.(166-167) Another feature of ecological relevance is FLA capability of forming biofilms due to the excretion of nutrients and thus offering protection to the remaining microorganisms in co-occupancy. A 2017 report contributed to this insight by pointing out *Legionella spp* and *Naegleria* spp coexisting at biofilm networks.(168) However, there have been few reports describing niches and occupancy patterns linking FLA and water microbiota.(131,169–171) Most of the available literature addressed this topic in terms of the FLA potential as a vehicle to a diversity of microorganisms, the so-called amoeba-resistant microorganisms (ARM).(72,172) Additional analyses have demonstrated FLA harboring intracellularly smaller cells and extra-biological material from the environment.(45) Altogether, these ecological features attributed to FLA the analogy to a "Trojan horse" regarding the microbial community.(45,80,173) Related to this, the intra-FLA bacterial community in natural sources was examined by metagenomics in 2013 in which results highlighted 21 bacteria genera living intra FLA. (160) Currently, FLA has been classified as a waterborne protozoan of emerging concern.(48) Although emergent, its ecological role as a vehicle to microorganisms and co-occupancy patterns in distinct habitats remain as major open questions to FLA scientific community.(167)

1.4 Brazil as a potential hotspot to FLA proliferation

The environmental distribution and diversity of FLA in the Brazilian context consist of a history that began 35 years ago. From 1985 to 2020 there have been published 58 papers concerned with FLA investigations. Here, they are classified on four major topics, as shown in Figure 1.8.

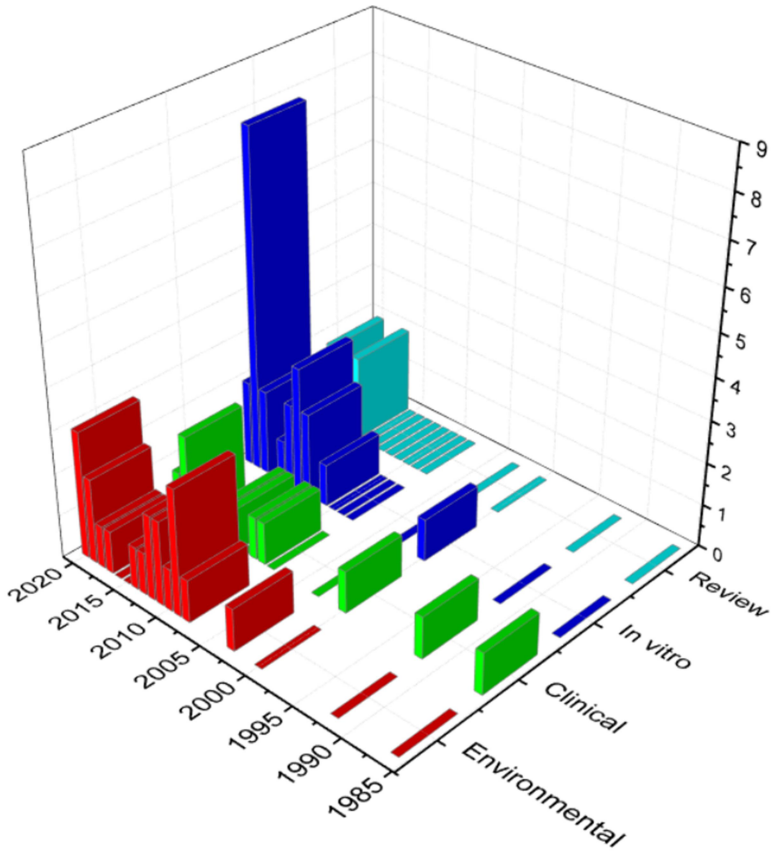

Figure 1.8 - FLA literature stressing the Brazilian context, from 1985 to 2020. The literature was distributed on four types of publications, classified as review, in vitro, clinical and environmental surveys.
Source: By the author.

As shown in figure 1.8, Brazilian FLA literature is an emerging theme. About 80% (46/58) of the literature was published over the past 10 years while the remaining 20% (12/58) was reported in a 25 years window. This lack of information observed until 2011 is reinforced by a review that ranked South American countries with a lack of information on *Naegleria* occurrence in contrast with the frequently reported data from European, North American and Asian researches.(81) However, the potential of the country to overcome this scene is endorsed by a 2017 review arguing that among all waterborne protozoa parasites, FLA outbreaks are currently in the fourth position in the Brazilian context. (174) Although the literature has expanded, a 2019 study reported that Brazil has likely misdiagnosed FLA environmental and clinical detections due to those studies whose culture-based method was the first line of choice, lacking complementary molecular approaches.(175)

On this concern, current Brazilian studies have used conserved regions of PCR amplified 18S rDNA to perform FLA identification. Regarding literature encountered between 2011 to

2020, mots of the FLA environmental and clinical investigations conducted a molecular based assay (127,141,143,150,176–182) in contrast with few studies based on amoeba immunodetection tools. (183-184) Classified as environmental isolated groups, the first one is dated from 1986 by pointing out *N. fowleri* presence in an artificial lake.(135) Further identifications broaden the knowledge on *Naegleria* genus by revealing five *Naegleria* species besides *N. fowleri* inhabiting river water samples. In addition, *Vermamoeba* isolates were shown coexisting with *Naegleria* species at the same River.(150) Brazilian river water evaluated through amplicon based metagenomics ranked positive to the presence of Amoebozoa, however without describing the class or genus that they belong.(180) Reports have amplified *Acanthamoeba* genes in tap water samples, (176-177,185) cooling towers (186) and swimming pools.(141,143-144) Not only freshwater but also estuarine systems were sampled in Brazilian habitats in which *Acanthamoeba* T3 and T4 genotypes were encountered.(179) Other matrices, as urban university buildings (187) and hospital units (181,188) also tested positive to *Acanthamoeba* and *Naegleria*. Other molecular based investigations of *Acanthamoeba* revealed its presence on domestic dust at the Espírito Santo state (178), in contact lens storage cases (189) and in hospital locations, (190) both in the Rio Grande do Sul state. A recent report describing hospital dust samples has identified a diversity of *Acanthamoeba* strains and a *Balamuthia mandrillaris* isolate.(182) A 2019 survey aiming at soil fungi predators has isolated *Vermamoeba vermifromis* and *Acanthamoeb*a spp strains discussing its food preference upon *Paracoccidioides* genus.(191) Similarly, another national survey on *Acanthamoeba* identification from drinking water, highlighted the importance of environmental isolation of FLA due to its role as a vehicle to pathogenic bacteria.(127) In this respect, the *Acanthamoeba* identification in air-conditioned cooling tower samples also revealed the potential of this FLA genus, as well as *Vermamoeba* and *Naegleria*, on harboring *Pseudomonas* spp..(186)

In Fig 1.8, 10 out of 58 publications are classified as clinical FLA reports. Among them, PAM (135), GAE (192) and amoebic keratitis (193-194) were reported in humans. The former includes five PAM cases from 1976 to 1983 (135). The second refers to two opportunistic GAE infections in an alcoholic (192) and an AIDS patient.(195) And the latter comprised a co-infection case in which the patient, contact lenses user, was diagnosed with both, *Acanthamoeba* genotype T4 and *Candida albicans*. (193)

Acanthamoeba keratitis has also been reported in Brazil. (178,196) *Acanthamoeba* presence in urine samples collected from critically ill patients has been indicated as a suitable niche for pathogenic bacteria proliferation and reinfection. The literature also suggested that bacteria can likely use the amoeba as a host to escape from drug treatments.(197) Apart from humans, two additional studies identified *N.fowleri* as the etiological agent of encephalitis in cattle grazing flooded pastures.(183-184) Both reports depict an important role that FLA can exert not only to human health but also to the ecosystem, as intermediate in this relation.

In figure 1.8, those reports grouped as in vitro comprise: gene silencing in *Acanthamoeba* (198); molecular detection of *Acanthamoeba* by showing randomly amplified polymorphic DNA (RAPD) as a suitable strategy to rapid genotyping new isolates; (196) metabolism studies in *Naegleria* (199-200) and *Acanthamoeba*, (201-202); interactions among FLA and intracellularly resistant microorganisms, (173,203–206); serach for antibodies as detection tool for *Acanthamoeba* infections, (207) and assays demonstrating amoeba capability of infecting mosquitoes, by using *Acanthamoeba polyphaga* and *Aedes aegypti* as studies of case. (208) In vitro assays by using natural substances as bacteriocin-like compounds (209) or synthetical substances as biguanides (e.g.: chlorhexidine) (210) in *Acanthamoeba* strains, whose dose-response assays confirmed amoebostatic and cysticidal effects related to these substances, respectvilly to bacteriocin and biguanides.

Regarding the association of virus with amoebas, two Tupanvirus strains, *Mimiviridae* family, have been identified to infect *Acanthamoeba* and *Vermamoeba* genera.(204,211) Belonging to these *Acanthamoeba polyphaga* mimivirus (APMV), a 2014 Brazilian report presented a novelty describing the so called Samba virus isolated from Amazon basin.(212) Complementary to this, in silico studies of genetic signature among *Acanthamoeba* and intra-*Acanthamoeba* living microorganisms demonstrated a strong correlation with the amoeba genus and its virus and bacteria content.(213) Other group of virus, the giant virus group, has been isolated from rive water and it has shown cytopathic effect in *Vermamoeba vermiformis*. As a defense strategy, amoeba releases signaling factors to the surrounding cells that initiate the encystment, aiming at resisting to further infections.(214) Genetic properties of giant virus used to infect FLA amoeba hosts have been investigated by Brazilian researchers enabling the discovery of a new genus, named Tupanvirus. (215) The newest amoeba resisting virus identified in 2020 comprises the discovery of a new lineage of virus hosted by *Acanthamoeba castellanii*.

Boratto *et al*. named them as Yaravirus in honor to the mother of the waters, the Brazilian mythological figure, Yara.(216)

Studies investigating the fungi infecting amoeba strains identified in vitro interactions in *Acanthamoeba* and *Cryptococus neoformans*. It is possible that amoeba can prior select fungus predation based on further benefit that this interaction can bring to the amoeba while hosting their vertebrate at a prospect of amoeba infections.(173)

Finally, composing the set of FLA reviews authored by Brazilian researchers, two comprehensive surveys addressed the main mechanisms developed by intra *Acanthamoeba* microrganisms to enhance its survival chances and consequently raising the hazard caused by FLA .(104,217) In addition two literature reviews presented the most common drugs used for FLA treatment and clinical features of FLA infections, caused by both *Naegleria* (39) (Appendix I) and *Acanthamoeba* infections.(218) Likewise, a 2019 review scrutinized the importance of extracellular vesicles to *A. castellanii* pathogenicity highlighting its cell singling roles, proteolytic activity relatedness and biomedical interest.(219) A 2020 review concerned with *Acanthamoeba* presence in hospitals indicated the extreme importance on assessing the ecological knowledge and distribution of *Acanthameoba* to comprehend its threat to humans. (220) Other recent reviews have discussed the interaction exerted by a giant virus and their *Acanthamoeba* host, manners of affect amoeba replication and trapping amoebic molecular mechanisms enabling it spread to new cells.(215,221)

Summarizing the Brazilian perspective on elucidating FLA epidemiology, about 28% (16/58) of publications have isolated amoeba in natural and man-made habitats, as aforementioned. This percentage exposes a binary issue: FLA investigation still lacks to be exploited in large extend [1], and the literature reinforces the relevance of the country as a fertile area to FLA spreading [2]. The second issue is confirmed by the increase in literature reports over the past decade with studies that point out the Brazilian potential on harboring FLA. Likewise, accounting hydrographic landscape of Brazil, there are important features that call attention to its potential to FLA dispersion. At a global extend, Brazilian hydrology has about twelve percent of the world total freshwater. Compared with South American countries, 53% of total surface water is located in Brazil.(222) According to the last Food and Agriculture Organization (FAO) report about world water resources by country, Brazil is ranked as the richest country in terms of volume of water. Moreover, following water reports written by

Brazil´s national water agency (ANA), the country is divided in twelve hydrographic regions that include rivers, lakes, wetland, amongst others [40], whose hydric heterogeneity covers all those water reservoirs commonly associated with FLA identifications (Table 1.1.). It reflects the potential of the country to harbor waterborne protozoan, as FLA and the consequent endangering affected populations, in a perspective of pathogenic FLA presence and human water exposure.

Altogether, these aspects enhance the role of the country for FLA epidemiological purpose, reinforce the need to establish comprehensive strategies to obtain faster and more effective environmental identification and highlight the relevance of the present PhD research.

Three complementary features related to free-living amoeba have been accounted to design our objectives: FLA as a waterborne protozoan, Brazilian hydric systems as a fertile country to FLA epidemiology and the urgent need to increase the ecological knowledge related to FLA.

1.5 Objectives

1.5.1 General objective

To propose an elucidative investigation of FLA diversity and distribution in Brazilian aqueous systems by initially targeting the local Monjolinho river located in the city of São Carlos, São Paulo state, as a model of study;

1.5.2 Specific objectives

Specific objectives are of three categories of interest: water quality evaluation to comprehend amoebic aqueous reservoir profile, morphological and molecular investigation of FLA diversity, as follows:

1. Aqueous reservoir profile:

1.1. To compare the diversity of FLA genera along longitudinal sections of the Monjolinho river, in sites with different human impact;

2. Morphological investigation of FLA

2.1. To evaluate the morphological diversity among environmental FLA isolates comparing trophozoite, cyst and flagellate typical features by performing a microscopic based analysis;

2.2. To test thermophilic capability of environmental isolates;

2.3. To investigate flagellation capability;

2.4. To establish axenic cultures of the trophozoites encountered in the Monjolinho River;

3. Molecular investigation of FLA

3.1. To elucidate FLA molecular identification through complementary PCR based analysis suitable to FLA detection, by using molecular targets established in the literature to perform PCR screening;

3.2. To determine species of FLA of Monjolinho river based on Sanger sequencing results and reveal its taxonomic identity;

The present PhD research is motivated by the hypothesis that the Monjolinho river is a water source containing FLA, it is in contact with the population and therefore can be a source of FLA contamination.

The aforementioned generic and specific objectives are in line with the ongoing BIOTA São Paulo Research Foundation (FAPESP) program, research grant #2018/20693-4, in which the student is a member of the scientific team. Both thesis supervisors, Prof. Otavio Henrique Thiemann and Prof. Jacob Lorenzo-Morales, have established a PhD cotutelle agreement that resulted in the present double PhD thesis. CAPES scholarships supported the PhD student on developing this research: a PhD scholarship (88882.328731/2019-01) and an internship scholarship (88887.368039/2019-00).

Chapter 2 Material and methods

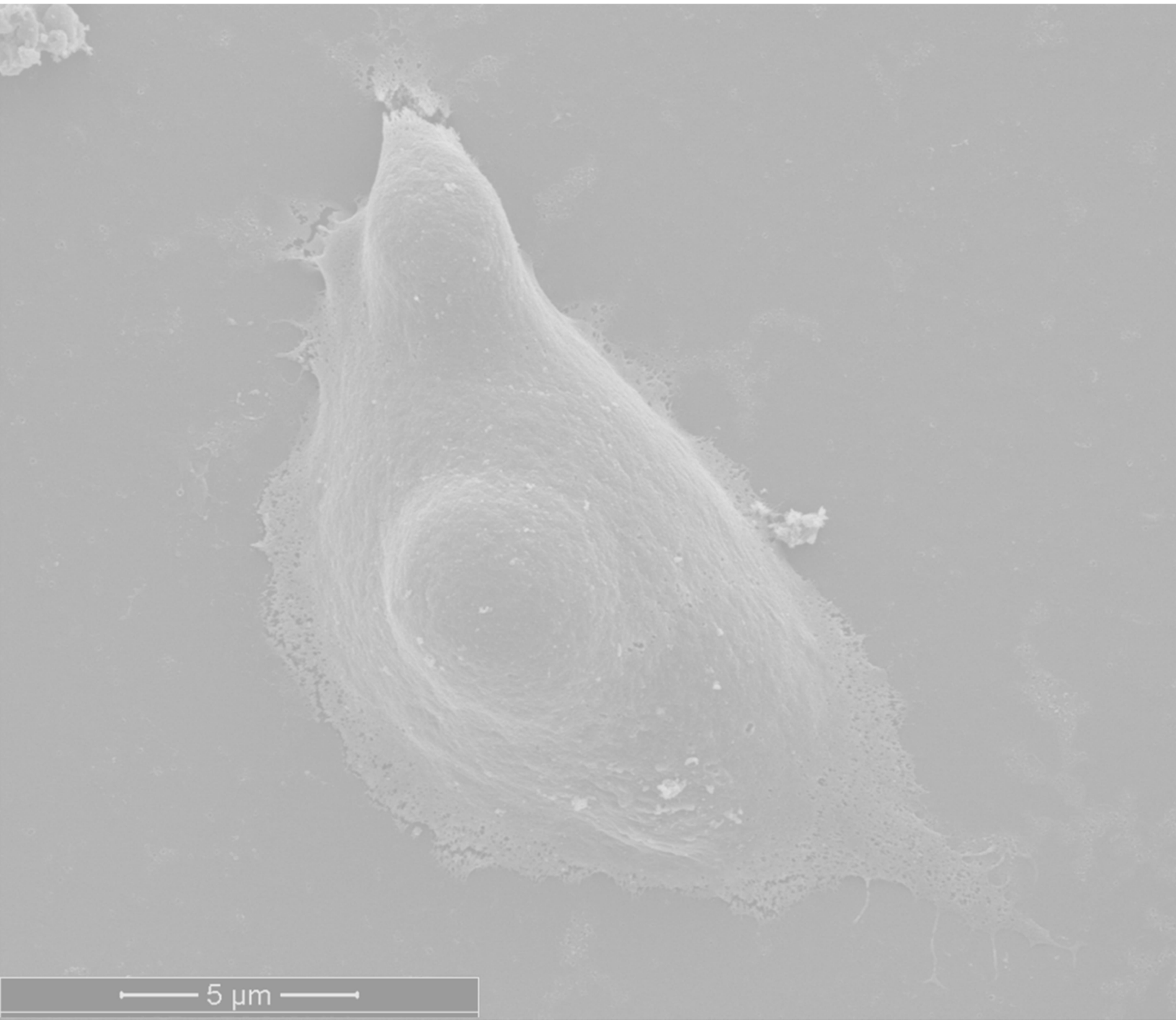

Scanning electron microscopy of *Naegleria gruberi* trophozoite emphasizing surface projections related with cell adhesion (lower right).

Source: By the author.

The methodology included in this thesis is summarized in Figure 2.1.

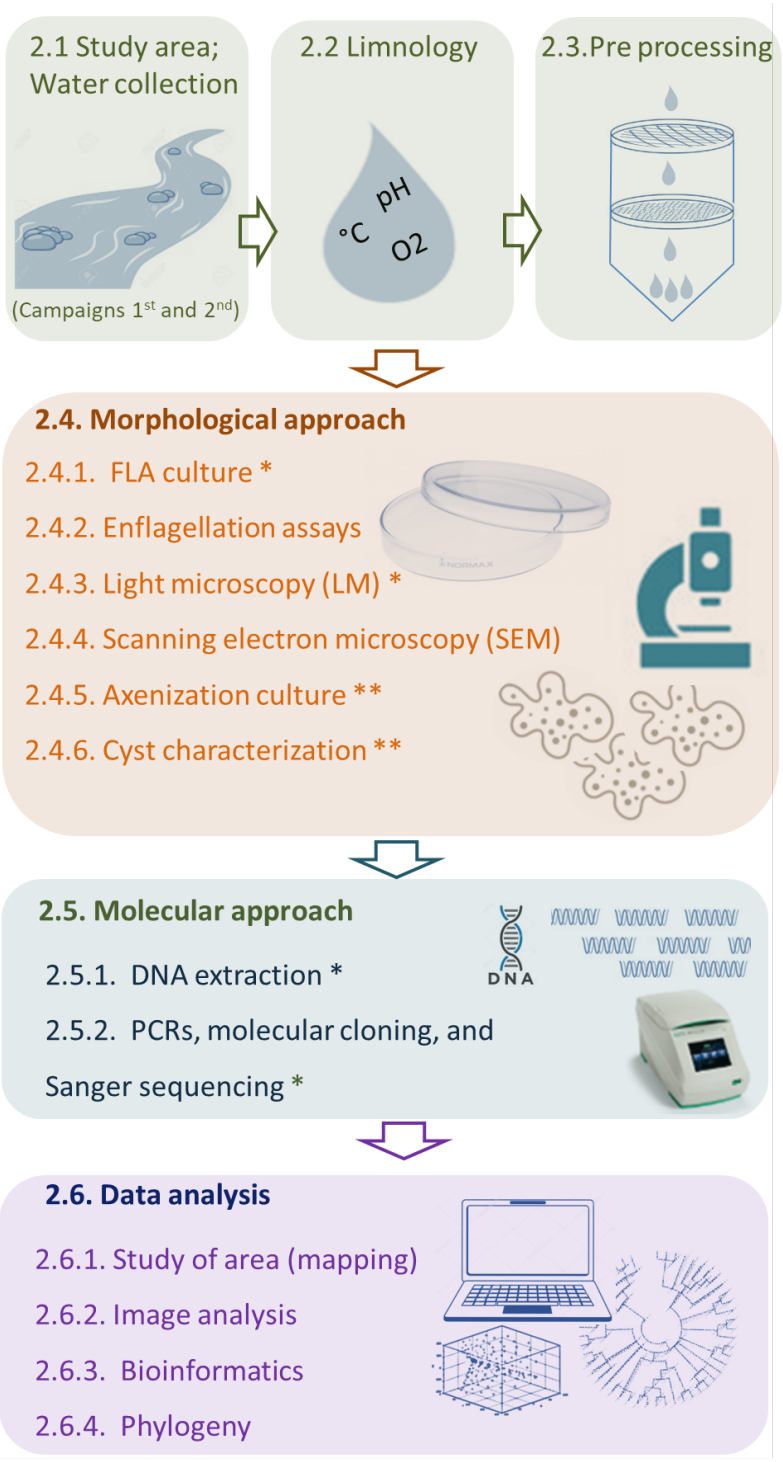

Figure 2.1 - This flow chart describes the methodological design performed to investigate FLA diversity in the Monjolinho River. Steps marked with * were performed in both universities, University of São Paulo (USP) and University of La Laguna (ULL). Steps marked with ** were performed only in the ULL and steps without marks only at USP.
Source: By the author.

Figure 2.1. summarizes experimental steps undertaken as strategies to investigate FLA diversity present in the river water samples, whose collection routine included two distinct campaigns at Monjolinho River, a pilot-scale and a full-scale design named first (1st) and second (2nd) samplings, accomplished in August 2017, and April 2018 respectively. The main differences among the two campaigns include improvements on molecular and morphological technical choices tackled by the second 2nd sampling. The student accomplished the whole methodology described in Figure 2.1 at the Structural Biology Laboratory (USP), accompanied by a six months training at the Laboratory of Free Living Amoeba, at the University of La Laguna (ULL), Spain. During the development of Brazilian assays, at USP, the PhD student has co-supervisioned, along with Prof. Otavio assistance, two undergraduate students: Ana Letícia Maria da Fonseca and Matheus Issa. Their projects shared part of the experimental steps depicted in Figure 1. Ana Letícia da Fonseca worked with items 2.1-2.5 at the pilot campaign (1st) and Matheus da Silva was committed with steps 2.5.1 and 2.5.2, second sampling (2nd). Regarding the ULL internship, it was motivated to perform axenization (2.4.5), light microscopy and cyst characterization (2.4.3. and 2.4.6.) whose assays were assisted by the head of the laboratory and co-advisor, Prof. Dr. Jacob Lorenzo-Morales, and Dr. Maria Reyes-Battle. Both, contributing to the progress of the internship.

Moreover, two other collaborations assisted in specific steps along this work: Prof. Dr. Odete Rocha and Prof. Dr. Douglas Cedrim. The former, ecologist research at the Federal University of São Carlos (UFSCar), assisted with the definition of the sampling sites, water collection and water limnologic characterization (Fig 2.1- 2.1 to 2.2). The latter, a computer scientist at the Federal Institute of Goiás (IF-Goiás), contributed with the development of an automated morphological characterization of cyst shape (Fig1.2 - 2.4.6). Finally, 2.4.4. has been conducted as a third-party service by the Materials Engineering Department, São Carlos School of Engineering (MED). Methodological details regarding each step shown at Figure 2.1. are described as follows.

2.1 Study of area and water sampling

The sampling site study was performed taking into account aquatic reservoirs commonly reported to harbor FLA (Table 1.1). Considering Brazilian surface water diversity along twelve hydrographic regions, as mentioned here (CHAPTER 1), this research focused in the Monjolinho River basin that belongs to one of the most relevant hydrographic regions, named the Paraná region. This hydrographic area covers seven Brazilian states in which the São Paulo state, the target of the present research, hosts the Monjolinho river basin. Since FLA can be present in particular aqueous systems in low concentration, rendering its detection challenging, we selected a diversity of five locations with different levels of human intervention throughout the river in the hope to comprehend FLA diversity, compliant with specific objective 1.1.

Five sampling areas of interest, A to E, were examined in both 1st and 2nd collections, at the river sub surface, of 30 cm, for all samples. In the 1st campaign, a volume of 1L of water was collected with sterile glass flasks and used to both, the direct FLA molecular detection (2.5.) and the cultivation method enrichment (2.4.1.). To the second campaign, besides a 1 L water sample site, used to culture purposes, an additional 10 L water sample was collected into sterile plastic bottles for metagenomics purpose, related to water microbiome monitoring. These latter experiments are under ongoing evaluation within the BIOTA FAPESP objectives (data not reported here).

Figure 2.2 - Overall workflow of water collection.
Source: By the author.

Figure 2.2 illustrates a representative image of water collection (2.1), as well as highlighted details of limnology and preprocessing topics (2.2 and 2.3), both described ahead.

2.2 Limnology

Limnologic characterization to monitor the chemical and physical water properties influencing the microbial community was performed in situ, as seen at Figure 2.2 (step 2.2.). By using a portable water quality checker, Horiba U-10, the dissolved oxygen (mg/L), hydrogenionic potential (pH), electric conductivity (µS/cm), water temperature (°C), and geographical location through Universal Transverse Mercator (UTM) coordinates were obtained. The dissolved oxygen

and electrical conductivity are often assessed as indicators of anthropogenic pressures in the environment, usually inform about organic matter availability that exerts a direct effect on the local species diversity. (223) Complementary, the temperature and pH values have been assessed to monitor temperature range in which FLA can be found and water acidity levels in which they are able to withstand, according to the literature description.(149,169,223) Afterward, all values were contrasted against Brazilian environmental legislation that provide the national standards about water quality status (e.g., CONAMA resolution 357/05). (224)

2.3 Water pre-processing

Immediately after the limnologic examination, the water samples were stored in proper flasks and water preprocessing steps (e.g. sieving, filtering and centrifugation steps) were performed within a maximum of 6 hours. Once at the laboratory, a representative sampling site from the first campaign was elected for the addition of cultured amoeba establishing a positive sample to determine the downstream methodology efficacy on identifying FLA (Figure 2.2, item 2.3). In its regard, D sampling site, due to its physicochemical profile, was selected to validate the experimental pipeline (Fig. 2.1.). To induce the positive control, *Naegleria gruberi* American Type Culture Collection (ATCC) 30224 was previously axenically cultured on ATCC 1034 medium according to the literature recommendations (225) and 1.10^5 trophozoites were harvested, centrifuged, and the precipitate was homogeneized with 100 µL of river water, next added directly into 1L of river water and mixed by vortexing at maximum speed for 30 sec.

To both 1st and 2nd sample sets, water sieving was performed through a granulometric ultra-sieve (BERTEL - ABNT/ASTM 400) to remove suspended material, as illustrated at Fig. 2.2 (step 2.3.1). Then, flowthrough fractions were conducted to both filtration and centrifugation whether aiming at a morphological or molecular characterization, respectively. 500mL of water was filtered through a sterile 0.45 µm cellulose nitrate membrane (Nalgene® Analytical Test Filter Funnel, 47mm) coupled to a vacuum filtration system, inside a biosafety cabinet, for amoeba enrichment purpose (Fig 2.2, 2.3.2.). Membranes were seed on nutrient agar plates (NNA) as detailed at 2.4.1. section. Simultaneously, water centrifugation was conducted at 3000 g for 15 min at room temperature (RT, 25 º C) in a Thermo Scientific™ Sorvall™ RC 3BP+ centrifuge, to access FLA community directly from river water (Fig 2.2 - 2.3.3.). After the first

centrifugation step, 5 ml of phosphate-buffered saline (PBS) was used to resuspend the pellet followed by a second centrifugation step in 15 ml tubes at 2500 g for 10 min, room temperature (RT), in an Eppendorf Centrifuge 5810 R, followed resuspending the pellet with 200-500 µL Tris-EDTA (TE) [Tris-HCl 10mM; EDTA 1mM; pH 8.0]. Thus, the material was stored at -20º C until the opportune nucleic acid extraction procedure, detailed at 2.5.1.

2.4 Morphological examination

Morphological characterization of environmental FLA isolates included culture-based evaluation coupled with microscopic analysis guided by classification keys for amoeba taxonomy.

2.4.1 In vitro culture

Proceeding with the water filtering step (Fig 2.2., item 2.3.3), cellulose membranes were transferred to 2% (w/v) non-nutrient agar (NNA) plates prepared with Page's amoeba Saline (PAS) solution by following literature recommendations. (226-227) The following image illustrates membrane handling and seeding onto NNA plates:

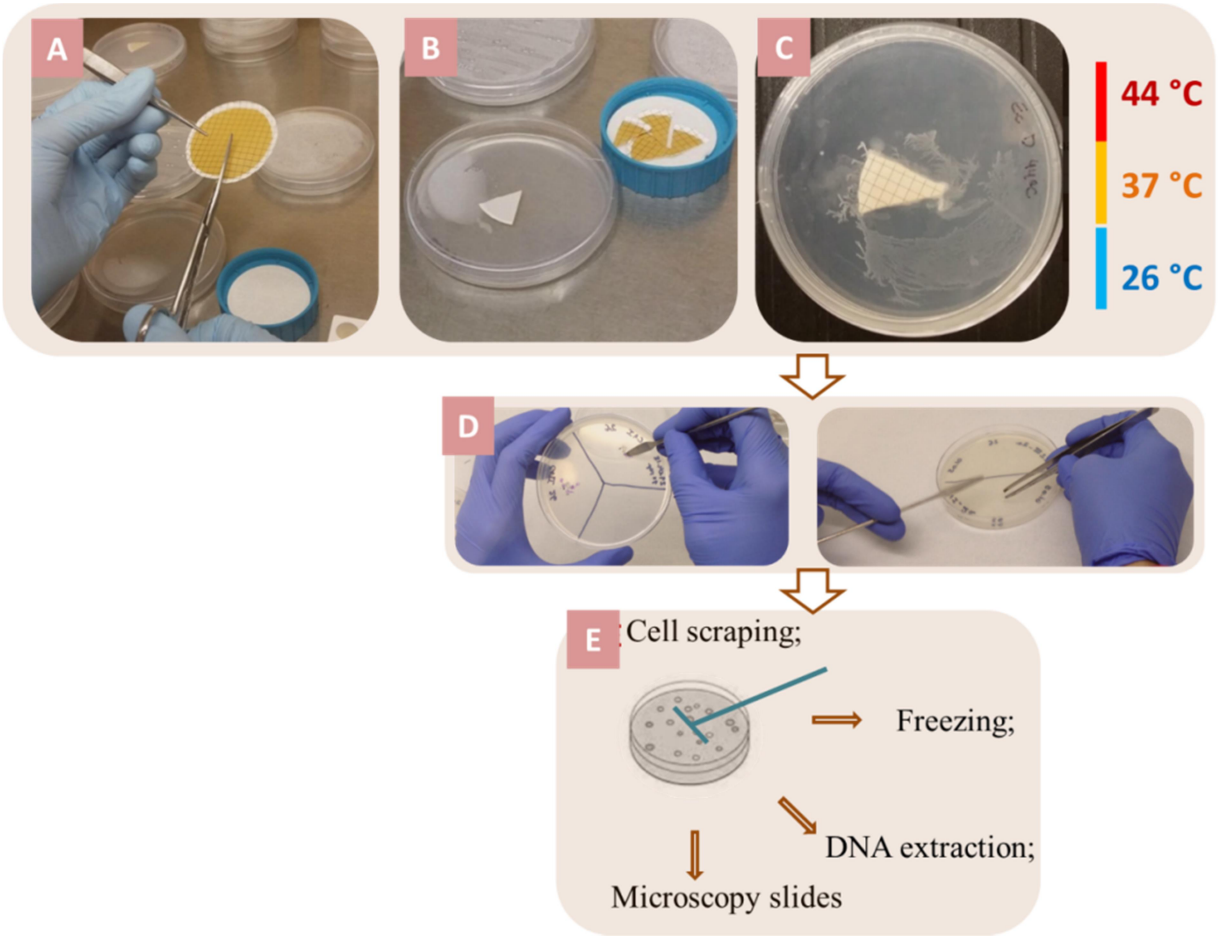

Figure 2.3 – Process to obtain non nutrient agar (NNA) plate cultures.
Source: By the author.

Cellulose membranes, partitioned into smaller fractions (Fig. 2.3, B), were seeded onto *Escherichia coli*-coated NNA plates (Fig. 2.3, C), owing to the fact that most FLA genera are bacterivorous. (19) NNA plates overcoated with 100 µl layer of inactivated *E. coli*, by exposing the bacteria culture in a 60 ºC water bath for 30 minutes, following the literature recommendation. (228). Addittionally, cellulose membranes (Fig. 2.3, B) were transferred onto pure NNA plates, without the bacteria layer, as a comparative essay. NNA plates were prepared in triplicate, and maintained in a temperature range of 26°C, 37°C and 44°C (Fig. 2.3, C), as recommended in the literature. (33,116,229) Amoeba growth was monitored for 14 days by using a Nikon-Eclipse TS100/F inverted microscope. Areas with trophozoites were carefully transferred, face down, onto new NNA plates as shown in Figure 2.3., D. This cloning step process was repeated every day aiming to remove of bacterial and fungi contaminants. By

following the literature recommendations, the cloning step was used as well to enrich the amoeba density.(113,117,230-231)

The next step (Fig 2.3, E) comprised amoeba harvesting to the morphological downstream characterization and the complementary DNA based confirmation. The agar surface was washed with 5 ml of PAS solution, plates were sealed with parafilm and gently mixed at 60 rpm for 10 min in an orbital shaker (Orbit™ 300 Multipurpose Vortexer). The suspended trophozoites floating at PAS solution were poured into a canonical 15 ml tube and centrifuged at 1000g, 10 min, RT (centrifugation step "c1"). Next, 1 ml PAS solution was added to homogenizing the precipitate followed by the second centrifugation, 10 min at 1500 g (centrifugation step "c2"). Finally, precipitates were used to cell cryopreservation, cell microscopic examination, and cell DNA extraction (Fig. 2.3, E). Each method has been detailed at following topics.

Adjustments in the pipeline shown in Figure 2.3 were performed to the second sampling in the Monjolinho River, including extension of the incubation period to 60 days with longer cloning step process, and new NNA formulations by adding antibiotics and antifungals to avoid heterogeneity of microorganism persisting in the amoeba cultures. Antibiotic mix (100 U/ml penicillin; 100 µg/ml streptomycin) and antifungal (100 µg/ml amphotericin B) were mixed with NNA after its temperature reached about 50 °C. The downstream morphological characterization of FLA included scanning electron microscopy (SEM), flagellation test and efforts to reach axenic cultures.

The most promising NNA plate samples, in both 1st and 2nd samplings, were harvested and frozen aiming to perform a deeper morphological investigation in the Laboratory of Free Living Amoeba, at the University of La Laguna (ULL), Spain. In ULL, each sample was seeded onto fresh 2% NNA plates and maintained at room temperature assuming prior temperature screening at USP (Fig. 2.3, C). NNA plates were daily examined with Leica DMi1 Inverted microscope. The remaining morphological and molecular examination carried during the internship (Fig. 2.1, * and **) are detailed along the present section.

2.4.2 Enflagellation test

Flagellation test was carried out by harvesting trophozoites from target NNA plates, as described at topic 2.4.1., washing cycles were adjusted and performed with 1x phosphate

buffered saline (PBS) [7.5 mM Na^2HPO^4, 3.3 mM NaH^2PO^4, 108 mM NaCl, ph 7.4] instead of PAS solution. The precipitate was homogenized with 1 ml of 20 mM NaCl solution and placed onto 24 wells plate to 4 hours incubation at 22º C, 100 rpm, as recommended in previous research focused on *Naegleria gruberi*. (225) Flasks were monitored each 30 min seeking and once positive to flagellate transforming, the suspension of cells was transferred to 1.5 ml microcentrifuge tubes and centrifuged 1500 rpm, 10 min. After precipitate homogenizing with 200 µl of 20 mM NaCl solution, a drop of flagellates was placed onto glass slides, stained with methylene blue stain (further detailed), covered with the coverslip and observed into the microscope. To obtain the flagellate taxonomic description, the features examined comprise: flagella number, nucleus and contractile vacuole position.

2.4.3 Light Microscopy (LM) examination

The morphological analysis of FLA was documented with distinct microscope settings according ro the availability of equipment in each institution, as summarized at Table 2.1.

Table 2.1 - Instrumentation used to perform the light microscopy evaluation.

1- Assay	2- Institution	3- Microscope	4- Camera
A - NNA plate	USP	Nikon-Eclipse TS100/F	Nikon Coolpix 990
	ULL	Leica DMi1 Inverted microscope	Samsung camera version 9.0.02.38
B - Staining slides	USP	in Nikon´s Eclipse E600	Nikon DS-Ri1
C - Wet mounts	ULL	Leica DM1000 LED	Leica ICC50W Camera

Source: By the author.

Regarding NNA plate visualization (Table 2.1, Line A), plates were directly examined at 40x, 100x, 200x and 400x magnification through microscopes described in column 3. The image acquirement was carried out with camera specifications as detailed in column 4, and the resultant images were evaluated to determining the greatest trophozoites dimension.

Staining slides (Table 2.1 - B) were employed to reveal morphological details, method composed of methylene blue, eosin and hematoxylin stains, with adaptations on literature reports. (232–237) To eosin and methylene blue, a 50 µl drop each dye was directly added to 25 µl suspension of trophozoites previously dropped into a glass slide, immediately covered with the

coverslip. To hematoxylin staining, samples were fixed with a 100 µl drop of 100% (v/v) absolute methanol added to a drop of amoeba culture, placed onto a glass slide, for 5 min fixing time. Three washing steps with 100 µL distilled water were performed, 3 min each washing. Then, a 50 µl hematoxylin drop was added and allowed to cover the attached cells for 5 min. Cells were rinsed with distilled water drops for 3 min each washing (3x). Glass slide was immersed into crescent solutions of 70%, 95% and 100% (v/v) absolute ethanol for 5, 5 and 1 min, respectively. Then, a drop of 20% (v/v) glycerol solution was added; the glass slide was mounted with a coverslip, sealed with Nail Polish and microscopically examined.

To wet-mounts preparation (Table 2.1, Line C), 2 ml PAS solution was added into NNA plates aiming trophozoites detaching. Plates were sealed with Parafilm® and maintained at 4 °C for 10 min. Next, an additional 2 ml PAS solution was added to trophozoites harvesting by means of a sterile Pasteur pipet. The suspending volume was collected, poured into 1.5 mL tubes and centrifuged at 1500 rpm, 10 min. 1 ml PAS solution was used to washing the precipitate, followed by a centrifugation step at 1500 rpm, 10 min. The washing step was repeated once and, after the last centrifugation, 900 µl supernatant was discarded and the precipitate was homogenized with the remaining 100 µl PAS solution. The suspension of cells (50 µl) was dropped into a slide and covered with a coverslip. Fresh mounts and staining slides were examined at 200x, 400x and 1000x magnifications. To enhance FLA morphological evaluation, not only its intracellular characterization was evaluated, by light microscopy, but also cell surface information was assessed by scanning electron microscopy.

2.4.4 Scanning electron microscopy (SEM)

Scanning electron microscopy (SEM) has been used in FLA studies to examine differentiation processes, (43) cell-to-cell interactions, (238) and to outline cell surface details. (239-240) Herein, SEM was prepared by using smaller fragments of glass slides, pre cleaned with 100% absolute methanol, and coated with a thin layer of poly-lysine (0.1% w/v poly-L-lysine Sigma). Trophozoites were harvested (as detailed in section 2.4.1), and the cell precipitated obtained in the last centrifugation step was homogenized with 200 µl of 2.5% (v/v) glutaraldehyde dissolved in PAS solution and, immediately, dropped into glass fragments for a 2 hours fixing, at room temperature (RT). Next, 2 ml of 30, 50, 70 and 100% absolute ethanol

solutions were poured onto 24 wells plate to serial dehydration. Glass fragments were sequentially immersed for 30 min per solution and finally in hexamethyldisilazane (HMDS Sigma) to reach the critical point drying (CDP). Each fragment was coated with an ultra-thin layer of platinum, attached to carbon stubs using conductive pants and placed in a JSM-5310 scanning electron microscope (JEOL, Tokyo, Japan). Coating and imaging were carried out as a third-party service at Materials Engineering Department, USP (São Carlos, SP). SEM photomicrographs were combined with light microscopy (LM) imaging and compared against Page´s Classification Key taxonomy, (23) as recommended by recognized surveys on searching FLA. (113,117,230-231) Additionally, Iva Dikova´s "Illustrated Guide to culture collection of Free Living amoeba" was included to evaluate amoebic cell morphology.

2.4.5 Axenic cultivation

Axenic culturing included NNA plates seeded with target samples sorted at both 1st and 2nd Monjolinho River samplings. Prior to selecting promising FLA samples to undertake its axenic growth, routinely cloning steps were conducted, as reported in the literature as an essential step before axenic culture achievement.(240) Moreover, antibiotic/antifungal NNA plates were used as a strategy of enhancing amoeba purity (as described at 2.4.1 section). Plates were daily examined in Leica DMi1 Inverted Microscope, and inside a biosafety cabinet, those agar pieces with trophozoites and even cysts were transferred into 24-well microplates, prepared with 1 ml of American Type Culture Collection (ATCC) Modified PYNFH Medium [ATCC medium 1034] and Peptone Yeast-extract Glucose (PYG) liquid mediums per well. ATCC 1034 is recommended to *Naegleria, Hartmannella* and *Vahlkampfia* (33,241-242) axenic cultivation and PYG appropriated to *Acanthamoeba* culture. (141,178,243) For PYG medium, 40 µg/ml of gentamicin was added as literature recommendations (141,178,243) and for ATCC 1034, 100 U/ml of penicillin and 100 mg/ml of streptomycin, according to literature reports. (33,241-242)

Plates were maintained at room temperature and monitored day-to-day in an inverted microscope, either EVOS® FL or Leica DMi1. Fresh medium, along with antibiotic restoration, was added to washing trophozoites in wells whose bacteria and fungi contamination persisted. Thus, promising cultures to amoeba proliferating were harvested by means of sterile Pasteur pipet and placed into 12.5 cm^2 cell culture flasks prepared with 5 ml PYG or ATCC1034 liquid medium as recommended in the literature. (113,227,230,244) Positive samples to axenic growth

in cell culture flasks were harvested, poured into 15 ml canonical tubes, centrifuged 1500 rpm for 10 min and the precipitate was homogeneized in a freezing solution composed of 9:1 of fetal bovine serum: dimethyl sulfoxide (DMSO). Cells were replaced to cryotubes, slowly frozen with a freezing container (Thermo Scientific™ Mr. Frosty™), and placed in an ultra-freezer (-80 C) for 24 hours. Finally, cryotubes were stored in a container with liquid nitrogen.

2.4.6 Cyst characterization

The development of cyst software in a hope of detecting FLA cysts in heterogeneous environmental samples was undertaken through collaboration with Prof. Douglas Cedrim to the computational analysis of the cyst images, software construction and implementation. The micrograph dataset creation was obtained by wet mounts prepared with amoeba cysts. The list of encystment assays and strains included here is summarized at the following Table 2.2.

Table 2.2 - List of FLA strains included to cyst software development.

	FLA	Method
1-	*V. vermiformis*	NNA plate (SD44°C_2nd)
2-	*N. australiensis*	NNA plate (SE44°C_2nd)
3-	*A. castellanii Neff*	literature based encystment

Source: By the author.

In Table 2.2, cysts of *V. vermiformis* [1] and *N. australiensis* [2] were obtained directly from NNA plates and observed with wet-mount slides, as described in section 2.4.3. To *Acanthamoeba* (Table 2.2, Line 3) encystment, the assay was performed as recommended in the literature.(245)

Image acquirement was conducted with Leica DM1000 LED Microscope coupled with Leica ICC50W Camera. The manual light features were examined, aiming to enhance the contrast between specimen and gray background. Light intensity, exposition, and saturation ranging comprised the first parameters setting evaluated. Computational details regarding imaging evaluation and software creation are described along ahead oi this chapter (section 2.6.2).

2.5 Molecular approach

2.5.1 DNA extraction

The DNA extraction of FLA culture was carried out by selecting NNA plates with profuse amoeba growth to cell harvesting. The precipitates resultant from the last centrifugation step (detailed in topic 2.4.1.) were solubilized by adding 50 µl of ultrapure water (MiliQ) and directly used to DNA extraction. At the University of São Paulo (USP), DNA extraction was performed with DNeasy PowerSoil® Kit (QIAGEN). Alternatively, NNA plates cultured in the University of La Laguna (ULL) were extracted by using Maxwell® 16 Tissue DNA purification kit (Promega), into a Maxwell® 16 System, as described in the literature.(227)

Addittionally, the DNA extraction directly from river water was conducted using samples provided by water centrifugation, precipitate washing and homogenization in 200-500 µl TE buffer, according to details at topic 2.3. The environmental DNA (eDNA) was extracted by using DNeasy PowerSoil® Kit (QIAGEN) and the final elution step included 100 µL ultra-pure water. The D sampling site was sampled in triplicate in the purpose of confirming the efficacy of Power Soil Kit to extract environmental DNA. Thus, after water centrifugation, the precipitate had the DNA extracted by using: DNeasy PowerSoil® Kit (PS), Mini Spin DNA Extraction Kit KASVI (K), according to manufacture recommendations, and the additional phenol-chloroform extraction, following literature recommendations.(246) Further comparison among these methods included DNA concentration and purity examination through an UV absorbance-method (Nanodrop 2000 Spectrophotometer, Thermo Scientific), and an amplification reaction searching *Acanthamoeba* 18S rDNA by using DNA templates provided from each method. Then, samples were stored at – 20 º C until its usage in polymerase chain reactions (PCRs).

2.5.2 PCRs, molecular cloning and Sanger sequencing

Polymerase chain reactions (PCRs) carried out at the present study embraced two main purposes: amplification of FLA genes to further genotyping environmental samples (I), and PCR reactions for molecular cloning confirmation (II). First (I), the DNA extracted from either NNA culture samples or directly from the river water microbiota, was used as input of PCRs by searching FLA genes amplification. The current literature uses 18S ribosomal RNA (18S rRNA) as a highly conserved region suitable to amplifying FLA group (153), as well as to identify

genus-specific, as shown to *Acanthamoeba* (121,247) and *Vermamoeba* identifications. (60,125) Regarding the genus *Naegleria*, PCRs commonly included primers flanking the ITS rRNA region, as shown in a 2018 review authored by the PhD student shedding light on the preference for ITS1/5.8S/ITS2 rRNA regions rather than 18S rRNA to *Naegleria* molecular characterization. (39) It consisted of a set of clinical and environmental molecular investigations targeting *Naegleria* (Appendix I, Fig. 1). The entire list with primer pairs selected to perform the molecular characterization of samples isolated in Monjolinho River is summarized in Table 2.3:

Table 2.3 - List of primer pairs used on FLA molecular searches addressed on this thesis. The PCR cycling details include: including annealing T ºC; extension time; and the nº of cycles.

Target	Gene/regio	Primer pairs	5'-3' sequence	PCR cycling details	Reference
FLA		AmeF977 / AmeR1534	GATYAGATACCGTCGTAGTC / TCTAAGRGCATCACAGACCTG	55ºC;1min;34x	(24)
Acanthamoeba (spp e ss)	18S rDNA	CRN5 / 373r	CTGGTTGATCCTGCCAGTAG / TCAGGCTCCCTCTCCGGAATC	51ºC;1min;34x	(121,248,249)
		JDP1 / JDP2	GGCCCAGATCGTTTACCGTGAA / TCTCACAAGCTGCTAGGGAGTCA	56ºC;1min;35x	(121,250)
Naegleria spp. (spp)	ITS	VeergsF / VeergsR	GAACCTGCGTAGGGATCATTT / TTTCTTTTCCTCCCCTTATTA	50ºC;1min;34x	(229,251)
Hartmannella (ss)	18S rDNA	HARTF / HARTR	GGAGGGCAAGTCTGGTGCC / GCCCGGAGAGTCATCCATG	54ºC;1min;34x	(125)

Source: By the author.

The primers listed in table 2.3 cover global FLA amplifications using the AmeF977/AmeR1534 target, asides a diversity of genus-specific primers to amplifying expected FLA genera, normally indicated by morphologically based evidence. Particulally, the JDP1/JDP2 primer pairs are recommended in the literature (250) due to amplifying a region termed diagnostic fragment 3 (DF3), elucidative to distinguish between *Acanthamoeba* genotypes. All primer pairs, commercially obtained from Sigma-Aldrich, were solubilized in TE buffer and use solutions were prepared at 10 µM primer concentration. The corresponding annealing

temperature was adjusted according to their melting temperatures (Tm), and the elongation time in accordance with the expected size of amplicon (Table 2.3, Column PCR cycling details).

The remaining PCR cycling condition and the concentration of reagents into PCR reaction mixtures followed the polymerase enzyme requirements. Experiments at USP were conducted with Taq Pol High Fidelity Master Mix 2X Red (Cellco), and at ULL with AmpONE™ α-Taq DNA polymerase (ThermoFisher Scientific). Overall, it has been used about 200 ng DNA template, 200 nmoles FW and RV primers, 1x Taq reaction buffer (2.5 mM $MgCl_2$), 200 µM deoxynucleoside triphosphate (dNTP) mix and 1U enzyme/10uL reaction volume. Reactions were carried out using a T100 Thermal Cycler (BIO-RAD) and an Arktik thermal cycler (Thermo Scientific), respectively at USP and ULL. The control samples were composed of the DNA from both commercial strains *Naegleria gruberi* (ATCC 30224) and *Acanthamoeba castellanii* Neff (ATCC 30010) to positive controls, and the DNA-free water to the negative control.

DNA products were examined in 2% agarose gels, 80 V, 400 mA for about 1.5 hours running in 1x TE buffer. At USP it involved SYBR Safe-stained agarose gels and, and at ULL, GelRed-stained gels. At ULL the downstream pipeline encompassed PCR product excision and purification from agarose gel by using Agarose Gel Extraction Kit (Jena Bioscience) for cases in which double bands appeared in the same agarose lane indicating a diversity of species/genus. For those cases with a single band, products were directly prepared to sequencing. Both DNA samples, purified from agarose, or directly taken from PCR products, were examined by Sanger sequencing as a third-party service performed by Macrogen Spain Company. At USP, the downstream pipeline included excision and agarose band purifying with either Agarose Gel Extraction Kit (Cellco Biotec) for double band visualization or PCR Purification Kit (Cellco Biotec) for DNA purification directly from PCR solution.

Regarding to molecular cloning assays (II), it included PCR amplicon ligation, transformation, and positive colonies screening by PCR confirmation. The ligation was performed into pJET 1.2/blunt cloning vector using the T4 DNA ligase, provided by CloneJET PCR Cloning Kit (Thermo-Scientific), following manufacture recommendations. Next, the ligation product was transformed into *E. coli* cells, chemically competent prepared according to literature recommendation.(252) Colonies resultant from the transformation were randomly collected from the Luria-Bertane (LB) agar plates and seeded onto 5 ml LB, liquid medium, until reached a mid-log growth. Cells were centrifuged for 14000 rpm, 1 min, and the last cycle was

repeated until precipitating the total 5 ml inoculum. Precipitate DNA was isolated with Fast-n-Easy Plasmid Mini-Prep Kit (Cellco Biotec) and used as a template onto investigative PCRs in which the DNA was flanked by the vector´s primer. PCR products were analyzed in 1.5% agarose gel, target bands were purified and sequenced in a 3130 Genetic Analyzer (Thermo Scientific), Sanger method, as a third-party service at Molecular Biophysics Groups (IFSC-USP-Brazil).

2.6 Data Analysis

The analysis of the data resultant from the methodology described in topics 2.1 to 2.5 encopmassed a diversity of computational tools summarized in Figure 2.4.

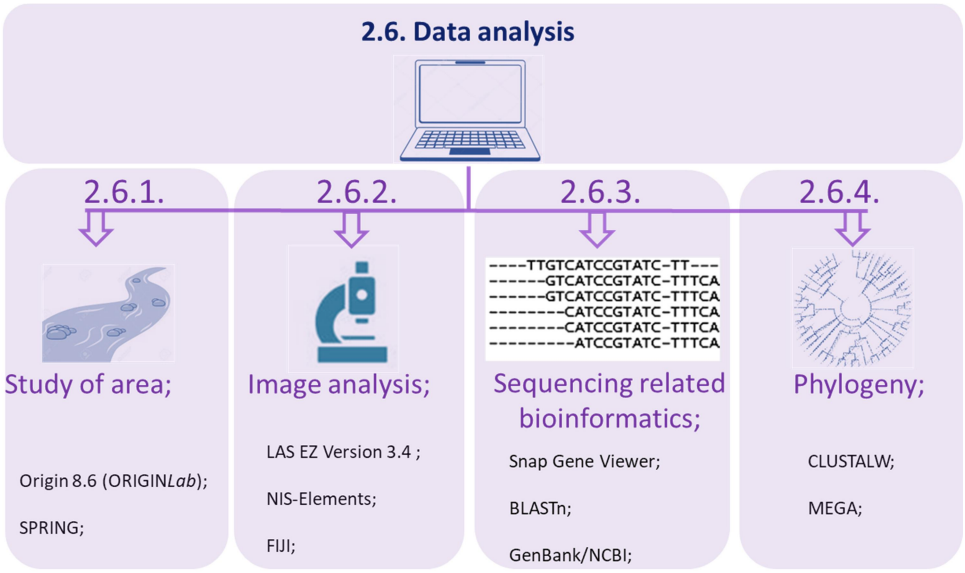

Figure 2.4 - Overview on data analysis software and computational tools used along this thesis.
Source: By the author.

2.6.1 Study of area - mapping sampling sites

To each sampling site targeted on this thesis, the corresponding UTM coordinates were integrated with the Monjolinho River basin digital cartography through a Georeferenced Information Processing System (SPRING 5.5.5). SRING is a Geographic Information System (GIS), created by the National Institute for Space Research (INPE). The original river basin map, available in the Center of Scientific and Cultural Diffusion (CDCC/USP) collection, was

processed with SPRING software to image vectorization, georeferencing and insertion of sampling site coordinates as graphical objects associated to the hydrography. Processing details were performed as documented in the SPRING official guideline. (253)

2.6.2 Image analysis

Ligh and scanning micrographs provided from the morphological characterization process were examined for processing, visualizing, scaling, and exporting images. The NIS-Elements and the LAS EZ Version 3.4 imaging software were applied to staining slides visualization, and fresh mounts preparation, respectively. Scanning electron microscopy images were recorded with SMile View™ Map. Additionally, FIJI image software (254) had been used as a complementary approach to digital processing, scaling images normalizing and time-lapse studying (Fig. 2.4, STEP 2.6.2).

2.6.3 Sanger sequencing related bioinformatics

Regarding Sanger sequencing data analysis, resultant chromatograms were carefully examined with a sequencing analyzing tool, SnapGene Viewer version 4.1, to recognize forward (FW) and reverse (RV) primers and to sequence quality checking, as illustrated in Figure 2.5.

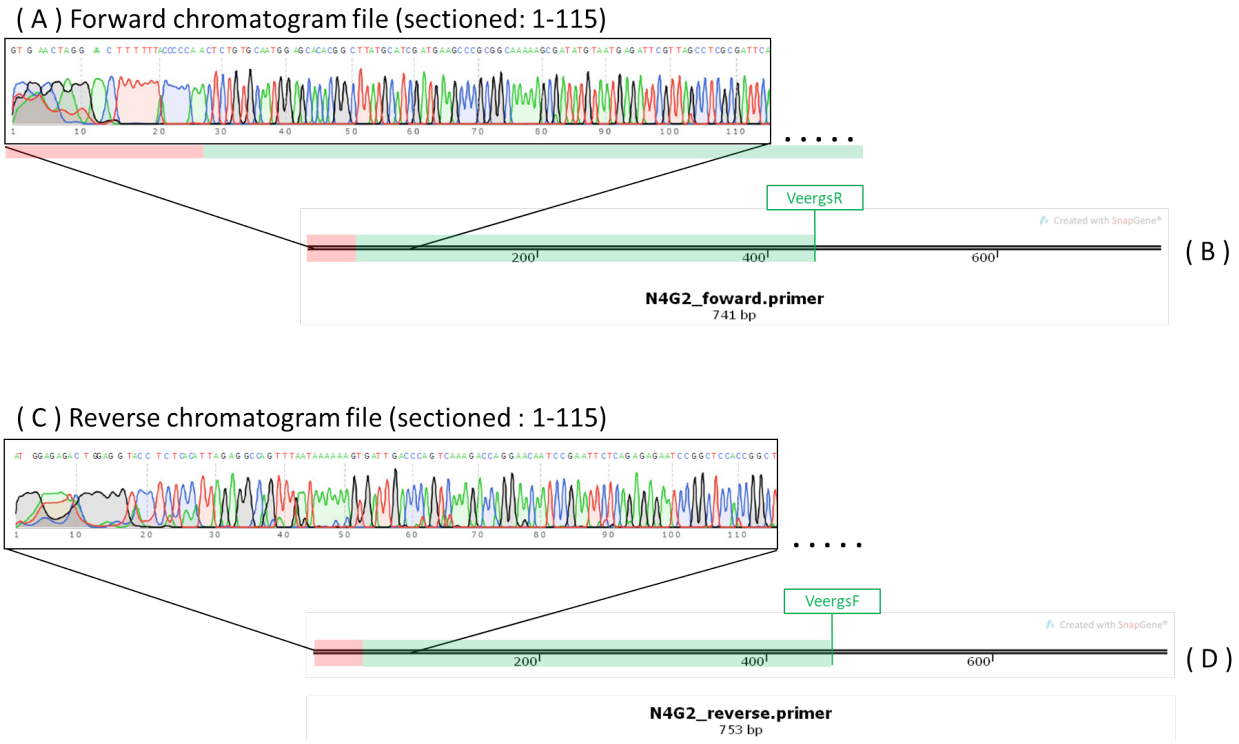

Figure 2.5 – Analysis of chromatogram and Sanger sequences in SnapGene Viewer. Forward (A) and reverse (C) chromatogram files. Corresponding forward (B) and reverse (D) snap gene-based representations. Low and high-quality regions are shown in red and green boxes, respectively.
Source: By the author.

As represented by target sequences termed N4G2, in Fig.2.5, low-quality regions were identified (Fig. 2.5, red boxes) to be removed from both strains. As well, nucleotides upstream to primer markers (Fig. 2.5, green flags) were removed. Next, curated N4G2 forward and curated N4G2 reverse strands were merged to create a consensus sequence, as shown in Figure 2.6.

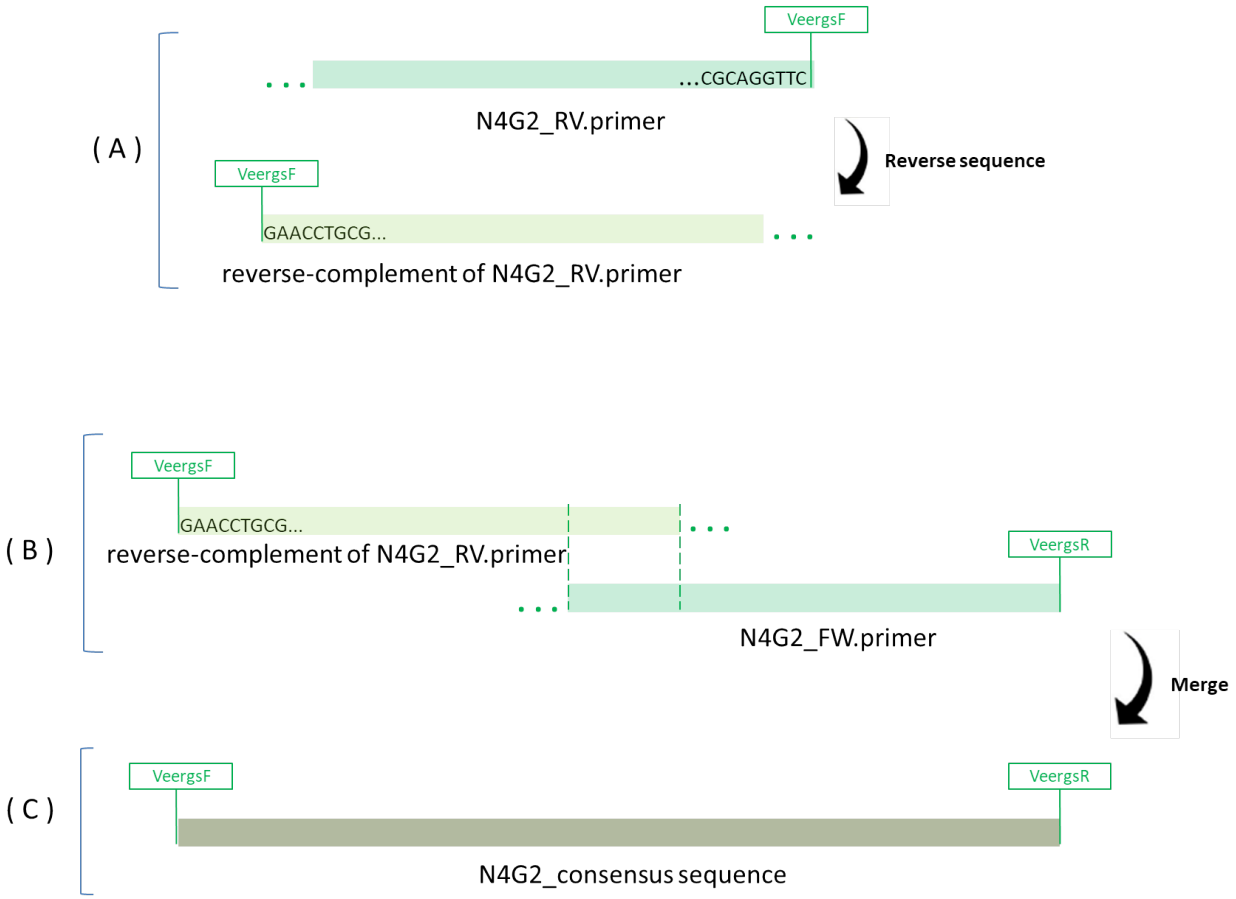

Figure 2.6 - Bioinformatic pipeline with Sanger sequencing data – creating consensus sequence (2). A – generating reverse-complement of N4G2_reverse.primer sequence. B – Building consensus sequence.
Source: By the author.

The consensus sequence was created by identifying the overlapping region between both sequences shown in B step (Fig. 2.6). Consensus sequences were used as query within BLASTn (Basic Local Alignment Search Tool nucleotide) platform, seeking against either all eukaryotic nucleotide sequences available in National Center for Biotechnology Information (NCBI) database, or against amoeba filtered searches. Additionally, the SnapGene software was used to predict amplicon sizes and to guide the interpretation of PCR results.

2.6.4 Phylogeny

The target Sanger sequencing results, along with reference homologs, whose FASTA data was downloaded from GenBank, were carefully examined to define phylogenetic relationships. Alignments were obtained by using the ClustalW software (255) in which 20/0.1 and 15/6.66

were selected to gap opening/extension for the pairwise and multiple alignments, respectively. Next, alignment outputs served as the seed in the Molecular Evolutionary Genetics Analysis (MEGA version 7.0) program to access taxonomic assignments. Most reliable phylogenetic trees were drawn in accordance with the literature recommendations emphasizing data analysis treatment by using MEGA.(256)

Chapter 3 Results and discussions

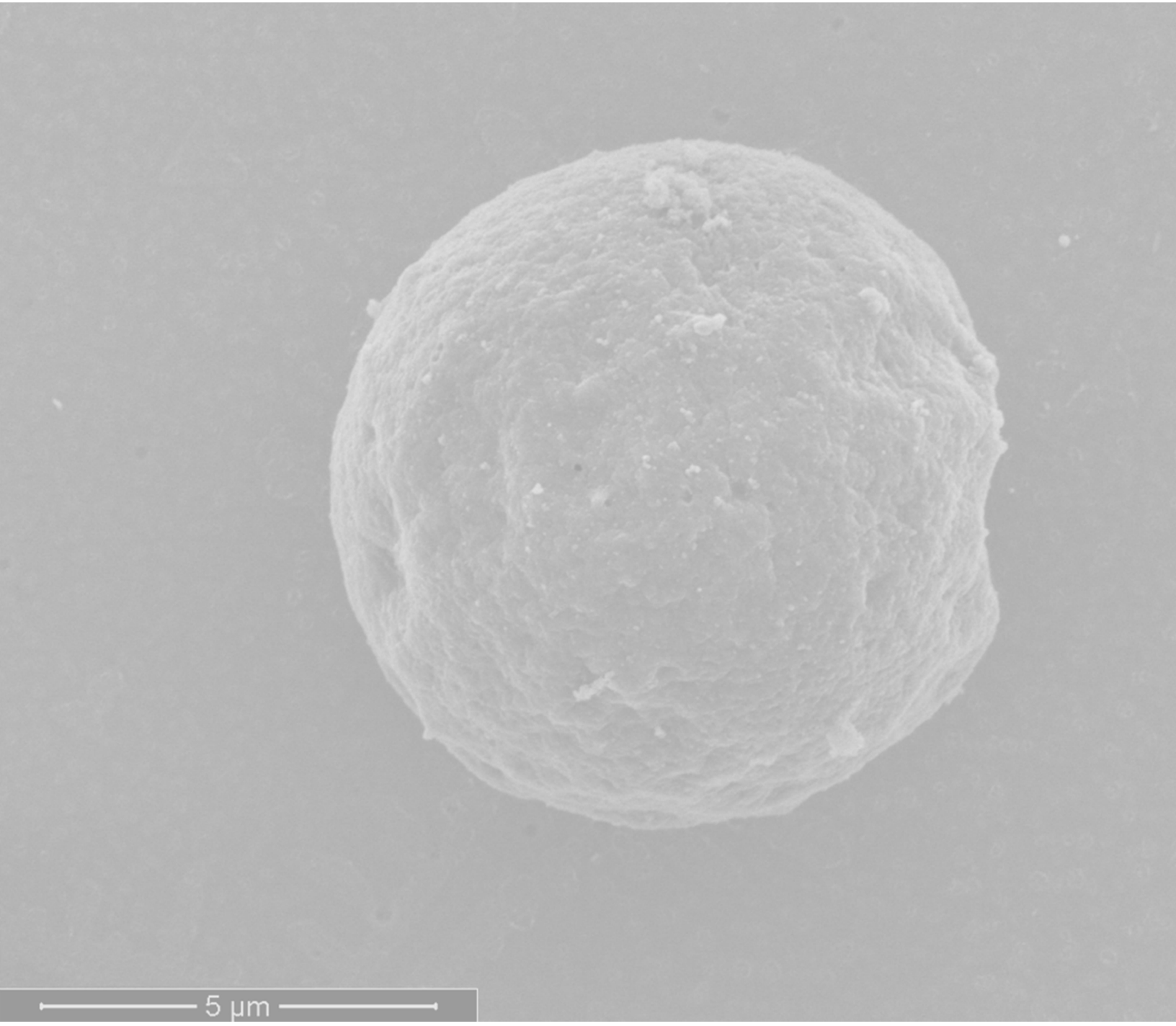

Scanning electron microscopy of *Naegleria gruberi* cyst with a suggestive pore (left side).

Source: By the author.

3.1 Area of study and physicochemical properties of water

3.1.1 Area of study and physicochemical properties of water – RESULTS

Monjolinho River study of the area was composed of five collection sites, graphically represented as follows:

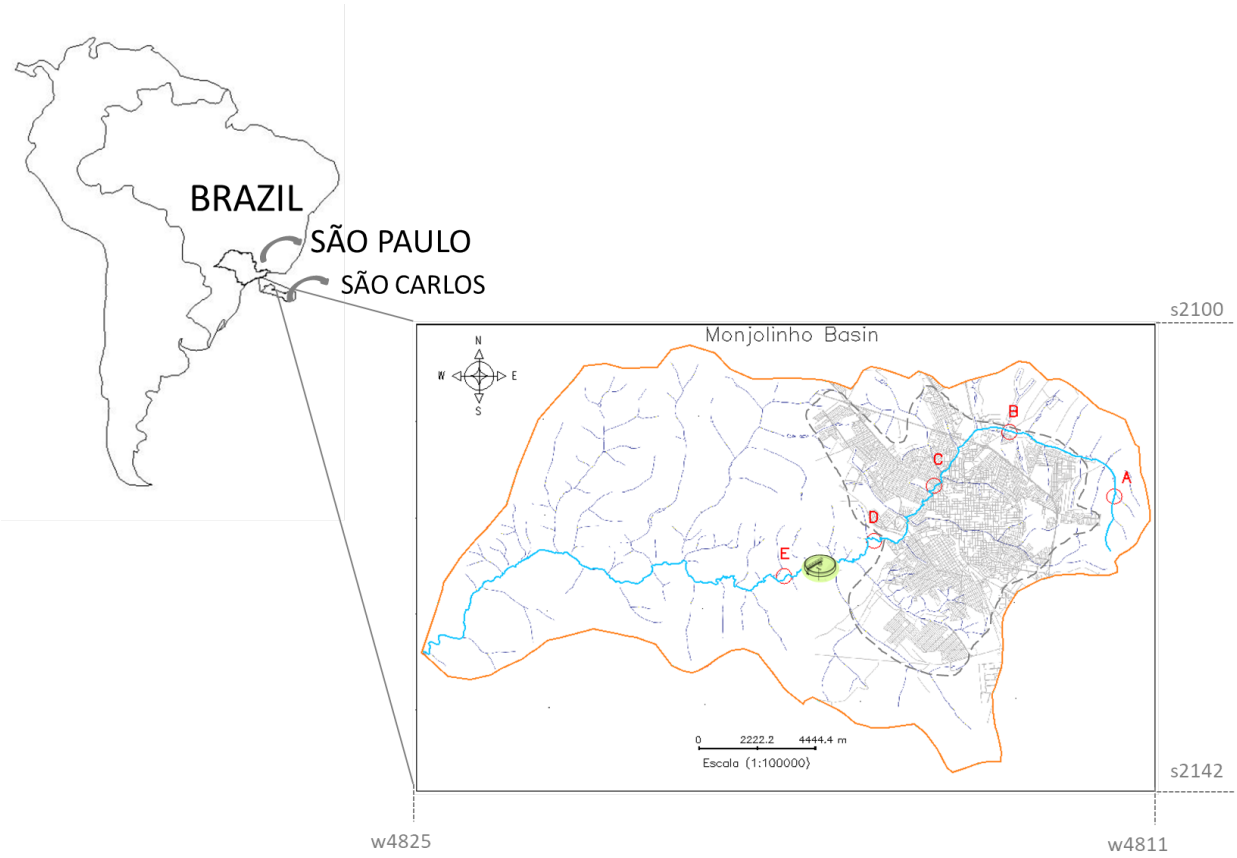

Figure 3.1 - Georeferenced cadastral map of Monjolinho River basin. Red circles (sampling sites A to E), light blue line (main course of the river), orange line (basin limit), grey dashed portion (urban area of São Carlos city). Sampling sites A to E also denote the order of sampling. WWTP - wastewater treatment plant.
Source: By the author.

Figure 3.1 illustrates the Monjolinho River sampling sites targeted at the present research in a cadastral map created with SPRING software (section 2.6.1.). At the rectangle corners of the Monjolinho basin are displayed the coordinates corresponding to the universal transverse Mercator system. The recorded geographical positions of each sampling site were: A (22° 0′ 2.87″ S, 47° 50′ 8.96″ W), B (21° 58′ 40.6884″ S, 47° 52′ 25.50″ W), C (21° 59′ 45.40″ S, 47°

54′ 6.32″ W), D (22° 0′ 52.41″ S, 47° 55′ 26.65″ W) and E (22° 1′ 34.92″ S, 47° 57′ 26.29″ W). Shown in red circles, letters A to E also denote the order of sampling accompanying the light blue route from which the river flows. Additionally, Monjolinho hydrographic limit (orange line) was highlighted to clarify the extension of the basin in comparison with the dashed urban area of São Carlos city. This representation (Fig 3.1.) illustrates to what extend Monjolinho hydrography is linked with the total area targeted by A to E sampling sites. Photographs taken while performing the water sampling process demonstrated the typical landscape encountered in each location (Figure 3.2).

Figure 3.2 - The environmental landscape of the sampling sites A to E throughout Monjolinho river samplings.
Source: By the author.

In Figure 3.2, headwaters and rural vegetation are typical of the first sampling ambient (Fig.3.2, A1). Once placed in a non-urban area, it was remarkable along the route, areas of agricultural livestock practices benefiting from the river as a source of water. B sampling site is located at a peri-urban area and, at upstream of sampling collection (Fig 3.2, B), the river course flows en route to Ecological Park of São Carlos, a zoo in which the river water and animals are in direct contact. Next, the C sampling site is located within an urbanized area as shown in both Fig. 3.2, C1 and C2, and Fig 3.1, sampling site C. It is surrounded by five neighborhoods, and is enclosed to the University of São Paulo, São Carlos campus. The D sampling site is placed at a peri-urban area and it is a stream impacted by domestic sewage (Fig. 3.2, D1). It is located upstream of a wastewater treatment plant (WWTP), and the subsequent E sampling site is placed downstream of WWTP (Fig 3.1), a rural area with forest fragment in its surroundings (Fig. 3.2, E.1). These sampling sites were analyzed, in situ, towards the assessment of physicochemical parameters of water with the aid of Horiba device (Fig. 3.2, A2, B2, C3, and D2). Values recorded to both 1st and 2nd samplings are summarized in Table 3.1.

Table 3.1 - Physicochemical properties of water obtained in the Monjolinho River by using a multiparameter analyzer, Horiba U10. Red numbers highlight the highest and lowest OD and conductivity values, respectively. Columns present four variables, examined into the first (1st) and the second (2nd) surveys. SS refer to the sampling sites.

SS	Dissolved oxygen (mg L-1)		Conductivity (µS/ cm-1)		Water temperature (°C)		pH	
	1st	2nd	1st	2nd	1st	2nd	1st	2nd
A	9.11	10.27	8	32	17.8	20.35	6	5.87
B	9.07	10.06	25	42	18	20.96	5.67	5.76
C	8.2	9.48	69	100	19.3	21.65	5.83	4.84
D	5.21	7.6	446	544	21.8	23.97	7.08	6.98
E	5.13	6.98	221	243	20.9	23.03	6.85	6.95

Source: By the author.

Overall, the results obtained from the first sampling did not exhibit remarkable fluctuation in comparison with the second sampling (Table 3.1, columns 1st and 2nd), with exception of water temperature. Values highlighted in red indicated limnologic properties that exerted an important role as discriminators of sampling points. Conductivity and dissolved oxygen features enabled to differentiate all sampling points in which more significant variations were observed to the last

sampling sites (D and E). Whereas the remaining variables, water temperature, and pH, presented values that kept reasonably constant. The entire discussion in regard of abiotic characterization of water is presented below.

3.1.2 Area of study and physicochemical properties of water – DISCUSSION

Results presented above, regarding the Monjolinho basin area of study, illustrated five sampling sites composed of forested and urban areas. The latter gathers effluents under anthropogenic activity impacts, as shown in Figure 3.2. Once the Monjolinho River watershed dimension embraces São Carlos city and thirteen neighboring districts,(257) the examination of FLA presence undertaken at the present research in a local scope can exert impacts to a major extent. From a perspective of water flow along meanders of the river, the general influence of A to E sampling sites is represented by branched lines originated from the light blue watercourse (Fig 3.1). The information provided in both Figures 3.1 and 3.2 clarifies the diversity of sampling sites in regard to its location (rural, peri-urban and urban), vegetation structure, and human involvement with distinct habitats. The intense anthropogenic activity that comes from these urbanized regions exerts high impacts on the water system, mainly due to domestic and industrial sewage. (257-258)

The results obtained from the lymnological evaluation of the five sampling sites reinforced the human impact in freshwater, according values displayed in Table 3.1. The electrical conductivity parameter reflects the total ion concentration,(125) and D sampling site exhibited the highest conductivity values, immediatlly followed by the E sampling site. This observation is coherent with the relative position of these sites within the river basin and is consistent with being highly impacted by domestic sewage discharge received from the upstream urbanized area (Fig 3.1). Water quality studies demonstrated that wastewater effluents provoke an increasing concentration of organic compounds dissolved in the water and lead to a consecutive high ionic load that raises electrical conductivity values. (259) Not only sewage but also agriculture runoff has been stressed by ecological studies as a contributor to organic and chemical inflow to freshwater systems, indicated as an important agent of eutrophication processes. (260) In comparison with D sampling site, the lowest conductivity values recorded to

E sampling site are likely due to the presence of the WWTP located between both areas (Table 3.1. and Fig. 3.1.).

Accompanying the increase in the conductivity, there is a concomitant decrease in dissolved oxygen values throughout the five sampling sites. As shown in Table 3.1, the lowest OD values were recorded in D and E sampling sites what is likely due to the higher levels of organic matter in decomposition linked with intense oxygen consumption by the microbiota present and a consecutive decrease in oxygen availability, as reported by Verani and collaborators in 2015. (257) Likewise, studies demonstrated that sewage discharge, and agriculture practices, mainly due to the use of fertilizers have been responsible for the OD decreasing and the growth of microorganisms in the water.(261) Thus, based on the aforementioned reports, the lowest OD values recorded to both D and E samples suggest high nutrient content in the water system, therefore indicative of anthropogenic effects. Although in the present study the chemical analyses of organic and inorganic compounds (e.g.: total organic carbon, phosphate, and nitrate) was not performed, these analytes are very elusive to determining water quality. (261) Afterwards, the literature has been statistically interpreting this chemical analysis along with the canonical physicochemical parameters by using principal component analysis (PCA) and partial redundancy analysis (pRDA). (169,262-263)

Limnological parameters of freshwater systems have been compared against Brazilian regulations concerned with establishing standards to classify water bodies according to its quality, ecological status, availability as drinking water supply, risks to human health, and human impacts acting in the aqueous ecosystem. In this regard, the Resolution No. 357/2005 is one of the most commonly assessed documents, provided by the National Environmental Council (CONAMA). (224,260,262,264-265) This resolution classifies water bodies in four levels of environmental quality, in which the level 1 defines the water as highly pure and suitable for several purposes including human water supply, after a mild disinfection process. In the opposite extreme, water bodies with the level 4 represent poor quality of water, harmful to microbiota and also unsuited to human use, even after severe disinfection procedures. (224) Sites D and E are classified as water level 3 in the first sampling. From the second sampling, both sites are classified as level 2, indicating a scenery less prone to microorganism proliferation. Whereas sites A to C were classified as level 1 in both 1st and 2nd samplings.

Regarding the water pH variation, both samplings ranged from neutral (7.08) to acid (4.84) pHs values (Table 3.1.). The increase of pH between C and D sampling sites is likely due to the intake of organic matter along the river in the direction of the D site, taking into account that higher organic matter content in decomposition leads to higher hydrogen consumption in water and a consequent pH increment. The lowest pH values recorded from A to C can pose a target to microorganism proliferation due to harmful compounds that can be dissolved in a chemically acidified environment. For this reason, Brazilian national regulations recommend pHs in a range of 6 to 9.5 as suitable values to water quality. (266) Finally, water temperatures revealed a fluctuation of about 3 °C from A to E sites in both sampling times. Collection routines were scheduled in the morning conducted in three hours from site A to E (8:50 AM – 11:02 AM) in the first sampling and four hours in the second sampling (8:20 AM – 01:10 PM). Thus, the temperature variation is likely due to the ambient effect, expressing the warming of the day during the sampling.

Summing up, Figure 3.1, 3.2 and table 3.1 indicated the environmental heterogeneity from each sampling site and reinforced the relevance of the study in urbanized, as well as rural areas. After qualifying sampling sites in regard to its geographical and physicochemical classifiers, water river samples were evaluated regarding its microbiological content aiming to comprehend FLA diversity throughout the Monjolinho River, and to predict potential FLA hotspots, as detailed in the following 3.2 and 3.3 sections. Once the Monjolinho basin has been pointed out as a public freshwater supply very important to the community inhabiting its surroundings,(257) examining FLA as a waterborne parasite on this freshwater system was critical in this research assuming the hydrological scope of the studied area.

3.2 Morphological examination

3.2.1 Morphological examination - RESULTS

The investigation of FLA presence in the river water samples included NNA agar plate cultures and the morphological characterization of trophozoite, flagellate, and cyst stages. The arsenal of microscopy techniques embraced here is summarized in Figure 3.3.

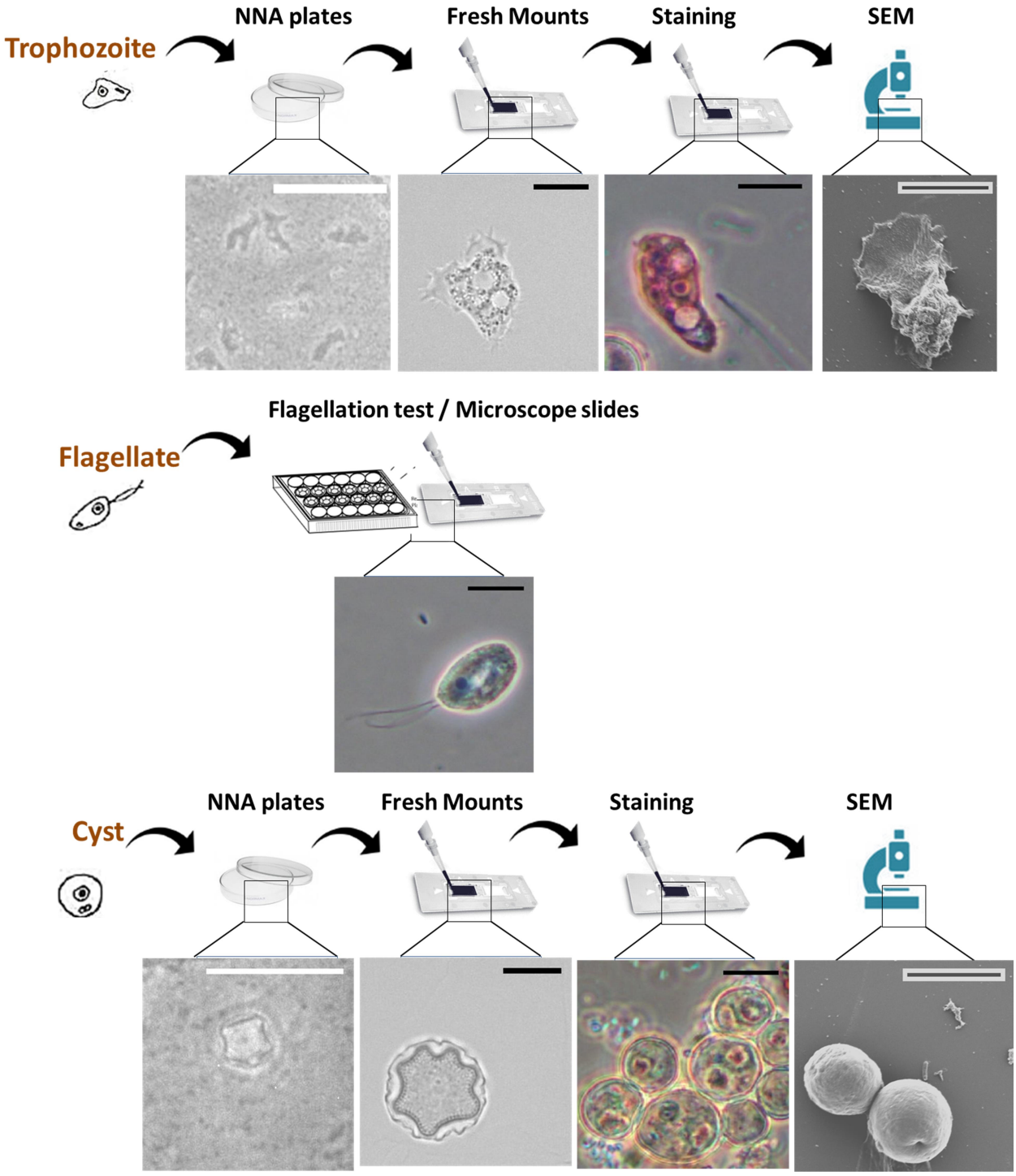

Figure 3.3 – Morphological based characterization of FLA isolated in Monjolinho river – a perspective of typical obtained result per method. White scale bar = 50 µm. Black scale bar = 10 µm. NNA – non-nutrient agar plates, SEM – scanning electron microscopy whose scale bar refers to 10 µm.
Source: By the author.

Inoculated NNA plates incubated at different temperatures were monitored daily by microscopic examination (Figure 3.3_NNA) resulted in the identification of amoeba in all five

sampling sites along the Monjolinho river, at both first and second sampling times. Together with the growth temperature, the results of NNA cultures are summarized in Table 3.2..

Table 3.2 –Amoeba growth in non-nutrient agar plates (NNA). Presence (+) or absence (-) of amoeba on agar surface; Colors blue, green, and red refer to growth temperatures 26 °C, 37 °C and 44 °C, respectively.

	Samples	26 °C		37 °C		44 °C	
		Trophozoite	Cyst	Trophozoite	Cyst	Trophozoite	Cyst
1ST sampling	SA_1st _*pure*	+	+	+	+		
	SA_1st _ *ecoli*	+	+	+	+		
	SB_1st _ *pure*	+					
	SB_1st _ *ecoli*	+					
	SC_1st _ *pure*	+		+	+		
	SC_1st _ *ecoli*	+		+	+		
	SD_1st _ *pure*	+	+	+	+	+	
	SD_1st _ *ecoli*	+	+	+	+	+	
	SD_1st _*ecoli* _Ng	+	+	+			
	SE_1st _ *pure*	+	+	+	+		
	SE_1st _ *ecoli*	+	+	+	+		
2ND sampling	SA_2nd			+	+		
	SB_2nd	+	+	+	+		
	SC_2nd	+	+	+	+		
	SD_2nd	+	+	+		+	+
	SE_2nd	+		+	+	+	+

Source: By the author.

The main information obtained from the data in table 3.2 is the gradual decreased of amoeba presence in response to the increment of temperature. Overall, amoeba growth was detected from four to seven days of incubation and cysts appeared within about 14 days after initiating the culture. In regard to the thermophilic feature here studied by including 44 °C as incubation temperature, among all positive samples to amoeba growth into NNA plates, solely trophozoites recovered at D sampling site presented the capability of withstanding to 44 °C at both 1st and 2nd

samplings. In addition to this, isolates from site E were also revealed to be thermophilic in the second sampling (Table 3.2).

Moreover, no remarkable difference in terms of the presence of amoeba was detected between NNA plates coated with *E.coli* (*ecoli*) and its corresponding plate without *E. co*li layer (*pure*), as shown in table 3.2, 1st sampling. To deeper evaluate this observation, trophozoites provided from C sampling site culture (37 °C) were used as a test to analytical microscopic comparisons between *pure* and *ecoli* conditions, by measuring its cell dimension and moving rate, as described ahead.

First, NNA plate images recorded by using an inverted microscope suggested the same portrait of non-distinguishable amoeba shape upon comparing both *pure* and *ecoli* NNA plate conditions (Figure 3.4).

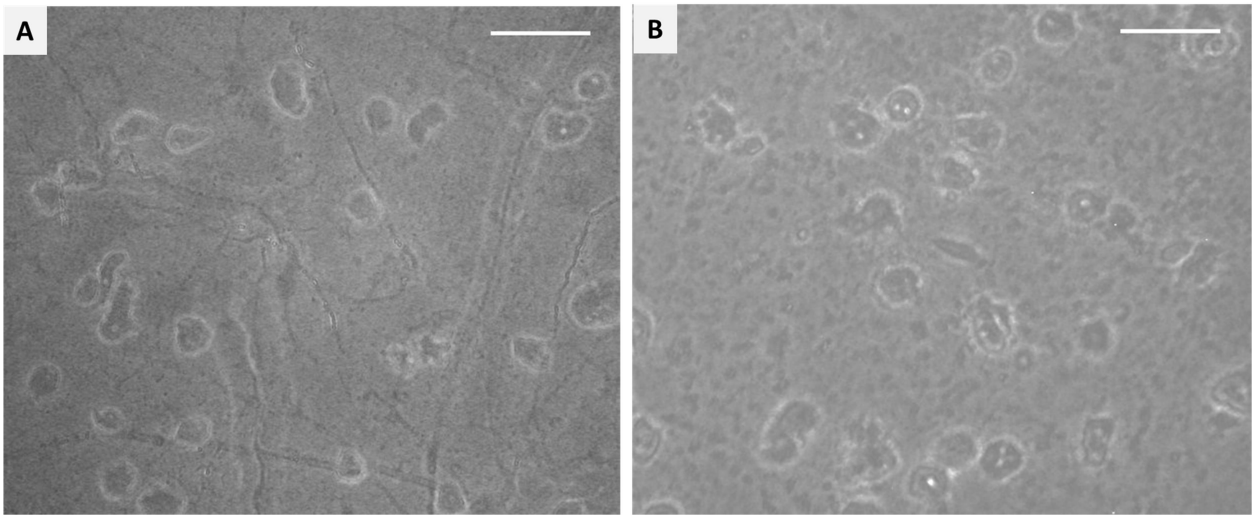

Figure 3.4 - FLA culture obtained to SC, after water filtering process and subsequent membrane seeding onto *pure* (A) and *ecoli* (B) NNA plates, maintained at 37 °C. SC: isolates obtained from filtering the water provided from C sampling site. Scale bar = 50 µm.
Source: By the author.

To perform a proper phenotypic evaluation of trophozoites encountered in *pure* and *ecoli* NNA plates (Figure 3.4.), analytical strategies based on cell measuring had been integrated into our analysis. Thus, a subset of three consecutive images per sample was recorded to measuring the cell dimension of trophozoites, as represented by the following example (Figure 3.5.).

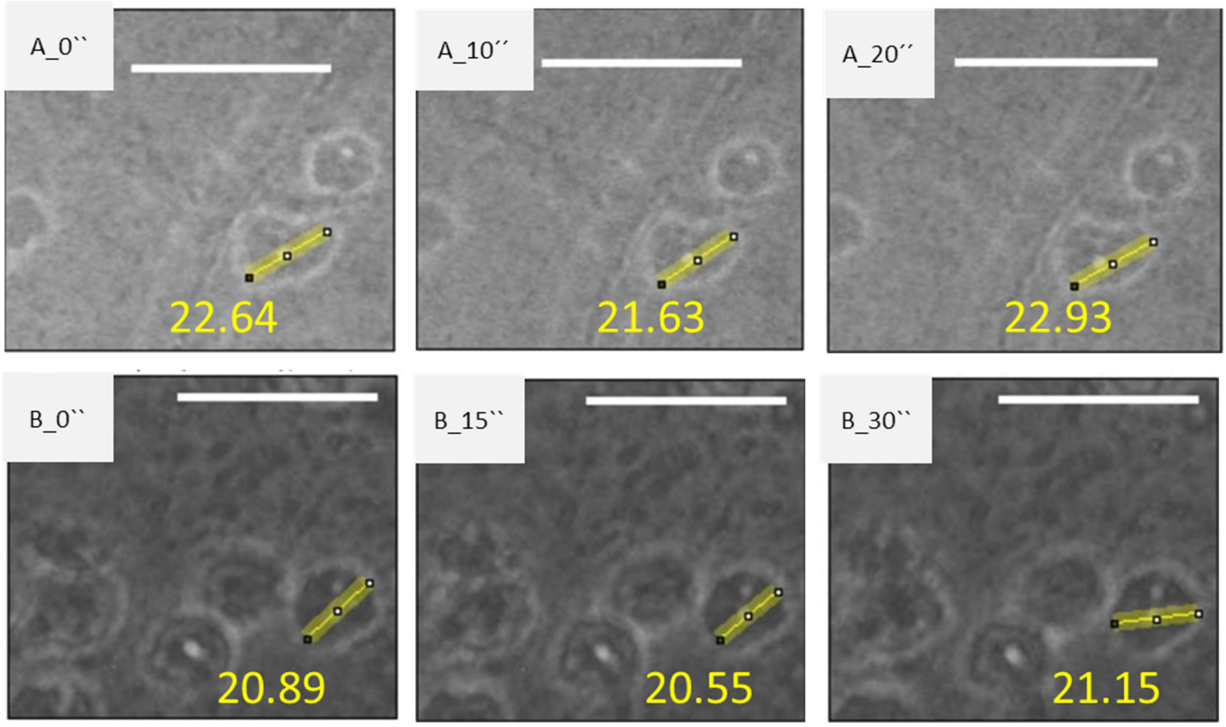

Figure 3.5 – Process of measuring the trophozoite's greatest dimension. Micrographs of representative trophozoites from SC37_1st samples growing onto *pure* (A) and *E.coli* supplied (B) NNA plates. Consecutive images were examined accounting trophozoite shape moving whose time window comprised 0, 10, and 20 seconds, to A samples, and 0, 15, and 30 seconds, to B samples. Scale bar: 50 µm.
Source: By the author.

One trophozoite per sample was targeted to demonstrate the cell measurement process revealing the slight amoeba shape variation in both time windows (Figure 3.5). This evaluation was made in 20 trophozoites resulting in average dimensions of 21.8 ± 0.6 µm and 22.3 ± 0.4 µm to *pure* and *ecoli* groups, respectively. Alternatively, the distribution of data was summarized as a boxplot representation in which the average of greatest trophozoite dimensions is disclosed on the Y-axis (Figure 3.6).

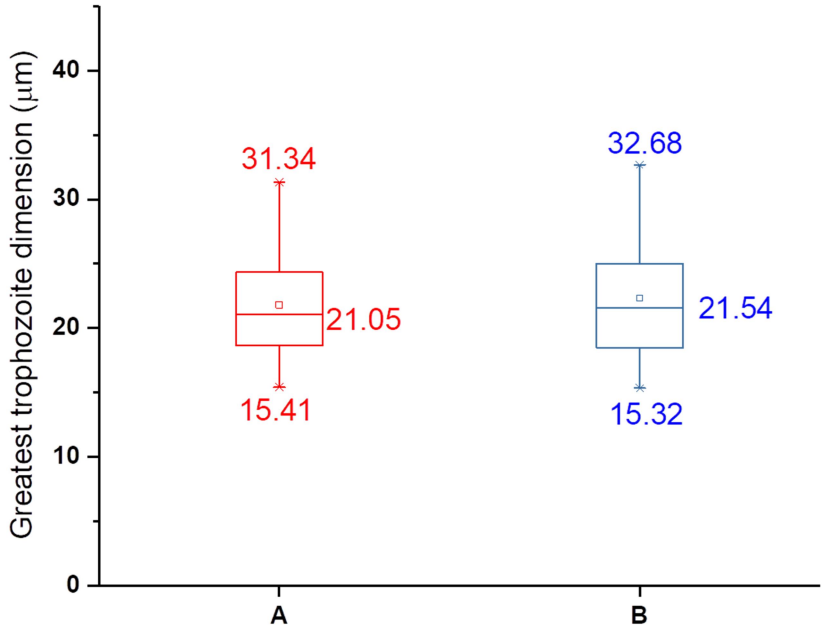

Figure 3.6 - Boxplot data of 20 trophozoites´ greatest dimension measuring. Maximum, mean, and minimum dimensions are highlighted accompanying boxplot distributions, numbers surrounding red (A), and blue (B) boxplots. The median is demonstrated by the horizontal line in the middle of the boxplot and the mean by the little square inside the boxplot. Trophozoite dimensions refer to SC37_1st samples growing onto pure (A) and *E.coli* supplied (B) NNA plates.
Source: By the author.

Figure 3.6 demonstrated that the shape variation encountered to trophozoite population cultured in both *pure* (A) and *ecoli* (B) conditions was ranked in the same dimension range. Going further on this microscopic-based comparison, not only dimensions but also motility patterns exerted by trophozoites acquired in both conditions had been characterized through the tracking of the cell movement. By following the trophozoites movement during a time frame, continuous lines could be traced as shown in Figure 3.7.

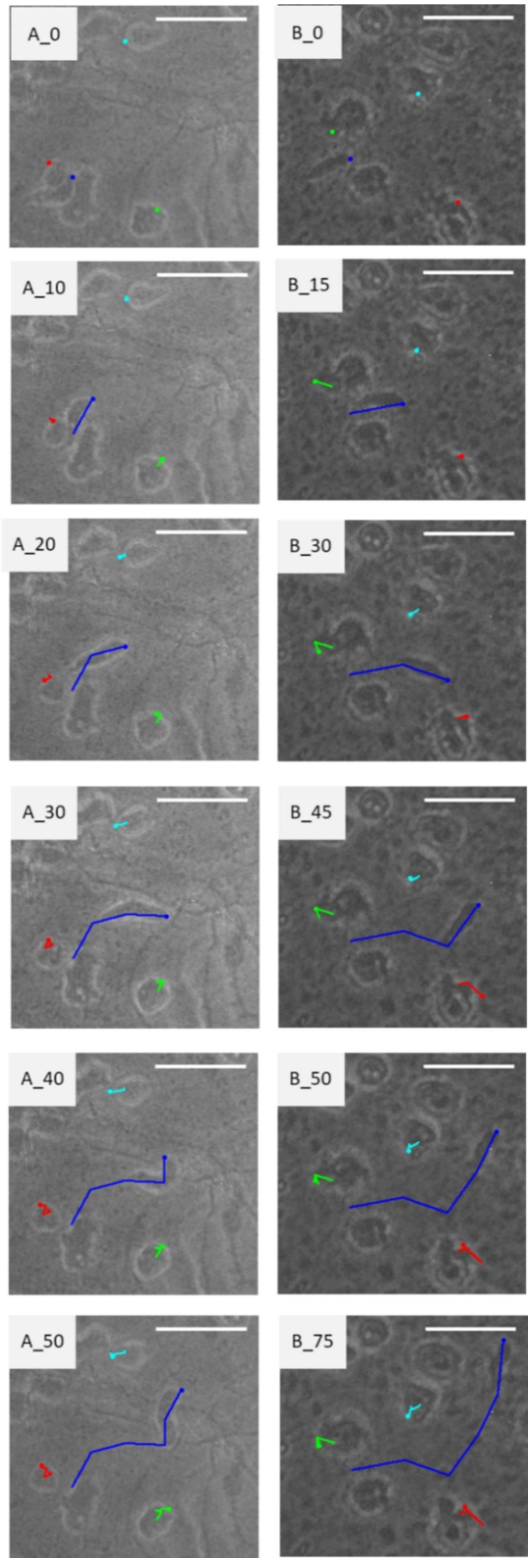

Figure 3.7 - Overview resultant from the tracking process of examining trophozoites´ movement onto NNA plates. Trophozoites observed from pure (A) and *E.coli* supplied (B) NNA plates. Scale bar: 50 µm

Source: By the author.

The first type of movement has shown a unidirectional pattern (Fig. 3.7, dark blue line), and the second type resembles the spider-like movement (Fig. 3.7, red, light blue, and light green lines). Thus, by measuring the total length of lines and normalizing by 60 seconds, rates of movement could be estimated (Table 3.3.).

Table 3.3 – Locomotion rates extracted from tracking trophozoites movement into NNA plates; Rates in µm/min.

# measured cells	Line	*pure* (A)	*ecoli* (B)
G1 (Non-FLA)	dark blue	111.45 ± 6.64	109.83 ± 3.23
G2	light blue + red + light green	18.39 ± 1.92	17.93 ± 1.14

Source: By the author.

These results suggest a mixed culture, classified as group 1 (G1) and group 2 (G2). Tracking analysis indicated that moving rates of group 1 (G1) were about six times more rapid than group 2 (G2) trophozoites, recorded to both *pure* and *ecoli* conditions. This pattern emphasized that both conditions consisted of the same FLA morphotype (G2) in coexistence with the same type of non-FLA microorganism (G1). To properly identify which non-FLA microorganism is G1, it should be isolated, its DNA extracted, and amplified by using generic eukaryote-based PCRs.

The remaining samples provided from the 1st sampling (e.g.: SA_1st_*pure* and SA_1st_*ecoli*) demonstrated the same pattern in which no distinguishable FLA population was observed to *pure* and *ecoli* plates. Thus, trophozoites cultured on both conditions were unified before the DNA extraction and samples were assumed as a unified code (e.g.: the term SA_1st refers to SA_1st_*pure* and SA_1st_*ecoli* together). The same was adopted to those samples obtained in the second sampling.

Progressing with the microscopic characterization of Monjolinho River isolates, a complementary approach based on light microscopy, wet mount preparation, staining methods, and scanning electron microscopy was carried out, as summarized in Table 3.4:

Table 3.4 - Overview on the morphological characterization of FLA. SEM – scanning electron microscopy.

	1-FLA culture		2-Trophozoite characterization			3-Cyst Characterization	4-Flagellation
Samples	NNA plate	Axenization	Staining slides	Wet mount	SEM		
SA26°C _1st	+					+	
SA37°C _1st	+					+	
SB26°C _1st	+						
SC26°C_1st	+						
SC37°C_1st	+	+		+		+	
SD26°C_1st	+	+		+		+	
SD37°C_1st	+					+	
SD44°C_1st	+						
SE26°C_1st	+	+		+			
SE37°C_1st	+	+		+			
SE44°C_1st	+						
SA37°C_2nd	+	+		+	+		
SB26°C_2nd	+		+		+		
SB37°C_2nd	+				+		
SC26°C_2nd	+	+			+		
SC37°C_2nd	+				+		
SD26°C_2nd	+	+	+	+	+		
SD37°C_2nd	+		+	+	+		
SD44°C_2nd	+	+	+	+	+	+	+
SE26°C_2nd	+		+	+	+		+
SE37°C_2nd	+	+	+	+	+		+
SE44°C_2nd	+	+			+	+	

Source: By the author.

The way each sample had been selected to perform its corresponding morphological assays depended on the conditions of the culture at that particular time in which the methodological step was carried out. For that reason, not all samples shown in Table 3.4 were investigated with the full list of essays, as well listed in Table 3.4.

3.2.1.1 NNA plates evaluation

To confirm the positive scoring for amoeba growth, marked with "+" in Table 3.4, NNA plates imaging has been carefully examined and most representative results were depicted in Figures 3.8 and 3.9 respective to the 1st and 2nd sampling cultures.

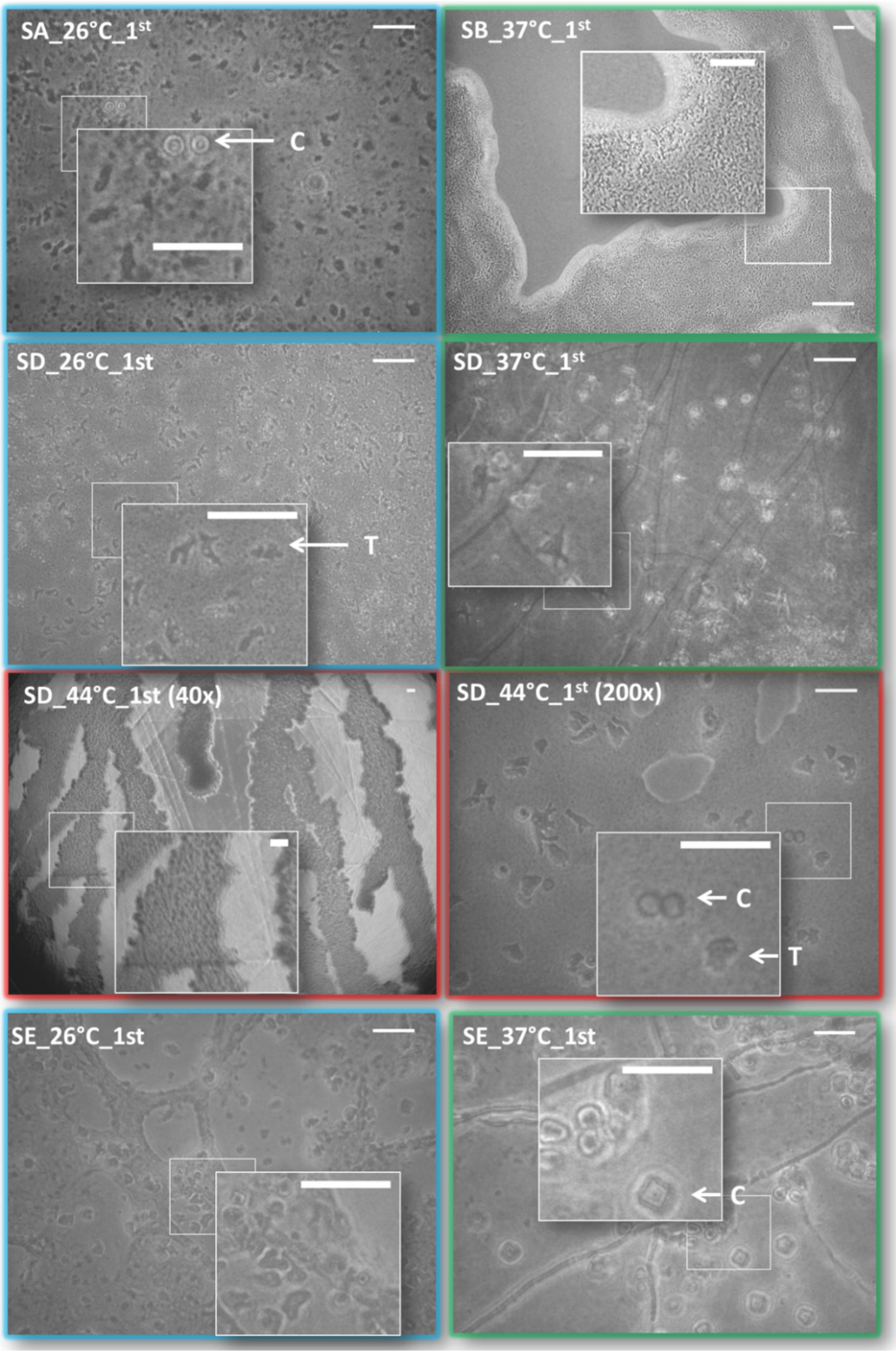

Figure 3.8 - Photomicrographs of amoeba growth onto NNA plate surfaces to samples recovered from the 1st sampling in the Monjolinho River. Green, blue and red colors are indicative of 26 ºC, 37 ºC, and 44 ºC respectively. Scale bar: 50 µm.

Source: By the author.

Figure 3.8 contains representative patters of amoeba growth observed from samples resulted from the 1st sampling. The C sampling site is not displayed oi this Figure once it has been prior analyzed in Figures 3.4, 3.5, and 3.7. In regard to NNA plates imaging performed to samples collected in the 2nd campaign, it had been produced a similar panel than observed in Figure 3.8, as follows:

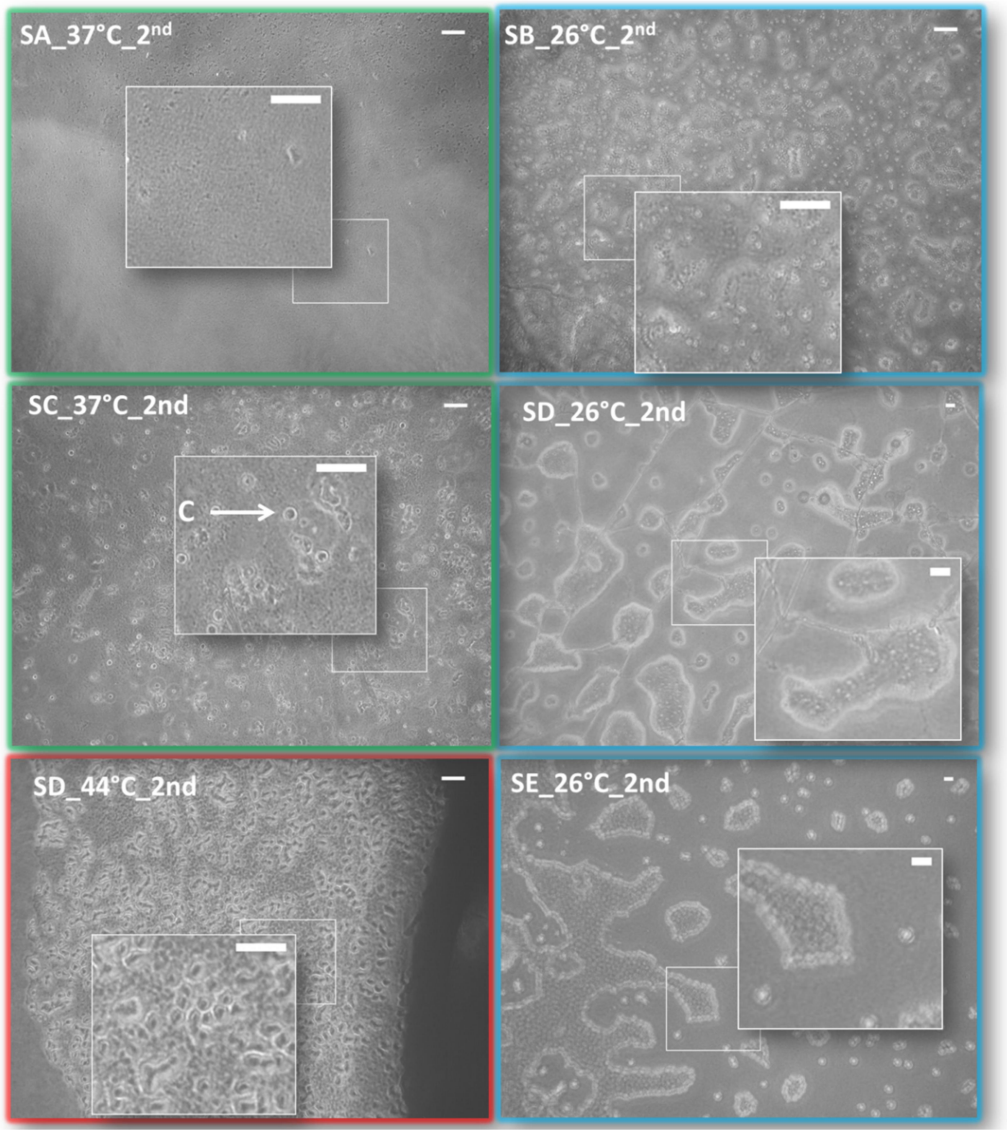

(to be continued)

(continuation)

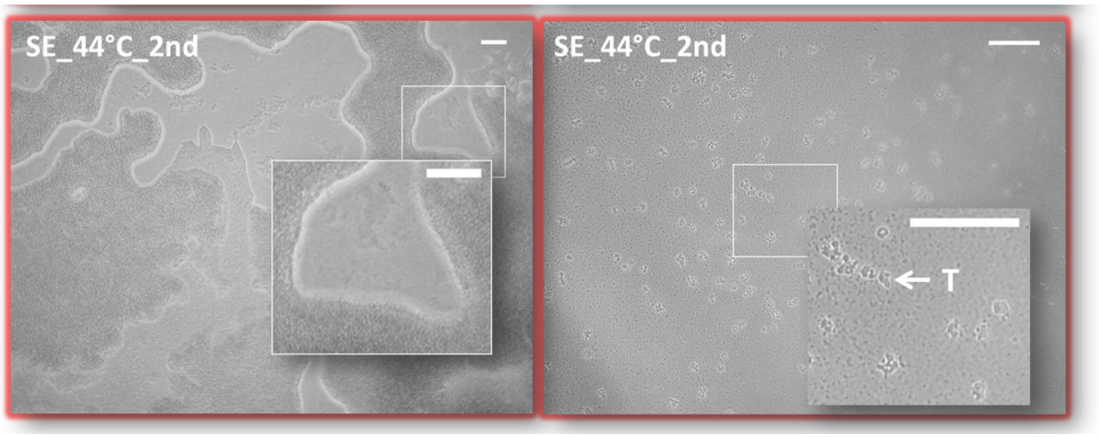

Figure 3.9 - Photomicrographs of amoeba growth onto NNA plate surfaces to samples recovered in the 2nd sampling in the Monjolinho River. Green, blue and red colors are indicative of 26 ºC, 37 ºC, and 44 ºC respectively. To the sample SD26ºC_2nd, trophozoites usually grew attached to hyphae of fungi. Scale bar: 50 µm.
Source: By the author.

Overall, the set of micrographs documented in Figures 3.8 and 3.9 highlighted the most typical landscape of amoeba growth onto NNA plates encountered to those FLA isolates from the Monjolinho River. It emphasized two main typical forms of FLA: trophozoite stage (T) able to move, feed, and divide, and the cyst (C) stage able to withstand extreme environments. Cyst formation revealed rounded and star-like forms, both with the typical double wall (Fig. 3.8, samples SA26_1st and SE37_1st; and Fig.3.9, sample SC37_1st). Cultures shown in Figure 3.8 and 3.9 were imaged after 10 days of growth with exception of sample SD44_2nd acquired two days inoculation in the new NNA plate in order to highlight the amoeba migration pattern (Fig 3.9).

Bacteria and fungi contaminations have been present on NNA cultures, as illustrated in Figure 3.8 (samples SD37_1st, SE_37_1st, SD26_2nd), and Figure 3.9 (samples SD26_1st, SD44_1st, SC37_2nd, SE44_2nd). Thus, several subculturing steps were performed to eliminate the fungi and bacteria contamination, as shown in Figure 3.10.

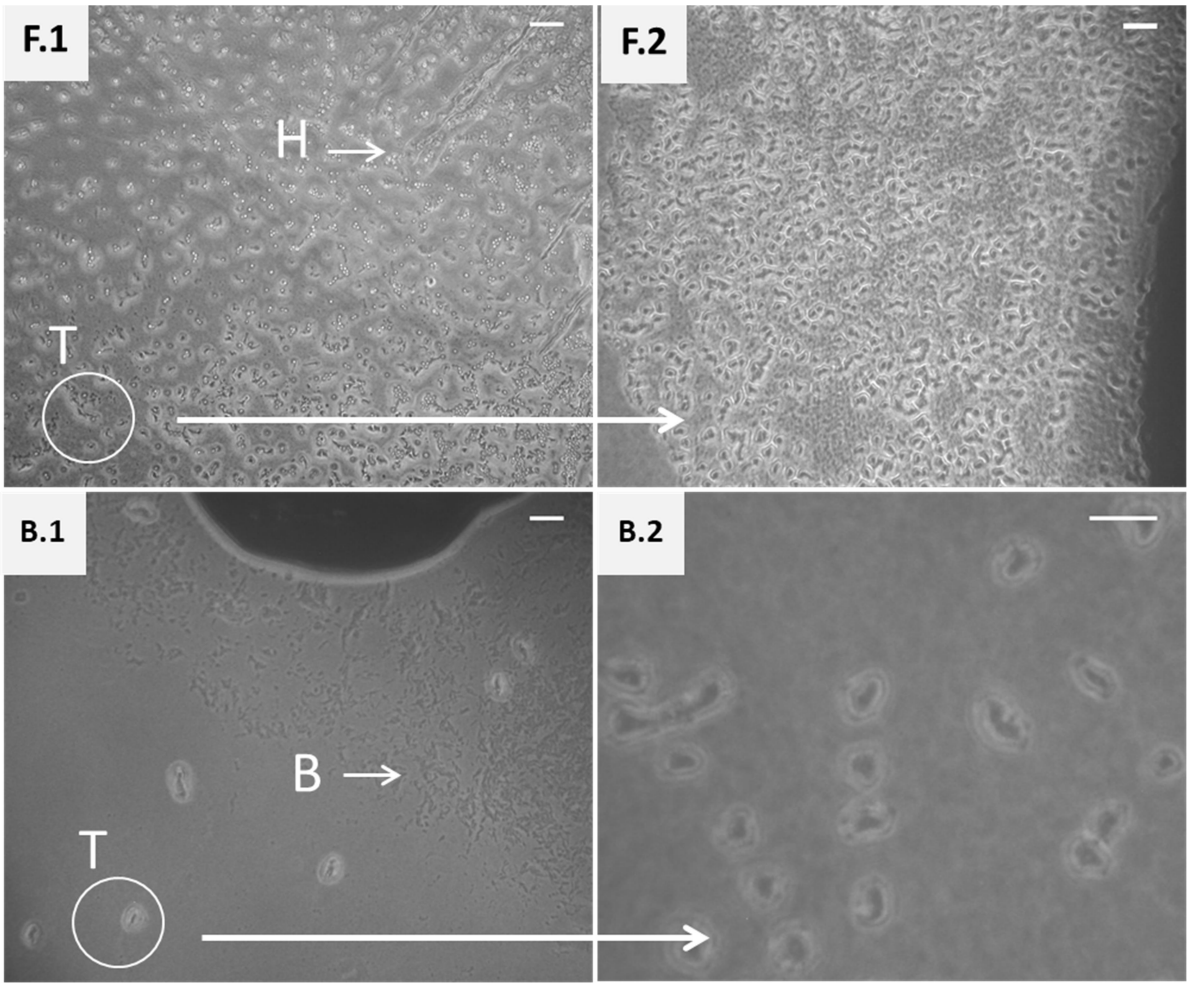

Figure 3.10 – Light microscopy of the cloning step process to remove fungi (F.1-F.2) and bacteria (B.1-B.2) contaminations onto NNA plates. H: hyphae of fungi.F1 and B1 refer to prior plates and F2 and B2 to new NNA plates. Scale bar = 50 µm.
Source: By the author.

As shown in Figure 3.10, not only a decrease in fungi and bacteria contamination, as well as amoeba enrichment could be obtained with subculturing. With the aim of reducing as much as possible the contamination, this practice was extended for approximately 3 months by selecting areas of interest to extract amoeba (white circle, Fig. 3.10, F.1 and B.1) and replacing the agar pieces to fresh NNA plates (Fig. 3.10, F.2 and B.2). Although daily subculturing, this process was not sufficient to eliminate the contamination. The procedure was optimized by introducing a multidrug based treatment. Target antibiotics (penicillin and streptomycin) and antifungal (amphotericin B) were added to the NNA media, as described in section 2.4.1. (Methods). However, most cultures were sensitive to this treatment and transformed into the cyst resistant form or directly died without encysting. Based on this experience, new cloning steps have been

performed, and trophozoites harvested along passages were used for morphological and molecular characterization.

3.2.1.2 Axenization

Resultant from cloning steps effort as a preliminary level to conduct axenization assays, the most cleaned areas of target NNA plates were selected, and trophozoites were harvested and seeded into 24 wells culture plate including those samples ranked as "+" in the axenization column, Table 3.4. Axenization results are summarized in Table 3.5.

Table 3.5 - Axenization scheme conducted with environmental FLA amoeba samples from the Monjolinho River. T1 – T3 refer to antibiotic treatments. Green squares to PYG (Y) medium and coral squares to ATCC1034 (A) medium are indicating those samples used to prepare the culture plates (PI – PVI). Cultures transferred from plates to 12.5 cm^2 tissue culture flasks were ranked with "F", and samples that reached axenization ranked with "X".

	T1				T2						T3	
	PI		PII		PIII		PVI		PV		PVI	
	Y	A	Y	A	Y	A	Y	A	Y	A	Y	A
SD26_2nd												
SE37_2nd												
SC37_1st			F									
SC_2nd												
SE26_1st			F									
SE37_1st												
SD26_1st												
SD44_2nd				F		X						
SE44_2nd				F								

Source:By the author.

Table 3.5. illustrated the development of axenization assays performed with a total of six plates (PI – PVI) in which one plate per month, in a time window of six months, enabled us to observe behaviors of target cultures in the prior assay (e.g.:PIII) and optimize new strategies to be adopted in the sequential attempt (e.g.: PVI). Thus, the first plate (PI and PII) combined both PYG and ATCC1034 mediums to the whole set of samples aiming to observe any medium

preference during one month culture observation. Each well was monitored daily in EVOS® FL Cell Imaging System with a representative result revealed in Figure 3.11.

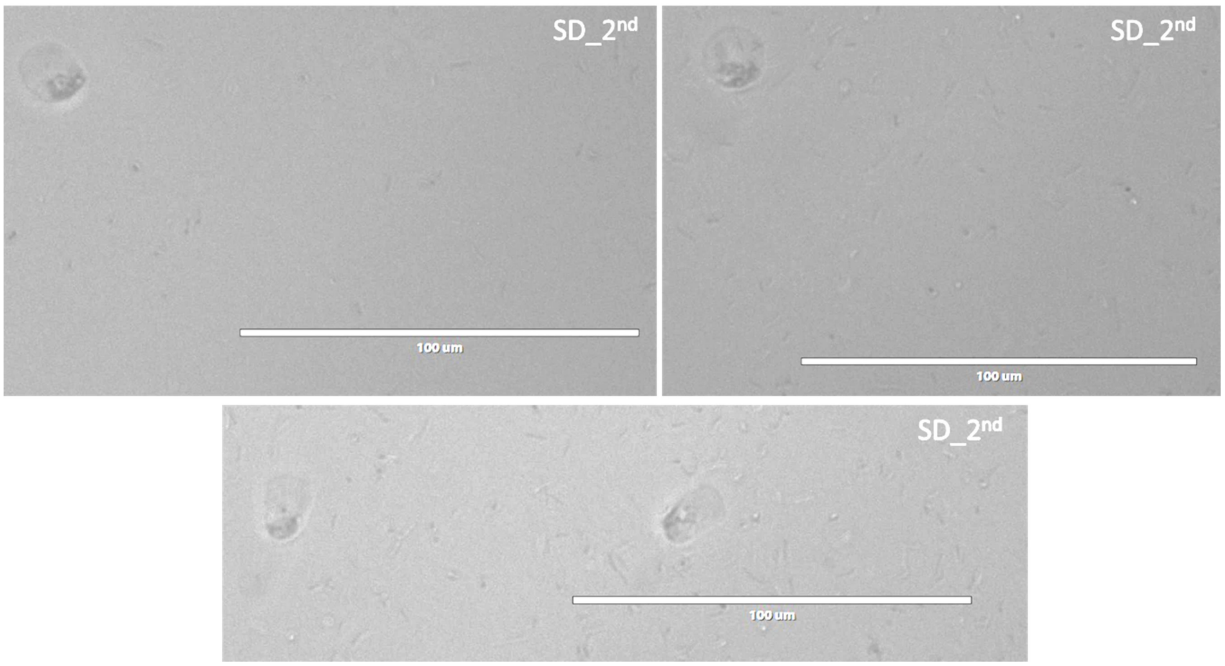

Figure 3.11 - Micrograph of trophozoites from SD26_2nd sample cultured onto 24 cell culture plate with ATCC1034 for the purpose of axenization.
Source: By the author.

Although continuous effort with cloning steps routine, the most common issue hampering the progress of amoebic proliferation, regardless of the choice of medium, was the bacteria contamination, as exemplified in Figure 3.11. Therefore media contamination was intrinsic of removing trophozoites from NNA plates, a process that carried contamination in the agar block. Thus, three distinct treatments were designed aiming to solve the issue, in which T1, T2, and T3 comprised:

(T1) Canonical culture mediums, ATCC1034, and PYG, with additional 10 µl/well of multi-spectrum antibiotic PANTA™ Antibiotic Mixture, BBL™ MGIT™ to bacteria contaminated wells and amphotericin B, 5 µg/ml, to fungi-contaminated wells;

(T2) Canonical culture mediums, ATCC1034, and PYG, with additional 10 µl/well of an antibiotic mix (100 U/ml Penicillin plus 100 µg/ml Streptomycin) to bacteria contaminated wells;

(T3) Modified ATCC 1034 and PYG culture mediums, both prepared without antibiotic adding.

A common routine for all treatments included careful washing six times each well with fresh medium to remove the previous contaminated medium. In the last washing step, antibiotics/antifungals were added regarding or T1 either T2 treatments. Some results revealed bacteria eliminating with coincident amoeba death, a similar behavior observed to isolates cultured on NNA plates supplied with antibiotics. Often, other cases have shown bacteria persistence due to its antibiotic resistance. The third attempt (T3) was aimed to enhance amoeba growth for those cultures sensitive to antibiotic treatment (plate IV).

From T1 to T2, four cultures revealed promising to be replaced to 12.5 cm^2 culture flasks with 5 ml medium (Table 2, letter F). Cells were detached with a scraper, replaced to culture flasks, and daily examined. Along one week of culturing, SD44_2^{nd} could be successfully axenized, enabling its freeze preservation in cryovials with FBS:DMSO (9:1). Although treatments T1-T3 somehow revealed improvement of amoebic growth in initial days of treatment, what allowed selecting samples to transfer to liquid flasks (F), after a couple of days, it resulted in bacteria contamination or amoebic density decreasing. Taking account that cloning steps have been exhaustively performed to remove bacteria/fungi from NNA plates prior to seed axenization plates, it was observed a growth pattern of days without contamination interspersed with days in which contamination reappeared to most of samples listed at Table 3.5. Thus, it was prepared a wet mount slide with SE26_1^{st} sample to evaluate the quality of samples. Figure 3.12. displayed an interesting scene.

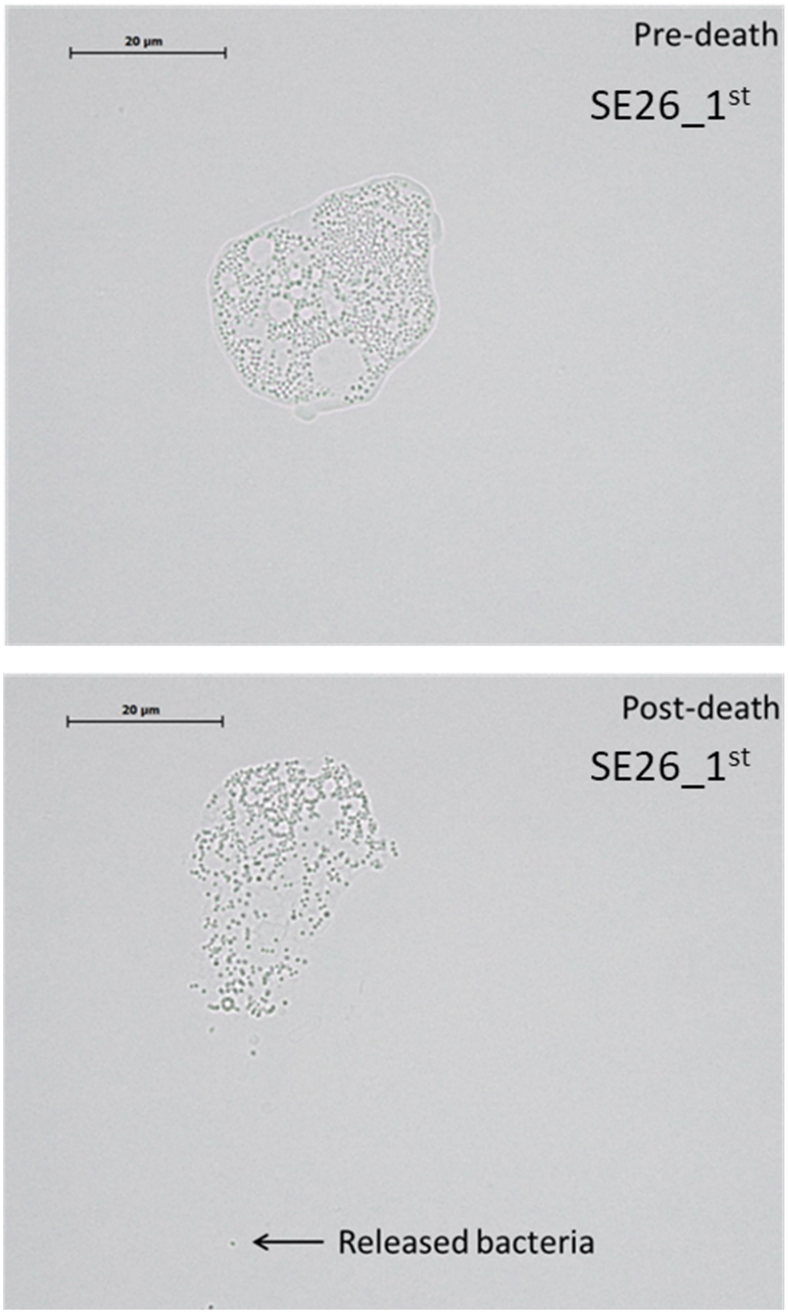

Figure 3.12 – Photomicrographs of an environmental FLA isolates recovered from an axenization plate.The sample, SE26_1st, suggests amoebic resistant bacteria presence living intra-FLA.
Source: By the author.

Figure 3.12 revealed that intra-FLA bacterial content is the most reasonable evidence for the difficulty of reaching axenic cultures with most of the FLA isolates targeted here. Although most samples did not work in an axenic system, target samples could be further investigated through slide microscopy, as documented ahead.

3.2.1.3 Morphology of free-living amoeba

The first morphological study carried out with FLA isolates included the measurement of the greatest trophozoite dimension into NNA plates. A total of 20 trophozoites has been randomly sampled per image, and its greatest dimension was monitored on three consecutive images concerning the diameter fluctuation due to amoeba locomotion, exactly as previously reported to C sampling site standardizing tests (Figure 3.5). Measures were graphed in a boxplot, as shown in Figure 3.13.

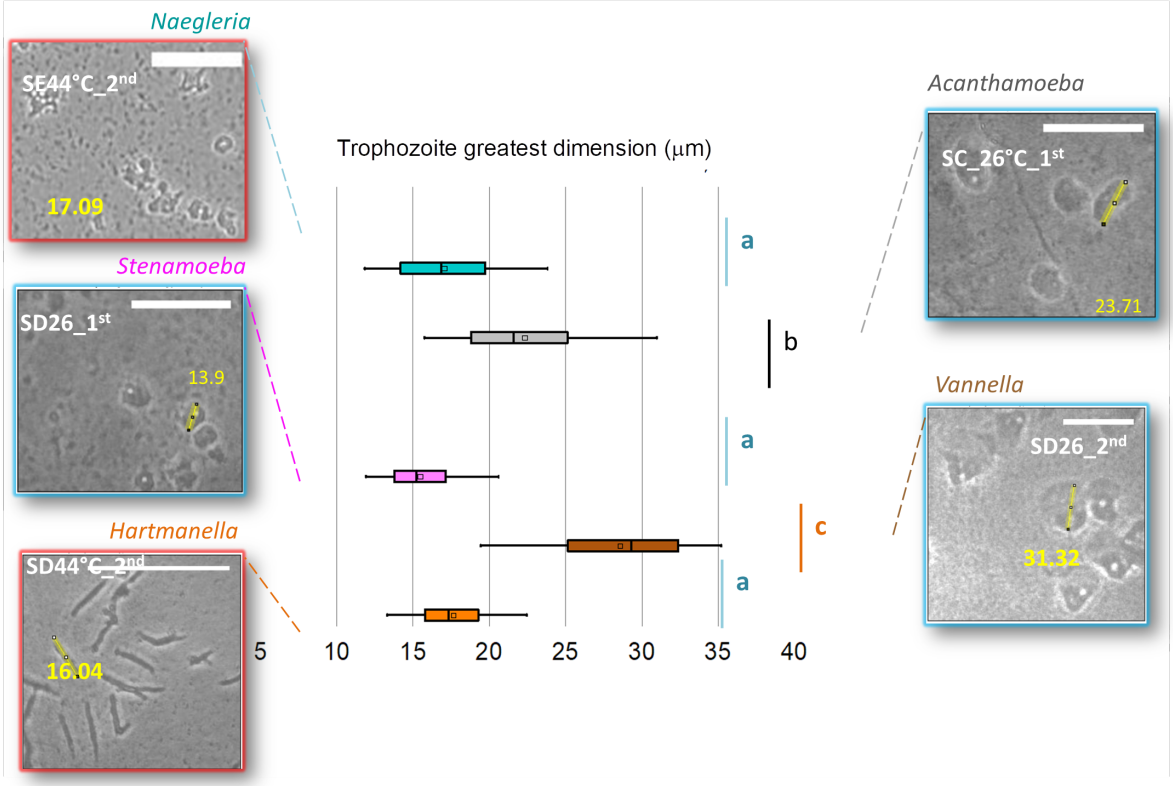

Figure 3.13 – Boxplot of trophozoite greatest dimensions evaluated into NNA plate images. Boxplot colors are indicative of FLA genera: *Naegleria, Acanthamoeba, Stenamoeba, Hartmanella*, and *Vannella*. Red and blue colors, in the micrographs, represent 44°C and 26°C respectively. Scale bar = 50 µm. The statistic is based in ANOVA and Post hoc (Tukey) tests considering a p-value<0.01.
Source: By the author.

Figure 3.13. depict the typical range from about 11 to 35 µm to all trophozoites encountered in the Monjolinho river samples, here represented by five NNA cultures belonging to the FLA genera *Naegleria, Acanthamoeba, Stenamoeba, Vannella, Hartmanella* (=

Vermamoeba) whose molecular characterization, as detailed in section 3.3, allowed to confirm the morphological findings. Another observation in Figure 3.13. is the overlap of trophozoite dimensions, as shown for *Stenamoeba, Naegleria* and *Hartmanella*, accompanied by a morphotypic divergence between the outline of each corresponding trophozoites. The statistical analysis proved that there is no sisgnificative divergence between the dimensions of the aforementioned genera once they are all placed as group "a". Thus, cyst morphology studies were included to clarify the issue, as shown in the Figure 3.14.

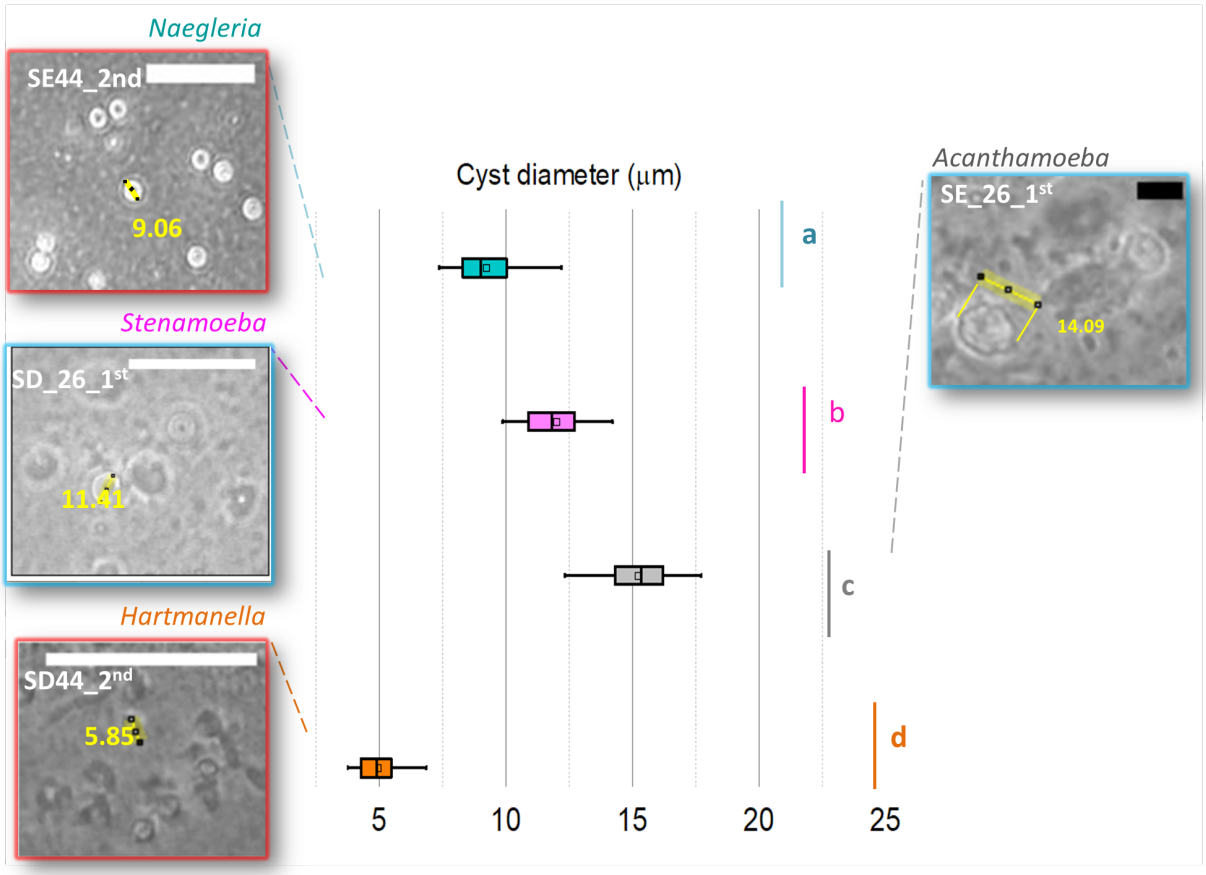

Figure 3.14 - Boxplot of cyst diameter ranges evaluated into NNA plate images. are indicative of FLA genera: *Naegleria, Acanthamoeba, Stenamoeba*, an d *Hartmanella*. Red and blue colors, in the micrographs, represent 44°C and 26°C respectively. White and black scale bars refer to 50 µm and 10 µm respectively. The statistic is based in ANOVA and Post hoc (Tukey) tests considering a p-value<0.01.
Source: By the author.

The results in Figure 3.14 clarify the morphotype distinction among the genera *Naegleria*, *Stenamoeba* and *Hartmanella* as they have been placed into distinct diameter ranges, as well as in three statistically divergent groups a, b, and d, respectivlly. It is observed that 50% of

Hartmanella data has 5 µm diameter, whereas *Naegleria* ranged from 7.5 – 10 µm and *Stenamoeba* ranged from 10-12.5 µm (Figure 3.14). Another observation provided from Figure 3.14. is that *Vannella* has no identifiable cyst formed, regardless of the method tested (non-nutrient agar plates imaging, staining and wet mount slides). However, we argue that several details may not be detected and could be observed with more accurate techniques as wet-mount and staining slides imaging, as illustrated in both. Figure 3.15 and the subsequent Figure 3.16.

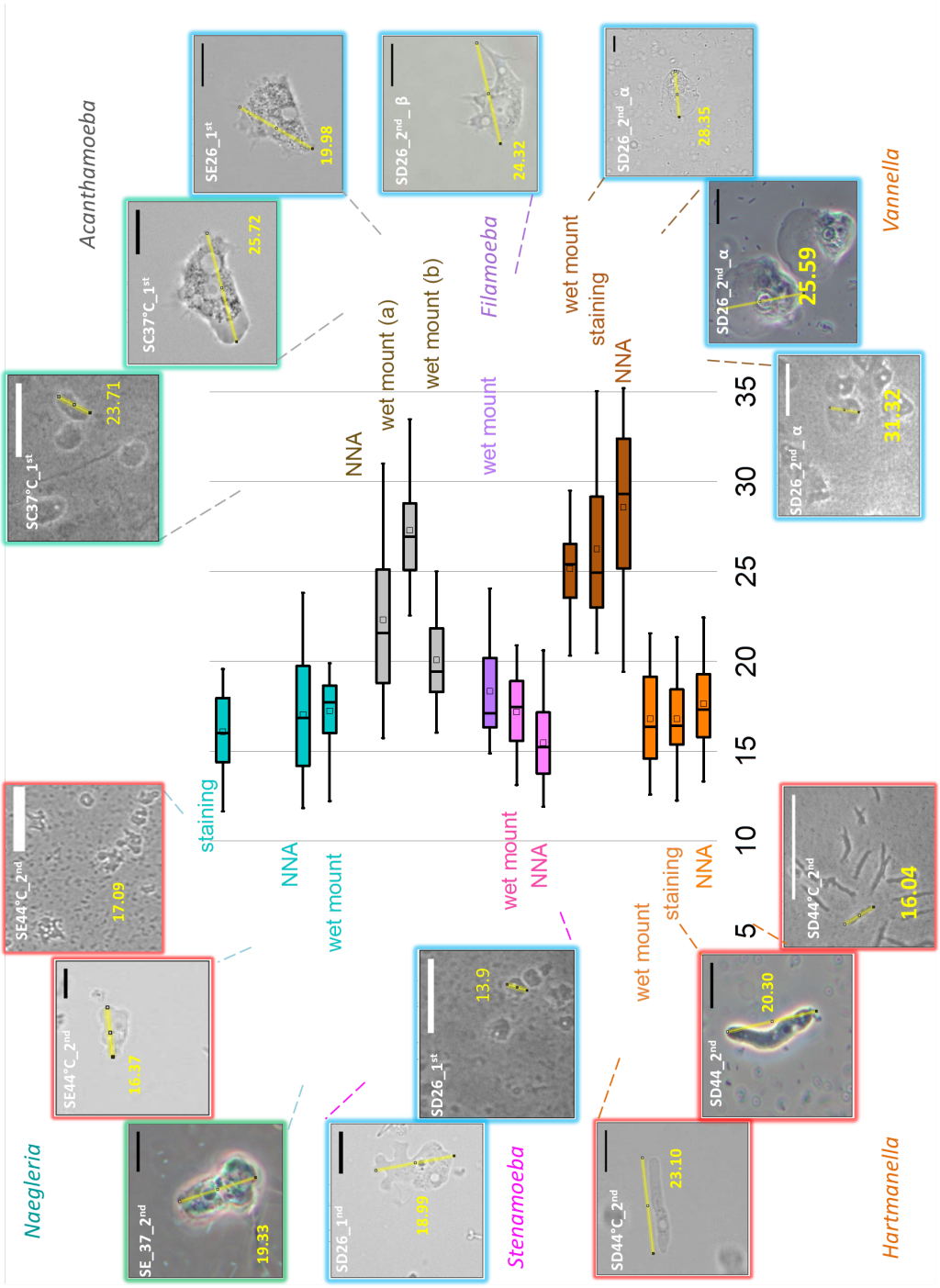

Figure 3.15 - Boxplot of **trophozoites'** greatest dimensions. Each FLA genus was evaluated employing one or more microscopic techniques: non-nutrient agar (NNA) plates imaging, wet-mount and staining method. The sample SD26_2nd was termed with α and β to demonstrate heterogeneity whithin this culture in which *Vanella* and *Filamoeba* genera were identified. White and black scale bars refer to 50 µm and 10 µm respectively

Source: By the author.

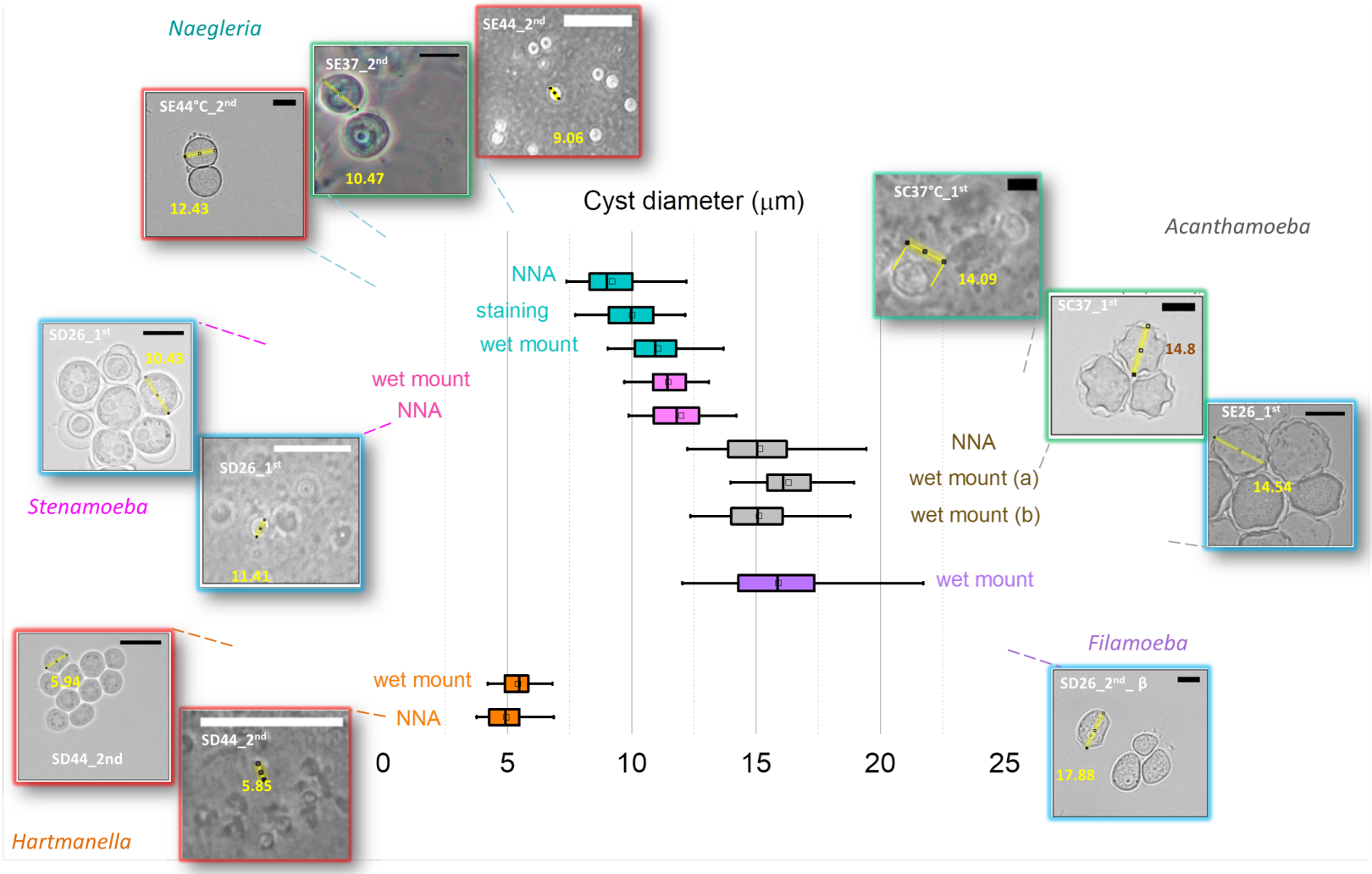

Figure 3.16 - Boxplot of cyst diameter recorded to FLA isolated in Monjolinho river. Each FLA genus was evaluated employing one or more microscopic tecchniques: non-nutrient agar (NNA) plates imaging, wet-mount and staining method. The sample SD26_2nd was termed with β to demonstrate heterogeneity whithin this culture in which not only *Filamoeba* (β) but also *Vanella* (α) genera were identified. The latter is not reported here accounting that it has no identifiable cyst formed. White and black scale bars refer to 50 µm and 10 µm respectively

Source: By the author.

The major finding shown in both Figure 3.15 and 3.16 is the largest boxplot ranges provided from NNA plate measurements, in comparison with the remaining staining and wet mount techniques. For instance, *Naegleria* trophozoites dimension has shown lower length ranges by staining method and wet mount compared to NNA ranges (Fig. 3.15). Exceptions to this pattern are seen to *Hartmanella* and *Filamoeba* (Fig. 3.15). The *Hartmanella* results provided equivalent dimension values observed to all of them, NNA, staining, and wet mounts (Fig. 3.15). The *Filamoeba* case is lacking of NNA imaging characterization, as well as staining method, once its presence was detected later in a sample previously characterized as *Vannella*, SD26_2nd, both presented in Figure 3.15. It reveals an example of mixed FLA culture outgrowing in a unique sample, here termed as α and β to distinguish both genera *Vannella* and *Filamoeba* respectively. Moreover, cyst based investigation illustrated in Figure 3.16 reinforced the divergence among these samples, since no cysts were found in *Vannella* samples.

Overall, Figures 3.15 and 3.16. show the morphological diversity regarding pseudopodia, hyaloplasmic projections, and cyst wall, among other features informative to identify each FLA genera. Therefore, the following sections are devoted to the description of FLA morphology isolated from the Monjolinho river.

Free-living amoeba characterization – *Naegleria* genus

Morphological characteristics typical of type N isolates are summarized in Figure 3.17. based on staining slides, wet mount preparations, and scanning electron microscopy results.

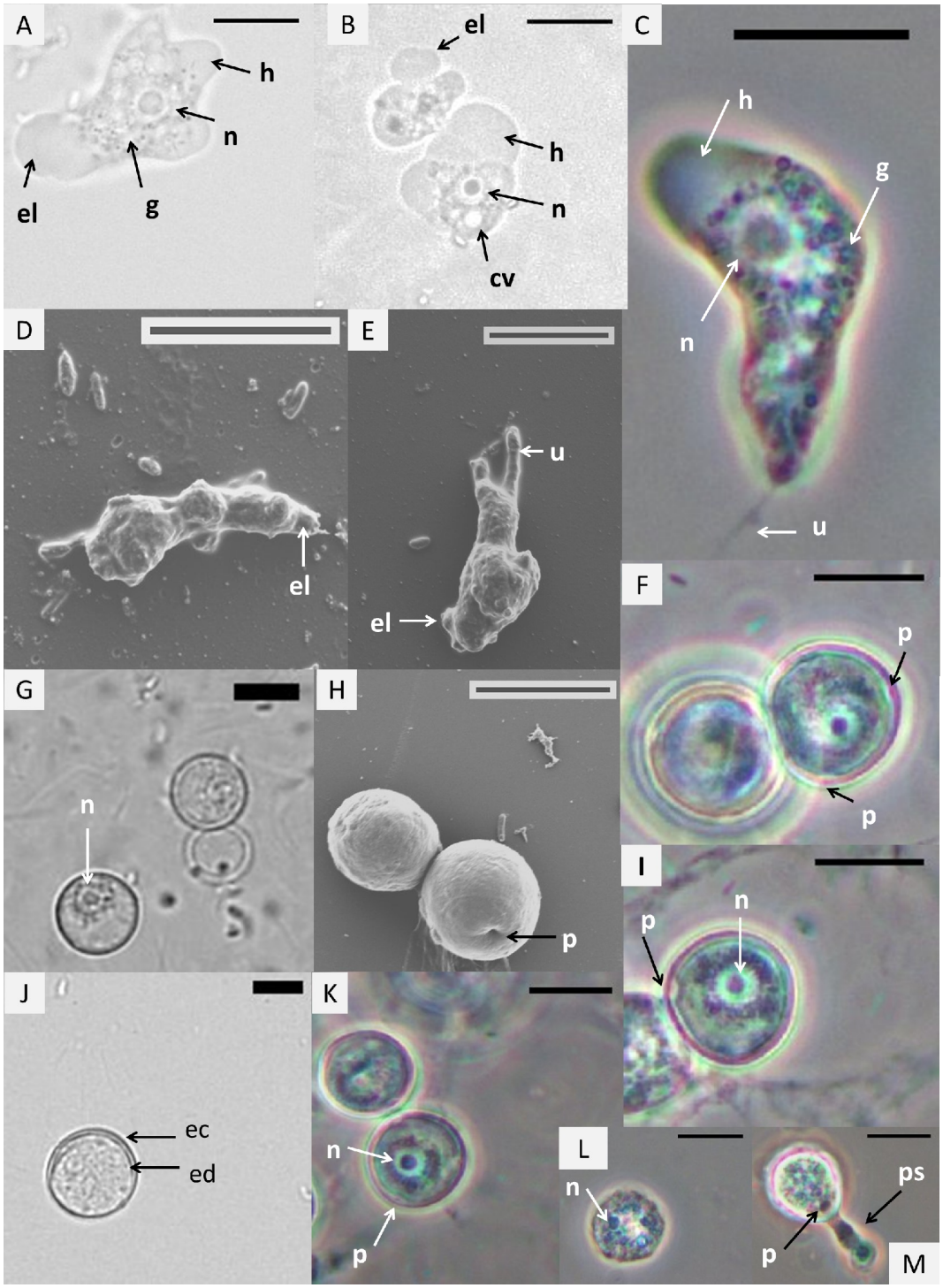

Figure 3.17 – Morphology of *Naegleria* isolates - trophozoites (A-E) and cysts (F-L). Light microscope techniques include wet mount slides (A,B,G,J) and methylene blue staining slides (C,F,I,K, L, M). Scanning electron microscopy images (D,E,H). Excystation process is represented by pre excistation stage (L) and initial excistation stage (M). ps – pseudopodia, h –hyaloplasm, w – cyst wall, eruptive lobopodia (el), p – pore, g – granuloplasm, ed – endocyst, ec – ectocyst. Isolates registered on this panel belongs to NNA cultures respective to SE44_2nd (A,C,F,G,H,K,L,M,J) and SE37_2nd (B,D,E,H). Scale bar = 10 µm. Based on ITS1/5.8S/ITS2 rDNA sequencing data, SE37_2nd and SE44 _2nd corresponded to *Naegleria australiensis*.

Source: By the author.

Figure 3.17. illustrates the main morphological features considered for the identification of a *Naegleria* genus isolate. The most evident cellular structures are: eruptive lobopodium (Fig 3.17 - A, B, D and E), posterior uroidal zone (Fig 3.17 - C and E), an elongated amoeba shape during locomotion (Fig 3.17 – C to E), and double-walled cysts (Fig 3.17 G, I and J) with pores (Fig 3.17 - F, H, I, K and L). Moreover, the hyaloplasm and granuloplasm areas are evident in which the latter contains all organellar content as the vesicular nucleus (n) and contractile vacuole (cv).

Although Figure 3.17. illustrated methylene blue stained slides, a prior evaluation, including eosin and hematoxylin stains, was carried out to both life cycle stages, trophozoites and cysts, as shown in Figure 3.18.

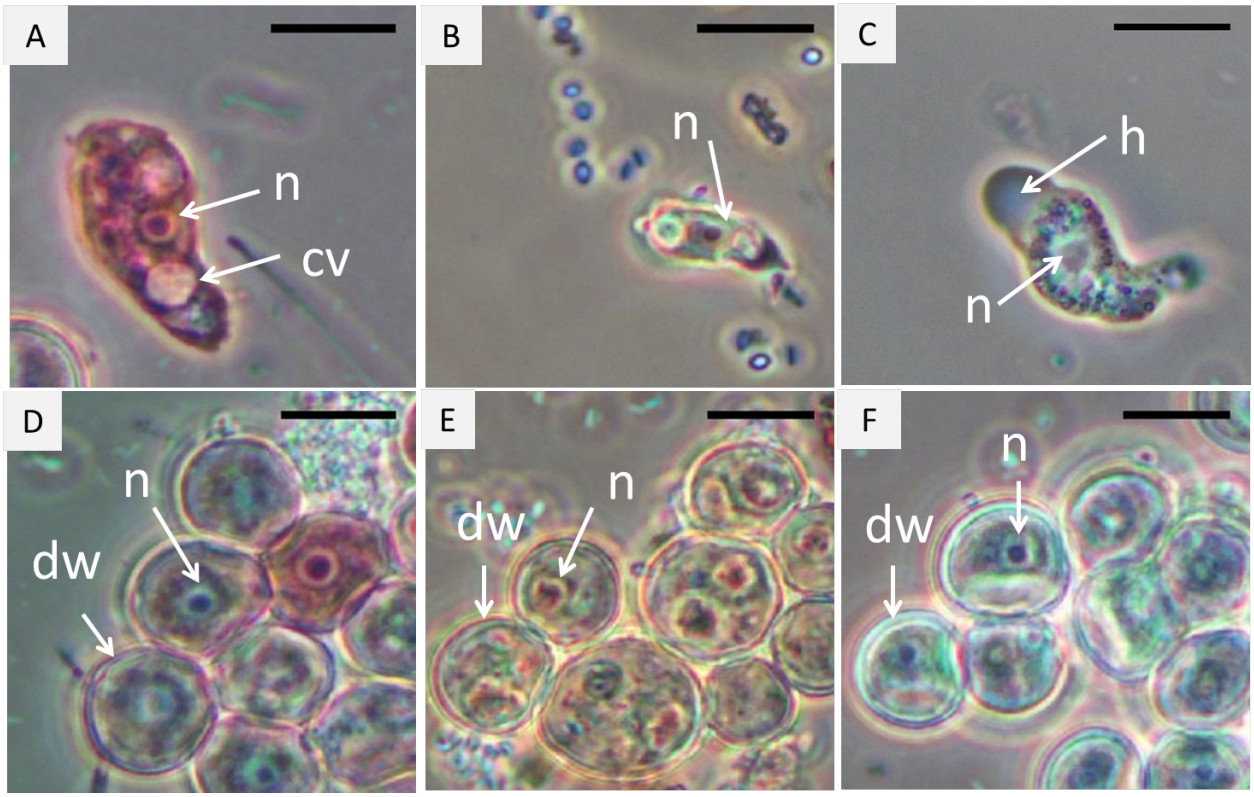

Figure 3.18 - Stained trophozoites (A-C) and cysts (D-F) of *Naegleria* observed through light microscopy images. Comparison among Eosin (A and D), Hematoxilin-Eosin (B and E) and methylene blue (C and F) stains. Annotations refer to nucleus (n), double wall (dw), contractile vacuole (cv), hyaloplasm (h). Trophozoites recovered from SE37_2nd NNA plate culture. Scale bar = 10 µm.

Source: By the author.

Figure 3.18 shows that the different staining methodologies do not reveal additional representative features. This analysis enabled us to use all staining options without any preference among them.

The genus *Naegleria* also exhibited the flagellate form, resultant from the enflagellation test, described in section 2.4.2. The results are summarized in Figure 3.19.

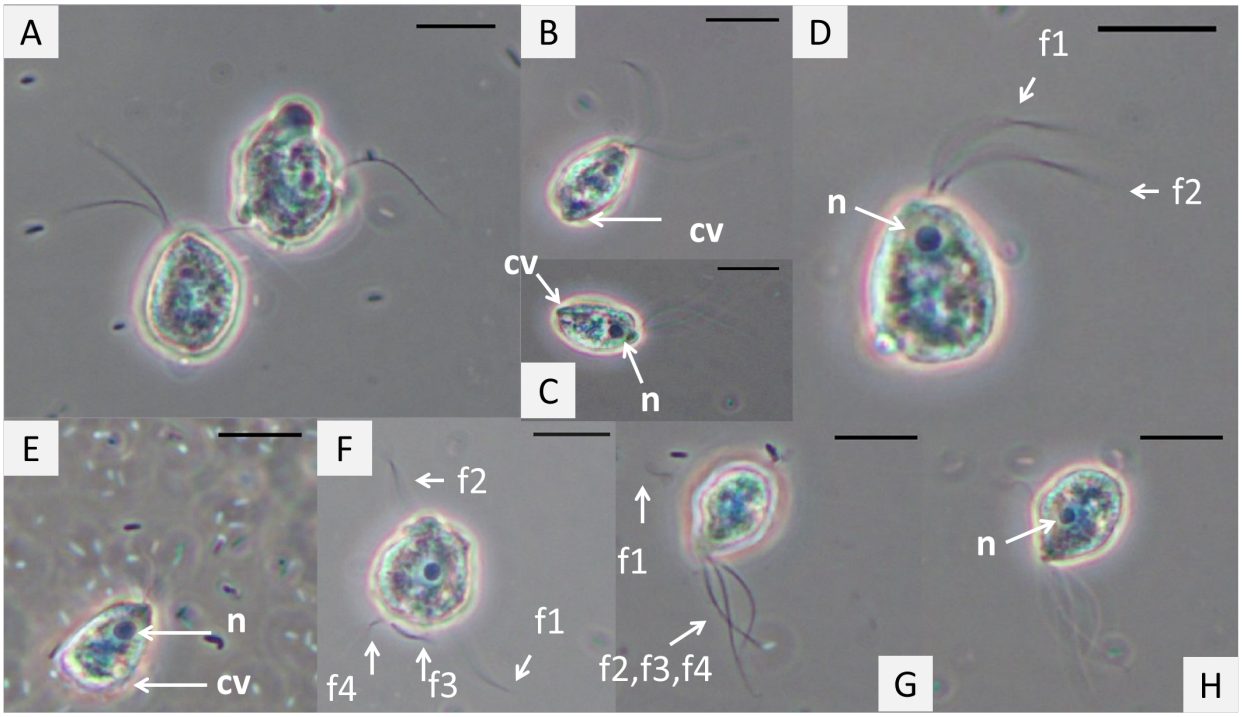

Figure 3.19 - Light microscopy of flagellate forms typical of *Naegleria* isolates, sample SE37_2nd (*N. australiensis*). Methylene blue stained slides. Scale bar: 10µm. Biflagellates (A,B,C,D,E,H) and tetraflagellates (F,G). Annotations f1-f4 refer to flagellate numbers; n- nucleus; and cv – contractile vacuole.
Source: By the author.

From the samples submitted to enflagellation experiments as listed in Table 3.4 (page 95), only SE37_2nd was successfully transformed into amoeboflagellates, consisting of biflagellate and multiflagellate forms. As shown in Figure 3.19, B - E, the nucleus is often positioned near the flagella and the contractile vacuole is observed in the opposite to the nucleus. Both are important to differentiate *Naegleria* from the remaining Heterolobosea amoeba-flagellates. After molecular characterization, the SE37_2nd sample has been identified as *N. australiensis*. The isolates that did not succeed to form flagella were identified as *Vermamoeba vermiformis* (SD44_2nd) and *Naegleria phillippinensis* (SE26_2nd).

Free-living amoeba - characterization of *Acanthamoeba*

Figure 3.20 summarizes the characteristics of *Acanthamoeba* genus.

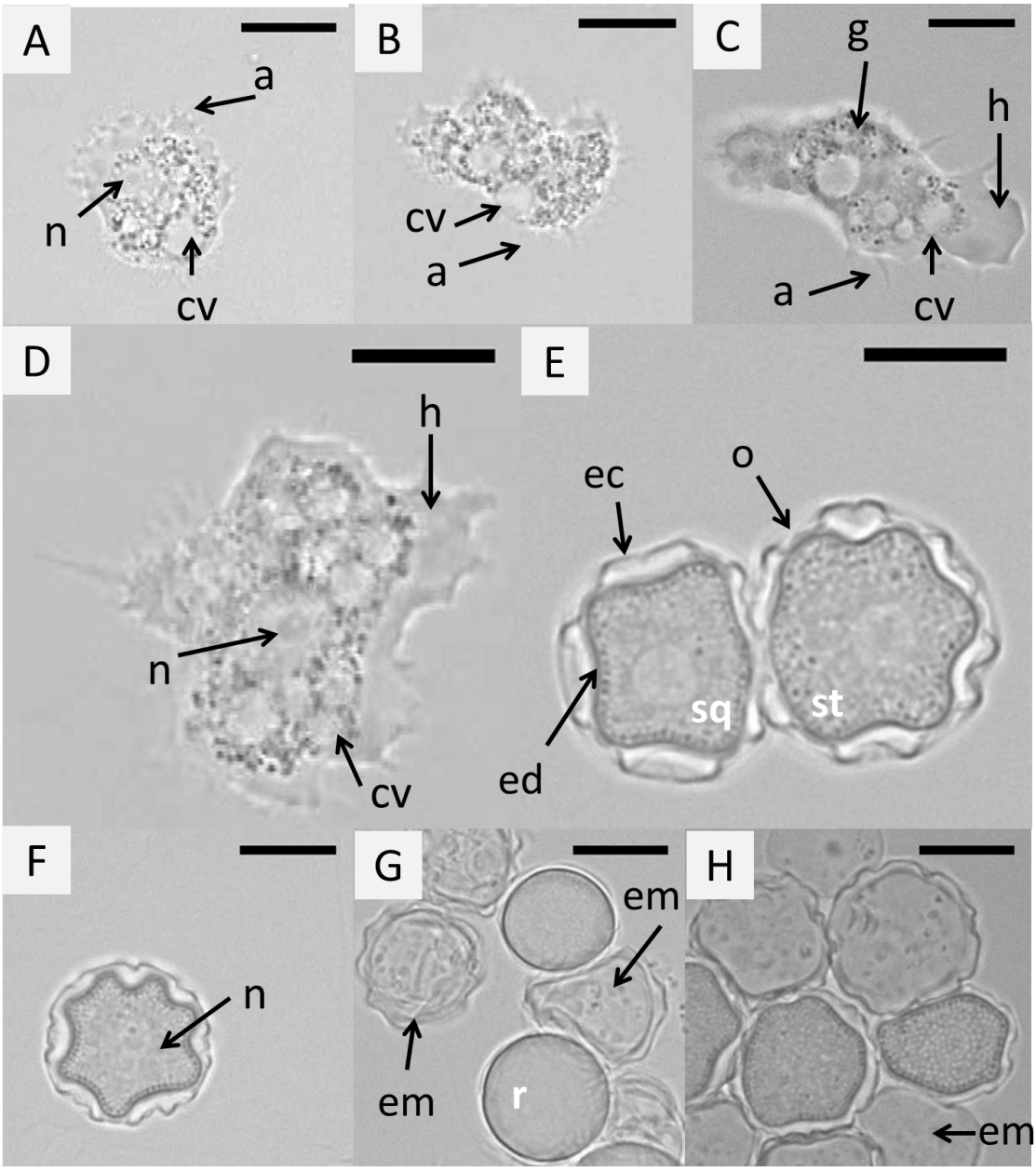

Figure 3.20 - Morphology of *Acanthamoeba* isolates - trophozoites (A-D) and cysts (E-H) observed with wet mount preparations. Annotations are highlighting contractile vacuole (cv), nucleus (nu), pseudopodia (ps), hyaloplasm (h), ectocyst (ec), endocyst (ed), acanthopodia (a), and opercula (o). The isolates belong to the samples SC37_1st (C-E) and SE26_1st (A, B, G, H). Based on 18 S rDNA sequencing data, SC37_1st corresponds to *Acanthamoeba hatchetti* and SE26_1st to *Acanthamoeba* spp. T4 genotype. Scale bar = 10 µm.

Source: By the author.

Trophozoites have shown the branched aspect of pseudopodium, with subpseudopodium protuberances that arose from the hyaline zones (Fig. 3.20, A - D), clearly differing from monopodial pseudopodium seen in *Naegleria* morphology (Fig. 3.17, A - C). The cyst walls of *Acanthamoeba* isolates have shown a wrinkled ectocyst, as in Figure 3.20 (E - H). An opercula is visible in those cysts whose ectocyst (ec) and endocyst (ed) contact each other (Fig. 3.20, E). Moreover, cysts ranged from round (r), square (sq) and star-like (st) shapes, Fig. 3.20, E and G. Likewise, empty (em) cysts were identified in those G and H micrographs (Fig. 3.17).

Free-living amoeba characterization – *Hartmanella* genus

The morphology of *Hartmanella* (= *Vermamoeba*) genus is illustrated in the following Figure 3.21:

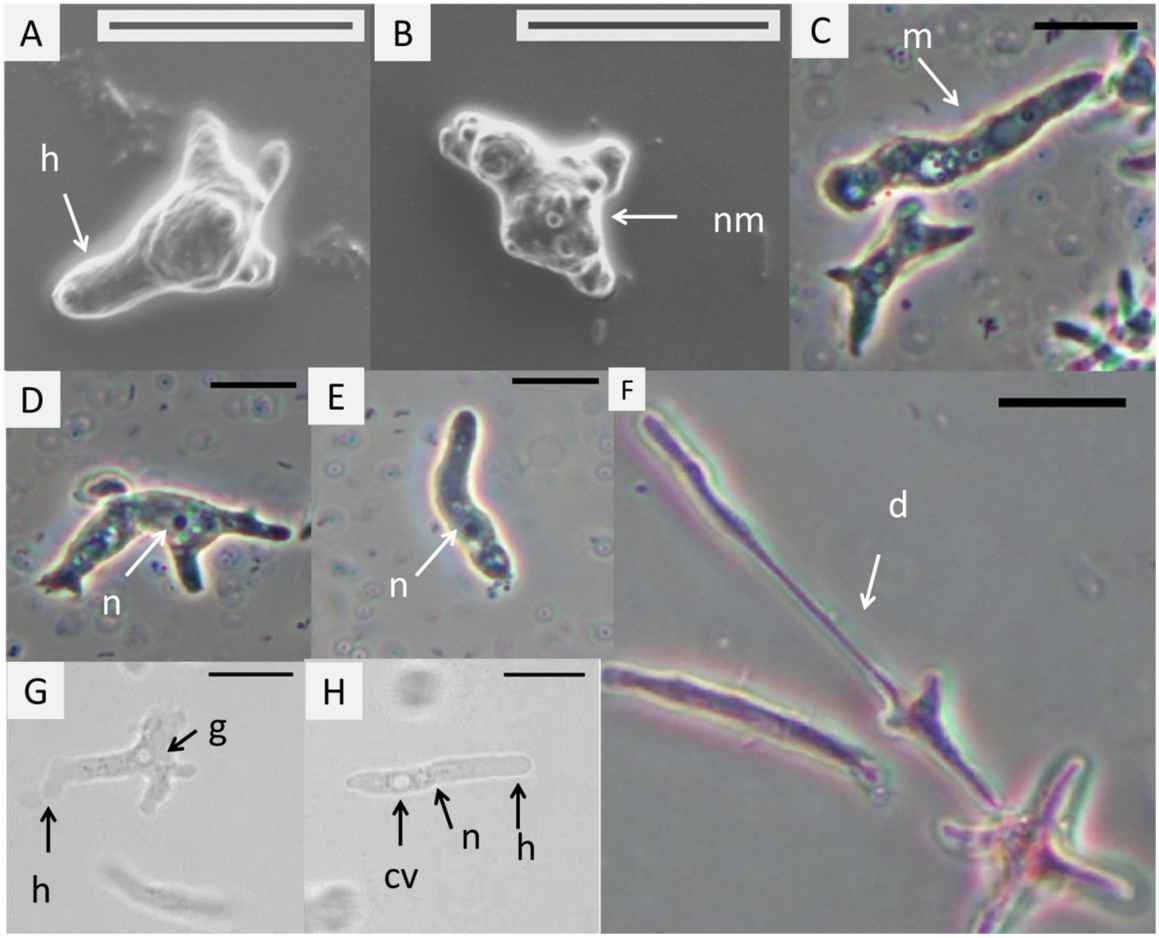

(to be continued)

(continuation)

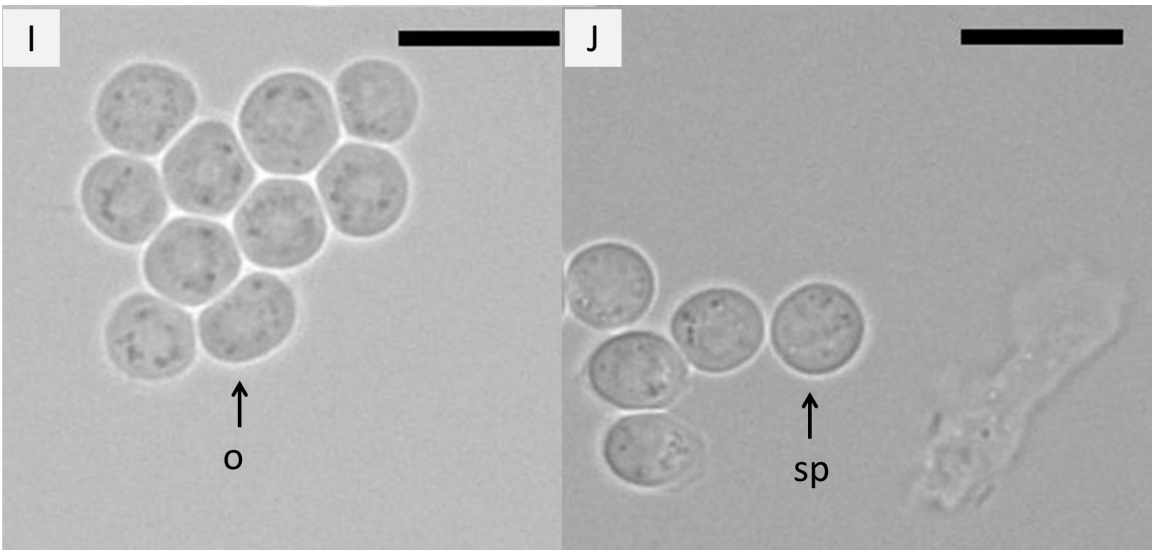

Figure 3.21 - Morphology of *Hartmanella* isolates - scanning electron microscopy (A and B) and light microscopy (C-J) overview. Trophozoites (C-F) and cysts (I and J) were examined through methylene blue stain (C-E), eosin stain (F) and wet mount preparations (I and J). Dividing (d) trophozoites are depicted in micrograph F. Annotations are highlighting contractile vacuole (cv), nucleus (n), hyaline cap (h), granuloplasm (g), dividing cell (d), actively moving (m) and non-actively moving (nm) cells; spherical (sp) and ovoid (o) cysts. The isolates belong to the sample SD44_2nd and, based on 18 S rDNA sequencing data, comprise *Vermamoeba vermiformis*. Scale bar = 10 µm.
Source: By the author.

The *Hartmanella* trophzoites are elongated and monopodial while moving (Fig 3.21, C, D, E and H), assuming other shapes during resting periods (Fig 3.21, A, B, G, and F). Sometimes, lateral hyaline fronts appear before a change in direction (Fig 3.21, D). Cysts are spherical or ovoids, and almost three times smaller than elongated trophozoites on moving (Fig 3.21, I and J).

Free-living amoeba characterization – *Stenamoeba* genus

The morphology of *Stenamoeba* genus is illustrated in the following Figure 3.22.

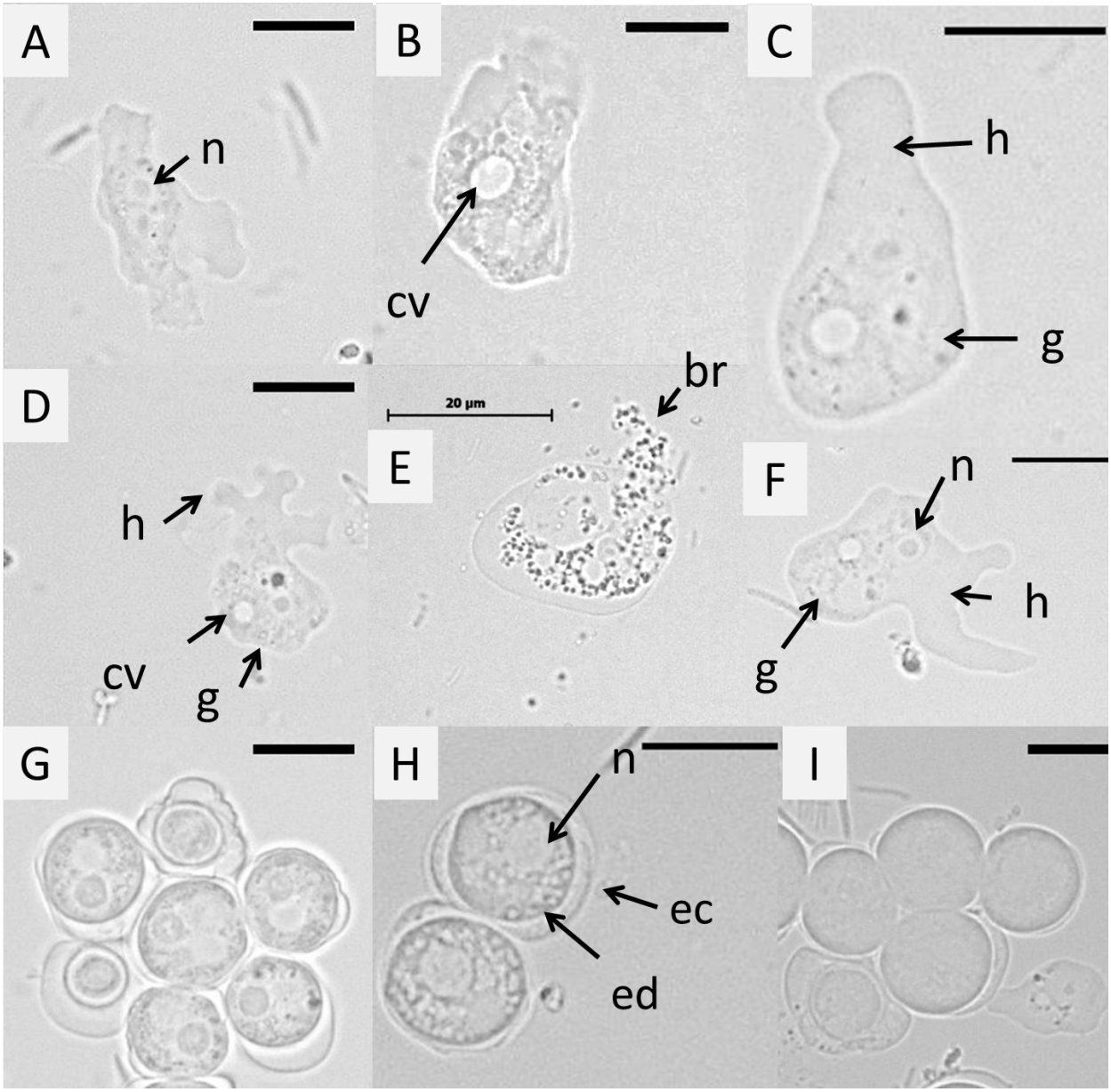

Figure 3.22 - Morphology of *Stenamoeba* isolates - trophozoites (A-F) and cysts (G-I). E - lysed trophozoite illustrating the suggestive bacteria release (br). Annotations are highlighting contractile vacuole (cv), nucleus (n), hyaline cap (h); granuloplasm (g), ectoplasm (ec) and endoplasm (ed). Based on 18 S rDNA sequencing data, these amoeba isolates from SD26_1st_α sample, correspond to *Stenamoeba sp.*. Scale bar = 10 µm.
Source: By the author.

Trophozoites illustrated in Figure 3.22. reveal the distinction between hyaloplasm (h) and granuloplasm (g) zones (Fig. 3.22, C, D and F). A contractile vacuole is distinguishable in the granuloplasm (Fig. 3.22, B,C,E and F) and the nucleus located in the granuloplasm and hyaloplasm boundary (Fig. 3.22, C and F). Occasionally, a branched pseudopodium has been observed (Fig. 3.22, F), as well as a dactylopodia like projections (Fig. 3.22, D). Figure 3.25, F,

illustrates a case in which intra-FLA resistant microorganisms leads to cell lysing and the subsequent release to the outer environment. Cysts stage (Fig 3.25 G to I) are round with two visible walls.

Free-living amoeba characterization – *Filamoeba* genus

A sample of *Filamoeba* isolates is shown in Figure 3.23:

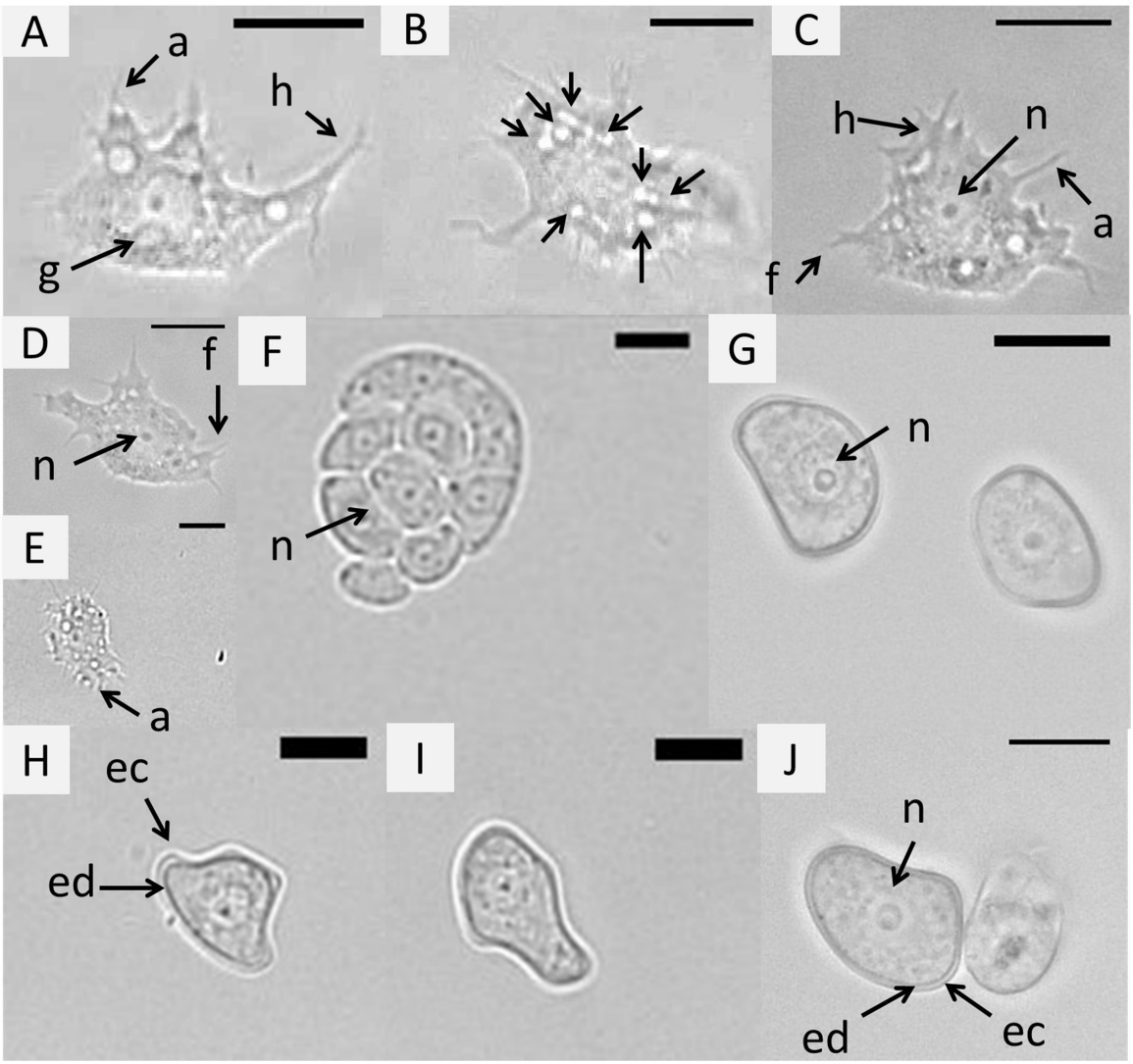

Figure 3.23 – Morphology of *Filamoeba* isolates - trophozoites (A-E) and cysts (F-J).B - multiple arrowed trophozoite demostrates the density of contractile vacuoles. Annotations are highlighting contractile contractile vacuole (cv), nucleus (n), hyaline cap (h), granuloplasm (g), ectoplasm (ec), endoplasm (ed), furcate pseudopodium (f), acanthopodia-like projections (a). Based on 18 S rDNA sequencing data, these isolates from SD26_2nd_β sample, correspond to *Filamoeba sp.*.

Source: By the author.

General characteristics of the trophozoite stage shown in Figure 3.23. called attention to the presence of irregular projections (Fig. 3.23, A - E). Although resembling acanthapodia like pseudopodia (Fig. 3.23, A,C and E), these projections are even finer than acanthapodia seen in *Acanthamoeba* (Figure 3.20.). Cytoplasmic content also shows numerous contractile vacuoles, observed in the granuloplasm of trophozoites (Fig. 3.23, B), and a central prominent nucleus can be easily identified (A-E). The cyst shape shows reniform (Fig. 3.23, G and J) to irregular forms (Fig. 3.23, H and I), uninucleated, with cyst wall separated in two thin layers, ectoplasm and endoplasm without the presence of pores (Figure 3.23, G and J). Cysts were also observed forming groups, as highlighted in Figure 3.23, F.

Free-living amoeba characterization – *Vannella* genus

Typical examples of *Vannella* cells can be observed in Figure 3.24.

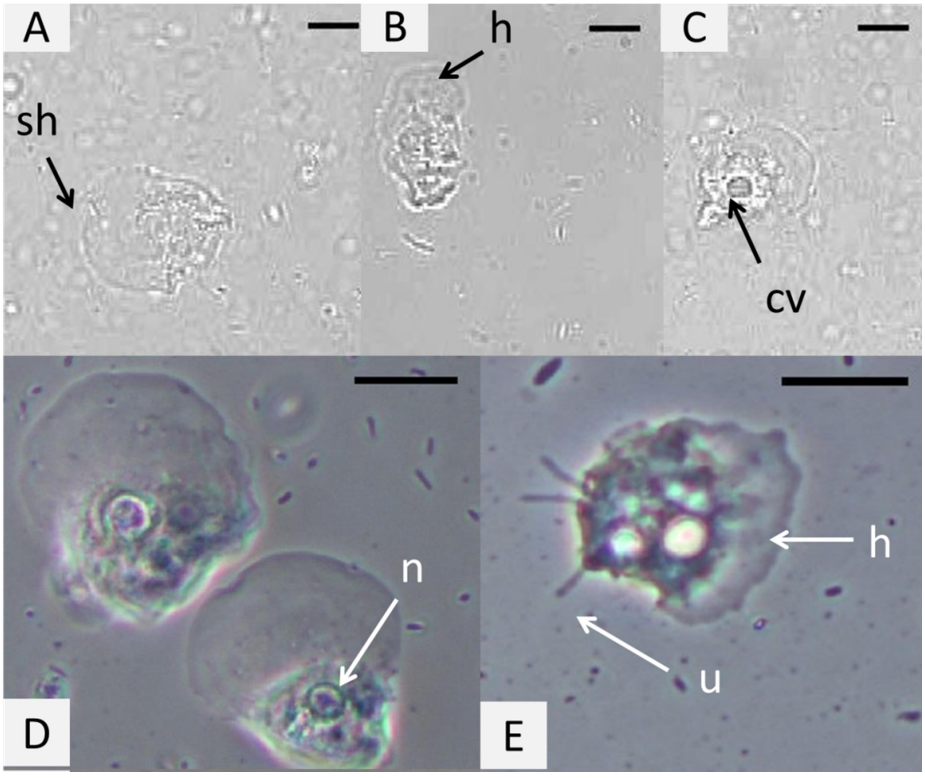

(to be continued)

(continuation)

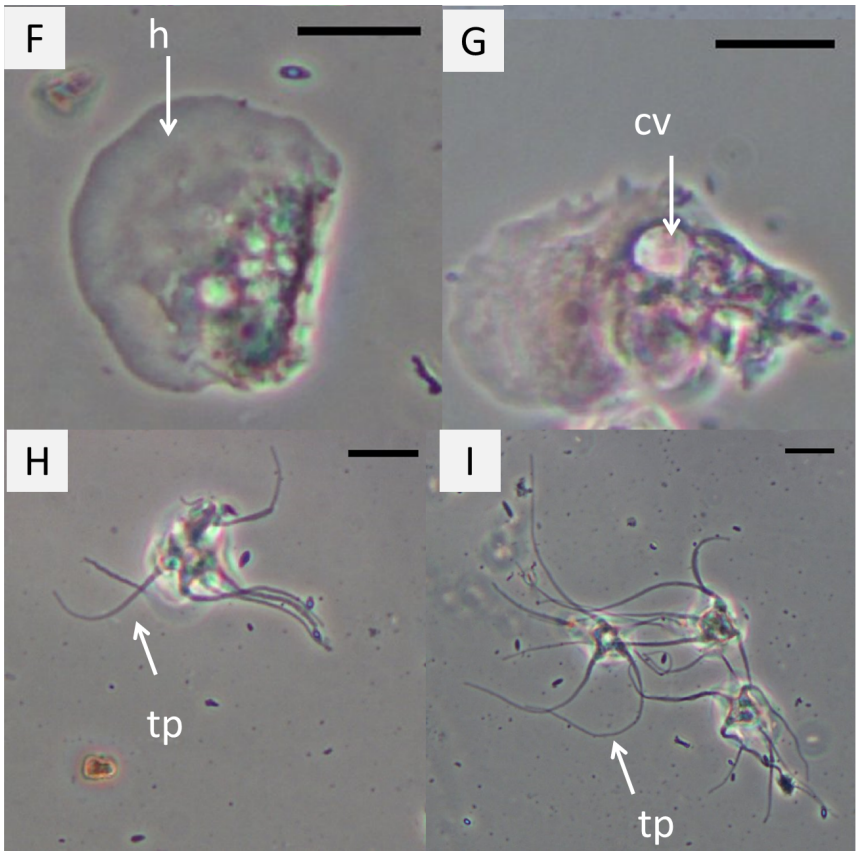

Figure 3.24- Morphology of *Vannella* isolates - trophozoites (A-G) and floating forms (H-I). Wet-mount microscope slides (A – C) and staining slides based on methylene blue (D-F and H-I) and eosin stains (G). Annotations are highlighting contractile contractile vacuole (cv), nucleus (n), hyaline cap (h), a split in the hyaline cap (sh), granuloplasm (g),and tapering pseudopodia (tp). Scale bar = 10 µm. Based on 18 S rDNA sequencing data, these isolates from SD26_2nd_α, correspond to *Vannella sp.* genotype.

Source: By the author.

Vannella trophozoites shown in Figure 3.24 are characterized by a prominent frontal hyaline zone located at the side of displacement of the cell, forming an anterior line semi-circular front (Fig. 3.24, A-G). Cells often present a posterior extension composed of granuloplasm (Fig. 3.24, G) and other cells seemed arch-shaped (Fig. 3.24, F) with no posterior end projection. Hyaline can also split into two main zones in cases of a change in the direction of the displacement (Fig. 3.24, A). The nucleolus is visible observed in methylene blue stained preparations (Fig. 3.24, D). Additionally, star-shaped floating forms were observed with long tapered pseudopodia (figure 3.27, H and I).

Table 3.6 – Comparative morphological data of the free-living amoeba genera isolated in the Monjolinho River. The values represent greatest dimensions to trophozoite and flagellate stages, and it represents the diameter to the cyst stage. Annotations refer to the minimum and maximum lengths (MIN-MAX), the error expresses the standard deviation considering a total of 20 cells measured thrice, the symbol # is indicating lines, and the symbol * indicates the highest intervals between min-max values associated with NNA plate measures. The colors are used to separate values by genera of FLA: *Naegleria*, *Acanthamoeba*, *Hartmanella*, *Stenamoeba*, *Filamoeba* and *Vannella*.

	TROPHOZOITE				**CYST**			**FLAGELLATE**		**Samples**
	#	MIN-MAX (µm)	Average±error (µm)	Method	MIN-MAX (µm)	Average±error (µm)	Method	MIN-MAX (µm)	Average±error (µm)	
Naegleria *(N. australiensis)*	1 2 3	11.65-19.57 11.82-23.81* 12.22-19.88	16.08±0.48 17.04±0.27 17.24±0.1	Staining NNA wet mount	7.73-12.14 7.74-13.87* 9.02-13.68	10±0.23 10.19±0.89 11.05±0.39	Staining NNA wet mount	9.6-18.4 (method: staining)	13.62±0.58 (method: staining)	SE37_2nd SE44_2nd
Naegleria *(N. phillipinensis)*	4	13.84-22.04*	17.74±0.32	NNA	Not a suggestive amount to collect measurements			Not found		SE26_2nd
Acanthamoeba *(A. spp T4)*	5 6	11.04-20.24* 16.03-25	15.17±2.15 20.07±0.72	NNA wet mount	12.35-18.80 12.23-19.49	15.12±0.44 15.17±0.58	NNA wet mount	Not found		SE37_1st; SE26_1rt;
Acanthamoeba *(A. hatchetti)*	7 8	15.73-30.99* 22.25-33.45	22.32±0.52 27.29±1.9	NNA wet mount	13.9-18.9	16.3±0.72	wet mount	Not found		SC37_1nd
Hartmanella	9 10 11	12.25-21.33 13.31-22.43* 12.57-21.55	16.79±0.84 17.64±0.37 16.80±0.94	Staining NNA wet mount	3.75-6.85* 4.2-6.8	4.95±0.21 5.14±0.16	NNA wet mount	Not found		SD44_2nd
Stenamoeba	12 13	13.12-20.08 11.91-18.51	17.18±0.68 15.49±0.52	NNA wet mount	9.86-16.00 8.03-15.49	11.99±0.12 11.76±0.30	NNA wet mount	Not found		SD26_1st
Filamoeba	14	14.88-24.04	18.34±0.89	wet mount	9.67-21.72	15.27±0.39	wet mount	Not found		SD26_2nβ
Vannella	15 16 17	20.46-35.05 19.41-35.19* 20.31-29.48	26.25±1.77 28.56±1.2 25.15±0.53	Staining NNA wet mount	Not found			Not found		SD26_2nα

Source: By the author.

The comparative panel of FLA morphology depicted in Table 3.6 revealed that dimensions obtained with NNA plates analysis commonly recorded the highest length intervals, marked with " * " (Table 3.6). It is suggesting that the remaining wet mount and staining methods are more accurate to perform morphological characterization of cells. For instance, *Naegleria* trophozoites ranged from 12-23 µm when evaluated with NNA plate based approach (Table 3.6, Line 2) and from about 12-19 µm when evaluated with both methods, the wet mount and staining methods (Table 3.6, Lines 1 and 3).

If comparing all amoeba stages, the trophozoites have recorded the largest ranges of dimensions whose variation seem to rely on the methodology employed (NNA plates, staining slides and wet mount). On the contrary, in general, the nearest values of diameter were obtained to cyst stage regardless the methodology employed. For instance, an interval of about 15 µm is recorded to *A. hatchetti* trophozoites evaluated in NNA plates (Table 3.6, Line 7), with a 5 µm of difference to the same stage upon wet mount preparation (Table 3.6, Line 8). However, the variations related to cysts ranked about 1 µm to *Naegleria* (Table 3.6, Lines 1-3) and *Acanthamoeba* (Table 3.6, Lines 5-7) across distinct methods. Basically, to *Stenamoeba*, no variation was remarked to the cyst averages comparing NNA and wet mount methods (Table 3.6, Lines 12 and 13). It indicates that the regular shape of cysts might be an informative discriminator to comprehend taxonomy. Moreover, the absence of cyst stage, as well as the presence of the flagellate stage, are both elucidative to comprehend FLA diversity. *Naegleria* genus is well known by the capability of transforming into flagellate stages, as morphological details documented in Table 3.6, Line 1.

All results summarized in table Table 3.6 were provided from the manual effort of measuring representative micrographs by using the FIJI software, as described in section 2.6.2. (methods). Complementary to this, we have been working on automated detection of cysts towards optimizing the morphological characterization process, as detailed in the next section.

3.2.1.4 Cyst characterization – automated detection

The cyst diameters analyzed for *Acanthamoeba, Hartmanella* and *Naegleria* revealed that the shape is a useful feature that distinguishes among amoeba genera, as mentioned along 3.2.1.3. section. Hence, an automated method to evaluate cyst diameter is been developed,

in collaboration with Prof. Dr. Douglas Cedrin (UFG), based on a machine learning approach, substituting the time-consuming and error-prone manual identification.

Initially, the standardization of the process was made based on tests with the microscopy properties, as the intensity of light and gamma correction. It was performed to obtain a clear contrast between the background and the target cells enabling the software to detect cyst cells, as shown in Figure 3.25.

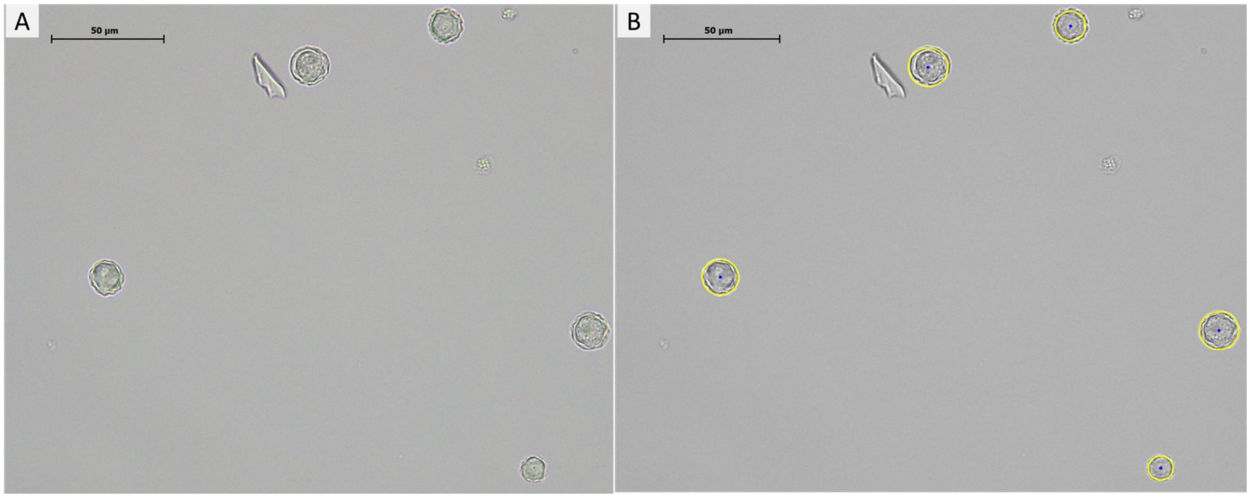

Figure 3.25 – Light microscopy of *A. castellanii* Neff (1) taken as example to set parameters prior to the image acquisition. Yellow rings correspond to automated cyst detection by the software. Scale bar = 50 µm.
Source: By the author.

Similar to *Acanthamoeba* example (Figure 3.25), cycles of optimization and data acquisition of 30 images, resulting in a minimum of 3000 cysts, were recorded to *Naegleria* and *Vermamoeba* whose integrated result is shown in Figure 3.26.

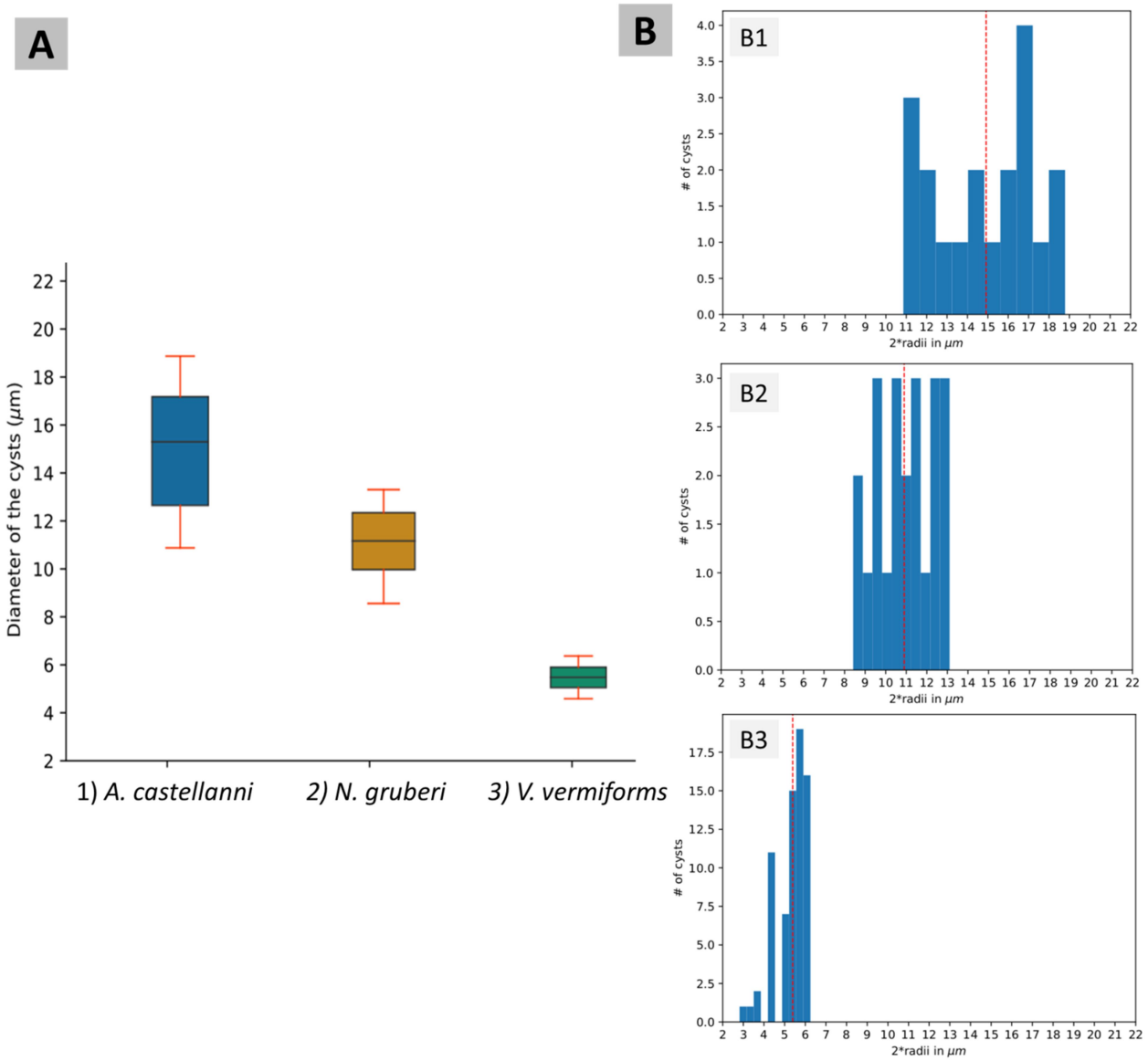

Figure 3.26 – Automated cyst diameter evaluation. A) Boxplot of cyst diameter ranges obtained trhough wet mount preparations. B – The sistribution of cyst diameters to *A. castellanii* (B1), *N. australiensis* (B2) and *V. vermiformis* (B3). In graphs B1 – B3, the number (#) of cysts was divided by 1000 to compose "y" axis.
Source: By the author.

The ranges illustrated in Figure 3.26. (A) are in line with the ranges manually acquired to *Acanthamoeba*, *Naegleria*, and *Vermamoeba* cysts, observed in wet mount preparations, as previously documented in Figure 3.16. However, by investigating in deep each boxplot data, B graphs highlighted three patters of diameter distribution to a minimum of 3000 cysts per sample (Fig. 3.26, B1, B2 and B3). Resultant from the experimental assay conducted here with three representative genera, further steps will be to propagate this analysis with additional FLA targets. Diameter distribution graphs to distinct FLA genera obtained by this pipeline can be assembled to

provide an image databank useful to automated comparisons between a query and the information previously archive on the databank.

The results provided from culturing trophozoites in both, NNA plates (section 3.2.1.1) and culture liquid mediums (section 3.2.1.2), along with the morphology of FLA documented in sections 3.2.1.3 and 3.2.1.4 are discussed in the following section in the light of the current literature.

3.2.2 Morphological examination - DISCUSSION

3.2.2.1 FLA culturing and correspondent morphology into NNA plates

Although there is a trend in the literature to the use of NNA coated with *E. coli* layer, (25,38,46,68,267) our experiments did not reveal an improvement of the FLA growth in the presence of bacterial overlay. This is probably due to the abundance of bacteria already present in the water samples. By monitoring the presence and diversity of amoebas seeded in agar, NNA plate analysis (Figures 3.8 and 3.9) indicated a diversity of FLA in the Monjolinho river samples. Diversity in pseudopodia morphology has been observed (Figure 3.8, samples SE_26 and SD_37 samples), as well as cyst diversity (Figure 3.8, samples SD_44 and SE_37). In regards to the cysts, the recorded diversity allowed inferring more than one FLA species in which a star-like morphology is suggestive of *Acanthamoeba* spp (Fig. 3.8, SE_37) and a rounded regular one can indicate the presence of *Naegleria* cysts (Fig. 3.8, SE_26). Overall, we observed cyst differentiation to NNA cultures whose growth reached density saturation or cultures growing on less hydrated agar surfaces.

Temperature screening demonstrated a distinct thermophilicity of the FLA isolates from different sampling sites, wherein solely D and E samples could withstand 44 ºC, suggestive of pathogenic FLA, since most thermophilic FLA strains have been related to pathogenicity (Table 3.2, Fig. 3.8 and Fig. 3.9).

Another observation provided from NNA plate analysis pointed out fungi and amoeba coexistence, in which groups of trophozoites were visualized attached to hyphae (Figure 3.9, sample SD26_2nd). In the literature (173) it has been proposed multiple reasons for the interaction between fungi and amoeba and most noticeable these interactions would be for

feeding purposes. Studies (59,268) confirmed that distinct fungi structures (e.g.: conidia, hyphae, spore) have been selected as food sources for a variety of FLA. On the other hand, there has been reported a diversity of fungi and bacteria that can resist to amoeba when phagocyted by them. (45,214,269) In the present thesis, most samples have shown a bacterial content as a background layer on the agar surface, and to a lesser extent, fungi contamination (Fig. 3.8 and 3.9.). We argue that this heterogeneous portrait is inherent of the river microbiota that persists when the water is filtered by a 0.22 µM pore size membrane, before seeding on NNA plates. By following the literature recommendation in which subculturing steps have been used as a successful approach leading to axenic amoeba cultures, (36) our results were indicative of fungi eliminating and bacteria reduction (Fig 3.10.). However, even by conducting massively passages of cloning steps, it was not possible to obtain axenic cultures for most of the samples, as demonstrated in the topic 3.2.1.2. To better discuss axenization results, a special section is presented ahead.

3.2.2.2 Axenization and intra-amoebic microorganisms

The probable reason for cycles of bacteria re-contamination into both axenization culture plates and liquid flasks is the possible bacteria content living inside the amoeba, as suggested to *Acanthamoeba* (Fig. 3.12) and *Stenamoeba* (Fig. 3.22, E) isolates. Moreover, even using antibiotic based treatments, amoeba cultures kept with the suggested intra-FLA content. Only the SD44_^{2nd} sample, from the *Hartmanella* genus, was successfully axenized. As proposed by the literature, (15,32) the difficulty of controlling contamination is aggravated taking into account the identification of more than one bacteria genus infecting amoeba strains. Some examples of bacteria strains already isolated from *Acanthamoeba* include *Heliobacter pylori*, known to cause gastric infections that can evolve to cancer, (123) *Campilobacter spp*. associated with human enteritis, (270) and *Legionella pneumophila* with lung inflammation complications. (271) Related studies demonstrated that about 20% of *Acanthamoeba* isolates harbor a type of bacteria. (54) Relevance to this intra-FLA microorganisms is the dual-threat that they can pose to human health, potentially worsening of diseases by combining the infection caused by the amoeba, in addition to the bacterial infection, as described by a *Legionella* infected *Acanthamoeba* spp. provoking pneumonia due to this association. (54) Such association may be advantageous to the bacteria by protecting it from antibacterial activities (19,104) as reported to *Acanthamoeba* spp.

co-infected with *Stenotrophomonas maltophilia*. (102) The bacterial community encountered as amoeba endocytobionts has been named amoeba-resistant bacteria (ARB) and among them, there are multidrug-resistant bacteria. (129,170) Among reasonable strategies proposed by the literature to overcome the issue, a Brazilian study (177) concerned on *Acanthamoeba* argued that transforming trophozoites to a monoxenic culture of cysts, along with micromanipulation, enhanced the success on obtaining amoeba in axenic cultures.

3.2.2.3 Taxonomy overview of FLA isolated in Monjolinho River and its correspondence with the literature

Morphological features were examined on this thesis based on NNA plate observations along with staining slides and wet mount preparations, as complementary techniques that demonstrated to be more accurate to reveal minor details of each FLA stage (cysts, trophozoites, and flagellates). Among them, cysts seemed to be more elusive to discriminate among FLA genera when compared to the greatest trophozoite dimensions, which revealed huge variations in the length according to the method of analysis.

We propose a discussion of FLA morphology consisted of: (A) results recorded into the present thesis, (B) its corresponding morphology reported in the amoeba classification guide proposed by F. C. PAGE, and (C) additional data available in the literature that reinforced placement of isolates on their respective genera. This comparison is outlined here, according to amoeba genera.

The main morphological characters obtained on this thesis to *Naegleria* genus are shown in Figure 3.27, in comparison with the literature findings.

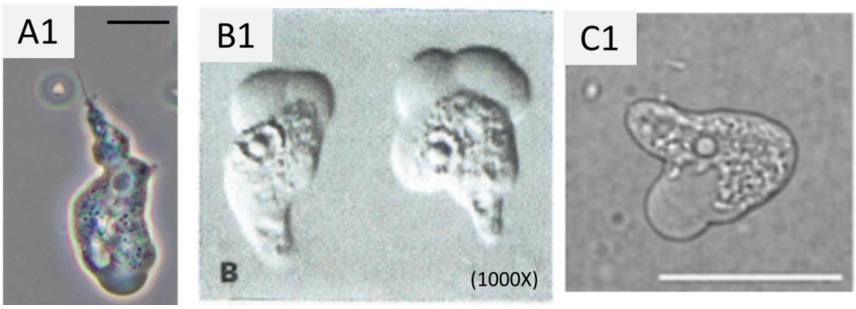

(to be continued)

(continuation)

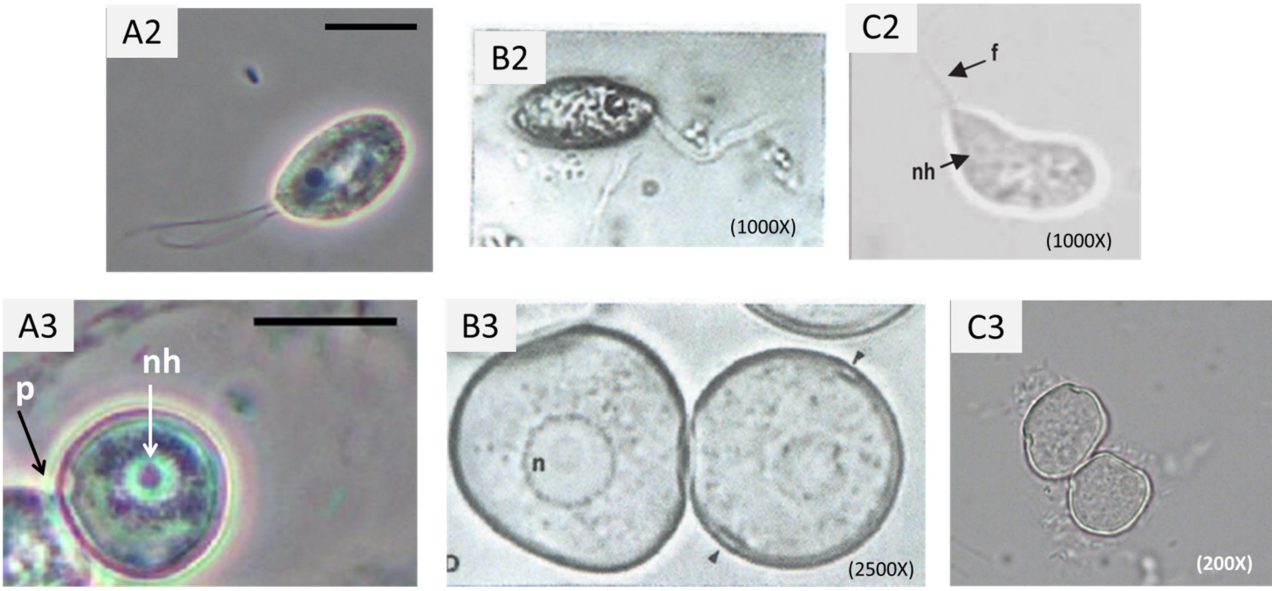

Figure 3.27 - The landscape of *Naegleria* spp. morphology based on light microscopy images acquired by the author (A), reported in the PAGE classification guide (B), and additional FLA literature (C1- (24); C2 – (145) and C3 - (272)). nh- nucleus with halo; f – flagella; p – pore. Black and white scale bars = 10 µm.
Source: A1-A3: By the author; B1-B3: Adapted from PAGE[24]; C1: adapted from LIANG *et al.*[25]; C2: Adapted from INIT *et al.*[143]; and C3: Adapted from REYES-BATLLE *et al.*[262]

The eruptive pseudopodia, which is characteristic of the locomotive activity of *Naegleria* like vegetative stage, (25,26) was visualized to all trophozoites displayed in Figure 3.27, A1, B1, and C1. *Naegleria* is termed as a "limax" amoeba in recognition to the monopodial cylindrical amoeba forms, according to F. C. PAGE (23), as well termed as limacine by the literature (25) due to the eruptive locomotion advancing in a unidirectional region. Uroidal filaments, as seen in Figure 3.27, A1, are structures associated with amoeba moving, posterior filaments as adhesion point or focal contact, (23) often accompanied by trailing filaments.(26) In the literature, (24,26) *Naegleria* trophozoites commonly ranged from 10-25 µm, and in this thesis from about 11-19 µm to *N. australiensis* (Table 3.6, Line 1 to 3) and 13-22 µm to *N. phillipinensis* (Table 3.6, Line 4). *Naegleria* isolates obtained on this work presented different capability of transforming to flagellates, in which only *N. australiensis* has shown the amoeboflagellate form, commonly biflagellates (Figure 3.27._A2). Likewise, FLA isolates from irrigation water samples (272) reinforced the enflagellation capability to *N. australiensis* (Figure 3.27._C2), as well demonstrated to *N. gruberi* strains (Figure 3.27._B2), according to the Page´s amoeba classification guide. (23) In the guide, (23) *Naegleria* flagellates normally range from 10-16 µm resembling the dimensions recorded on this thesis, whose flagellates ranged from 9-18 µm (Table

3.6, Line 1). Although *N. philippinensis* was included in enflagellation tests, it did not transform into flagellates (Table 3.6, Line 4). In regard to the resistance stage, typical features of *Naegleria* cysts comprise a double smoothed wall, pores used to amoeba excystment (Fig 3.27, A3-C3), and often visible nucleus with the conspicuous nucleolus.(26) In the literature, *Naegleria* cysts commonly ranged from 7-14 µm, (24) and to the present work, it ranged from 7-12 µm to *N. australiensis* (Table 3.6, Line 1). Samples of *N. phillipinensis* did not present a suggestive amount of cysts to enable its measurement (Table 3.6, Line 4).

In regard of *Acanthamoeba* genus, trophozoites revealed finer projections to the outside of hyaline lobes Figure 3.28. (A1-C1), named spin-like protuberances, or acanthopodia. (51)

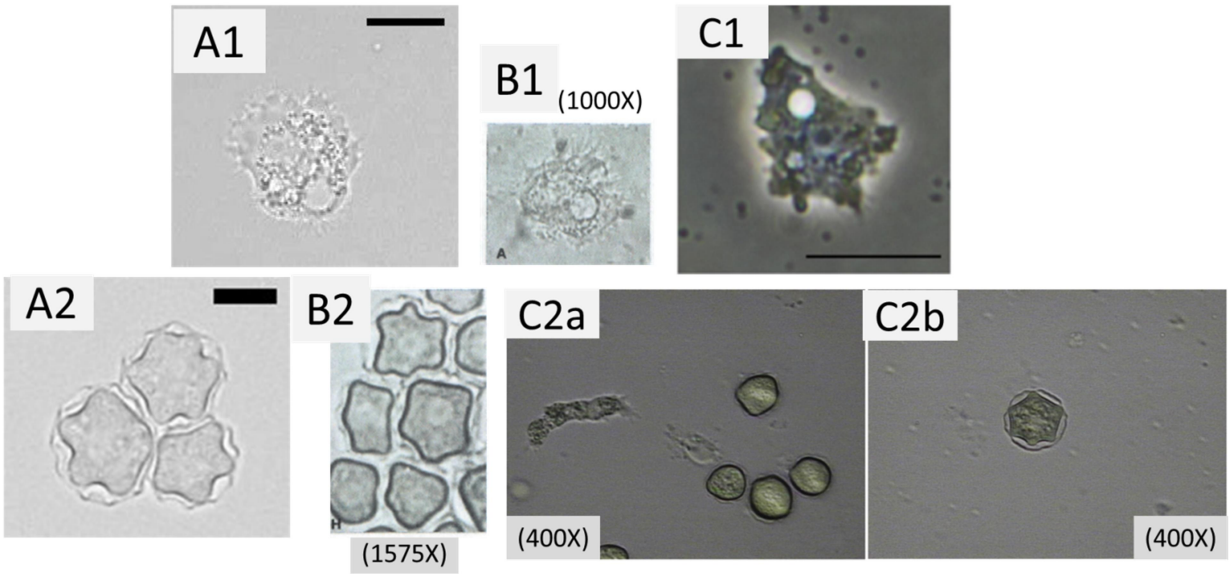

Figure 3.28 – *Acanthamoeba* morphology landscape based on light microscopy images acquired in the present thesis (A), reported in PAGE classification guide (B) and in additional FLA available literature (C1-(273) and C2 –(218)) . Black scale bars represents 10µm (A1, A2) and 20 µm (C1).
Source: A1-A2: By the author; B1-B2: Adapted from PAGE[24]; C1: Adapted from CHAVETTE *et al.*[263]; C2: Adapted from CARRIJO-CARVALHO *et al.*[208]

Acanthamoeba trophozoites are well-known by a sluggish moving stile, (33) besides being larger and more compressed than limax amoebas. (23) Literature findings reported lengths of 15-25 µm to *A. castellanii* T4 isolate, (24) and 14-40 µm (26) to *Acanthamoeba* spp.. In this thesis, we obtained 16-25 µm to *A.* spp T4 and 22-35 µm to *A. hatchetti* (Table 3.6, Lines 6 and 8, respectively). The pleomorphism is inherent of *Acanthamoeba* cysts, forms consisting of round and stellate like shapes, (218) whose diversity was depicted in Figure 3.28. (C2a and C2b), as well as illustrated in our findings (Figure 3.20, E to H). *Acanthamoeba* cyst diameters generally

ranked from 10 to 25 µm, (26) and on this thesis, it ranged from about 12-19 µm (Table 3.6, Lines 6 and 7). Most cysts contain evident pores, also termed ostiole, (51) that can be formed in the confluence of inner and out cyst walls, being closed by an opercula, (23) as shown in Figure 3.20, E. Ectocyst and endocyst regions of contact are also named arms, always equivalent to the number of pores, and primary morphological based taxonomy suggested the number of arms as a discriminator to classify *Acanthamoeba* spp. into three major groups (I, II, III).(23,177,230) Presently, studies concerned with resolving differences within *Acanthamoeba* isolates have been using modern non-morphological based taxonomy, mainly based on 18S rDNA sequencing. (274)

In regard to *Hartmannella* (=*Vermamoeba*) morphology, features are resumed in Figure 3.29.

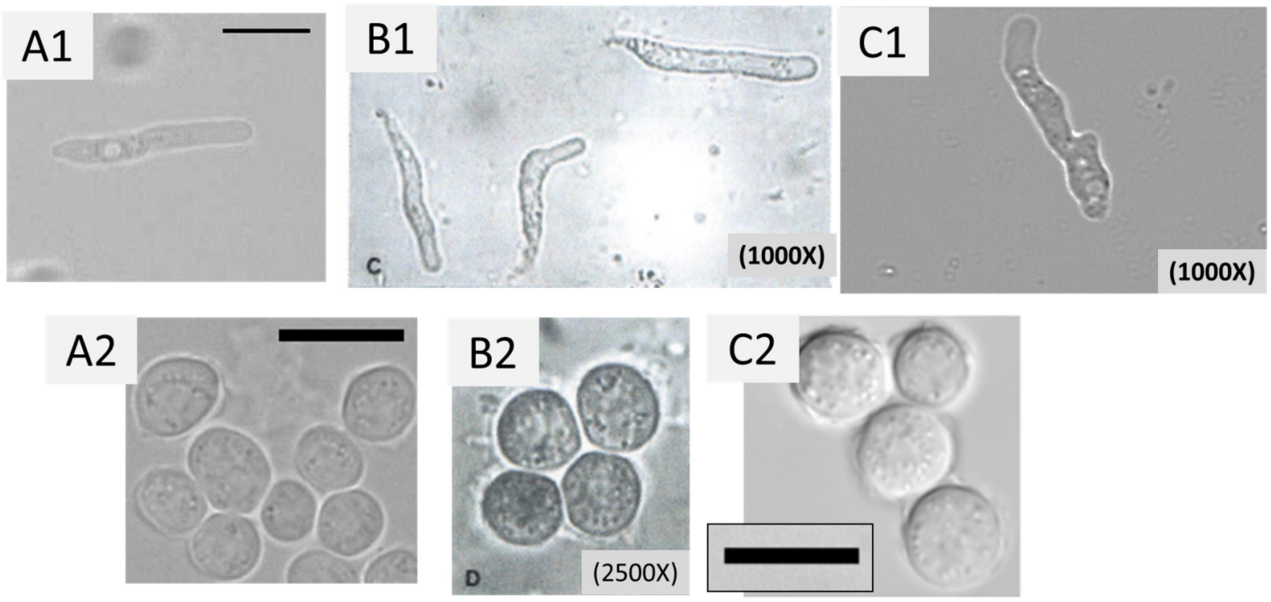

Figure 3.29 – *Hartmannella* morphology landscape based on light microscopy images acquired in the present thesis (A), reported in PAGE classification guide (B) and additional FLA available literature (C1- (275) and C2 - (167)) . Scale bars - 10µm.
Source: A1-A2: By the author; B1-B2: Adapted from PAGE[24]; C1 and C2: Adapted from REYES-BATLLE *et al.*[229]; and SAMBA-LOUAKA *et al.*[162], respectively.

Vermamoeba genus, grouped as a limax amoeba, can be distinguished from *Naegleria*, as well as a limax amoeba, due to the absence of eruptive pseudopodia in *Vermamoeba* trophozoites, (23) according to Figure 3.29. (A1 – C1). Althoug secondary pseudopodium emissions can be seen to *Vermamoeba* (Fig 3.21, E and H), the monotactic moviment is more

common. (29) Trophozoite dimensions commonly range from 12 – 37 µm, (23) in which our data is compliant with, due to dimensions varying from about 12-22 µm (Table 3.6, Lines 9 to 11). Regarding the cyst stage, its outline can be rounded to ovoid, double layered, (241) and occasionally forming groups, as demonstrated in Figure 3.29 (A2-C2). In the literature, cysts diameters ranged from 4.4 to 9.5 µm.(33) Our results recorded min and max values of 4.2 to 6.28 µm (Table 3.6., Line 10).

To the morphology of *Stenamoeba*, the discussion does not contain data collected from PAGE´s classification guide, since the Thecamoebidae family, to which *Stenamoeba* belongs, (276) is not included on it. Thecamoebidae family also gathers *Sappinea* and other naked lobosea amoebas, as *Techamoeba* genus. (277) These are striate and rugose amoebas, discriminated by a lingulated or polytatic shape. (277) *Stenamoeba* morphology is resumed in Figure 3.30.

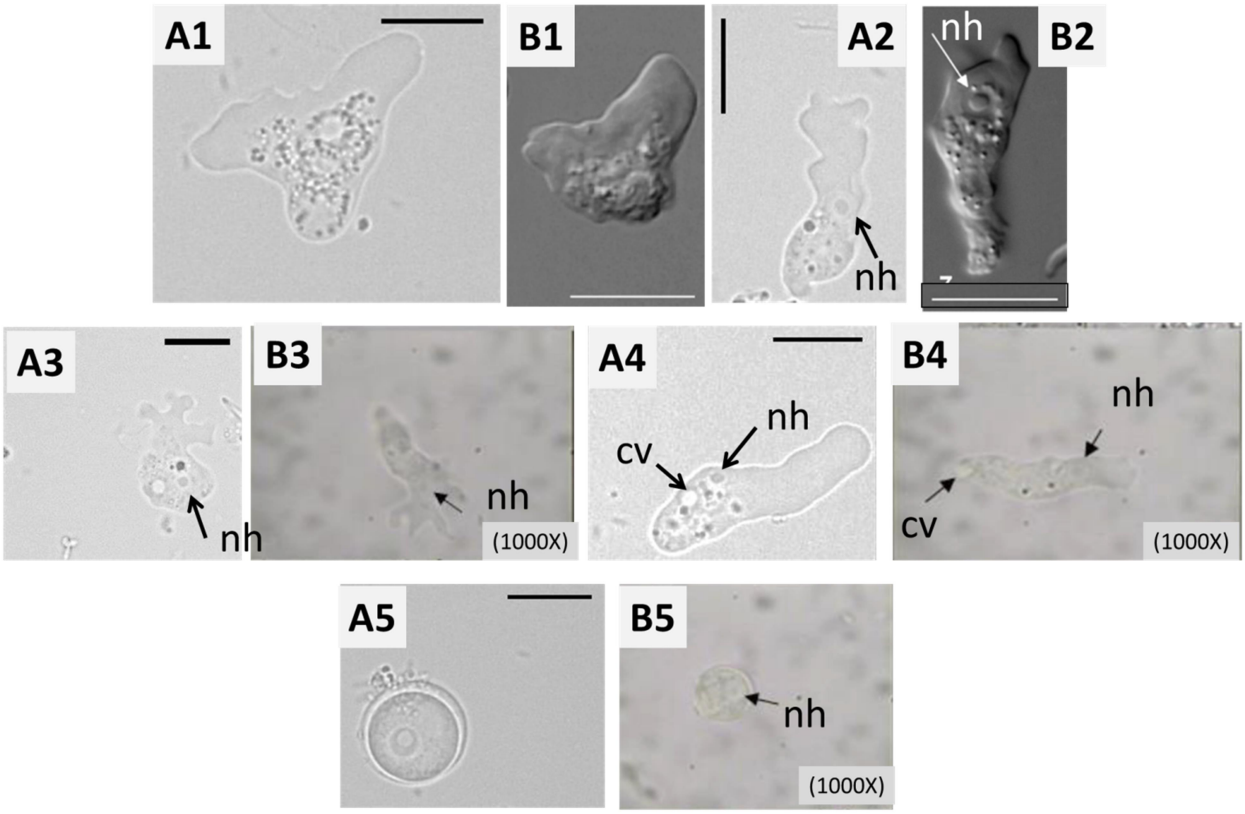

Figure 3.30 - *Stenamoeba* morphological landscape based on light microscopy images acquired in the present thesis (A), and reported in FLA available literature (B1, B2 - (278)and B3, B4, B5 –(279)) . nh- nucleus with halo; contractile vacuole. Black and white scale bars represent 10µm.

Source: A1-A5: By the author; B1-B2: Adapted from GEISEN *et al.*[268]; B3-B5: Adapted from BORQUEZ-ROMÁN *et al.*[269]

Stenamoeba moving forms are recognized with an oblong to fan-shaped outline, (278) as in Figure 3.30 (A1-B4). The granuloplasm of trophozoites is commonly placed in the terminal end of the cell, and the hyaloplasm, whose proportion can reach half or more of whole cell size, occupies a huge portion of the anterior area, (278) as shown in Figure 3.30., A2 and A4. Likewise, similar features can be seen in Figure 3.22., C, D and F. Contractile vacuole number (one), its corresponding position (posterior end), and nucleus position (the boundary of hyaloplasm and granuloplasm) registered to *S. sardiniensis,* shown in Fig. 3.30, B2, (278) and *S. dejonckheerei,* shown in Fig. 3.30, B4, (279) were similarly observed to the Monjolinho River isolates, illustrated in Fig. 3.30, A2 and A4. Moreover, dactilopodia-like pseudopodia (279) was identified to the literature provided isolate (Fig. 3.30, C3), as well as trophozoites collected on this thesis (Fig. 3.30, A3). Trophozoites greatest dimensions of 13-24 µm and 15-29 µm were attributed to *S. sardiniensis* and *S. limacina*, respectively. (278) Cysts are double walled and rounded with an average of 10 µm diameter to *S. sardiniensis* (278) and *S. dejonckheerei*. (279) No cysts were seen to *S. limacine*.(278) Our isolates ranged from 11-18 µm and 8-15 µm, respectively to trophozoite and cyst stages (Table 3.6, Line 13). Although we performed many attempts to axenizate *Stenamoeba*, the process was not achieved to this genus likely due to bacteria contamination provided from intra-amoebic microorganisms as we suggest in Figure 3.22, E. The literature, as well as using the most suitable media to FLA growth, reported the same difficulty on axenization of *Stenamoeba* isolates.(279)

In regard of *Filamoeba*, its morphology is summarized in Figure 3.31:

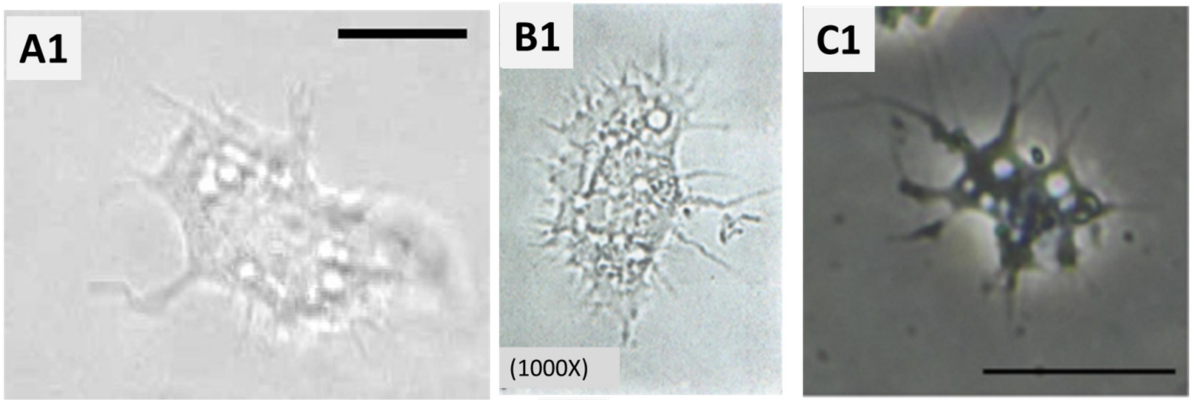

(to be continued)

(continuation)

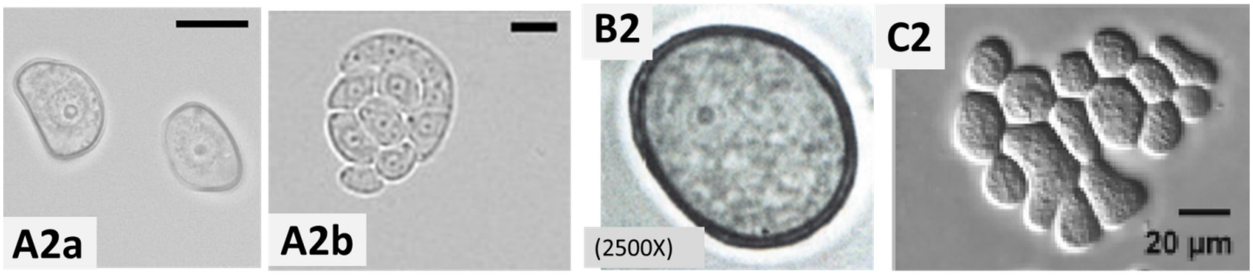

Figure 3.31 - *Filamoeba* morphology landscape based on light microscopy images acquired in the present thesis (A), reported in PAGE classification guide (B) ,and in additional FLA available literature (C1 - (273) and C2 – (280)) . Black scale bars represent 10µm (A1 - A2b) and 20 µm (C1).
Source: A1-A2: By the author; B1-B2: Adapted from PAGE[24]; C1: Adapted from CHAVATTE *et al.*[263]; C2: Adapted from PECKOVA *et al.*[270]

The hyaline zone contains a large number of spine-like subpseudopodia, rather than an evident lobule, (277) although lobulated *Filamoeba* spp. have been previously disclosed to few cases. (23) The general outline of *Filamoeba* comprises irregularly shaped trophozoites, sometimes elongated in the posterior end (Figure 3.23, A) or semi-circular in the hyaline front (Figure 3.31. B1), and no clear boundary is seen between the granuloplasm and the hyaloplasm (Fig. 3.31, A1 to C1). The multibranched pseudopodia is suggested by the literature as acanthopodial morphotype,(281) or filiform subpseudopodia.(23) We observed a large number of contractile vacuoles (Figure 3.23, B), in accordance with the description in Page´s classification guide, in which trophozoites with about 15 contractile vacuoles have been noted to *Stenamoeba* isolates.(23) Cysts are ranging from circular, ovoid, or reniform, as proposed by the latest identification of a new *Filamoeba* specie, *Filamoeba sinensis* (280) and as well observed on this thesis (Fig. 3.31, A2a and A2b). Dimensions comprised intervals of 15 to 50 µm and 8 to 15 µm, respectively to trophozoites and cyst stages, (23) and our isolates ranged from 14-24 µm and 9-21 µm to trophozoites and cyst respectively (Table 3.6, Line 14).

Figure 3.32. comprises the most representative morphological features typical of *Vannella* spp..

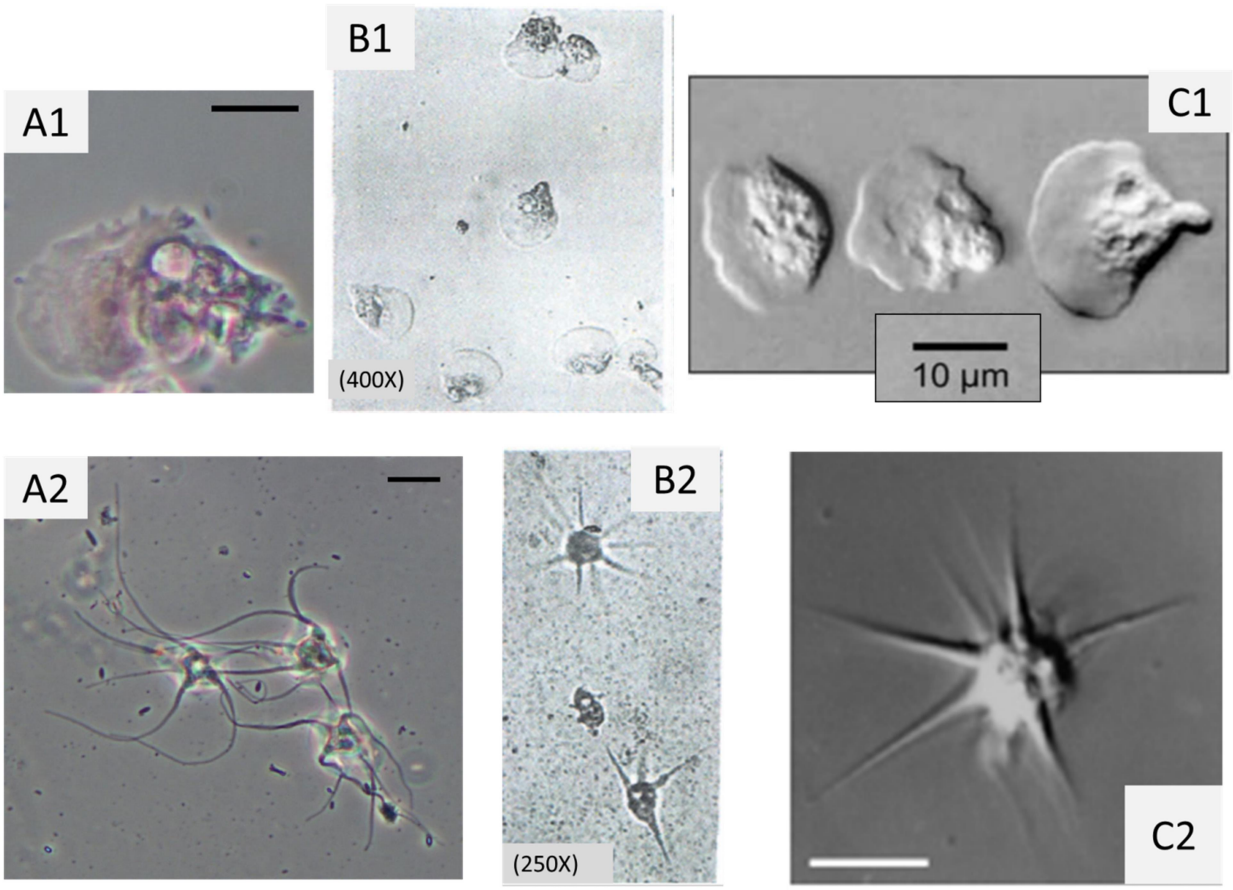

Figure 3.32 - Landscape of *Vannella* morphology based on light microscopy images acquired in the present thesis (A), reported in PAGE classification guide (B), and in additional FLA available literature (C1- (282) and C2 –(27)). Black and white scale bars = 10µm.

Source: A1-A2: By the author; B1-B2: Adapted from PAGE[24]; C1: Adapted from DYKOVÁ *et al.*[272]; C2: Adapted from SMIRNOV *et al.*[28], respectively.

The hyaloplasm of *Vannella* trophozoites is predominantly positioned in the frontal area of the cell, (24) occupying 1/3 to half of cell size,(31) as illustrated in Figure 3.32. (A1-C1). Due to presenting flattened pseudopodia, the trophozoite outline is commonly termed fan-shaped. In locomotion, the hyaloplasm produces a crescent-shaped outline.(29) A remarkable feature of *Vannella* spp., is the tapering pseudopodia typical of floating forms, (23) whose outline is also referred to star-shaped, (31) and the length can exceed three times the trophozoite dimensions. (23) Our results, consistent with the literature findings (Figure 3.32, B2, and C2), depicted such floating form outlines (Figure 3.32, A2). Trophozoites commonly ranged from 15-25 µm length to *Vanella spp.*, reported in FLA isolates from rice field samples. (24) Larger ranges were recorded to *V. lata* and *V.cirrifera* with 24 to 46 µm, and 25 to 55 µm, respectively. (23) Our results revealed *Vanella* dimensions of 20-35 µm to trophozoites (Table 3.6, Line 15). No cyst

form was observed to *Vannella* isolates in the present work (Table 3.6, Line 16), a result demonstrated in related studies.(124,273)

In regard to FLA cysts, the proposed automated approach to detect and measure cysts (Figure 3.26) may help to remove manual effort on qualitative evaluating cyst images, as well as to optimize analysis conducted with huge data sets. However, intraspecific comparisons remain a challenge to be overcome by the software (e.g.: the distinction between *N. australiensis* and *N. philippinensis*). So far, our methodology, still in progress, can be assessed as a prior step to select molecular targets of PCR to further access species-specific information. To a major extent, we expect to use the software approach to build a cyst diameter distribution dataset to be available to the FLA community to classify isolates onto corresponding genera and even species, based on cyst features. To the best of our knowledge, there is no such tool in the FLA field. Although the computational approach is currently in progress, we expect that investigative slides with unknown cysts and its distribution ranges would be compared against the diversity of portraits from the data bank that is being settled. Moreover, preliminary results with software development demonstrated to bring improvements to further morphological studies on FLA taxonomy, as it provided an updated strategy to report cyst diameter intervals taking into account the inner distribution of diameters, information unexplored by PAGE's Classification guide.

To sum up, the morphological features evaluated to each FLA genus along this work demonstrated to be potential discriminators to classify the isolates in its corresponding genera, even to the extent of species (e.g.: flagellation capability typical of *N. australiensis*). However, the current literature (15,46,47,227-228,230,273-274) is combining mitochondrial based analysis as complementary data to define FLA taxonomy, commonly accessed with transmission electron microscopy (TEM). Although this ultrastructural morphology analysis was not included here, the literature has been using transmission electron microscopy as well to comprehend the intra amoebic microorganisms diversity, meanly in respect of amoeba as a host to virus replication,(204,212,217) and amoeba as a container to fungi spore (285) and bacteria. (286) Moreover, interaction processes between FLA and its host during an infection onset have been elucidated with TEM, as to *Acanthamoeba* keratitis in vitro analysis.(287-288) Nonetheless, in the present thesis, light and electron scanning microscopy also demonstrated to be useful to assess distinct cell processes occurring in FLA. For instance, excystation process (Fig 3.17, M), floating form presence (Fig. 3.32, A2), cell division (Fig. 3.21, F), amoeba cell lysis potentially

evoked by microorganisms infecting trophozoites as suggested in both Fig. 3.12 and Fig. 3.22, E. Moreover, a diversity of amoeba shape and cysts forms could be evidenced on this thesis, and cell dimensions recorded to our isolates were comparable with related supporting literature as described in the present discussion (section 3.2.2.3).

Morphological findings aforementioned were confirmed through complementary molecular investigation whose details are presented in the following topics.

3.3 Molecular approach

3.3.1 Molecular approach – RESULTS

Initial steps to perform the molecular characterization of FLA isolates included the validation of the DNA extraction method by using environmental DNA (eDNA) extracted from the D sampling site, SD. This study enabled us to select Power Soil Kit as the most efficient method according to results shown in Table 3.7. and Figure 3.33.

Table 3.7 - DNA concentration and absorbance rates of eDNA extracted from the D sampling site. Ratios 260/280 and 260/230 indicate protein and acid contaminations, respectively. Values were recorded with an UV-Vis Nanodrop spectrophotometer.

Methods	DNA concentration (ng/µl)	A_{260}/A_{280} rate	A_{260}/A_{230} rate
1 – KASVI Kit	500.1 ± 10.87	2.03 ± 0.06	1.95 ± 0.07
2 – Phenol-chloroform	572.57 ± 25.91	1.66 ± 0.15	1.58 ± 0.11
3 – Power Soil Kit	772.84 ± 15.45	1.87 ± 0.09	2.18 ± 0.18

Source: By the author.

Taking into account that all methods employed the same water volume of the site D, the highest DNA concentration recorded to Power Soil extraction is more efficient on treating samples containing significant levels of organic matter, characteristic of this site (Table 3.7, Line 3). Going further on verifying the DNA availability and stability to allow a proper downstream application we also investigated the DNA amplification patterns on PCR reactions targeting *Acanthamoeba* spp.. By using the CRNS/373r nucleotide primer pair (Table 2.3, page 77), PCR products were electrophoresed and the corresponding results are illustrated in Figure 3.33, A,

accompanied by the amplicon length prediction, by using Genbank reference sequence (Fig. 3.33, B).

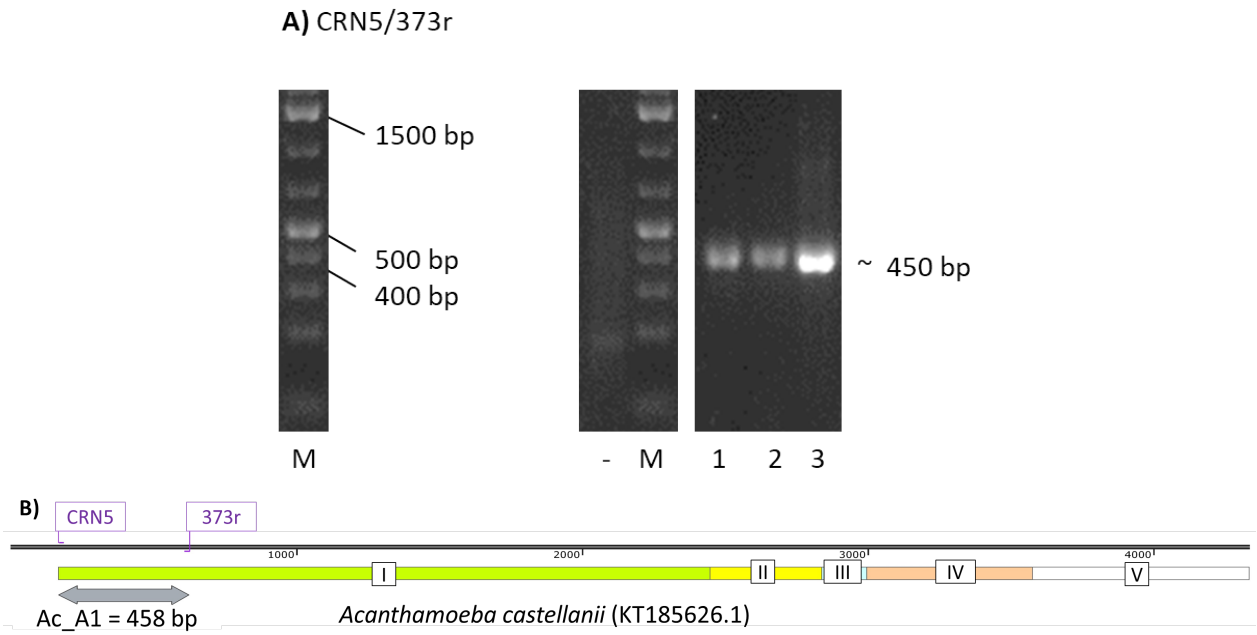

Figure 3.33 – Amplification of *Acanthamoeba* 18S rDNA gene by using CRN5 and 373r primer pair. (A) 2% Agarose gel revealing amplicon bands obtained from eDNA samples extracted with KASVI Kit (Lane 1), Phenol-chloroform (Lane 2) and Power Soil Kit (Lane 3) methods. Negative control (-) refers to DNA-free water sample, and the molecular marker (M) refers to DNA ladder PCRBio Ladder IV; (B) Partial ribosomal DNA sequence of *Acanthamoeba castellanii* (Genbank KT165626.1). Highlighted regions correspond to 18S rRNA gene (I), ITS1 (II), 5.8S rRNA gene (III), ITS2 (IV) and 28S (V). Grey arrowed region indicates the target amplicon (A1) of about 450 base pairs (bp) length.
Source: By the author.

As shown in Figure 3.33. (A), Power Soil Kit called attention due to the highly intense amplification band (Fig 3.33. - A, Lane 3), assuming a 200 ng DNA template as a constant DNA input concentration to all reactions. After accomplished the initial screening towards the selection of a suitable DNA isolating treatment, PCR amplifications were conducted as follows.

3.3.1.1. PCR and electrophoretic analyses

The DNA extracted from the D sampling site was selected as a target to test the list of nucleotide primer pairs of interest (Table 2.3, page 77) and to evaluate PCR cycling effectiveness. The positive control consisted of an equivalent D site water sample with added *Naegleria gruberi* (ATCC) 30224 culture. Samples with and without added *N. gruberi* were

named +D and D respectively. A DNA sample extracted directly from *N. grube*ri (ATCC) 30224 axenic culture was included in the PCR reactions as the second positive control, termed +N (Fig. 3.34).

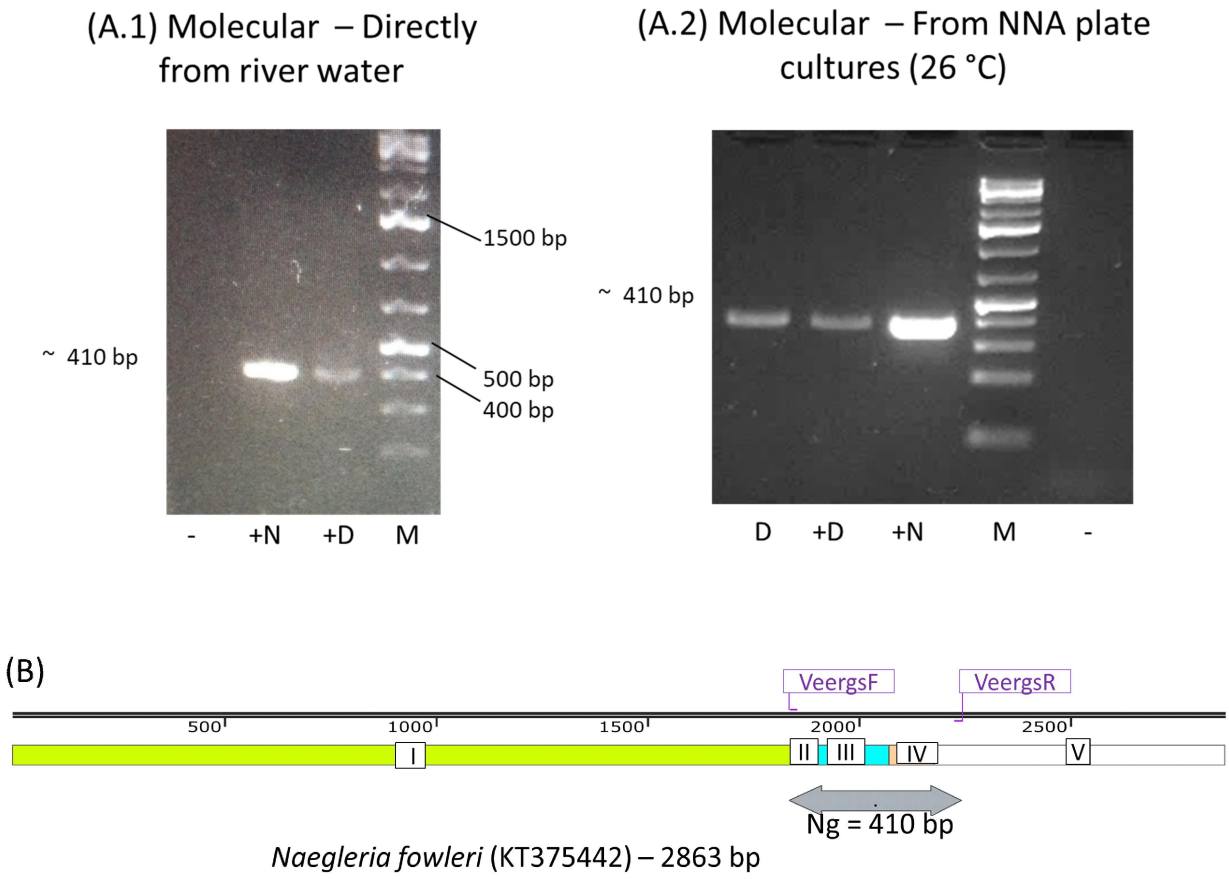

Figure 3.34 - Validation of river water pre-processing steps. 2% agarose gel with PCR results to *Naegleria* evaluating DNA samples extracted directly from river water (A.1), and NNA cultures (A.2). Positive controls consisted of river water from D sampling site supplied with *N. gruberi* (+D), and *N. gruberi* DNA extracted from axenic culture (+N). The negative control (-) consisted of a DNA-free water solution. Figure B with the in silico prediction of the expected amplicon length (gray arrowed region). I - 18S rRNA gene; II - ITS1; III - 5.8S rRNA gene; IV - ITS2; V - 28S gene.
Source: By the author.

The results in Figure 3.34. A1 and A2 have shown the amplification of a band of approximately 410 bp in samples of DNA extracted from the site D that had added *N. gruberi* DNA (+N) or whole cells (+D) showing that the extraction method does not inhibit the PCR amplification. The DNA band obtained from the target D sampling site (Fig. 3.34, gel A2, lane D) was analyzed by nucleotide sequencing and revealed a 100% identity with *Naegleria*

australiensis. Thus, the molecular characterization of FLA isolates to the remaining sampling sites and the remaining PCR targets are described as follows.

First, *Naegleria* based PCR reactions performed with eDNA from Monjolinho River resulted in a diversity of five species, N1 – N5, retrieved from A-E samples in the first sampling. Figure 3.35 illustrates the most representative results.

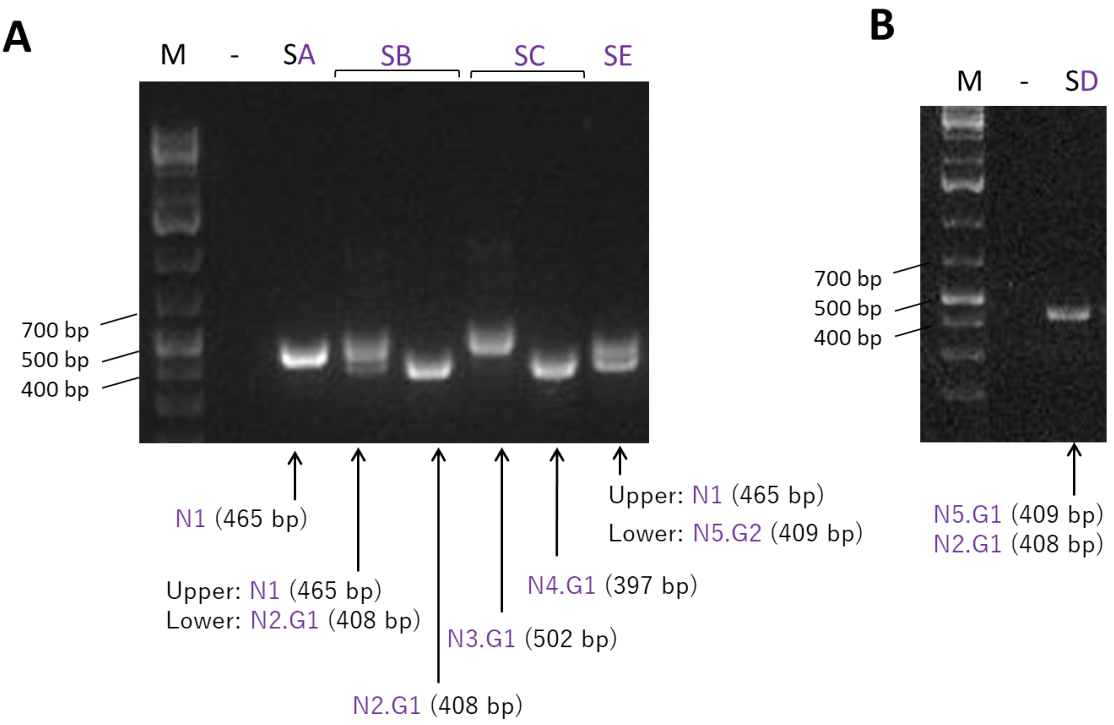

Figure 3.35 - PCR amplification of the *Naegleria* ITS rDNA region. SA to SE refers to the sampling sites screened in the 1st sampling in the Monjolinho River. Notes M and (-) refer to the DNA ladder PCRBio Ladder IV, and the negative control based on a DNA-free water solution, respectively. The purple color indicates that the DNA was extracted directly from the river water precipitate after the centrifugation step. Codes N1 to N5.G2 correspond to distinct *Naegleria* sequence types.
Source: By the author.

Figure 3.35 shows that *Naegleria* is ubiquitous in all five sampling sites of the Monjolinho River. Its corresponding amplicons revealed a length variation from 397 bp (Fig. 3.35, amlplicon N4.G1) to 502 bp (Fig. 3.35, amlplicon N3.G1). Moreover, derived from the sequencing analysis, N1 to N5 belonged to five *Naegleria* species and N2 to N4 to more than one sequence type, termed G1 and G2, as shown in Fig. 3.35. Amplifications of more than one sequence type were often visibly distinguished (Fig. 3.35, gel A). However, particular cases resulted in two amplified products resultant from a single band (Fig. 3.35, B), latter confirmed by

cloning and sequencing of amplicons. Complementary to the molecular information obtained directly from the river water investigation (Fig. 3.35.) it had been performed a similar screening by using the DNA extracted from NNA plate cultures. Representative electrophoresis results are shown ahead, in Figure 3.36.

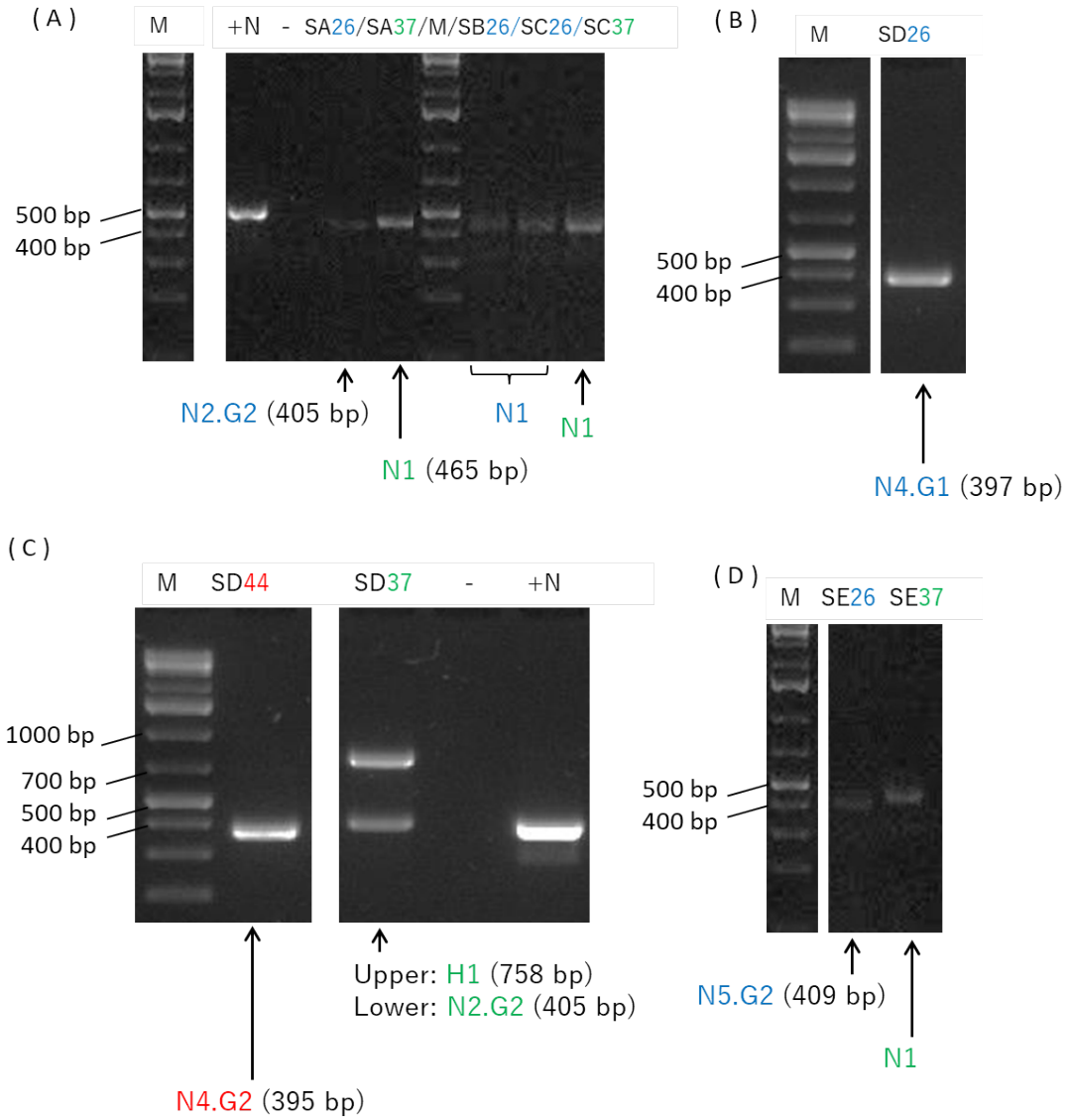

Figure 3.36 - PCR amplification of *Naegleria* ITS rDNA regions of NNA plate samples extracted from the sampling sites SA, SB, SC (gel A), sampling site SD (gels B and C) and sampling site SE (gel D). Positive (+N) and negative (-) controls comprise *Naegleria gruberi* _ ATCC 30224 and DNA-free water sample, respectively. M refers to the GeneRuler 1kb Plus DNA Ladder. Blue, green and red colors are indicative of maintenance temperatures of 26 ºC, 37 ºC, and 44 ºC, respectively. Codes N1 to N5.G2 correspond to distinct *Naegleria* sequence types and the code H1 corresponds to *Hartmanella* genus.

Source: By the author.

Results in Figure 3.36 enabled to confirm the diversity of species previously detected in the directly-from the river approach (Fig. 3.35), besides detecting another FLA genus, *Hartmanella*. Those amplification bands of 400-500 bp correspond to *Naegleria* sequences, N codes (Fig. 3.36). A double band was observed in SD37 in which the higher fragment, of approximately 800 bp, was identified as a *Vermamoeba vermiformis* (Figure 3.36, gel C, amplicon H1). In addition to the prior in silico prediction of the expected *Naegleria* amplicons (Fig. 3.34, B), the following image illustrates the compatible rDNA region of a *Vermamoeba* gene originated with the *Naegleria*-specific primer pair (Figure 3.37).

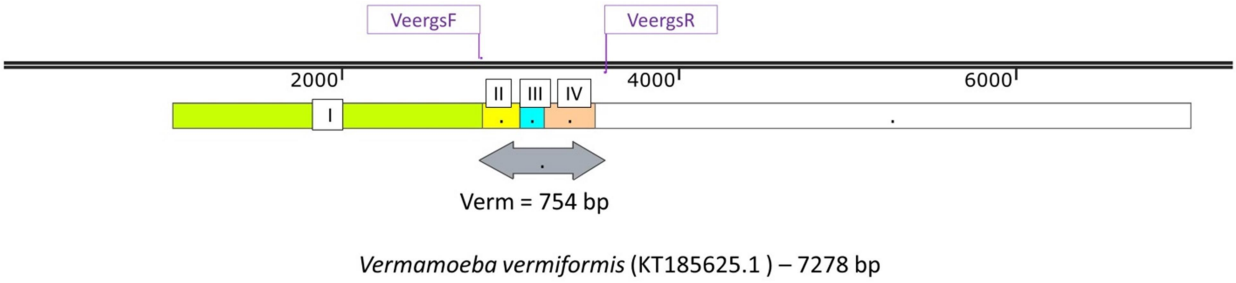

Figure 3.37 - Amplicon length (bp) prediction, gray arrowed fragment, to *Vermamoeba vermiformis* fragments obtained with VeergsF/VeergsR based PCR. Annotations refer to: I - 18S rRNA gene; II - ITS1 region; III - 5.8S rRNA gene; IV - ITS2 region; V - 28S gene.
Source: By the author.

As shown in Figure 3.37 the primer-pair is able to amplify the *Vermamoeba* rDNA region whose amplicon of about 750bp is in line with the amplicon band H1 obtained to SD37 (Fig. 3.36, C). The second sampling in the river resulted in simillar results, i.e. both *Naegleria* spp and *Vermamoeba vermiformis* ITS amplicons (Figure 3.38) of DNA extracted from NNA cultured cells at 44°C.

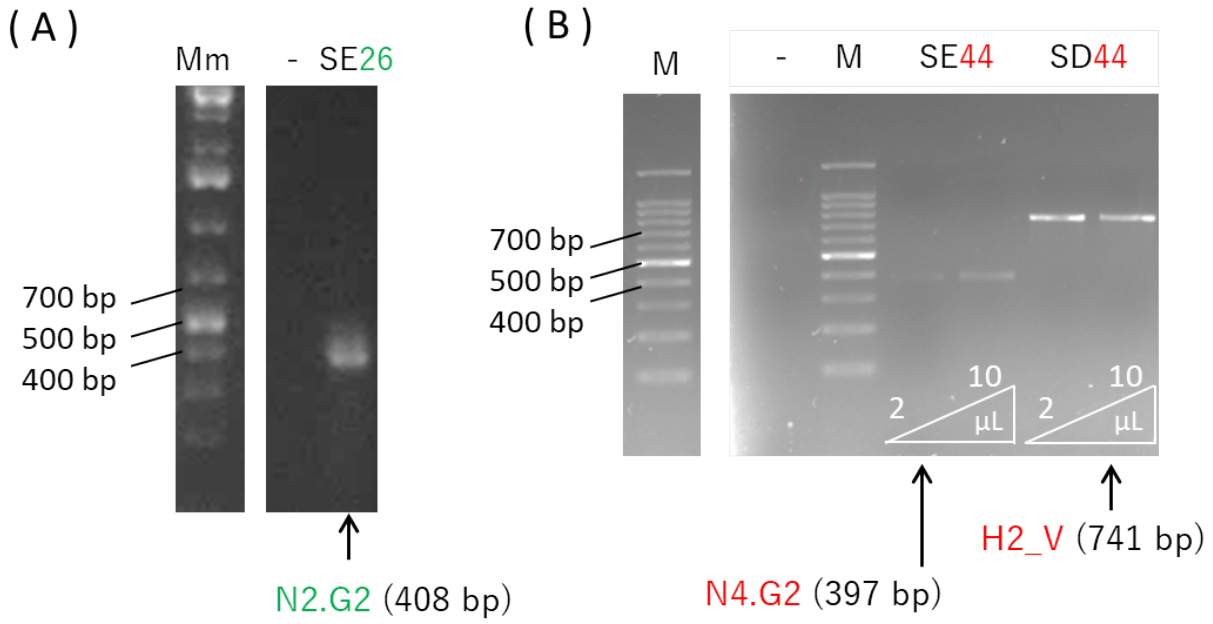

Figure 3.38 - *Naegleria* spp. PCR products electrophoresed on 2% agarose gels with DNA samples extracted from NNA plates. SE and SD refer to DNA samples extracted from sampling sites E and D, whose cultures were maintained at 26 °C or 44 °C. Molecular markers correspond to DNA ladder PCRBio Ladder IV (M) and GeneRuler 1kb Plus DNA Ladder (Mm). Codes N2.G2 and N4.G2 correspond to *Naegleria* amplicons and the code H2_V correspond to *Hartnmanella* amplicon. PCRs performed with VeergsF/VeergsR primer pairs.
Source: By the author.

The amplicons obtained in Figure 3.38 were identified as *N. philippinensis* (N2.G2), *N. australiensis* (N4.G2), and *Vermamoeba vermiformis* (H2.V) upon sequencing.

To confirm the *Vermamoeba* finding (Fig. 3.36 and Fig. 3.38), *Vermamoeba*-specific primers, HartF/HartR, were used as summarized in Figure 3.39.

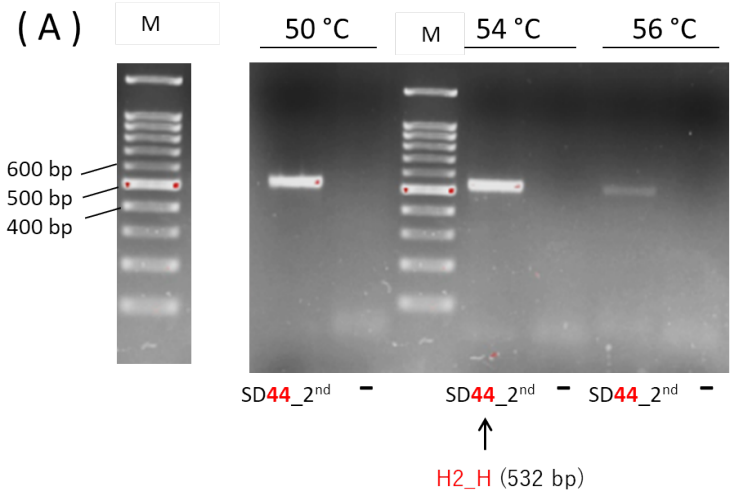

(to be continued)

(continuation)

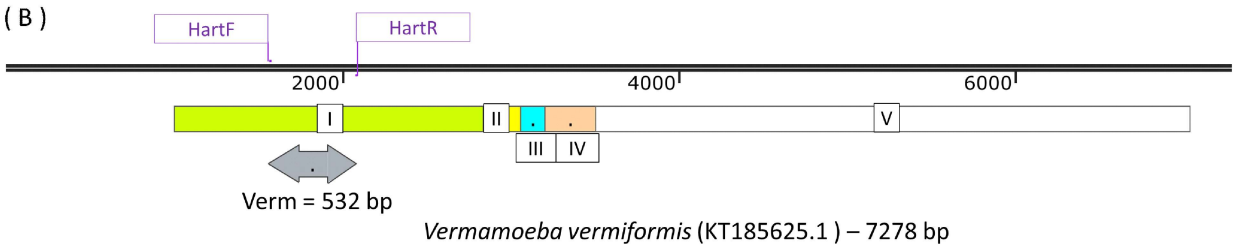

Figure 3.39 - Detection of *Vermamoeba vermiformis* 18s rDNA region by using HartF/HartR primer pair. (A) 2% agarose gel electrophoresis with *Vermamoeba vermiformis* PCR products, H2_H, validating annealing temperature conditions (50 ºC, 54 ºC and 56 ºC). M corresponds to DNA ladder PCRBio Ladder IV and the negative control (-) is based in DNA free water solution. Part (B) contains the amplicon length (bp) prediction indicated by the gray arrowed area. I - 18S rRNA gene; II - ITS1; III - 5.8S rRNA gene; IV - ITS2; V - 28S gene. Code H2_H and N4.G2 correspond to *Naegleria* ITS rDNA regions.
Source: By the author.

Figure 3.39. elucidates the amplification pattern found to *Vermamoeba* positive samples amplified in a range of annealing temperatures whose amplicon length placed between 500 to 600 bp was compliant with the correspondent in silico prediction of about 530 bp (Fig. 3.39, B). The amplified fragment H2_H, Fig. 3.39, was sequenced and identified as *Vermamoeba vermiformis* 18S rDNA (Table 3.8 – Line 17).

The *Acanthamoeba* spp. PCR-based approach included amplification of two distinct targets, named amplimers Am1 and Am2 obtained respectively by using primer pairs CRN5/373r and JDP1/JDP2. The former is shown in Fig. 3.33, and the latter is illustrated ahead in Figure 3.40:

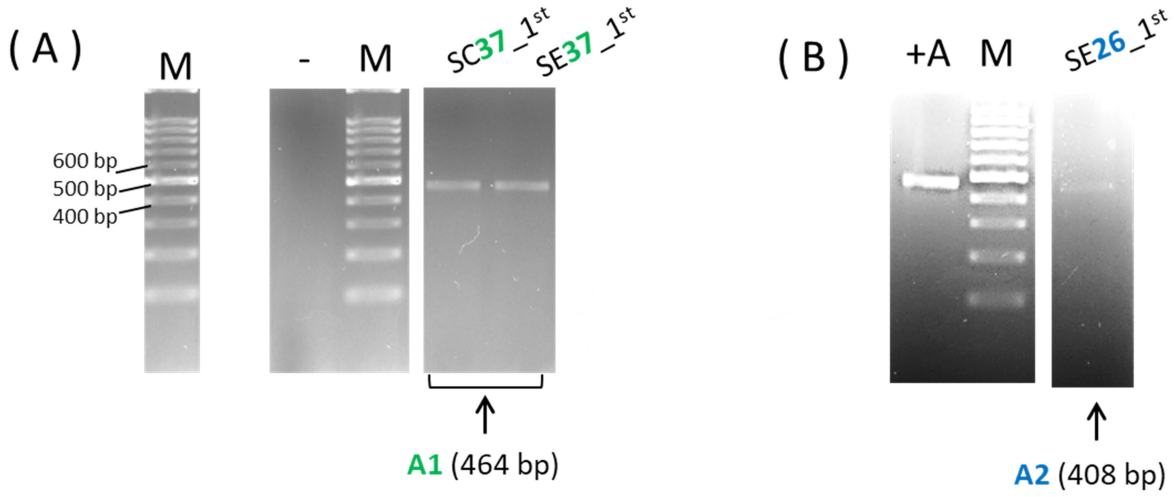

(to be continued)

(continuation)

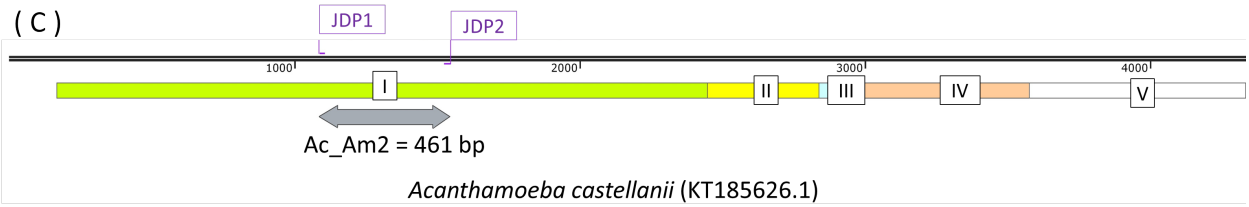

Figure 3.40 - Molecular characterization of *Acanthamoeba* spp. amplimer Am2 by using JDP1/JDP2 primer pairs. PCR products electrophoresed in 2% agarose gel containing SC37_1st and SE37_1st samples (gel A) and the sample SE26_1st (gel B). Respectively, M, - and +A correspond to DNA ladder PCRBio Ladder IV, DNA-free water sample, and *Acanthamoeba castellanii* Neff (ATCC 30010) DNA. Codes A1 and A2 correspond to *Acanthamoeba* 18S rDNA genes. Part (C) contains the amplicon length prediction (bp) indicated by the gray arrowed area. I - 18S rRNA gene; II - ITS1; III - 5.8S rRNA gene; IV - ITS2; V - 28S gene.
Source: By the author.

Figure 3.40 confirmed the expected amplification of *Acanthamoeba* amplimer Am2 whose PCR products have shown bands between 400 and 500 bp (Fig. 3.40, agarose gels A and B), as predicted (Fig. 3.40, C). Both PCR products, A1 and A2, upon sequencing analysis, revealed gene fragments of 464 bp and 408 bp respectively to *A. hatchetti* (A1) and *Acanthamoeba* genotype T4 (A2).

Apart from the genus-specific targets highlited in Figures 3.35 to Figure 3.40, we also included PCR amplifications targeting generic FLA rDNA genes in which global primer pairs enabled to retrieve distinct FLA genera. In this regard, a diversity of five distinct genera could be obtained by screening our isolates, as illustrated by Figure 3.41.

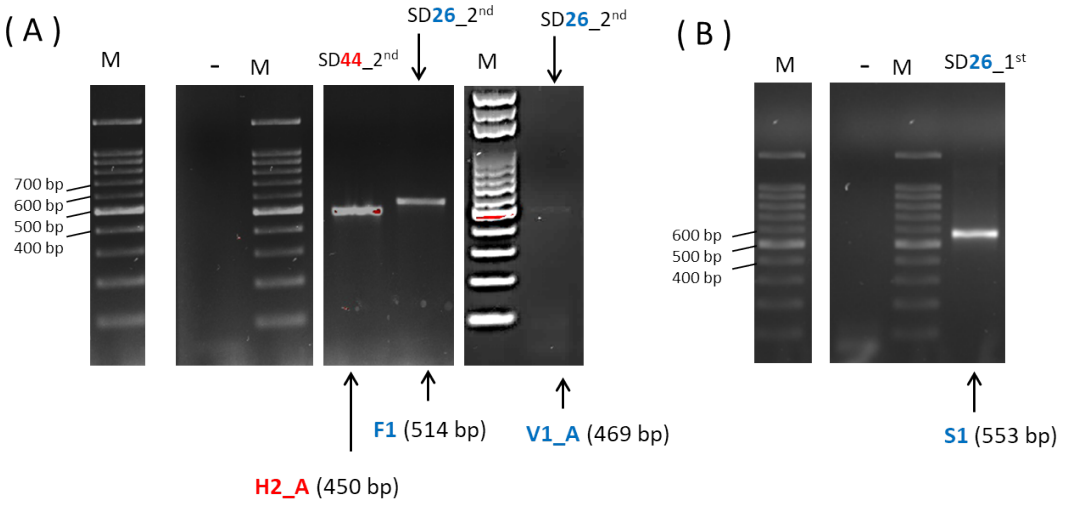

(to be continued)

(continuation)

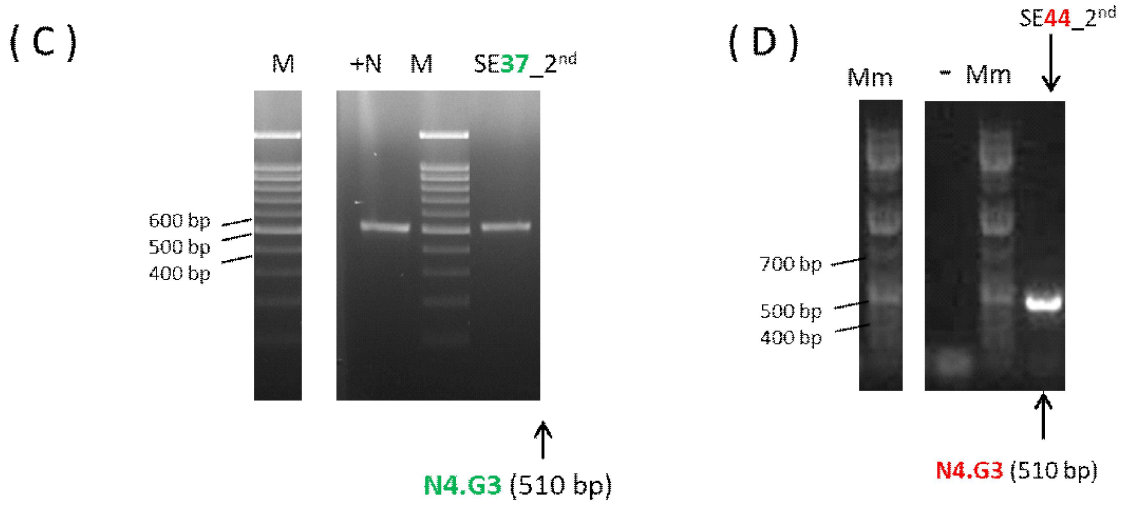

Figure 3.41 - Set of PCR results against generic FLA primer pairs (AmeF977/AmeR1534). DNA samples include NNA plates cultures from both first (1st) and second (2nd) Monjolinho River samplings. Molecular markers M and Mm correspond to DNA ladder PCRBio Ladder IV and GeneRuler 1kb Plus DNA Ladder, respectively. Positive (+N) and negative (-) controls comprise *Naegleria gruberi* _ ATCC 30224, and DNA-free water sample, respectively. Codes H, F, V, S and N correspond to 18S rDNA amplicons of *Hartmannella*, *Filamoeba*, *Vannella*, *Stenamoeba*, and *Naegleria* genera, respectively.

Source: By the author.

Results obtained through generic-FLA-based PCRs showed a variety of amplification bands, ranging from 400 bp to 700 bp length (Fig. 3.41). Upon sequencing, those samples extracted from 44 ºC (codes in red, Figure 3.41) revealed amplification of thermophilic *Naegleria* (Fig.3.41, amplicon N4.G3) and *Vermamoeba* isolates (Fig.3.41, amplicon H2_A), as previously described in this word by amplifications with genus-specific primers, in Figure 3.39 and 3.38 respectively. Overall, the migration of PCR products on agarose gels shown in Figure 3.41 seemed to be compatible with the in silico predictions as illustrated above, in Figure 3.42.

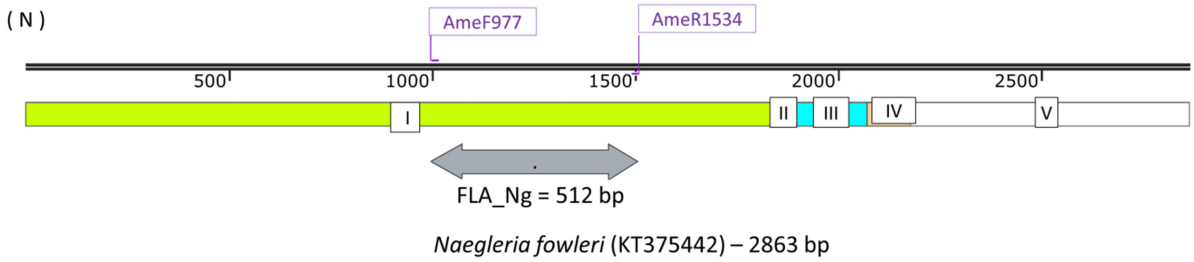

(to be continued)

(continuation)

Figure 3.42 - Amplicon length prediction in base pair (bp) to FLA genera by using primer pairs AmeF977/AmeR1534J. Annotations refer to 18S rRNA gene (I); ITS1 (II); 5.8S rRNA gene (III); ITS2 (IV); and 28S gene (V). Gray arrowed regions indicate amplimer lengths to *Naegleria* (N), *Acanthamoeba* (A), *Vannella* (V), *Filamoeba* (F), and *Stenamoeba* (S) genera.
Source: By the author.

These molecular results confirmed the efficacy in the adopted molecular surveillance towards the microbiological assessment of FLA species in river water samples either using genus-specific primer pairs (Fig. 3.34 to 3.39) or targeting the generic FLA PCRs (Figure 3.41). Thus, the following list (Table 3.8) summarizes the positive amplifications, integrates its corresponding sequencing code, and the corresponding reference sequence from GenBank whose identity was detected, based on sequencing evaluation.

Table 3.8 - Assemble of positive PCR reactions performed with environmental DNAs extracted either directly from river water samples or NNA plate culture seeded with water from Monjolinho river. # is indicating lines and bp indicates amplicon length in base pairs.

#	Primer pairs	Agarose ref. (Fig_nº)	bp	Amplicon codes	Species	SAMPLES
1	VeergsF/ VeergsR	Fig. 3.38; Fig. 3.36	465	N1	*N. canariensis*	SC37_1st ; SC26_1st; SB26_1st ; SA37_1st SE_direct; SA_1st_direct SE37_1st SB_1st_direct
2		Fig.3.38; Fig. 3.40	405	N2.G2	*N. philippinens*	SE26_2nd ; SD37_1st ; SA26_1st
3		Fig 3.36	408	N2.G1	*N. philippinensis*	SB_1st_direct, SD_1st_direct
4		Fig 3.36	502	N3.G1	*N. dobsoni*	SC_1st_direct
		(not documented)	502	N3.G2	*N. dobsoni*	SC_1st_direct
5		Fig. 3.36; Fig.3.38	397	N4.G1	*N. australiensis*	SC_1st_direct ; SD26_1st
6		Fig 3.38; Fig. 3.40	397	N4.G2	*N. australiensis*	SE44_2nd ; SD44_1st
7		Fig 3.36	397	N5.G1	*N. gruberi*	SD_1st_direct
8		Fig 3.38	397	N5.G2	*N. gruberi*	SE_1st_direct; SE26_1st
9		Fig 3.38	758	H1	*Hartmanella*	SD37_1st
10	JDP1/ JDP2	Fig 3.42	464	A1	*Acanthamoeba hatchethi T12*	SE37_1st ; SC37_1st
11		Fig 3.42	408	A2	*Acanthamoeba genotype T4*	SE26_1st
12	AmeF977/ AmeR1534	Fig 3.46	553	S1	*Stenamoeba polymorpha*	SD26_1st
13		Fig 3.45	469	V1_A	*Vannella* sp	SD26_2nd α
14		Fig 3.45	514	F1	*Filamoeba sinensis*	SD26_2nd β
15		Fig 3.45	450	H2_A	*Hartmanella vermiformis*	SD44_2nd
16		Fig 3.45	510	N4.G3	*N. australiensis*	SE37_2nd ; SE44_2nd
17	HartF/ HartR	Fig 3.41	532	H2_H	*Hartmanella vermiformis*	SD44_2nd

Source: By the author.

Generally, in Table 3.8, PCRs performed with the genus-specific primer pairs revealed a diversity of species within the targeted genus. For instance, all positive bands termed with "N" codes are corresponding to *Naegleria* genes obtained with VeergsF/VeergsR primer pairs, useful to discriminate intra specific divergences on ITS1/5.8S/ITS2 rDNA regions (Table 3.8, Lines 1-8). Global FLA PCRs, by using AmeF977/AmeR1534 primer pairs, confirmed those genera prior detected with the genus-specific PCRs (e.g.: *Naegleria* genus, Table 3.8, Line 16), besides to

revealing other FLA genera as *Vannella*, *Filamoeba*, and *Stenamoeba* (Table 3.8, Lines 13-14). Moreover, to each DNA sample extracted from NNA plates one or more PCR target amplifications were carried out (e.g.: sample SD44_2nd, Lines 15 and 17). In the next section, a description of sequencing results and phylogenetic relations is provided.

3.3.1.2. Sequencing and phylogenetic analysis

All Sanger sequencing data obtained from the Monjolinho River were used as queries for nucleotide similarity searches in the NCBI database with the BLASTn tool, as detailed in methods (section 2.6.3., page 80). The corresponding results are summarized in Table 3.9 with an emphasis on *Naegleria* genus.

Table 3.9- BLASTn searches to consensus generated Sanger sequences obtained from PCRs against VeergsF/VeergsR primer pairs. Codes N and H refer to *Naegleria* and *Hartmannella* genera. Annotations indicate: ID – identity; AN[a] - accession number for strains characterized in this thesis; AN[b]– accession numbers for reference sequences; terms S, I, and D refer to the number of substitutions, insertions and deletions, respectively.

#	Code	AN[a]	ID (%)	BLASTn result	AN[b]	S	I	D
1	N1	MN781116.1	100	*N. canariensis*	FJ475124.1			
2	N2.G1	MN781117.1	99	*N. philippinensis*	AY033618.1	1	1	2
3	N2.G2	MN781118.1	99	*N. philippinensis*	LC191904.1		1	2
4	N3.G1	MN781119.1	99	*N. dobsoni*	KU380484.1	1		
5	N3.G2	MN781120.1	97	*N. dobsoni*	KU380484.1	1	2	2
6	N4.G1	MN781121.1	100	*N. australiensis*	AB128053.1			
7	N4.G2	MN781122.1	100	*N. australiensis*	AB128052.1			
8	N5.G1	MN781123.1	100	*N. gruberi*	MG699123.1			
9	N5.G2	MN781124.1	99	*N. gruberi*	MG699123.1	4		
10	H1	MN781125.1	99	*Hartmanella sp*	HE617186.1	6		2

Source: By the author.

The diversity of *Naegleria* genes shown in Table 3.9, Lines 2 - 9 is resultant from evaluating corresponding chromatograms to validated sequencing mismatches and confirm the distinction between groups, G1 and G2 (as shown in Fig. 3.43). Here, *N. australiensis* sequences (Table 3.9, Lines 6 and 7) were used as a study of case in which codes N4.G1 and N4.G2 were compared in Figure 3.43 to exemplify groups G1 and G2 origin.

(A)

Description	Max Score	Total Score	Query Cover	E value	Per. Ident	Accession
Naegleria australiensis genes for SSU rRNA, ITS1, 5.8S rRNA, ITS2, LSU rRNA, partial and complete sequence, isolate: Yodo5	734	734	100%	0.0	100.00%	AB128052.1
Naegleria sp. isolate N4.G1 internal transcribed spacer 1, partial sequence; 5.8S ribosomal RNA gene and internal transcribed spacer 2, com	721	721	100%	0.0	99.50%	MN781121.1

(B)

Score	Expect	Identities	Gaps	Strand
721 bits(390)	0.0	395/397(99%)	2/397(0%)	Plus/Plus

```
Query  1    GAACCTGCGTAGGGATCATTTCTGGTAAAAAGGTGAAAACCTTTTTTACCCCCAAACTCT  60
            ||||||||||||||||||||||||||||||||||||||||||||||||||||||||||||
Sbjct  1    GAACCTGCGTAGGGATCATTTCTGGTAAAAAGGTGAAAACCTTTTTTACCCCCAAACTCT  60

Query  61   GTGCAATGGAGCACACGGCTTATGCATCGATGAAGCCCGCGGCAAAAAGCGATATGTAAT  120
            ||||||||||||||||||||||||||||||||||||||||||||||||||||||||||||
Sbjct  61   GTGCAATGGAGCACACGGCTTATGCATCGATGAAGCCCGCGGCAAAAAGCGATATGTAAT  120

Query  121  GAGATTCGTTAGCCTCGCGATTCATCAAATTGGTGAACACATACTGGACCTCTTCGGAGG  180
            ||||||||||||||||||||||||||||||||||||||||||||||||||||||||||||
Sbjct  121  GAGATTCGTTAGCCTCGCGATTCATCAAATTGGTGAACACATACTGGACCTCTTCGGAGG  180

Query  181  TACTTGCGTTAGAGTGCTAGTTTTCTATCAATTGATCCTGGTAAAAGGTGTTTGAATCGT  240
            ||||||||||||||||||||||||||||||||||||||||||||||||||||||||||||
Sbjct  181  TACTTGCGTTAGAGTGCTAGTTTTCTATCAATTGATCCTGGTAAAAGGTGTTTGAATCGT  240

Query  241  TAGGTTCTTACGCCCTAGCCGGTGGAGCCGGATTCTCTCTGAGAATTCGGATTGTTCCTG  300
            ||||||||||||||||||||||||||||||||||||||||||||||||||||||||||||
Sbjct  241  TAGGTTCTTACGCCCTAGCCGGTGGAGCCGGATTCTCTCTGAGAATTCGGATTGTTCCTG  300

Query  301  GTCTTTGACTGGGTCAATCACTTTTTTATTAAACTGGCCTCTAATGTGAGAGGGTACCCC  360
            |||||||||||||||||| ||||||||||||||||||||||||||||||||||||||||
Sbjct  301  GTCTTTGACTGGGTCAATCAC--TTTTATTAAACTGGCCTCTAATGTGAGAGGGTACCCC  358

Query  361  CTGGATTTAAGCATATTAATAAGGGGAGGAAAAGAAA  397
            |||||||||||||||||||||||||||||||||||||
Sbjct  359  CTGGATTTAAGCATATTAATAAGGGGAGGAAAAGAAA  395
```

N4G2
N4G1

(C)

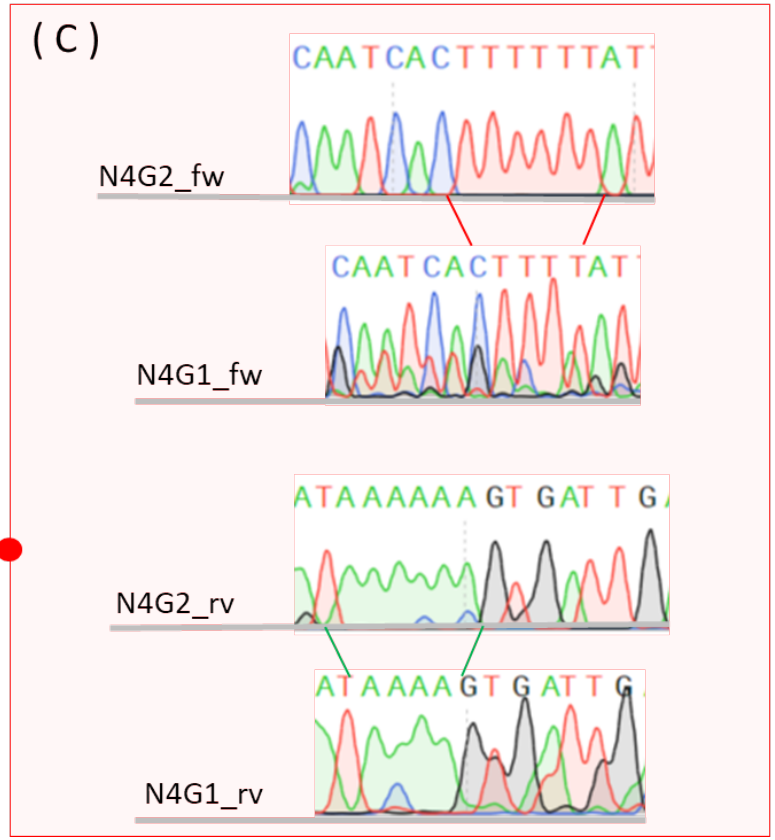

Figure 3.43 - Alignment of consensus sequence N4G2 on BLASTN searches. A – BLASTn typical result; B – sequence alignment details between N4G2 and N4G1; C – chromatogram comparison aiming to resolve mismatches. The red circle, in part A, is showing the identity between N4G2 (query) and N4G1, another Naegleria sequence isolated on this thesis and previously deposited in GenBank with the accession number MN781121.1.

Source: By the author.

Figure 3.43 illustrates a typical BLASTn result in which N4.G2 sequence corresponds to *Naegleria australiensis*, supported by 100% identity with the AB128052.1 reference gene. Moreover, an identity of about 99% was detected to N4.G1, another consensus sequence isolated at the present thesis (Fig. 3.43, A, red circle). N4.G1 also demonstrated a 100% identity with *N. australiensis* (Table 3.9, Line 7). By peering into the alignment of N4G2 and N4G1 (Fig. 3.43, part B), an insertion of two nucleotides represented the mismatch between both sequences, as shown in Fig. 3.43, part C. As listed in Table 3.9, variants G1 and G2 also occurred to the remaining *N. philippinensis* (N2), *N. dobsoni* (N3), and *N. gruberi* (N5) identifications, and above all *Naegleria* codes are compared in terms of length (Table 3.10).

Table 3.10 - Variability of length and position, in base pairs (bp), within the ITS1/5.8S/ITS2 rDNA locus for *Naegleria* strains. The column amplicon size refers to the length of the entire sequence amplified with VeergsF/VeergsR primer pairs.

Codes	ITS1	5.8S	ITS2	Amplicon size
N1	34 (22-55)	175 (56-230)	169 (231-399)	465
N2.G1	34 (22-55)	175 (56-230)	112 (231-342)	408
N2.G2	34 (22-55)	175 (56-230)	112 (231-342)	408
N3.G1	35 (22-56)	176 (56-231)	205 (232-436)	502
N3.G2	34 (22-55)	175 (56-230)	206 (231-436)	502
N4.G1	34 (22-55)	175 (56-230)	99 (231-329)	395
N4.G2	34 (22-55)	175 (56-230)	101 (231-331)	397
N5.G1	34 (22-55)	175 (56-230)	113 (231-343)	409
N5.G2	34 (22-55)	175 (56-230)	113 (231-343)	409

Source: By the author.

Table 3.10 revealed the ITS2 region as the most variable sequence given the heterogeneity in *Naegleria* strains. To express these divergences, the corresponding phylogenetic tree based on ITS1-5.8S-ITS2 regions to *Naegleria* sequences, along with the *Hartmanella* identification, is summarized in Figure 3.44.

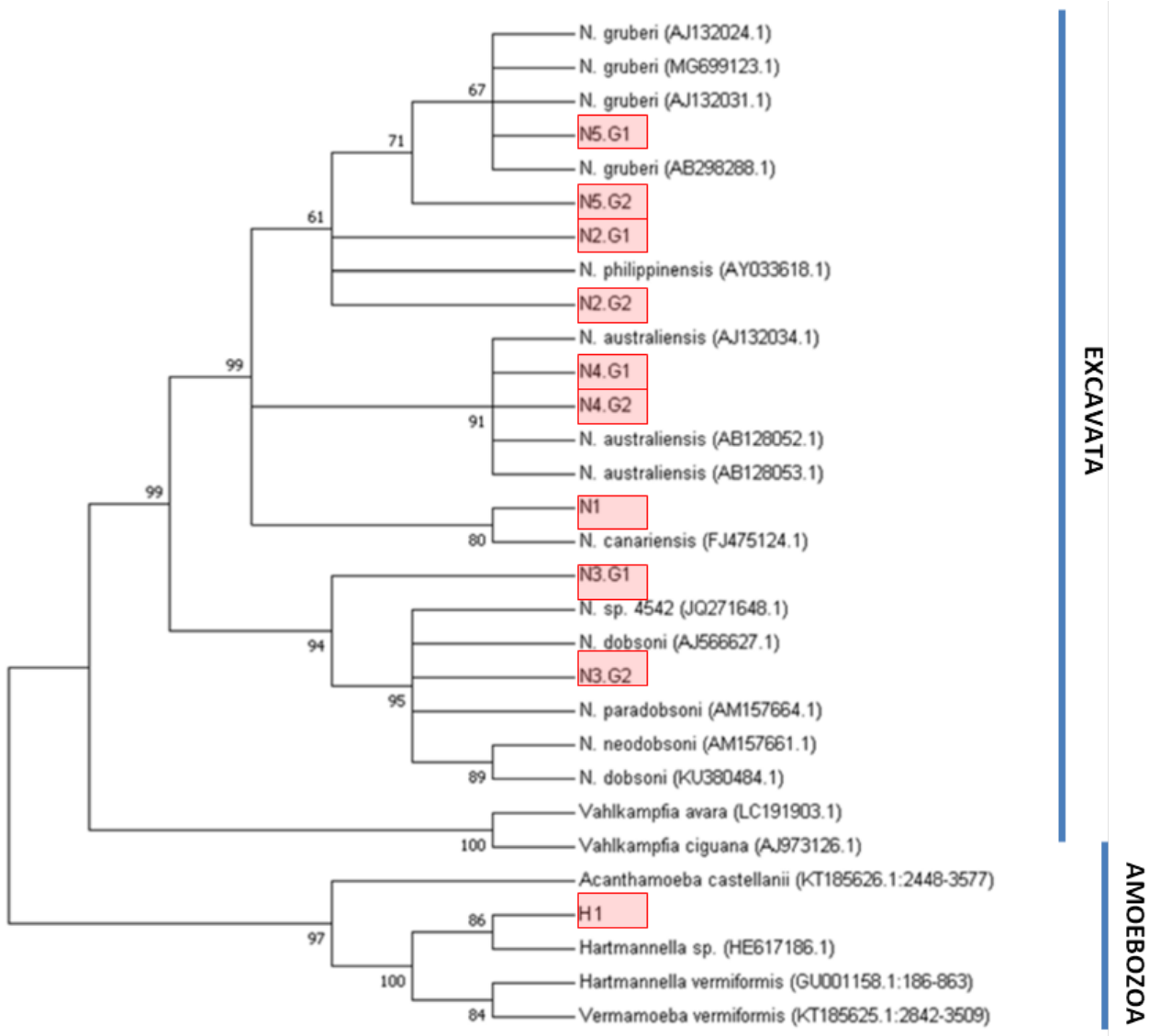

Figure 3.44 – Neighbor-joining phylogeny of *Naegleria* and *Hartmanella* isolates reconstructed from the ITS1-5.8S-ITS2 rDNA locus. Numbers show the bootstrap significance, in percentage, accounting 1000 replicates. Values below 50% are not shown.
Source: Adapted from BELLINI *et al*. (150)

Figure 3.44 demonstrated *Naegleria* and *Vahlkampfia* clustered in the Excavata supergroup and the remaining *Vermamoeba* and *Acanthamoeba* genera in the Amoebozoa supergroup. Within *Naegleria* clusters, those species grouped in the same clade indicated less polymorphism or divergence found between their corresponding ITS2 regions, as well suggested in Table 3.10 (e.g.: *N. philippinensis* and *N. gruberi*). The detailed characterization regarding these *Naegleria* isolations in Monjolinho River is described in section 3.3.2.1, as well as in the

paper “Isolation of *Naegleria* spp. from a Brazilian water source” (Appendix IIa) with alignment details in the supplementary material (Appendix IIb).

Apart from *Naegleria* identifications based on ITS regions, the extended evaluation of FLA in Monjolinho River enabled to the enhancement of the diversity of isolates based on 18S rDNA molecular identification revealing the species listed in Table 3.11.

Table 3.11- Results of BLASTn searches to Sanger sequences obtained after PCRs targeting HartF/HartR primer pairs (Line 1), AmeF977/AmeR1534 (Lines 2-6), and JDP1/JDP2 (Lines 7-8). Codes H, N, S, V, F, and A refer to *Hartmannella*, *Naegleria*, *Stenamoeba*, *Vannella*, *Filamoeba* and *Acanthamoeba* genus, respectively. Annotations indicate: ID – identity; AN– accession numbers for reference sequences; terms S, I and D refer to the number of substitutions, insertions and deletions, respectively.

#	Amplicon Code	ID (%)	BLASTn result	AN	S	I	D
1	H2_H	100	*Hartmanella vermiformis*	AY502959.1			
2	H2_A	100	*Hartmanella vermiformis*	AY502959.1			
3	N4 .G3	100	*N. australiensis*	MG945025.1			
4	S1	99	*Stenamoeba polymorpha*	KU955320.1	1	1	
5	V1_A	99	*Vannella sp.*	HM363632.1	3		
6	F1	99	*Filamoeba sinensis*	AY714369.1	3	1	
7	A1	100	*Acanthamoeba hatchetti (T11)*	KC164235.1			
8	A2	99	*Acanthamoeba genotype T4*	MN153018.1		1	

Source: By the author.

Hence, those sequences obtained with the generic FLA primer pair (Table 3.11, Lines 2-6) were aligned along with their corresponding reference genes (Table. 3.11, column AN), and the 18S rDNA-based phylogenetic relationship is expressed in Figure 3.45.

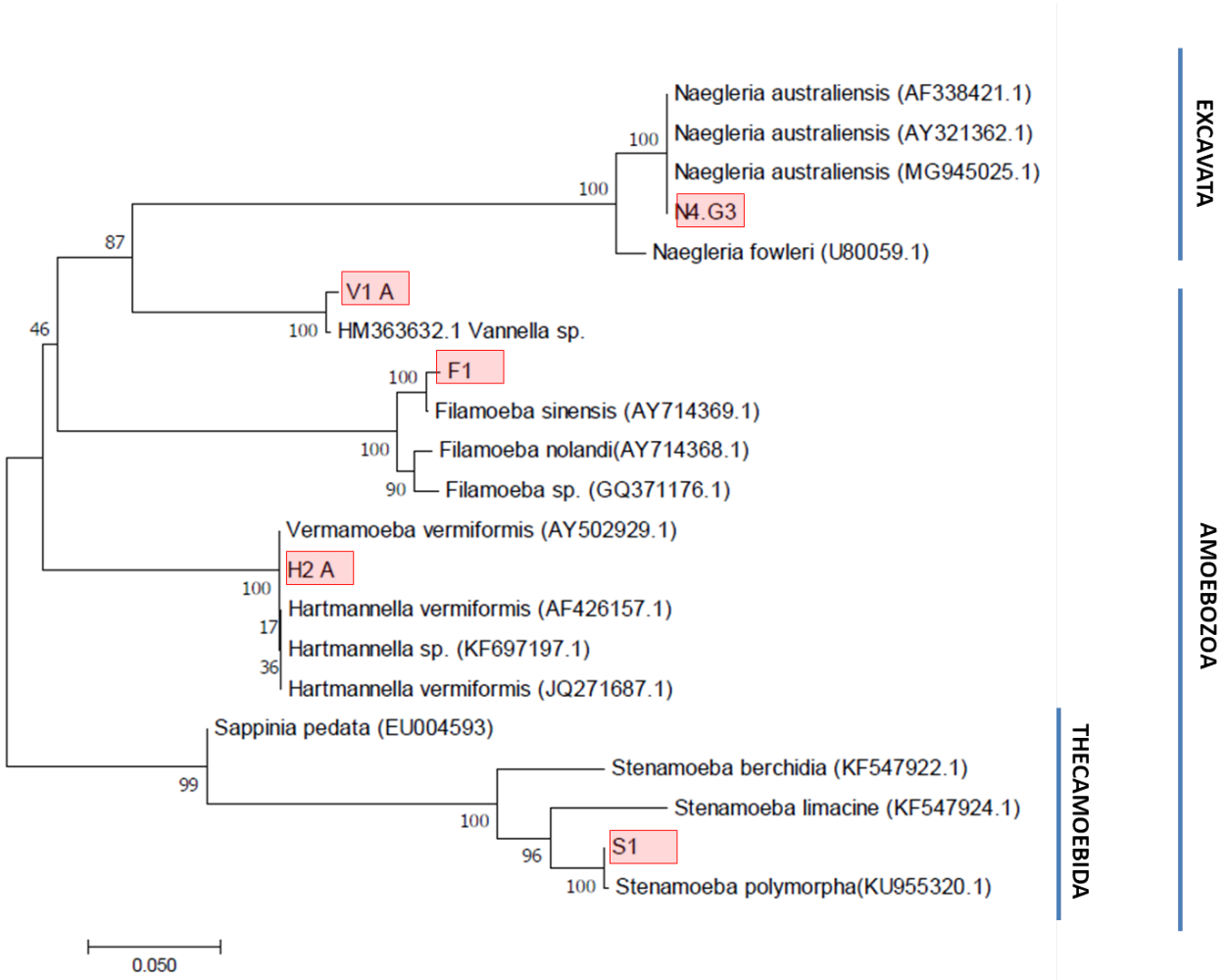

Figure 3.45 – FLA 18s rDNA based tree performed with Neighbor-joining (NJ) analysis model. Numbers refer to bootstrap percentages on 1000 replications.
Source: By the author.

The phylogenetic tree illustrated in Figure 3.45 supported the molecular characterization of target strains N4G3, V1_A, F1, H2_A, and S1 grouped within its corresponding clades *Naegleria, Vanella, Filamoeba, Hartmanella*, and *Stenamoeba.* Apart from *Naegleria*, belonging to Excavata, the remaining genera are composing the Amoebozoa supergroup (Fig. 3.45), similar as shown to the phylogeny based on ITS locus of *Naegleria* targets (Fig. 3.44). Moreover, S1 (*Stenamoeba*) is forming a clade with *Sappinia*, within the Thecamoebida clade (Fig. 3.45).

Finally, to *Acanthamoeba* identifications, whose primer pairs JDP1/JDP2 produced amplicons A1 and A2 (Table 3.11, Lines 7 and 8), the following Figure 3.46 summarizes the phylogeny that best represented the relation among our targets (A1, A2), those sequences

retrieved from the GenBank (MN153018.1 and KC164235.1) and representative sequences reported in a Brazilian survey (289) concerned on isolating *Acanthamoeba*.

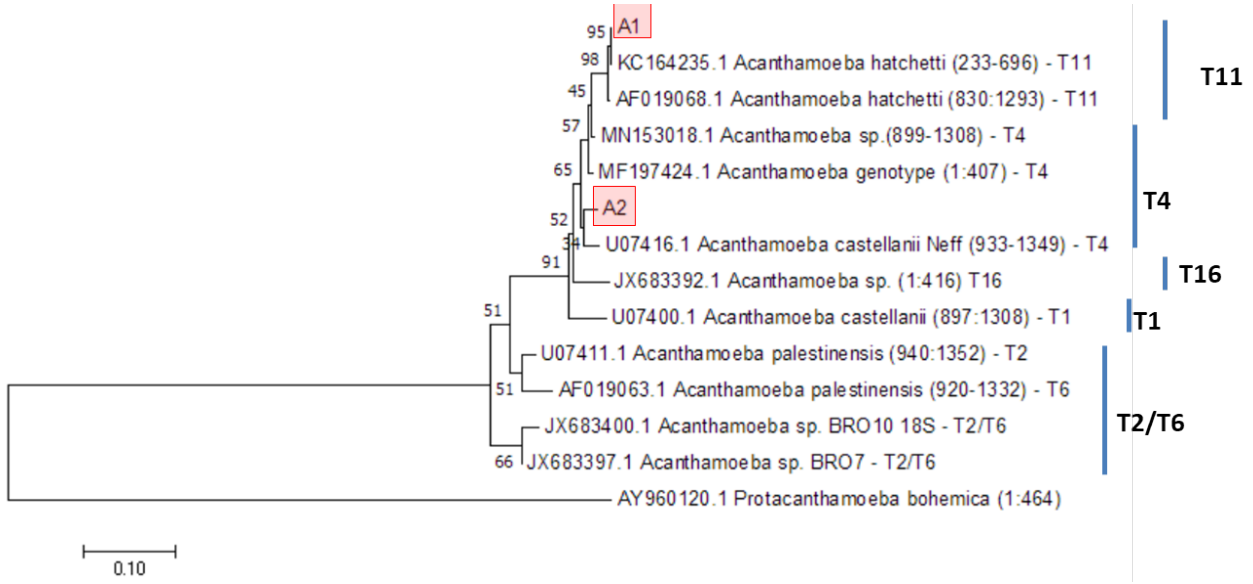

Figure 3.46 – Phylogeny of *Acanthamoeba* isolates reconstructed from diagnostic fragment 3, DF3 region, obtained with JDP1/JDP2 primer pairs. Neighbor-joining (NJ) analysis model, and bootstrap percentages based on 1000 replications. Accession numbers are shown in each terminal node depicting the corresponding species, the nucleotide region corresponding to the DF3 sequence within 18S rDNA gene, and the genotype to each they belong.
Source: By the author.

Amplicons A1 and A2 are supported by booststrapping values displaying on each node whose clade T11 presented the highest support due to an identity of 100% with *A. hatchetti* reference gene (KC164235.1). Regarding the amplicon A2, inserted within T4 clade, it has 99% identity with the remaining T4 sequences and 95% with *A. castellanii* (T1).

The discussion of the phylogenetic characterization of all genotypes obtained in Monjolinho River is described in the nesxt section.

3.3.2 Molecular approach – DISCUSSION

3.3.2.1 Molecular characterization and phylogeny of FLA isolates

After testing different extraction methods, the DNeasy PowerSoil® Kit has shown the best results, likely due to its additional mechanical cell lysing process at the initial steps of the protocol (Table 3.7). Also, the absorbance ratios revealed small differences regarding DNA

purity in which the phenol/chloroform method exhibited a decrease in A260/A230 absorbance likely due to the phenol contribution (Table 3.7). Similarly, its corresponding A260/280 rate likely indicates protein contamination, suggested by related studies concerned with DNA quality to downstream analysis. (290) On the other hand, commercial Kits have shown quite similar values indicative of higher DNA purity (Table 3.7, Lines 1 and 3), in which higher DNA concentration was recorded to the DNeasy PowerSoil® Kit method (Table 3.7). PCR results showing Power Soil Kit efficacy on producing a DNA compatible with PCRs reinforced our preference (Figure 3.34), as well as elected as a suitable option by the literature concerned with isolating DNA from environmental FLA samples. (132,168)

To confirm the efficacy of the DNA extraction protocols, the most contaminated samples, from the D site, had *N. gruberi* cells added. After performing the entire procedure, it was possible to amplify *N. gruberi* DNA (Fig 3.34) as well as *Acanthamoeba* (Fig 3.33) confirming that no preprocessing steps (e.g.: centrifugation and filtering river water) impaired the downstream molecular analysis.

Subsequently to this validation step, FLA isolates recovered from A to E sampling sites were molecularly characterized. Overall, most of the PCR products shown a single amplification band pattern (Fig. 3.38 – Fig. 3.40), however, some double band cases were observed, suggesting mixed amoeba cultures (Figure 3.36-C). The expressive diversity of *Naegleria* strains recognized by screening A to E DNA samples exemplified multiple amplicon lengths being obtained in a single sample (Figure 3.35, part A). Also, a single band can constitute sources of amplicon diversity (Figure 3.35, part B). However, to elucidate such refined information, cloning and subsequent screening of colonies shown to be imperative, results in line with a 2013 study recommending cloning based investigation to examine *Naegleria* directly from hot spring water. (291) However, most environmental surveys commonly assessed FLA diversity by analyzing the gel electrophoresis migration of the amplified bands and the presence or absence of an amplicon correlating with genus-specific primers used. (30,130,157,292–294) Numerous reports withdrew the need of cloning PCR products provided from amplicon heterogeneity due to alternatively performing culture-based identifications, obtaining monoclonal cultures of amoeba and corresponding molecular identifications that express homogeneity of amplicons. (16,229,295–297)

Among *Naegleria* identifications, after Sanger sequencing analysis, some results called attention to intra-specific genetic variation to the ITS1/5.8s/ITS2 rDNA locus (Table 3.10). The divergences were conserved within all replicates, which allowed us to keep genotypes as variants G1 and G2, as demonstrated to N4.G1 and N4.G2 (Fig. 3.43). As highlighted by the literature, most *Naegleria* species (229) have shown one or more variants to the same species. To *Naegleria fowleri* six variants have been recognized so far. (298) Accounting for many interstrain differences reported within *Naegleria* genus, it is important to report new identifications by discriminating strains divergences to the same species, especially these ITS regions carrying intra-specific variability. (299)

Apart from the intra-specific *Naegleria* diversity with amplicons ranging from about 500 bp length (Fig. 3.35), longer sequences were detected and revealed *Vermamoeba* genes, code H1 (Fig. 3.36, C). The potential of VeergsF/VeergsR primer pairs to amplifying the ITS regions from *Naegleria* and *Vermamoeba* has been recently reported in studies investigating: Nile River samples, Egypt;(154) environmental water and dust samples in Malaysia;(229) and drinking water sources in Iran. (130) Phylogeny of *Naegleria* and *Hartmanella* isolates reconstructed based on ITS regions demonstrated two major clusters consisted of *Naegleria* and *Valhkampfia* clades forming a group, so-called Excavata supergroup, and *Acanthamoeba* and *Hartmanella* composing the second clade, namely Amoebozoa supergroup (Fig. 3.44). Our results, to Excavata supergroup, are consistent with phylogenetic representations built to *Naegleria* isolates from Malaysia, (229) as well reconstructed from ITS locus, whose strains belonging to *N. gruberi* and *N. philippinensis* were grouped within the same taxa and both were externally grouped with *N. australiensis* by one branch of separation. The polymorphism of ITS regions, (299) mainly ITS2, is the main feature grouping them, as demonstrated in the alignment of *Naegleria* strains available in the literature (229) and similarly suggested by the ITS length variability listed in Table 3.10 (this thesis, page 152).

Regarding the primer pairs used to detect *Vermamoeba* (=*Hartmannella*), HartF/HartR, it has shown an amplicon of 500-600 bp length in agarose gel, named H2_H, detected to the sample SD44_2nd (Fig. 3.39, A). Sequencing analysis clarified a PCR product of 532 bp length to H2_H (Table 3.8, Line 17). It revealed 100% of identity with *Hartmanella vermiformis* (AY502959.1), a GenBank sequence isolated from aquatic biofilms. (300) The DNA from the SD44_2nd sample was detected positive as well to PCRs targeting the global FLA primer pairs,

AmeF977/AmeR1534 (Fig. 3.41, part A). Its corresponding amplicon, named H2_A has shown 100% identity with the same reference strain, *Hartmanella vermiformis* (AY502959.1). To the purpose of establishing a phylogenetic relationship among our isolates, we prioritized using the H2_A amplicon to perform alignments and to conduct the phylogeny (Fig. 3.45).

Additional PCRs based on AmeF977/AmeR1534 primer pairs revealed amplicons ranging from 450 to 550 base pairs as shown in Table 3.8, Lines 12-16. The amplicon V1_A (Fig. 3.41, A), after examining its corresponding Sanger sequencing data, was equivalent to a PCR product of 469 bp length, with 99% identity with *Vannella sp*. (HM363632.1) (table 3.11, Line 5). This reference strain, HM363632.1, was isolated from nodular gill disease (NGD) in rainbow trout.(301) Findings revealed *Hartmanella* sp. and *Acanthamoeba* sp. as causative agents of NGD. Although *Vannella* sp. was also isolated in the fish, authors argued it could not be conclusive as a causative agent considering that as the negative controls, gills of many healthy fishes also detected positive to Vannella. (301) The remaining samples amplified with AmeF977/AmeR1534 target primer pairs (Fig. 3.41), produced amplicons termed N4G3, S1, and F1 corresponding to *Naegleria*, *Stenamoeba*, and *Filamoeba* 18S rRNA genes, according to the Table 3.11, lines 3, 4, and 6 respectively. Firstly, the amplicon N4G3 found in SE37_2nd and SE44_2nd samples revealed an identity of 100% with *Naegleria australiensis* identity, MG945025.1, a reference strain isolated from thermal pool samples in Turkey.(302) In the regard of *Stenamoeba* and *Filamoeba* amplicons, amplification patterns around 500 bp were observed in agarose gel confirmations (Figure 3.41), whether compared with in silico predictions using reference genes available in GenBank revealed to be equivalent in terms of length as shown above in Figure 3.42.

In line with amplicon length prediction, Sanger sequencing analysis revealed 514 and 553 bp to F1 and S1, Table 3.8, Lines 12 and 14, respectively. Additionally, nucleotide similarity searches revealed 99% identity between F1 and S1 with *Stenamoeba polymorpha* (KU955320.1) and *Filamoeba sinensis* (AY714369.1), Table 3.11, lines 6 and 4 respectively. By examining corresponding phylogenetic analysis supporting our data (Figure 3.45), the sequence of *Stenamoeba* isolated on this study, S1, was clustered in a monophyletic group with the remaining three reference sequences of *Stenamoea*, upon 100% bootstrap support. All of them are related to the *Sappinea* sequence (Fig. 3.46) whose clade is well known for composing the Techamoeba group. (303) Then, *Vannela*, *Filamoeba* and *Vermamoeba* branches were shown to be supported

by 100% bootstrapping confidence each one (Fig. 3.45). Between them, *Filamoeba* and *Vannella* demonstrated to be closely related, consistent with literature findings. (278) Along with the Thecamoeba clade, all of them, *Vannela*, *Filamoeba*, and *Vermamoeba* isolates are clustered within the Amoebozoa supergroup what is supported by related SSU rRNA based phylogenies reported in the literature. (303)

Next PCR molecular target evaluated on this thesis relied upon *Acanthamoeba* based investigations, summarized in topic 3.3.1.1., what gave origin to amplicons A1 and A2 whose amplicons revealed 100% identity with *Acanthameoba hatchetti* (T11), KC164235.1, and 99% with *Acanthameoba* genotype T4 strains, MN153018.1, respectively to the amplicons A1 and A2 (Table 3.11, Lines 7 and 8). The corresponding phylogenetic inference demonstrated supported both amplicons belonging to *Acanthamoeba* genotypes T11 and T4 (Fig. 3.46), in comparison with reference sequences obtained from a related Brazilian study concerned with *Acanthamoeba* identifications. (289) The representative sequences BRO10 and BRO7 (Fig. 3.46), extracted from Brazilian environmental samples, were designed by the authors as belonging to T2/T6 genotypes, (289) which result was reproduced on the phylogeny built in this thesis (Fig. 3.46). Studies conducted in other parts of Brazil, revealed similar results than Monjolinho River isolates in which both T4 and T11 genotypes were isolated from mineral water samples. (127) Currently, *Acanthamoeba* genotype T4 was isolated from a keratitis patient wearing contact lenses, in Brazil. (194) Additionally, T4 isolates were recovered from samples collected in Brazilian swimming pools in the city of Brasília. (143) Although T11 is less frequent in *Acanthamoeba* epidemiological reports, it has been isolated from both clinical and environmental samples.(127)

Meanwhile, those samples that are missing to be reported in Table 3.8 (e.g.: SA, SB, and SC at the 2nd campaign) did not produce conclusive results on genotyping isolates. Therefore, further surveys will have the potential to contribute to enlarging the knowledge of FLA diversity in the Monjolinho River. For instance, the metagenomics based investigation under current analysis by the ongoing BIOTA FAPESP project (mentioned in Chapter 1, section 1.5.2) has the potential to bring complementary information expanding our findings, especially to those sampling sites not conclusive on this thesis investigations.

Nevertheless, the variety of amplicons retrieved in the present thesis (section 3.3.1.1.) enabled to the identification of six FLA genera: *Naegleria*, *Vermamoeba*, *Acanthamoeba*, *Vannella, Filamoeba* and *Stenamoeba* (Tables 3.15) whose distribution throughout the

Monjolinho basin and its consequent impact on the hydric system and concerns to the human health are discussed ahead.

3.3.2.2 Epidemiological contributions - potentially pathogenic species

Naegleria target PCRs employed against eDNA from all sampling sites, A – E, in the first Monjolinho River sampling enabled us to propose a comprehensive landscape of *Naegleria* spp and *Vermamoeba vermiformis* distribution in the hydrographic basin, as illustrated in the following map (Figure 3.47).

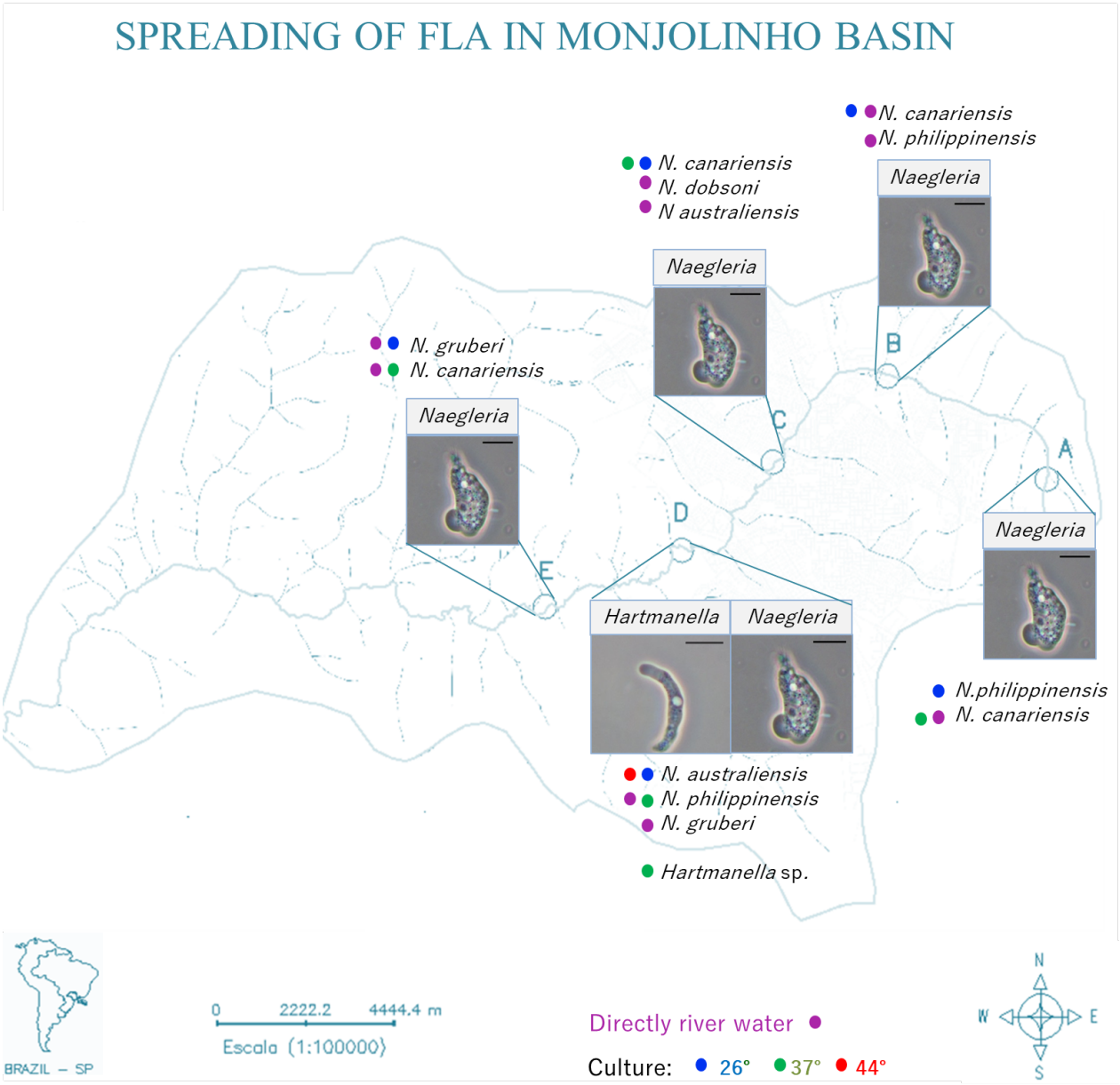

Figure 3.47 - The landscape of FLA isolates identified along the Monjolinho River basin during the first sampling, with emphasis on *Naegleria* spp. and *Vermamoeba* spp. genera. Trophozoites identified either from culture plates maintained at 26 ºC (blue), 37 ºC (green), and 44 ºC (red), or directly from river water (purple).
Source: By the author.

Figure 3.47 shown a diversity of five *Naegleria* species (*N. philippinensis, N. canariensis, N.dobsoni, N.australiensis* and *N.gruberi*) in addition to the *Hartmanella* spp., recovered in the first sampling campaign. This view enabled us to discriminate between results provide with cultivation-based analysis (Fig. 3.47, blue, green, and red circles) and those results provided directly from river water DNA characterization (Fig. 3.47, purple circles). The first observation exposed *Naegleria* as a ubiquitous genus to all sampling sites addressed in this research. On the

contrary, *Hartmanella* comprised a focal identification, detected through culture-based identification (D sampling site, Figure 3.47). Accounting no *Hartmanella* detection was obtained by directly examining water samples (Fig. 3.47, purple circles), we suggest that this result is likely a matter of low cell concentration in water, hampering its molecular detection. Thus, NNA plate cultivation seemed to be useful to enable the enrichment of *Hartmanella* population, confirmed by its subsequent molecular analysis (section 3.3.1.1). In the same regard, *Naegleria* species revealed this pattern for *N. canariensis* and *N. australiensis* identifications. The former, isolated in A sampling site through culture-based method (26 ºC), and the latter as well as isolated by culture, in D sampling site at 44 ºC (Fig. 3.47). Both identifications were not achieved by directly evaluating river water samples, only by culture (Fig. 3.47). The opposite pattern was also observed, in which samples demonstrated to be successfully diagnosed with eDNA extracted directly from the river, but not retrieved from cultivation based detection (e.g.: *N. dobsoni*, C sampling site, Fig. 3.47). These examples remarked the need for a complementary approach based on morphological and molecular investigations to obtain a thorough screening of the microbiological profile inhabiting water sources.

Concerned on the range of temperature suitable to the outgrowth of *Naegleria* strains, the D sampling site called attention (Figure 3.47). Genotyped as *Naegleria australiensis*, this strain standed out as the unique thermophilic species recovered in the first Monjolinho River campaign whit capability of growing at 44 ºC (Fig. 3.47, red circle). Although *N. australiensis* is renowned as thermotolerant, none of the earlier studies demonstrate its tolerance to 44 ºC, neither from environmental samples nor at laboratory conditions.(304) As an example, two out of five *N. australisnsis* strains isolated in the Nile River did not growth at 40 °C. (118) Thus, *N. australiensis* withstanding to 44 °C was a surprising result obtained on this thesis.

To discuss the impact of amoeba contaminated water to the surrounding areas of the Monjolinho river basin, those results documented to the first sampling (Fig. 3.47) were complemented with the extended survey addressed in this work by collecting results from the second sampling in the river. Thus, the following map illustrates the updated landscape of FLA distribution on the Monjolinho River (Figure 3.48).

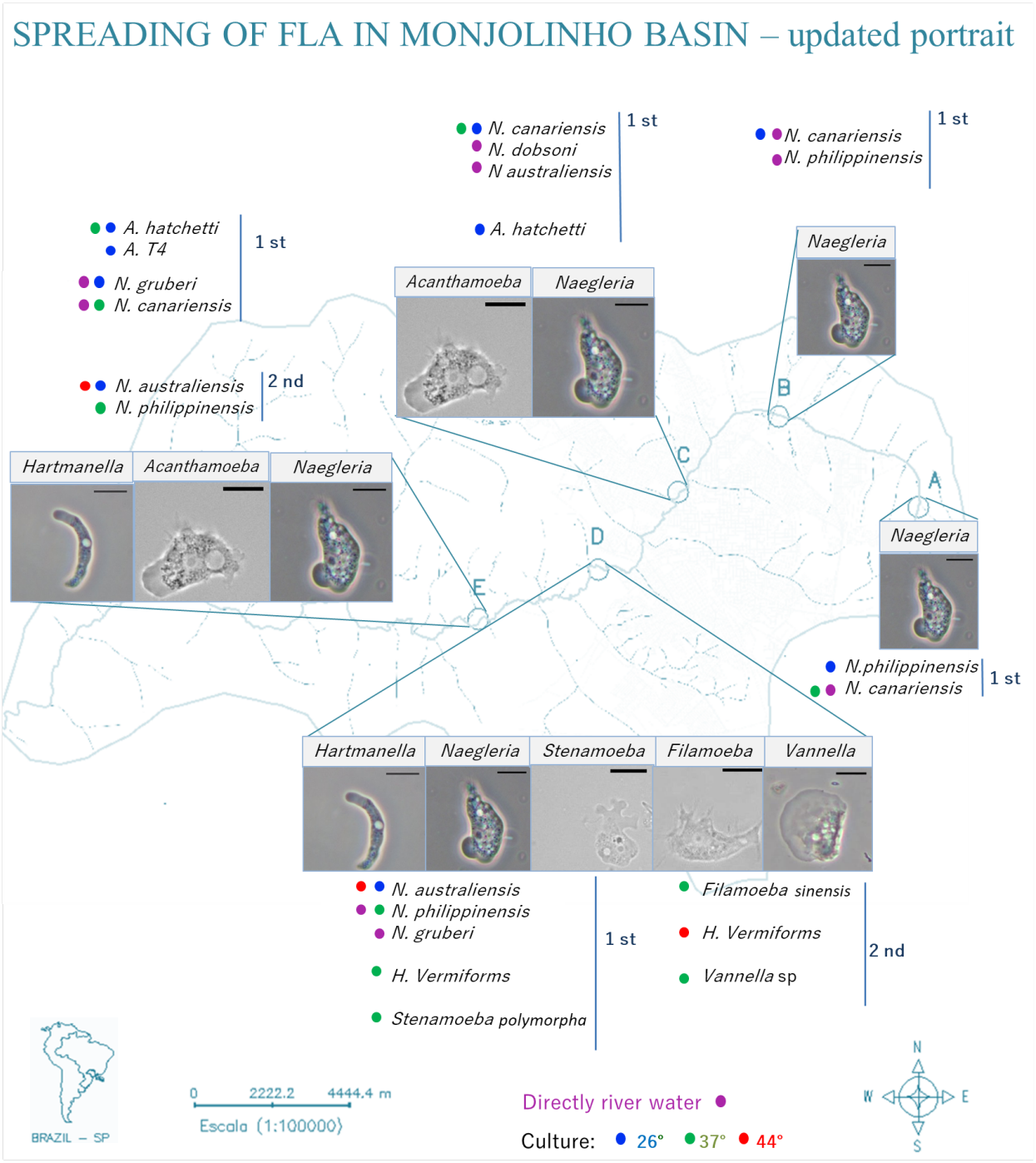

Figure 3.48 - The landscape of FLA isolates identified throughout the Monjolinho River basin during both, the 1st and 2nd samplings. Blue, green, red, and purple circles refer to the trophozoites identified either from culture plates maintained at 26 ºC, 37 ºC and 44 ºC, or directly from the river water, respectively.
Source: By the author.

In comparison, the updated view (Fig. 3.48) leveraged the identification demonstrated in the first mural (Fig 3.47) by broadening the diversity of species apart from *Naegleria* and *Hartmanella* findings. Results in Figure 3.48 demonstrated those genera able to withstand in

environments suggested to be harmful to life proliferation (e.g.: D and E sampling sites) whose abiotic factors of water indicated highly eutrophicated areas with a low concentration of dissolved oxygen (section 3.1.2). It was observed an increase in FLA diversity in the sampling site upon the higher human activity impact (Fig. 3.48, D sampling site). The E sampling site diversity revealed the capability of FLA persisting in water regardless of the treatment routines employed in the wastewater treatment plant, placed between both D and E sampling sites (Fig. 3.1). However, this research did not undergo quantitative evaluation to properly confirm the correlation between physico-chemical features and the FLA outgrowth. Thus, our analysis, to this concern, revealed suggestive findings. In agreement to this, studies have confirmed that the correlation among physicochemical, hydrologic, and microbiological factors modulating FLA presence and behavior is still poorly understood by the literature.(21,68)

Figure 3.48 demonstrated *Naegleria* and *Vermamoeba* detections to both 1st and 2nd collections in Monjolinho River. In regard to *Naegleria*, the identification of *N.australiensis* and *N.philippinensis* brings an important issue to be explored due to its capability of causing encephalitis in experimental models and freshwater isolated fishes. (19,240) Literature reports demonstrated *N. australiensis* as a causative agent of subacute meningoencephalitis on the nervous system of mice. (9,81,299,305-306) Potentially pathogenic *Naegleria* species has been a constant from the headwater (A) to the last sampling site (E), as shown in Fig. 3.48.

Moreover, accounting that *N. australiensis* demonstrated to be able to grow into 44ºC at both cultivation-based studies (1st and 2nd samplings), the availability of environmental niches for such thermophilic species is likely to be prevalent regarding global warming effects. (307–309) This concern has been currently argued to *N. fowleri* environmental distribution.(147) Another species isolated in the Monjolinho river that can likely be favored in a water heating context evoked by global warming refers to *Vermamoeba vermiformis*, able to withstand at 44 ºC (Fig. 3.48). Several studies highlighted the potential of water temperature on modulating microbiological complexity in which amoebic outbreaks have been ranked among a list of waterborne microorganisms whose growth can be impacted in a perspective of water temperature warming. (147,165)

In regard to *Acanthamoeba* identifications along Monjolinho river, *Acanthamoeba* genotype T4 and *A. hatchetti*, with recognized human health importance, were detected in C and E samples (Fig 3.48). *Acanthamoeba* genotype T4 isolates have been indicated as the most

prevalent strains linked with ocular infections, as well as a causative agent of neurological impairments (250) and demonstrated to be the most pathogenic genotype of *Acanthamoeba*. (273,310) A current Brazilian survey concerned on the investigation of *Acanthamoeba* in urban environments detected air-conditioned samples positives to *Acanthamoeba* T4.(182) *A. hatchetti* comprises the list of *Acanthamoeba* strains commonly associated with human infections, (311) as reported to amoeba keratitis suffering patients, diagnosed with *A. hatchetti* clinical reports from Mexico. (312)

Accounting for the non-pathogenic FLA identifications in Monjolinho river, *Vannela*, *Steanamoeba*, and *Filamoeba* (Fig. 3.48), they can also pose a concern to human health due to cases of pathogenic bacteria reported proliferating intra-FLA. (263,313) *Vannella* spp. has been reported as a vehicle to microsporidia-like parasites evoking keratistis onset on contact lenses wearing patients. *Vannella* extracted from pieces of contact lenses was isolated, cultured and enabled to confirming the endocytobionts causative of keratitis. (314) Even though we did not found literature reports confirming bacteria and fungi infecting *Filamoeba* and *Stenamoeba*, these genera have been important due to being isolated in the environment and in animals suggesting its potential as pathogenic. *Stenamoeba* has been isolated from horses, (315) fishes, (316), and several water sources. (317) By examining *Stenamoeba* growth in temperatures equivalent to the human body, the genus has been suggested as potentially amphizoic FLA amoeba. (315) In regard to *Filamoeba*, it has been isolated in drinking water samples, (318) fishes, (280) and pigs. (273) In this thesis, *Filamoeba*, along with *Vannela* and *Stenamoeba*, demonstrated to be also capable of inhabiting one of the most eutrophic water samples from Monjolinho river basin, D sampling site (Fig 3.48).

The outcomes summarized here contributed to broaden the epidemiological knowledge of FLA in Brazil. Comparing FLA spread throughout five sampling sites in Monjolinho river (Fig. 3.48), critical areas were highlighted and may need continuous surveillance to pathogenic FLA presence as future risk management measures. As environmental amoebas infect the host by direct contact (111-112) it is of great public health importance the knowledge of FLA occurrence, lightened up on the regional scale based on Monjolinho river (Fig. 3.47 and Fig. 3.48). Even though we have focused on a regional scale, the advances experienced in this research can be useful to similar freshwater systems investigated in foreign related surveys.

Chapter 4 Conclusions

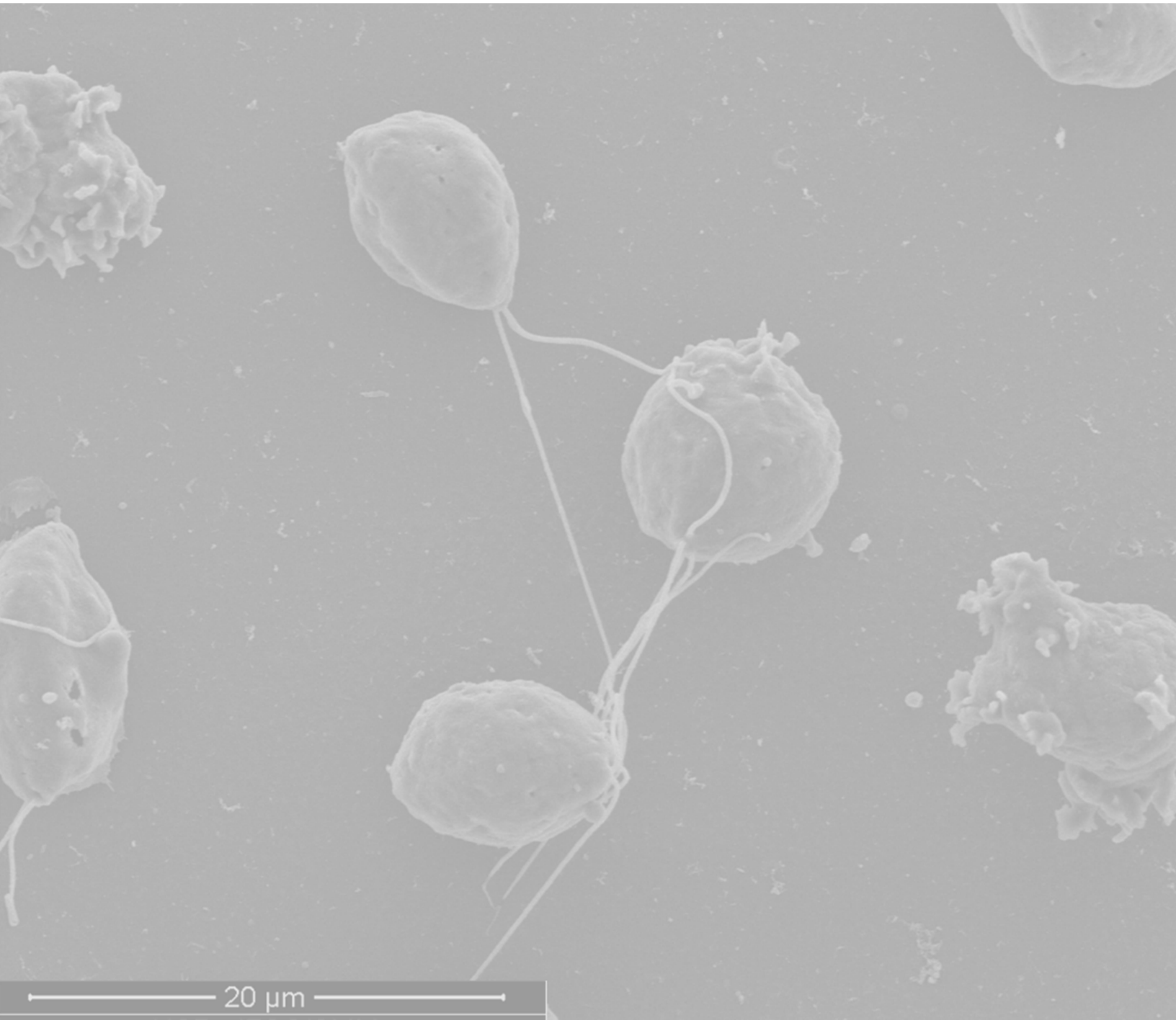

Scanning electron microscopy of *Naegleria gruberi* flagellates.

Source: By the author.

Overall, the findings described at the present research enriched Brazilian scenery on FLA based studies due to contributing with: expertize on isolating environmental FLA, knowledge about useful methods to classify FLA, to maintain cultures at NNA plates and to perform correspondent morphological and molecular characterizations. Results provided from this PhD study enabled the identification of the Monjolinho River as an emerging freshwater source to FLA proliferation. Physicochemical analysis of Monjolinho river water demonstrated that A to C sampling sites fitted in Brazilian legislations of water quality and the upstream locations, D and E sampling sites ranged with values in the limit of acceptance. Among four abiotic parameters investigated in this research, conductivity and dissolved oxygen configured as useful parameters to inspect anthropogenic driving forces acting upon the hydric ecosystem once both played as major discriminators to differentiate all sampling sites. Both physicochemical parameters allowed us to indicate D sampling site as the most impacted area in consequence of anthropogenic input in Monjolinho aquatic ecosystem.

By sampling Monjolinho River to the characterization of FLA, the preset research described *Naegleria* genera as prevalent in all sampling sites, from A to E, accompanied by a diversity of five related genera, *Vannela, Stenamoeba, Acanthamoeba, Filamoeba*, and *Hartmanella*. These findings highlighted the potential of this freshwater system to harbor amoeba proliferation. Thus, to the point of view of water quality and microbiological assessment of potentially pathogenic FLA in water, techniques outlined here can be adopted as suitable methodologies enabling the identification of this waterborne protozoan. Overall, fresh mount slides, staining, and scanning electron imaging enabled to set these techniques as reliable methods to be assessed in hope of performing morphotype differentiation and taxonomy. The entire set of micrographs acquired with morphological-based characterization allowed us to measure trophozoites lengths, evaluating pseudopodia branching patterns, uroidal protuberances, organelle positions, details of flagellate forms, cyst diameter, pores structure, among others. Each morphologic feature demonstrated to be typical of each FLA genera isolated in this thesis was properly assured by comparing our findings with Page´s classification guide descriptions, besides being compliant with taxonomy discussed on current FLA literature. Additionally, cyst software proposition, a non-canonical methodology proposed here, although at initial stages of development, is demonstrated as a potential strategy towards automatization of taxonomic studies. Up to now, this method can be adopted as a morphological step of filtering information

aiming to reach higher chances of obtaining positive amplifications with genera specific molecular targets.

Complementary to that, molecular-based investigation allowed us to confirm the previous culture-based suggestions, besides discriminating intrinsic diversity of FLA species identified on river water samples. Due to cloning PCR products and screening positives colonies, sequencing-based results demonstrated that a diversity of amplimer, a diversity of strains, was detected to those samples that, roughly viewed, seemed to be homogeneous. The major outcome provided from the 1st sampling study, standed out to the importance on taking into account both culture-based investigations, here including 26 ºC, 37 ºC and 44 ºC, along with the molecular characterization directly from river water evaluation. Aiming to reach a thorough microbiological characterization, our full-scale evaluation on Monjolinho river samples allowed us to obtain positive amplifications not only to *Naegleria* PCR-based target but also to *Vermamoeba* and *Acanthamoeba* genus-specific primer pairs, besides the universal FLA target. Results provided with the second sampling leveraged our findings in which the whole list of isolates comprises potentially pathogenic FLA strains (*N. australiensis*, *N. phillipinensis*, *A. genotype T4*, *A. hatchetti*, *V. vermifoms*), and non-pathogenic FLA (*N. dobsoni, N. gruberi, N. canariensis, S. polymorpha, F. sinensis* and *Vannella* spp). Thus we highlighted the relevance of assessing FLA due to serious sanitary problems pathogenic may represent, as well as the non pathogenic, if carrying pathogenic microbiome. In this study, thermotolerant potentially pathogenic identifications, e.g. *N. australiensis* and *V. vermiformis*, called attention as strains that will likely be prevalent in a global warming forthcoming condition. Its distribution along Monjolinho river, together with *Acanthamoeba* pathogenic strains, suggested those sites that can be regularly evaluated aiming to avoid future outbreaks.

Altogether, results documented in this thesis contributed to broaden the knowledge on FLA biodiversity in a Brazilian freshwater model.

REFERENCES

1 PAWLOWSKI, J. The twilight of Sarcodina: a molecular perspective on the polyphyletic origin of amoeboid protists.*Protistology*, v.5, n.4, p.281–302, 2008.

2 MARTINEZ, A. J. *et al*. Free-living, amphizoic and opportunistic amebas. *Brain Pathology*, v. 7, n. 1, p. 583–598, 1997.

3 WHITTAKER, R. H. New concepts of kingdoms of organisms. *Science,* v.163, n. 3863, p.150-160, 1969.

4 GRAY, M. W. Lynn Margulis and the endosymbiont hypothesis : 50 years later. *Molecular Biology of the Cell*, v. 28, n.10, p.1285–1287, 2017.

5 SOGIN, M. L. History assignment : when was the mitochondrion founded ? *Current Opinion in Genetics and Development*, v.7, n. 6, p.792-799, 1977.

6 SIMPSON, A. G. B. *et al*. The real "kingdoms" of eukaryotes. *Current Biology*, v. 14, n. 17, 693–696, 2004.

7 ADL, S.M. *et al.* The new higher level classification of eukaryotes with emphasis on the taxonomy of protists. *Journal of Eukaryotic Microbiology,* v. 52, n. 5, p. 399–451, 2005.

8 BALDAUF, S. L. *et al.* A Kingdom-level phylogeny of eukaryotes based on combined protein data. *Science*, v. 290, n. 5493, p. 972–978, 2000.

9 FRITZ-LAYLIN, L. K. *et al*. The genome of *Naegleria gruberi* illuminates early eukaryotic versatility. *Cell*, v. 140, n. 5, p. 631–642, 2010.

10 SIMPSON, A. G. B.; INAGAKI, Y.; ROGER, A. J. Comprehensive multigene phylogenies of excavate protists reveal the evolutionary positions of " primitive " eukaryotes. *Molecular Biology and Evolution*, v. 23, n. 3, p. 615-625, 2006.

11 KEELING, P. J.; BURKI, F. Progress towards the tree of eukaryotes. *Current Biology*, v. 29, n. 16, p. R808–R817, 2019.

12 BURKI, F.; ROGER, A. J.; BROWN, M.W.; SIMPSON, A. G. B.. *Trends in Ecology & Evolution*, v. 35, n. 1, p. 43–55, 2020.

13 GARCIA, A.; GOÑI, P.; CIELOSZYK, J.; FERNANDEZ, M.T.; CALVO-BEGUERÍA, L.; RUBIO, E.; FILLAT, M.F.; PELEATO, M.L.; CLAVEL, A. Identification of free-living amoebae and amoeba-associated bacteria from reservoirs and water treatment plants by molecular techniques. *Environmental Science & Technology*, v. 47, n. 7, p. 3132–3140, 2013

14 MICHEL, R.; MILITARY, C.; KOBLENZ, H.; WYLEZICH, C.; GERMANY, G.R.; HAUROEDER, B.; KOBLENZ, B.; ALEXEY, S. Protistology phylogenetic position and notes on the ultrastructure of *Sappinia diploidea* (Thecamoebidae). *Protistology*, v. 4, n. 4, p. 319-

325, 2006.

15 THOMAS, V.; LORET, J. F.; JOUSSET, M.; GREUB, G. Biodiversity of amoebae and amoebae-resisting bacteria in a drinking water treatment plant. *Environmental Microbiology*, v. 10, n. 10, p. 2728–2745, 2008.

16 DE JONCKHEERE, J.F. The isolation of *Naegleria italica* from Peru indicates that this potentially pathogenic species occurs worldwide. *Parasitology International*, v. 54, n. 3, p. 173–175, 2005.

17 VISVESVARA, G. S. Free-living amebae as opportunistic agents of human disease. *Journal Neuroparasitology*, v. 1, p.1–13, 2010. DOI: 10.4172 / 2314-7326.1000106

18 DUGGAL, S. D.; RONGPHARPI, S. R. Role of *Acanthamoeba* in Granulomatous encephalitis : a review. *Journal of Infectious Diseases & Immune Therapies*, v.1, n. 1, p.1-12, 2017.

19 VISVESVARA, G.S.; MOURA, H.; SCHUSTER, F.L. Pathogenic and opportunistic free-living amoebae: *Acanthamoeba* spp., *Balamuthia mandrillaris* , *Naegleria fowleri* , and *Sappinia diploidea*. FEMS *Immunology & Medical Microbiolog*y, v. 50, n. 1, p. 1–26, 2007.

20 PAGNIER, I.; VALLES, C.; RAOULT, D.; LA SCOLA, B. Isolation of *Vermamoeba vermiformis* and associated bacteria in hospital water. *Microbial Pathogenisis*. v. 80, p.14–20, 2015. DOI: 10.1016 / j.micpath.2015.02.006.

21 DELAFONT, V.; RODIER, M.; MAISONNEUVE, E.; CATEAU, E. *Vermamoeba vermiformis* : a free-living amoeba of interest. *Microbial Ecology*, v. 76, n. 4, p. 991–1001, 2018.

22 SCHUSTER, F. L.; VISVESVARA, G. S. Free-living amoebae as opportunistic and non-opportunistic pathogens of humans and animals. *International Journal Parasitology*, v. 34, n. 9, p.1001–1027, 2004.

23 PAGE, F.C. *A new key to freshwater and soil gymnamoebae.* Pennsylvania: Freshwater Biological Association, 1988.

24 LIANG, S.Y.; JI, D.R.; HSIA, K.T.; HUNG, C.C.; SHENG, W.H.; HSU, B.M.; CHEN, J.S.; WU, M.H.; LAI, C.H.; JI, D.D. Isolation and identification of *Acanthamoeba* species related to amoebic encephalitis and nonpathogenic free-living amoeba species from the rice field. *Journal of Applied Microbiology*, v. 109, n. 4, 1422–1429, 2010.

25 VISVESVARA, G. S.; DE JONCKHEERE, J. F.; MARCIANO-CABRAL, F.; SCHUSTER, F. L. Morphologic and molecular identification of *Naegleria dunnebackei* n. sp. isolated from a water sample. *Journal Eukaryotic Microbiology*, v. 52, n. 6, p. 523–531, 2005.

26 VISVESVARA, G.S. Infections with free-living amebae. *In:* VISVESVARA, G.S.*Handbook of clinical neurology*, Amsterdan: Elsevier,2013. v. 114; 2013. DOI: 10.1016 / B978-0-444-53490-3.00010-8

27 SMIRNOV, A. *et al*. Phylogeny and systematics of leptomyxid amoebae (Amoebozoa, Tubulinea, Leptomyxida). *Protist*, v. 168, n. 2, p. 220–252, 2017.

28 SOHN, H. J.; KIM, J. H.; SHIN, M. H.; SONG, K. J.; SHIN, H. J. The Nf-actin gene is an important factor for food-cup formation and cytotoxicity of pathogenic *Naegleria fowleri*. *Parasitology Research,* v. 106, n. 4, p. 917–924, 2010.

29 SMIRNOV, A. V.; CHAO, E.; NASSONOVA, E.S.; CAVALIER-SMITH, T. A revised classification of Naked Lobose amoebae (Amoebozoa: Lobosa). *Protist*, v. 162, n. 4, p. 545–570, 2011.

30 EDAGAWA, A.; KIMURA, A.; KAWABUCHI-KURATA, T.; KUSUHARA, Y.; KARANIS, P. Isolation and genotyping of potentially pathogenic *Acanthamoeba* and *Naegleria* species from tap-water sources in Osaka, Japan. *Parasitology Research*, v. 105, n. 4, p. 1109–1117, 2009.

31 KUDRYAVTSEV, A.; GLADKIKH, A. Two new species of Ripella (Amoebozoa , Vannellida) and unusual intragenomic variability in the SSU rRNA gene of this genus. *European Journal Protistology*, v. 61, Part A, p. 92–106, 2017.

32 CORSARO, D.; WYLEZICH, C.; WALOCHNIK, J.; VENDITTI, D.; MICHEL, R. Molecular identification of bacterial endosymbionts of *Sappinia* strains. *Parasitology Research*, v. 116, n. 2, p. 549–558, 2017.

33 TSVETKOVA, N.; SCHILD, M.; PANAIOTOV, S.; KURDOVA-MINTCHEVA, R.; GOTTSTEIN, B.; WALOCHNIK, J.; ASPÖCK, H.; LUCAS, M.S.; MÜLLER, N. The identification of free-living environmental isolates of amoebae from Bulgaria. *Parasitology Research*, v. 92, n. 5, p. 405–413, 2004.

34 KHAN, N.A. *Acanthamoeba* : biology and increasing importance in human health. *FEMS Microbiology Reviews*, v. 30, n. 4, p. 564–595, 2006.

35 TODD, S. R..; KITCHING, J. A. Effects of high hydrostatic pressure on morphogenesis in *Naegleria gruberi* (Schardinger)*. *Journal of Protozoology*, v. 20, n. 3, p. 421–424, 1973.

36 SCHUSTER, F.L. Cultivation of pathogenic and opportunistic free-living amebas. *Clinical Microbiology Reviews*, v. 15, n. 3, p. 342–354, 2002.

37 LORENZO-MORALES, J.; CABELLO-VÍLCHEZ, A.M.; MARTÍN-NAVARRO, C.M.; MARTÍNEZ-CARRETERO, E.; PIÑERO, J.E.; VALLADARES, B. Is *Balamuthia mandrillaris* a public health concern worldwide? *Trends in Parasitology*, v. 29, n. 10, p. 483–488, 2013.

38 ABDUL MAJID, M.A. *et al*. Pathogenic waterborne free-living amoebae: An update from selected Southeast Asian countries. *PLoS One*, v. 12, n. 2, p. e0169448, 2017.

39 BELLINI, N. K.; SANTOS, T. M.; DA SILVA, M. T. A.; THIEMANN, O. H. The

therapeutic strategies against *Naegleria fowleri*. *Experimental Parasitology*, v. 187, p. 1–11, 2018. DOI: 10.1016/j.exppara.2018.02.010

40 SCHAAP, P.; SCHILDE, C. Encystation: the most prevalent and underinvestigated differentiation pathway of eukaryotes. *Microbiology (United Kingdom)*, v. 164, n. 5, p. 727–739, 2018.

41 MARCIANO-CABRAL, F.; CABRAL, G. *Acanthamoeba* spp. as agents of disease in humans. *Clinical Microbiology Reviews*, v. 16, n. 2, p. 273–307, 2003.

42 CHÁVEZ-MUNGUÍA, B. *et al*. Ultrastructural study of the encystation and excystation processes in *Naegleria* sp. *Journal of Eukaryotic Microbiology*, v. 56, n. 1, p. 66–72, 2009.

43 CHÁVEZ-MUNGUÍA, B.; SALAZAR-VILLATORO, L.; LAGUNES-GUILLÉN, A.; OMAÑA-MOLINA, M.; ESPINOSA-CANTELLANO, M.; MARTÍNEZ-PALOMO, A. *Acanthamoeba castellanii* cysts: new ultrastructural findings. *Parasitology Research*, v. 112, n. 3, p. 1125–1130, 2013.

44 PATTERSON, M.; WOODWORTH, T.W.; MARCIANO-CABRAL, F.; BRADLEY, S.G. Ultrastructure of *Naegleria fowleri* enflagellation. *Journal of Bacteriolog*y, v. 147, n. 1, p. 217–226, 1981.

45 SCHEID, P. Relevance of free-living amoebae as hosts for phylogenetically diverse microorganisms. *Parasitology Research*, v. 113, n. 7, p. 2407–2414, 2014.

46 SCHUSTER, F.L. *et al*. Environmental isolation of *Balamuthia mandrillaris* associated with a case of amebic encephalitis. *Journal of Clinical Microbiology*, v. 41, n. 7, p. 3175–3180, 2003.

47 KRÓL-TURMIŃSKA, K.; OLENDER, A. Human infections caused by free-living amoebae. *Annals of Agricultural and Environmental Medicine*, v. 24, n. 2, p. 254–260, 2017.

48 MACIVER, S.K.; PIÑERO, J.E.; LORENZO-MORALES, J. Is *Naegleria fowleri* an emerging parasite? *Trends in Parasitology*, v. 36, n.1, p. 19–28, 2020.

49 LAURA GERTISER, M.; VISCIARELLI, E.; BASABE, N.; JOSE PEREZ, M.; RAUL COSTAMAGNA, S. *Acanthamoeba* spp. in indoor swimming pools in Bahia Blanca city, Buenos Aires province, Argentina. *Acta Bioquimica Clinica Latinoamericana*, v. 44, n. 4, p. 697–703, 2010.

50 LORENZO-MORALES, J.; KHAN, N.A.; WALOCHNIK, J. An update on *Acanthamoeba* keratitis: diagnosis, pathogenesis and treatment. *Parasite,* v. 22, 2015. DOI: 10.1051/parasite/2015010.

51 LORENZO-MORALES, J.; MARTÍN-NAVARRO, C.M.; LÓPEZ-ARENCIBIA, A.; ARNALICH-MONTIEL, F.; PIÑERO, J.E.; VALLADARES, B. *Acanthamoeba* keratitis: an emerging disease gathering importance worldwide? *Trends in Parasitology,* v. 29, n. 4, p. 181–187, 2013.

52 SCHAFER, K.R.; SHAH, N.; ALMIRA-SUAREZ, M.I.; REESE, J.M.; HOKE, G.M.; MANDELL, J.W.; ROY, S.L. Disseminated *Balamuthia mandrillaris* Infection. *Journal of Clinical Microbiology*, v. 53, n. 9, p. 3072–3076, 2015.

53 SCHEID, P.L.; LÂM, T.T.; SINSCH, U.; BALCZUN, C. *Vermamoeba vermiformis* as etiological agent of a painful ulcer close to the eye. *Parasitology Research*, v. 118, p. 1999–2004, 2019. DOI:10.1007/s00436-019-06312-y.

54 SCHUSTER, F.L.; VISVESVARA, G.S. Opportunistic amoebae: challenges in prophylaxis and treatment. *Drug Resistance Updates*, v. 7, n. 1, p. 41–51, 2004.

55 ARNALICH-MONTIEL, F.; MARTÍN-NAVARRO, C.M.; ALIÓ, J.L.; LÓPEZ-VÉLEZ, R.; MARTÍNEZ-CARRETERO, E.; VALLADARES, B.; PIÑERO, J.E.; LORENZO-MORALES, J. Successful monitoring and treatment of intraocular dissemination of *Acanthamoeba*. *Archives of Ophthalmology*, v. 130, n. 11, p. 1474, 2012.

56 CARNT, N.A.; SUBEDI, D.; CONNOR, S.; KILVINGTON, S. The relationship between environmental sources and the susceptibility of *Acanthamoeba* keratitis in the United Kingdom. *PLoS One*, v. 15, p. 1–11, 2020. DOI: 10.1371/journal.pone.0229681

57 ABEDKHOJASTEH, H.; NIYYATI, M.; RAHIMI, F.; HEI-DARI, M.; FARNIA, S.; REZAEIAN, M. First report of *Hartmannella* keratitis in a cosmetic soft contact lens wearer in Iran. *Iranian Journal Parasitology*, v. 8, p. 481–485, 2013.

58 SIDDIQUI, R.; KHAN, N.A. Biology and pathogenesis of *Acanthamoeba*. *Parasites and Vectors*, v. 5, p. 6, 2012. DOI: 10.1186/1756-3305-5-6

59 SCHEID, P.L. *Vermamoeba vermiformis* - a free-living amoeba with public health and environmental health significance. *Open Parasitology Journal*, v. 7, n. 1, p. 40–47, 2019.

60 HAJIALILO, E.; NIYYATI, M.; SOLAYMANI, M.; REZAEIAN, M. Pathogenic free-living amoebae isolated from contact lenses of keratitis patients. *Iranian Journal of Parasitology*, v. 10, n. 4, p. 541–546, 2015.

61 LORENZO-MORALES, J.; MARTÍNEZ-CARRETERO, E.; BATISTA, N.; ÁLVAREZ-MARÍN, J.; BAHAYA, Y.; WALOCHNIK, J.; VALLADARES, B. Early diagnosis of amoebic keratitis due to a mixed infection with *Acanthamoeba* and *Hartmannella*. *Parasitology Research,* v. 102, n. 1, p. 167–169, 2007.

62 NIYYATI, M.; DODANGEH, S.; LORENZO-MORALES, J. A review of the current research trends in the application of medicinal plants as a source for novel therapeutic agents against *Acanthamoeba* infections. *Iranian Journal Pharmaceutical Research,* v. 15, n. 4, p. 893–900, 2016.

63 MARTÍN-NAVARRO, C.M. *et al*. Amoebicidal activity of caffeine and maslinic acid by the induction of programmed cell death in *Acanthamoeba*. *Antimicrobial Agents and Chemotherapy,*

v. 61, n. 6, p. e02660-16, 2017.

64 LORENZO-MORALES, J.; ORTEGA-RIVAS, A.; FORONDA, P.; ABREU-ACOSTA, N.; BALLART, D.; MARTÍNEZ, E.; VALLADARES, B. RNA interference (RNAi) for the silencing of extracellular serine proteases genes in *Acanthamoeba*: Molecular analysis and effect on pathogenecity. *Molecular and Biochemical Parasitology*, v. 144, n. 1, p. 10–15, 2005.

65 SIFAOUI, I.; RODRÍGUEZ-EXPÓSITO, R.L.; REYES-BATLLE, M.; RIZO-LIENDO, A.; PIÑERO, J.E.; BAZZOCCHI, I.L.; LORENZO-MORALES, J.; JIMÉNEZ, I. A. Ursolic acid derivatives as potential agents against *Acanthamoeba* Spp. *Pathogens*, v. 8, n. 3, p. 130, 2019.

66 CARTUCHE, L.; SIFAOUI, I.; CRUZ, D.; REYES-BATLLE, M.; LÓPEZ-ARENCIBIA, A.; JAVIER FERNÁNDEZ, J.; DÍAZ-MARRERO, A.R.; PIÑERO, J.E.; LORENZO-MORALES, J. Staurosporine from streptomyces sanyensis activates programmed cell death in *Acanthamoeba* via the mitochondrial pathway and presents low in vitro cytotoxicity levels in a macrophage cell line. *Scientific Reports*, v. 9, n. 11651, p.1–12, 2019.

67 KHAN, N.A.; ONG, T.Y.Y.; SIDDIQUI, R. Targeting brain-eating amoebae infections. ACS *Chemical Neuroscience*, v. 8, n. 4, p. 687–688, 2017.

68 MATIN, A.; SIDDIQUI, R.; JAYASEKERA, S.; KHAN, N. A. Increasing importance of *Balamuthia mandrillaris*. *Clinical Microbiology Reviews*, v. 21, n. 3, p. 435–448, 2008.

69 ROCHA-AZEVEDO, B.; TANOWITZ, H.B.; MARCIANO-CABRAL, F. Diagnosis of infections caused by pathogenic free-living amoebae. *Interdisciplinary Perspectives on Infectious Diseases.* v. 2009, p. 21-26. doi:10.1155/2009/251406

70 QVARNSTROM, Y.; SILVA, A.J.; SCHUSTER, F.L.; GELMAN, B.B.; VISVESVARA, G.S. Molecular confirmation of *Sappinia pedata* as a causative agent of amoebic encephalitis. *Journal of the Infectious Diseases,* v. 199, n. 8, p. 1139–1142, 2018.

71 ONG, T.Y.Y.; KHAN, N.A.; SIDDIQUI, R. Brain-eating amoebae: predilection sites in the brain and disease outcome. *Journal of Clinical Microbiology*, v. 55, n. 7, p. 1989–1997, 2017.

72 SCHEID, P. Relevance of free-living amoebae as hosts for phylogenetically diverse microorganisms. *Parasitolology Research*, v. 113, n. 7, p. 2407–2417, 2014.

73 TAVARES, M. *et al*. Diagnosis of first case of *Balamuthia* amoebic encephalitis in Portugal by immunofluorescence and PCR. *Journal of Clinical Microbiology*, v. 44, n. 7, p. 2660–2663, 2006.

74 COPE, J.R.; ALI, I.K. Primary amebic meningoencephalitis: what have we learned in the last 5 years? *Current Infectious Disease Reports*, v. 18, n. 10, p. 1–7, 2016. DOI: 10.1007/s11908-016-0539-4

75 VARGAS-ZEPEDA, J.; GÓMEZ-ALCALÁ, A. V.; VÁZQUEZ-MORALES, J.A.; LICEA-AMAYA, L.; DE JONCKHEERE, J.F.; LARES-VILLA, F. Successful treatment of *Naegleria*

fowleri meningoencephalitis by using intravenous amphotericin B, fluconazole and rifampicin. *Archives of Medical Research*, v. 36, n. 1, p. 83–86, 2005.

76 CARY, L.C.; MAUL, E.; POTTER, C.; WONG, P.; NELSON, P.T.; GIVEN, C.; ROBERTSON, W. *Balamuthia mandrillaris* meningoencephalitis: survival of a pediatric patient. *Pediatrics*, v. 125, n. 3, p. 699-703, 2010.

77 DEETZ, T.R.; SAWYER, M.H.; BILLMAN, G.; SCHUSTER, F.L. Successful treatment of *Balamuthia* amoebic encephalitis: presentation of 2 cases. *Clinical Infectious Diseases*, v. 37, n. 10, p. 1304–1312, 2003.

78 STUBHAUG, T.T.; REIAKVAM, O.M.; STENSVOLD, C.R.; HERMANSEN, N.O.; HOLBERG-PETERSEN, M.; ANTAL, E.; GAUSTAD, K.; FØRDE, I.S.; HEGER, B. Fatal primary amoebic meningoencephalitis in a Norwegian tourist returning from Thailand. JMM *Case Reports*, v. 3, n. 3, p. 1-5, 2016.

79 MCKELLAR, M.S.; MEHTA, L.R.; GREENLEE, J.E.; HALE, D.C.; BOOTON, G.C.; KELLY, D.J.; FUERST, P.A.; SRIRAM, R.; VISVESVARA, G.S. Fatal granulomatous *Acanthamoeba* encephalitis mimicking a stroke, diagnosed by correlation of results of sequential magnetic resonance imaging, biopsy, in vitro culture, immunofluorescence analysis, and molecular analysis. *Journal of Clinical Microbiology*, v. 44, n. 11, p. 4265–4269, 2006.

80 BISWAL, I. *et al*. Role of *Acanthamoeba* in granulomatous encephalitis: a review. *Journal of Infectious Diseases & Immune Theraphy*, v. 1, n. 1, p. 1–12, 2017.

81 DE JONCKHEERE, J. F. Origin and evolution of the worldwide distributed pathogenic amoeboflagellate *Naegleria fowleri. Infection, Genetics and Evolution*, v. 11, n. 7, p. 1520–1528, 2011.

82 RIZO-LIENDO, A. *et al*. In vitro activity of statins against *Naegleria fowleri*. *Pathogens*, v. 8, n. 3, p. 122, 2019.

83 GELMAN, B.B.; POPOV, V.; CHALJUB, G.; NADER, R.; RAUF, S.J.; NAUTA, H.W.; VISVESVARA, G.S. Neuropathological and ultrastructural features of amebic encephalitis caused by *Sappinia diploidea*. *Journal of Neuropathology & Experimental Neurology*, v. 62, n. 10, p. 990–998, 2003.

84 LINAM, W. M.; AHMED, M.; COPE, J. R.; CHU, C.; VISVESVARA, G. S.; DA SILVA, A. J.; QVARNSTROM, Y.; GREEN, J. Successful treatment of an adolescent with *Naegleria fowleri* primary amebic meningoencephalitis. *Pediatrics,* v. 135, n. 3, p. 744-748, 2015.

85 GRENINGER, A.L. *et al*. Clinical metagenomic identification of *Balamuthia mandrillaris* encephalitis and assembly of the draft genome: the continuing case for reference genome sequencing. *Genome Medicine*, v.7, p. 1–14, 2015. DOI: 10.1186/s13073-015-0235-2

86 PARIJA, S.; VENUGOPAL, H.; DINOOP, K. P. Management of granulomatous amebic encephalitis: laboratory diagnosis and treatment. *Tropical Parasitology*, v. 5, n. 1, p. 23, 2015.

87 BAIG, A.M.; KULSOOM, H.; KHAN, N.A. Primary amoebic meningoencephalitis: amoebicidal effects of clinically approved drugs against *Naegleria fowleri*. *Journal of Medical Microbiology*, v. 63, Pt. 5, p. 760–762, 2014.

88 CERVANTES-SANDOVAL, I.; SERRANO-LUNA, J. DE J.; MEZA-CERVANTES, P.; ARROYO, R.; TSUTSUMI, V.; SHIBAYAMA, M. *Naegleria fowleri* induces MUC5AC and proinflammatory cytokines in human epithelial cells via ROS production and EGFR activation. *Microbiology*, v. 155, Pt. 11, p. 3739–3747, 2009.

89 DEBNATH, A.; TUNAC, J.B.; GALINDO-GÓMEZ, S.; SILVA-OLIVARES, A.; SHIBAYAMA, M.; MCKERROW, J. H. Corifungin, a new drug lead against *Naegleria*, identified from a high-throughput screen. *Antimicrobial Agents and Chemotheraphy*, v. 56, n. 11, p. 5450–5457, 2012.

90 VISVESVARA, G.S. Amebic meningoencephalitides and keratitis: challenges in diagnosis and treatment. *Current Opinious of Infectious Diseases*, v. 23, n. 6, p. 590–594, 2010.

91 ANWAR, A.; KHAN, N.A.; SIDDIQUI, R. Repurposing of drugs is a viable approach to develop therapeutic strategies against central nervous system related pathogenic amoebae. *ACS Chemical Neuroscience*, v. 11, n. 16, p. 2378, 2020.

92 TRABELSI, H. *et al*. Pathogenic free-living amoebae: epidemiology and clinical review. *Pathologie-Biologie*, v. 60, n. 6, p. 399–405, 2012.

93 PETRY, F. *et al*. Early diagnosis of *Acanthamoeba* infection during routine cytological examination of cerebrospinal fluid. *Journal of Clinical Microbiology*, v. 44, n. 5, p. 1903–1904, 2006.

94 BAIG, A.M.; KHAN, N.A. Tackling infection owing to brain-eating amoeba. *Acta Tropica,* v. 142, p. 86–88, 2015. DOI: 10.1016/j.actatropica.2014.11.004.

95 BAGINSKI, M.; CZUB, J. Amphotericin B and its new derivatives - mode of action. *Current Drug Metabolism*, v. 10, n. 5, p. 459–469, 2009.

96 PEROUTKA-BIGUS, N.; BELLAIRE, B.H. Antiparasitic activity of auranofin against pathogenic *Naegleria fowleri*. *Journal of Eukaryotic Microbiolo*gy, v. 66, n. 4, p. 684–688, 2019.

97 ESCRIG, J.I.; HAHN, H.J.; DEBNATH, A. Activity of auranofin against multiple genotypes of Naegleria fowleri and its synergistic effect with amphotericin B in vitro. *ACS Chemical Neuroscience*, v. 11, n. 16, p. 2464, 2020.

98 RICE, C.A.; LARES-JIMÉNEZ, L.F.; LARES-VILLA, F. In vitro screening of the open-source medicines for malaria venture malaria and pathogen boxes to discover novel compounds with activity against *Balamuthia mandrillaris*. *Antimicrobial Agents and Chemotherapy,* v. 64, n.5, p.02233-19, 2020.

99 MOREIRA, R.A.; MENDANHA, S.A.; FERNANDES, K.S.; MATOS, G.G.; ALONSO, L.; DORTA, M.L.; ALONSO, A. Miltefosine increases lipid and protein dynamics in *Leishmania* membranes at similar concentrations to those needed for cytotoxicity activity. *Antimicrobial Agents and Chemotheraphy*, v. 58, n. 6, p. 3021–3028, 2014.

100 SCHAFER, K.R.; SHAH, N.; ALMIRA-SUAREZ, M.I.; REESE, J.M.; HOKE, G.M.; MANDELL, J.W.; ROY, S.L.; VISVESVARA, G. Disseminated *Balamuthia mandrillaris* infection. *Journal of Clinical Microbiology*, v.53, n.9, 3072–3076, 2015.

101 GOÑI, P.; FERNÁNDEZ, M.T.; RUBIO, E. Identifying endosymbiont bacteria associated with free-living amoebae. *Environmental Microbiology*, v. 16, n. 2, p. 339–349, 2014.

102 CATEAU, E.; DELAFONT, V.; HECHARD, Y.; RODIER, M.H. Free-living amoebae: What part do they play in healthcare-associated infections? *Journal of Hospistal Infection*, v. 87, n. 3, p. 131–140, 2014.

103 MORENO-MESONERO, L.; HORTELANO, I.; MORENO, Y.; FERRÚS, M.A. Evidence of viable *Helicobacter pylori* and other bacteria of public health interest associated with free-living amoebae in lettuce samples by next generation sequencing and other molecular techniques. *International Journal of Food Microbiology*, v. 318, 2020. DOI: 10.1016/J.IJFOODMICRO.2019.108477

104 GUIMARAES, A. J.; GOMES, K. X.; CORTINES, J. R.; PERALTA, J. M.; PERALTA, R. H. S. *Acanthamoeba* spp. as a universal host for pathogenic microorganisms: One bridge from environment to host virulence. *Microbiological Research*, v. 193, p. 30–38, 2016. DOI: 10.1016/j.micres.2016.08.001

105 TAN, B.F.; NG, C.; NSHIMYIMANA, J. P.; LOH, L. L.; GIN, K. Y. H.; THOMPSON, J. R. Next-generation sequencing (NGS) for assessment of microbial water quality: Current progress, challenges, and future opportunities. *Frontiers in Microbiology*, v. 6, 2015. DOI: 10.3389/fmicb.2015.01027.

106 NIGRO, S. J.; POST, V.; HALL, R. M. Aminoglycoside resistance in multiply antibiotic-resistant Acinetobacter baumannii belonging to global clone 2 from Australian hospitals. *Journal of Antimicrobial Chemotheraphy*, v. 66, n. 7, p. 1504–1509, 2011.

107 BATRA, P.; MATHUR, P.; MISRA, M. *Aeromonas* spp.: an emerging nosocomial pathogen. *Journal of Laboratory of Physicians*, v. 8, n. 1, p. 1-6, 2016.

108 NIYYATI, M. *et al*. Morphological and molecular survey of *Naegleria* spp. in water bodies used for recreational purposes in Rasht city, Northern Iran. *Iranian Journal of Parasitology*, v. 10, n. 4, p. 523–529, 2015.

109 MARCIANO-CABRAL, F. Free-living amoebae as agents of human infection. *Journal of Infectious Diseases*, v. 199, n. 8, p. 1104–1106, 2009.

110 SU, M.Y.; LEE, M.S.; SHYU, L.Y.; LIN, W.C.; HSIAO, P.C.; WANG, C.P.; JI, D. DER;

CHEN, K.M.; LAI, S.C. A fatal case of *Naegleria fowleri* meningoencephalitis in Taiwan. *Korean Journal of Parasitology*, v. 51, n. 2, p. 203–206, 2013.

111 MORENO, Y.; MORENO-MESONERO, L.; AMORÓS, I.; PÉREZ, R.; MORILLO, J.A.; ALONSO, J.L. Multiple identification of most important waterborne protozoa in surface water used for irrigation purposes by 18S rRNA amplicon-based metagenomics. *International Journal Hygiene Environmental Health*, v. 221, n. 1, p. 593–594, 2018.

112 FARRA, A.; BEKONDI, C.; TRICOU, V.; MBECKO, J.R.; TALARMIN, A.; ACCESS, O. Free-living amoebae isolated in the central african republic: epidemiological and molecular aspects. *Pan African Medical Journal*, v. 26, p. 57, 2017. DOI: 10.11604/PAMJ.2017.26.57.9021.

113 CASTRO-ARTAVIA, E.; RETANA-MOREIRA, L.; LORENZO-MORALES, J.; ABRAHAMS-SANDÍ, E. Potentially pathogenic *Acanthamoeba* genotype T4 isolated from dental units and emergency combination showers. *Memórias do Instituto Oswaldo Cruz*, v. 112, n. 12, p. 817–821, 2017.

114 PLUTZER, J.; KARANIS, P. Neglected waterborne parasitic protozoa and their detection in water. *Water Research*, v. 101, p. 318–332, 2016. DOI: 10.1016/J.WATRES.2016.05.085.

115 O'CARROLL, R.E.; CONWAY, S.; RYMAN, A.; PRENTICE, N. Presence of rotavirus and free-living amoebae in the water supplies of Karachi, Pakistan Farzana. *Psychological Medicine*, v. 27, p. 967–971, 2017.

116 PUZON, G.J.; WYLIE, J.T.; WALSH, T.; BRAUN, K.; MORGAN, M.J. Comparison of biofilm ecology supporting growth of individual *Naegleria* species in a drinking water distribution system. *FEMS Microbiology Ecology*, v. 93, n. 4, p. 1–8, 2017.

117 REYES-BATLLE, M.; WAGNER, C.; LÓPEZ-ARENCIBIA, A.; SIFAOUI, I.; MARTÍNEZ-CARRETERO, E.; VALLADARES, B.; PIÑERO, J.E.; LORENZO-MORALES, J. Isolation and molecular characterization of a *Naegleria* strain from a recreational water fountain in Tenerife, Canary Islands, Spain. *Acta Parasitologica*, v. 62, n. 2, p. 265–268, 2017.

118 LATIFI, A.R.; NIYYATI, M.; LORENZO-MORALES, J.; HAGHIGHI, A.; JAVAD, S.; TABAEI, S.J.S.; LASJERDI, Z.; AZARGASHB, E. Occurrence of *Naegleria* species in therapeutic geothermal water sources, Northern Iran. *Acta Parasitologica*,v. 62, n. 1, p. 104–109, 2017.

119 WAGNER, C. *et al*. Isolation of *Naegleria fowleri* from a domestic water tank associated with a fatal encephalitis in a 4 month-old Venezuelan child. *Tropical Biomedicine*, v. 34, n. 2, p. 332–337, 2017.

120 LE CALVEZ, T.; TROUILHÉ, M.C.; HUMEAU, P.; MOLETTA-DENAT, M.; FRÈRE, J.; HÉCHARD, Y. Detection of free-living amoebae by using multiplex quantitative PCR. *Molecular and Cell Probes*, v. 26, n.3, p.116–120,2012.

121 SCHROEDER, J.M.; BOOTON, G.C.; HAY, J.; NISZL, I.A.; SEAL, D. V; MARKUS, M.B.; FUERST, P.A.; BYERS, T.J. Use of subgenic 18S ribosomal DNA PCR and sequencing for genus and genotype identification of *Acanthamoeba* from humans with keratitis and from sewage sludge. *Journal Clinical Microbiology*, v. 39, n.5, p.1903–1911,2001.

122 BENITO, M.; LAPLANTE, D.; TERESA FERNANDEZ, M.; MIGUEL, N.; MARTA LASHERAS, A.; GOMEZ, J.; PENA ORMAD, M.; RUBIO, E.; PILAR GONI, M. Free-living amoebas (FLAs) in sewage and sludges: their role as a natural reservoir of potentially pathogenic bacteria. *Revista de Salud Ambiental*, v. 18, p. 69–77, 2018.

123 MORENO-MESONERO, L.; MORENO, Y.; ALONSO, J.L.; FERRÚS, M.A. Detection of viable helicobacter pylori inside free-living amoebae in wastewater and drinking water samples from Eastern Spain. *Environmental Microbiology*, v. 19, n. 10, p. 4103–4112, 2017.

124 RAMIREZ, E.; ROBLES, E.; MARTINEZ, B.; AYALA, R.; SAINZ, G.; MARTINEZ, M.E.; GONZALEZ, M.E. Distribution of free-living amoebae in a treatment system of textile industrial wastewater. *Experimental Parasitology*, v. 145, p. S34–S38, 2014. DOI: 10.1016/j.exppara.2014.07.006

125 SCHEIKL, U.; SOMMER, R.; KIRSCHNER, A.; RAMEDER, A.; SCHRAMMEL, B.; ZWEIMÜLLER, I.; WESNER, W.; HINKER, M.; WALOCHNIK, J. Free-living amoebae (FLA) co-occurring with legionellae in industrial waters. *European Journal of Protistology*, v. 50, n. 4, p. 422–429, 2014.

126 NIYYATI, M.; LASGERDI, Z.; LORENZO-MORALES, J. Detection and molecular characterization of potentially pathogenic free-living amoebae from water sources in Kish Island, Southern Iran. *Microbiology Insights*,v. 8, n. 1, p. 1–6., 2015

127 MASCHIO, V.J.; CHIES, F.; CARLESSO, A.M.; CARVALHO, A.; ROSA, S.P.; VAN DER SAND, S.T.; ROTT, M.B. *Acanthamoeba* T4, T5 and T11 isolated from mineral water bottles in southern Brazil. *Current Microbiology*, v. 70, n.1, p. 6–9, 2014.

128 COPE, J. R. *et al*. The first association of a primary amebic meningoencephalitis death with culturable naegleria fowleri in tap water from a US treated public drinking water system. *Clinical Infectious Diseases*, v. 60, n. 8, p. e36–e42, 2015.

129 GOMES, T.S. *et al*. Presence and interaction of free-living amoebae and amoeba-resisting bacteria in water from drinking water treatment plants. *Science of the Total Environment*, v. 719, 2020. DOI: 10.1016/J.SCITOTENV.2020.137080

130 JAVANMARD, E. *et al*. Molecular identification of waterborne free living amoebae (*Acanthamoeba*, *Naegleria* and *Vermamoeba*) isolated from municipal drinking water and environmental sources, Semnan province, north half of Iran. *Experimental Parasitolog*y.v. 183, p.240–244.2017.

131 PUZON, G. J.; MILLER, H. C.; MALINOWSKI, N.; WALSH, T.; MORGAN, M. J. *Naegleria fowleri* in drinking water distribution systems. *Current Opinion in Environmental*

Science & Health,v. 16, p. 22–27, 2020. DOI: 10.1016/j.coesh.2020.02.003.

132 MILLER, H.C.; WYLIE, J.T.; KAKSONEN, A.H.; SUTTON, D.; PUZON, J. Competition between *Naegleria fowleri* and free living amoeba colonizing laboratory scale and operational drinking water distribution systems. *Environmental Science & Tecnology*, v. 52, n. 5, p. 2549-2557, 2018.

133 RICHARD, R.L.; ITHOI, I.; MAJID, M.A.A.; WAN SULAIMAN, W.Y.; TAN, T.C.; NISSAPATORN, V.; LIM, Y.A.L. Monitoring of waterborne parasites in two drinking water treatment plants: a study in Sarawak, Malaysia. *International Journal of Environmental Research and Public Health*, v. 13, n. 7, p. 641, 2016.

134 BAGHERI, H.R.; SHAFIEI, R.; SHAFIEI, F.; SAJJADI, S.A. Isolation of *Acanthamoeba* spp. from drinking waters in several Hospitals of Iran. *Iranian Journal of Parasitology*, v. 5, n. 2, p. 19–25, 2010.

135 SALAZAR, H.C.; MOURA, H.; FERNANDEZ, O.; PERALTA, J.M. Isolation of *Naegleria fowleri* from a lake in the city of Rio de Janeiro. *Transactions of the Royal Society of Tropical Medicine and Hygiene*, v. 80, n. 2, p. 348–349, 1986.

136 TYNDALL, R.L.; IRONSIDE, K.S.; METLER, P.L.; TAN, E.L.; HAZEN, T.C.; FLIERMANS, C.B. Effect of thermal additions on the density and distribution of thermophilic amoebae and pathogenic *Naegleria fowleri* in a newly created cooling lake. *Appllied & Environmental Microbiology*, v. 55, n. 3, p. 722–732, 1989.

137 STOCKMAN, L.J.; WRIGHT, C.J.; VISVESVARA, G.S.; FIELDS, B.S.; BEACH, M.J. Prevalence of *Acanthamoeba* spp. and other free-living amoebae in household water, Ohio, USA - 1990-1992. *Parasitology Research*, v. 108, n. 3, p. 621–627, 2011.

138 YODER, J.S. *et al*. Primary amebic meningoencephalitis deaths associated with sinus irrigation using contaminated tap water. *Clinical Infectious Diseases*, v. 55, n. 9, p. 79–85, 2012.

139 DORSCH, M.M.; CAMERON, A.S.; ROBINSON, B.S. The epidemiology and control of primary amoebic meningoencephalitis with particular reference to South Australia. *Transactions of the Royal Society of Tropical Medicine and Hygiene*, v. 77, n. 3, p. 372–377, 1983.

140 PUZON, G.J.; LANCASTER, J.A.; WYLIE, J.T.; PLUMB, I.J. Rapid detection of *Naegleria fowleri* in water distribution pipeline biofilms and drinking water samples. *Environment Science Technology,* v. 43, n. 17, p. 6691–6696, 2009.

141 CAUMO, K.; ROTT, M. B. *Acanthamoeba* T3, T4 and T5 in swimming-pool waters from Southern Brazil. *Acta Tropica*, v. 117, n. 3, p. 233–235, 2011.

142 GERTISER, M.L.; VISCIARELLI, E.; BASABE, N.; PEREZ, M.J. *Acanthamoeba* spp. en piscinas cubiertas de la ciudad de Bahía Blanca, provincia de Buenos Aires, Argentina. *Acta Bioquímica Clínica Latinoamericana;* v. 44, n. 4, p. 697-703, 2010.

143 ALVES, DSMM,, *et al*. Occurrence and characterization of *Acanthamoeba* similar to genotypes T4 , T5 , and T2 / T6 isolated from environmental sources in Brasília , Federal District , Brazil. *Experimental Parasitology.* v. 131, n.2, p.239–44, 2012.

144 CAUMO K, *et al*. Potentially pathogenic *Acanthamoeba* in swimming pools : a survey in the southern Brazilian city of Porto Alegre. *Annals of Tropical Medicine & Parasitology*. v.103, n.6, p. 477–85, 2009.

145 INIT, I.; LAU, Y.L.; ARIN FADZLUN, A.; FOEAD, A.I.; NEILSON, R.S.; NISSAPATORN, V. Detection of free living amoebae, *Acanthamoeba* and *Naegleria*, in swimming pools, Malaysia. *Tropical Biomedicine*, v. 27, n. 3, p. 566–577, 2010.

146 REYES-BATLLE, M.; NIYYATI, M.; MARTÍN-NAVARRO, C.M.; LÓPEZ-ARENCIBIA, A. Unusual *Vermamoeba vermiformis* strain isolated from snow in upon observation of the snow samples cultured in. *Novelty in Biomedicine*, v. 3, n. 4, p. 189-192, 2015.

147 XUE, J.; LAMAR, F.G.; ZHANG, B.; LIN, S.; LAMORI, J.G.; SHERCHAN, S.P. Quantitative assessment of *Naegleria fowleri* and fecal indicator bacteria in brackish water of Lake Pontchartrain, Louisiana. *Science of the Total Environment*, v. 622–623, p. 8–16, 2018. DOI: 10.1016/j.scitotenv.2017.11.308.

148 RAHDAR, M.; TAVALLA, M.; EBADI, S.; SALEHI, M. The identification of free-living amoebae in water and soil from in and around Ahvaz, Southwest Iran. *Biochemical and Cellular Archives*, v. 16, n. 2, p. 379–382, 2016.

149 BONILLA-LEMUS, P. *et al*. Occurrence of free-living amoebae in streams of the Mexico Basin. *Experimental Parasitology*,v. 145, p. S28–S33, 2014. DOI:10.1016/j.exppara.2014.07.001

150 BELLINI, N.K. *et al*. Isolation of *Naegleria* spp. from a brazilian water source. *Pathogens*, v. 9, n. 2, p. 90, 2020.

151 ETTINGER, M. R. *et al*. Distribution of free-living amoebae in James River, Virginia, USA. *Parasitology Research*, v. 89, n. 1, p. 6–15, 2003.

152 RUSIÑOL, M. *et al*. Metagenomic analysis of viruses, bacteria and protozoa in irrigation water. *International Journal of Hygiene Environmental Health*, v. 224, 2020. DOI: 10.1016/j.ijheh.2019.113440.

153 KANG, H.; SOHN, H.J.; SEO, G.E.; SEONG, G.S.; HAM, A.J.; PARK, A.Y.; JUNG, S.Y.; LEE, S.E.; CHO, S.H.; SHIN, H.J. Molecular detection of free-living amoebae from Namhangang (southern Han River) in Korea. *Science Reports*,. v.10, p.1–10, 2020. DOI: 10.1038/s41598-019-57347-1

154 EL-BADRY, A.A.; AUFY, S.M.; EL-WAKIL, E.S.; RIZK, E.M.; MAHMOUD, S.S.; TAHA, N.Y. First identification of *Naegleria* species and *Vahlkampfia ciguana* in Nile water, Cairo, Egypt: Seasonal morphology and phylogenetic analysis. *Journal of Microbiology, Immunology and Infection*, v.53, n.2, p.259-269,2020.

155 LARES-JIMÉNEZ, L.F.; BORQUEZ-ROMÁN, M.A.; LARES-GARCÍA, C.; OTERO-RUIZ, A.; GONZALEZ-GALAVIZ, J.R.; IBARRA-GÁMEZ, J.C.; LARES-VILLA, F. Potentially pathogenic genera of free-living amoebae coexisting in a thermal spring. *Experimental Parasitology*, v. 195, p.54–58, 2018.

156 MONTALBANO DI FILIPPO, M.; BERRILLI, F.; DI CAVE, D.; NOVELLETTO, A. Novel data from Italian *Vermamoeba vermiformis* isolates from multiple sources add to genetic diversity within the genus. *Parasitology Research*. v.118, p.1751–1759,2019.

157 KAO, P.M.; HSU, B.M.; CHEN, N.H.; HUANG, K.H.; HUANG, S.W.; KING, K.L.; CHIU, Y.C. Isolation and identification of *Acanthamoeba* species from thermal spring environments in southern Taiwan. *Experimental Parasitology*. v.130, p.354–358,2012.

158 SOLGI, R.; NIYYATI, M.; HAGHIGHI, A.; NAZEMALHOSSEINI MOJARAD, E. Occurrence of thermotolerant *Hartmannella vermiformis* and *Naegleria* spp. in hot springs of Ardebil Province, Northwest Iran. *Iran Journal Parasitology*, v.7, n,2,p.47–52,2012.

159 SHI, P.; JIA, S.; ZHANG, X.X.; ZHANG, T.; CHENG, S.; LI, A. Metagenomic insights into chlorination effects on microbial antibiotic resistance in drinking water. *Water Research*. v. 47, n.1, p.111–120, 2013.

160 DELAFONT, V.; BROUKE, A.; BOUCHON, D.; MOULIN, L.; HÉCHARD, Y. Microbiome of free-living amoebae isolated from drinking water. *Water Research*. v. 47, n.19, p.6958–6965.2013.

161 MUCHESA, P.; MWAMBA, O.; BARNARD, T.G.; BARTIE, C. Detection of free-living amoebae using amoebal enrichment in a wastewater treatment plant of gauteng province, South Africa. *Biomedical Research International*, v. 2014,n.535297.p.1-10,2014.

162 PAINTER, S.M.; PFAU, R.S.; BRADY, J.A.; MCFARLAND, A.M.S. Quantitative assessment of *Naegleria fowleri* and *Escherichia coli* concentrations within a Texas reservoir. *Journal Water Health*,v. 11, n.2., p.346–357.2013.

163 SIDDIQUI, R.; KHAN, N.A. *Balamuthia* amoebic encephalitis: An emerging disease with fatal consequences. *Microbiological Pathogenesis*, v. 44, n.2, p. 89–97, 2008.

164 MILLER, H.C.; WYLIE, J.; DEJEAN, G.; KAKSONEN, A.H.; SUTTON, D.; BRAUN, K.; PUZON, G.J. Reduced efficiency of chlorine disinfection of naegleria fowleri in a drinking water distribution biofilm. *Environmental Science Technology*, v, 49, n.11, p.11125–11131,2015.

165 NICHOLS, G.; LAKE, I.; HEAVISIDE, C. Climate change and water-related infectious diseases. *Atmosphere (Basel)*, v.9, n.10, p.1–60, 2018.

166 RODRIGUEZ-ZARAGOZA, S. Ecology of free-living amoebae. *Critical Review in Microbiology*, v.20, n.3, p. 225–241, 2008.

167 SAMBA-LOUAKA, A.; DELAFONT, V.; RODIER, M.-H.; CATEAU, E.; HÉCHARD, Y. Free-living amoebae and squatters in the wild: ecological and molecular features. *FEMS Microbiology Review.* v.43, n.4, p.415–434, 2019.

168 MILLER, H.C.; MORGAN, M.J.; WYLIE, J.T.; KAKSONEN, A.H.; SUTTON, D.; BRAUN, K.; PUZON, G.J. Elimination of *Naegleria fowleri* from bulk water and biofilm in an operational drinking water distribution system. *Water Research* . v. 110, n.1, p.15–26, 2017.

169 DELAFONT, V.; BOUCHON, D.; HÉCHARD, Y.; MOULIN, L. Environmental factors shaping cultured free-living amoebae and their associated bacterial community within drinking water network. *Water Research*, v.100, n.1, p.382–392, 2016.

170 DELAFONT, V.; MOUGARI, F.; CAMBAU, E.; JOYEUX, M.; BOUCHON, D.; HÉCHARD, Y.; MOULIN, L. First evidence of oebae-mycobacteria association in drinking water network. *Enviromental Science Technology*, v.48, n.20, p. 11872–11882, 2014.

171 PERRIN, Y.; BOUCHON, D.; DELAFONT, V.; MOULIN, L.; HÉCHARD, Y. Microbiome of drinking water: A full-scale spatio-temporal study to monitor water quality in the Paris distribution system. *Water Research*. v,149 , p.375–385, 2019. DOI: 10.1016/j.watres.2018.11.013.

172 WASO, M.; DOBROWSKY, P.H.; HAMILTON, K.A.; PUZON, G.; MILLER, H.; KHAN, W.; AHMED, W. Abundance of *Naegleria fowleri* in roof-harvested rainwater tank samples from two continents. *Enviromental Science Polluion Researc International*. v. 25, n.6, p.5700–5710,2018.

173 CASADEVALL, A.; FU, M.S.; GUIMARAES, A.; ALBUQUERQUE, P. The “amoeboid predator-fungal animal virulence” hypothesis. *Journal of Fungi*,v.5, n.1, p.10, 2019.

174 ROSADO-GARCÍA, F.M.; GUERRERO-FLÓREZ, M.; KARANIS, G.; HINOJOSA, M.D.C.; KARANIS, P. Water-borne protozoa parasites: The Latin American perspective. *International Journal Hygiene Environmental Health* , v.220, n.5, p.783–798, 2017.

175 LENTENDU, G.; BUOSI, P.R.B.; CABRAL, A.F.; TREVIZAN SEGÓVIA, B.; RAMOS MEIRA, B.; LANSAC-TÔHA, F.M.; VELHO, L.F.M.; RITTER, C.D.; DUNTHORN, M. Protist biodiversity and biogeography in lakes from four brazilian river–floodplain systems. *Journal Eukaryotic Microbiology*, v. 66, n.4, p.592–599, 2019.

176 WINCK, M.A.T.; CAUMO, K.; ROTT, M.B. Prevalence of *Acanthamoeba* from tap water in Rio Grande do Sul, Brazil. *Current Microbioogy*, v. 63, n.5, p.464–469, 2011.

177 ZANELLA, J.; DA COSTA, S.O.P.; ZACARIA, J.; ECHEVERRIGARAY, S. A Rapid and reliable method for the clonal isolation of *Acanthamoeba* from environmental samples. *Brazilian Archive Biology Technology*. v.55, n.1, p.1–6, 2012.

178 DUARTE, J.L.; FURST, C.; KLISIOWICZ, D.R.; KLASSEN, G.; COSTA, A.O. Morphological, genotypic, and physiological characterization of *Acanthamoeba* isolates from

keratitis patients and the domestic environment in Vitoria, Espírito Santo, Brazil. *Experimental Parasitology*, v.135, n.1, p.9–14, 2013.

179 LEAL, D.A.G.; SOUZA, D.S.M.; CAUMO, K.S.; FONGARO, G.; PANATIERI, L.F.; DURIGAN, M.; ROTT, M.B.; BARARDI, C.R.M.; FRANCO, R.M.B. Genotypic characterization and assessment of infectivity of human waterbore pathogens recovered from oysters and estuarine waters in Brazil. *Water Research*, v. 137, p.273–280,2018. DOI 10.1016/j.watres.2018.03.024.

180 MACHADO, K.B.; TARGUETA, C.P.; ANTUNES, A.M.; SOARES, T.N.; TELLES, M.P.D.C.; LOGARES, R.; VIEIRA, L.C.G.; HUSZAR, V.L.D.M.; NABOUT, J.C. Diversity patterns of planktonic microeukaryote communities in tropical floodplain lakes based on 18S rDNA gene sequences. *Journal Plankton Research*, v.41, n.3, p.241–256,2019.

181 WOPEREIS, D.B.; BAZZO, M.L.; DE MACEDO, J.P.; CASARA, F.; GOLFETO, L.; VENANCIO, E.; DE OLIVEIRA, J.G.; ROTT, M.B.; CAUMO, K.S. Free-living amoebae and its relationship with air quality in hospital environments: Isolation and characterization of *Acanthamoeba* spp. From air-conditioning system. *Parasitology*, v.147, n.7, p.782-790,2020.

182 FONSECA, J.D.G.; GÓMEZ-HERNÁNDEZ, C.; BARBOSA, C.G.; REZENDE-OLIVEIRA, K. Identification of t3 and t4 genotypes of acanthamoeba sp. in dust samples isolated from air conditioning equipment of public Hospital of Ituiutaba-MG. *Current Microbiology*, v.77, n.5, p.3–8,2020.

183 HENKER, L.C.; CRUZ, R.A.S. DA; SILVA, F.S. DA; DRIEMEIER, D.; SONNE, L.; UZAL, F.A.; PAVARINI, S.P. Meningoencephalitis due to *Naegleria fowleri* in cattle in southern brazil. *Revista Brasileira de Parasitologia*. *Veterinaria*, , v.28, n.3,p.514–517.2019.

184 PIMENTEL, L.A.; DANTAS, A.F.M.; UZAL, F.; RIET-CORREA, F. Meningoencephalitis caused by *Naegleria fowleri* in cattle of northeast Brazil. *Research in Veterinary Science*, v.2012, n. 93, p.811–812, 2012.

185 MAGLIANO, A.C.M.; DA SILVA, F.M.; TEIXEIRA, M.M.G.; ALFIERI, S.C. Genotyping, physiological features and proteolytic activities of a potentially pathogenic *Acanthamoeba* sp. isolated from tap water in Brazil. *Experimental Parasitology*, v.123, n.3, p.231–235, 2009.

186 CANTARELLI, V. V.; SOARES, S.S.; SOUZA, T.K.; BERTE, F.K.; ROTT, M.B. Occurrence of infected free-living amoebae in cooling towers of southern Brazil.*Current Microbiology*, v.74, n.12, p.1461–1468, 2017.

187 TEIXEIRA, L.H.; ROCHA, S.; PINTO, R.M.F.; CASEIRO, M.M.; COSTA, S.O.P. DA Prevalence of potentially pathogenic free-living amoebae from *Acanthamoeba* and *Naegleria* genera in non-hospital, public, internal environments from the city of Santos, Brazil. *Brazilian Journal Infectious Diseases*, v.13, n.6, p.395–397,2009.

188 APARECIDA, M.; ARISTEU, J. Isolation of potencially pathogenic free-living amoebas in hospital dust. *Revista de Saude Publica*,v. 37, n.2,p.242–246,2003.

189 PENS CJ, *et al*. *Acanthamoeba* spp . and bacterial contamination in contact lens storage cases and the relationship to user profiles. *Parasitology Research.* v.103, n.6, p.1241–5, 2008.

190 ARTUSO, L. Potentially pathogenic acanthamoeba isolated from a hospital in Brazil. *Current Microbiology*, v.60,n.3, p.185–190,2010.

191 ALBUQUERQUE, P. *et al*. A hidden battle in the dirt: Soil amoebae interactions with *Paracoccidioides* spp. PLoS Neglected. *Tropical Diseases*,v. 13.n.10,p.e007742,2019.

192 CHIMELLI, V. *et al*.Granulomatous amoebic encephalitis due to leptomycid amoebae: report of the first brazilian case. *Transactions of the Royal Society of Tropical Medicine & Hygiene*,v.86, n.6, p.635, 1992.

193 BUCHELE M.L.C*., et al*. Contact lens-related polymicrobial keratitis : *Acanthamoeba* spp . genotype T4 and *Candida albicans* saline solution for cleaning contact lenses and storage cases. *Parasitology Research*. v.117, n.11, p.3431-3436, 2018. DOI: 10.1007/s00436-018-6037-x.

194 ALVES, D.S.M.M*., et al*. Case Report The first *Acanthamoeba keratitis* case in the midwest region of Brazil : diagnosis, genotyping of the parasite and disease outcome. *Revista da Sociedade Brasileira de Medicina Tropical.* v.51, n.5, p.716–9, 2018.

195 SILVA, R.A.; ARAÚJO, S.D.A.; AVELLAR, I.F.D.F.; PITTELLA, J.E.H.; DE OLIVEIRA, J.T.; CHRISTO, P.P. Granulomatous amoebic meningoencephalitis in an immunocompetent patient. *Archives of Neurology*. v. 67,n.12, p. 1516–1520, 2010.

196 ALVES, J.M.P., *et al.* Random amplified polymorphic DNA profiles as a tool for the characterization of Brazilian keratitis isolates of the genus *Acanthamoeba*. *Brazilian Journal Medical Biology Research,* v.33, n.1, p.19–26, 2000.

197 SANTOS, L.C.; OLIVEIRA, M.S.; LOBO, R.D.; HIGASHINO, H.R.; COSTA, S.F.; VAN DER HEIJDEN, I.M.; GIUDICE, M.C.; SILVA, A.R.; LEVIN, A.S. *Acanthamoeba* spp. in urine of critically ill patients. *Emerging Infectious Diseases*.v. 15, n.7, p. 1144–1146,2009.

198 ZORZI, G.K.; SCHUH, R.S.; MASCHIO, V.J.; BRAZIL, N.T.; ROTT, M.B.; TEIXEIRA, H.F. Box Behnken design of siRNA-loaded liposomes for the treatment of a murine model of ocular keratitis caused by *Acanthamoeba*. *Colloids Surfaces B Biointerfaces* , v.173, p.725–732,2019.DOI 10.1016/jconsulfb2018.10044.

199 DA SILVA, M.T.A.; CALDAS, V.E.A.; COSTA, F.C.; SILVESTRE, D.A.M.M.; THIEMANN, O.H. Selenocysteine biosynthesis and insertion machinery in *Naegleria gruberi*. *Molecular and Biochemical Parasitology*. v.188, n.2, p.87–90, 2013.

200 MOURA, H.; IZQUIERDO, F.; WOOLFITT, A.R.; WAGNER, G.; PINTO, T.; DEL AGUILA, C.; BARR, J.R. Detection of biomarkers of pathogenic *Naegleria fowleri* through mass spectrometry and proteomics. *Journal Eukaryotic Microbiology*. v. 62, n.12, p. 12–20, 2015.

201 CAUMO, K.S. *et al.* Proteomic profiling of the infective trophozoite stage of *Acanthamoeba polyphaga*. *Acta Tropica* .v.140, p. 166–72, 2014.

202 POSSAMAI C.O. *et al. Acanthamoeba* of three morphological groups and distinct genotypes exhibit variable and weakly inter-related physiological properties. *Parasitology Research.* v.117, n.5, p.1389-1400, 2018.

203 MEDINA, G. *et al.* Transcriptional analysis of flagellar and putative virulence genes of *Arcobacter butzleri* as an endocytobiont of *Acanthamoeba castellanii*. *Archives of Microbiology*, v. 201, n.8, p.1075–1083, 2019.

204 SILVA, L.C.F. *et al.* Microscopic analysis of the tupanvirus cycle in *Vermamoeba vermiformis*. *Frontiers in Microbiology*, v.10, p. 1–9, 2019.

205 STAGGEMEIER R. *et al*. Detection and quantification of human adenovirus genomes in *Acanthamoeba* isolated from swimming pools. *Anais da Academia Brasileira de Ciencias,* v.88, n.1, p.635-42, 2016.

206 MASCHIO, V.J.. *et al.* Identification of *Paenibacillus* as a symbiont in *Acanthamoeba*. *Current Microbiology.* v.71, n.3, p.415–20, 2015.

207 WEBER-LIMA, M. *et al. Acanthamoeba* spp. monoclonal antibody against a CPA2 transporter: A promising molecular tool for acanthamoebiasis diagnosis and encystment study. *Parasitology*, v.147, n.14, p.1678-1688, 2020.

208 ROTT, M.B.; CAUMO, K.; SAUTER, I.; ECKERT, J,; DA ROSA, L,; DA SILVA O. Susceptibility of *Aedes aegypti* (Diptera : Culiveae) to *Acanthamoeba*. *Parasitology Research*. v. 107, n. 1, p.195-8, 2014.

209 BENITEZ, L.B.; CAUMO, K.; BRANDELLI, A.; ROTT, M.B. Bacteriocin-like substance from *Bacillus amyloliquefaciens* shows remarkable inhibition of *Acanthamoeba polyphaga*. *Parasitology Research*. v.108, n.3, p.687–91, 2011.

210 MAFRA, C,S. *et al.* Antimicrobial action of biguanides on the viability of *Acanthamoeba* cysts and assessment of cell toxicity. *Investigative Ophthalmology Visual Science*, v.54, n.9, p.6363-72, 2013.

211 ABRAHÃO, J.*et al*. Tailed giant Tupanvirus possesses the most complete translational apparatus of the known. *Nature Communications.* v.9, n.749, p.1-12, 2018. |DOI: 10.1038/s41467-018-03168-1.

212 CAMPOS, R.K.*et al*. Samba virus : a novel mimivirus from a giant rain forest , the Brazilian Amazon. *Virology Journal*, v.11, n.95, p.1–11,2014.

213 SERRANO-SOLÍS, V.; TOSCANO SOARES, P.E.; DE FARÍAS, S.T. Genomic signatures among *Acanthamoeba polyphaga* entoorganisms unveil evidence of coevolution.*Journal*

Molecular Evolution. v.87, n.1, p.7–15, 2019.

214 BORGES, I.; RODRIGUES, R.A.L.; DORNAS, F.P.; ALMEIDA, G.; AQUINO, I.; BONJARDIM, C.A.; KROON, E.G.; LA SCOLA, B.; ABRAHÃO, J.S. Trapping the enemy: *Vermamoeba vermiformis* circumvents faustovirus mariensis dissemination by enclosing viral progeny inside cysts. *Journal of Virology*, v. 93, n.14, p.1–19, 2019.

215 ARAÚJO, R.; RODRIGUES, L.; MOUGARI, S.; COLSON, P.; LA, B.; JÔNATAS, S.; ABRAHÃO, S. "Tupanvirus", a new genus in the family Mimiviridae. *Archives of Virology*, v. 164, p.325–331,2019.DOI 10.1007/s00705-018-4067-4.

216 BORATTO, P.V.M. *et al*. Yaravirus: a novel 80-nm virus infecting *Acanthamoeba castellanii*. *Proceedings of the National Academy of Science*, v. 117, n.28,p.16579-16586, 2020.

217 ARAUJO, R.;ABRAHA, S.; RODRIGUES, L.; DRUMOND, P.; KROON, E.G. Giants among larges : how gigantism impacts giant virus entry into amoebae.*Current Opinion in Microbiology*, v.31,p.88–93, 2016.DOI 10.1016/j.mib.2016.03.009.

218 CARRIJO-CARVALHO, L.C.; PERACINI, V.; FORONDA, A.S.; FREITAS, D. DE; RAMOS, F.; CARVALHO, D.S. Therapeutic review therapeutic agents and biocides for ocular infections by free-living amoebae of *Acanthamoeba* genus. *Survey Ophthalmology*, v.62, n.2,p.203-218,2016.

219 GONÇALVES, D. D.E S.; FERREIRA, M. D.A S.; GUIMARÃES, A.J. Extracellular vesicles from the protozoa *Acanthamoeba castellanii*: their role in pathogenesis, environmental adaptation and potential applications. *Bioengineering*, v.6, n.1, p.13,2019.

220 BULLÉ, D.J. *et al*. Occurrence of *Acanthamoeba* in hospitals: a literature review. *Journal of Epidemiology and Infection Control.* v.10, n.2, p.1–17, 2020.

221 OLIVEIRA, G.; LA SCOLA, B.; ABRAHÃO, J. Giant virus vs amoeba: fight for supremacy. *Virology Journal*, v.16,p.1-12, 2019.DOI 10.1186/s12985-019-1244-3.

222 ELABRAS VEIGA, L.B.; MAGRINI, A. The brazilian water resources management policy: fifteen years of success and challenges. *Water Resources Management*. v. 27, p.2287–2302, 2013.DOI 10.1007/s11269-013-0288-1.

223 ARRIEIRA, R.L.; SCHWIND, L.T.F.; BONECKER, C.C.; LANSAC-TÔHA, F.A. Temporal dynamics and environmental predictors on the structure of planktonic testate amoebae community in four neotropical floodplains. *Journal of Freshwater Ecology*, v.32, n.1, p.35–47, 2017.

224 BRASIL.Conselho Nacional do Meio Ambiente.CONOMA. Resoluçao N. 357, de 17 de março de 2005. Dispõe sobre a classificação dos corpos de água e diretrizes ambientais para o seu enquadramento, bem como estabelece as condições e padrões de lançamento de efluentes, e dá outras providências. *Diario Oficial da Uniao*, n.53, de 18/03/2005, p. 58-63.

225 BELLINI, N.K. *Estudo celular , bioquímico e biofísico da enzima selenofosfato sintetase de Naegleria gruberi*. 2015.159p. Dissertacao (Mestrado em Ciências) - Instituo de Fisica de São Carlos, Universidade de São Paulo, São Carlos,2015.

226 ITHOI, I.; AHMAD, A.F.; MAK, J.W.; NISSAPATORN, V.; LAU, Y.L.; MAHMUD, R. Morphological characteristics of developmental stages of *Acanthamoeba* and *Naegleria* species before and after staining by various techniques. *Southeast Asian Journal Tropical Medicine Public Health,* v.42, n.6,p.1327–1338,2011.

227 REYES-BATLLE, M.; HERNÁNDEZ-PIÑERO, I.; RIZO-LIENDO, A.; CHIBOUB, O.; BETHENCOURT-ESTRELLA, C.J.; LÓPEZ-ARENCIBIA, A.; SIFAOUI, I.; VALLADARES, B.; PIÑERO, J.E..; LORENZO-MORALES, J. Isolation and molecular identification of free-living amoebae from dishcloths in Tenerife , Canary Islands , Spain. *Parasitology Research*, v.118, n.3,p.927–933,2019.

228 DI FILIPPO, M.M.; SANTORO, M.; LOVREGLIO, P.; MONNO, R.; CAPOLONGO, C.; CALIA, C.; FUMAROLA, L.; D'ALFONSO, R.; BERRILLI, F.; DI CAVE, D. Isolation and molecular characterization of free-living amoebae from different water sources in Italy. *International Journal Environmental Research Public Health,* v.12, n.4,p.3417–3427,2015.

229 ITHOI, I.; AHMAD, A.F.; NISSAPATORN, V.; LAU, Y.L.; MAHMUD, R.; MAK, J.W. Detection of *Naegleria* species in environmental samples from Peninsular Malaysia. *PLoS One*, v. 6, n.9,p.e24327,2011.

230 ORTEGA-RIVAS, J.L.E.A. Isolation and identification of pathogenic *Acanthamoeba* strains in Tenerife , Canary Islands , Spain from water sources. *Parasitology Research*, v.95,n.4,p. 273–277,2005.

231 LORENZO-MORALES, J.; ORTEGA-RIVAS, A.; MARTÍNEZ, E.; KHOUBBANE, M.; ARTIGAS, P.; PERIAGO, M.V.; FORONDA, P.; ABREU-ACOSTA, N.; VALLADARES, B.; MAS-COMA, S. *Acanthamoeba* isolates belonging to T1, T2, T3, T4 and T7 genotypes from environmental freshwater samples in the Nile Delta region, Egypt. *Acta Tropica*, v. 100, n.1-2,p.63–69, 2006.

232 KOMANOFF, C.; LI, G.; BAKER, S.P. Amoebic encephalitis due to *Sappinia diploidea*. *Journal American Medicine Association,* v.285,n.19, p.2445–2446,2001.

233 KINDE, H.; READ, D.H.; DAFT, B.M.; MANZER, M.; NORDHAUSEN, R.W.; KELLY, D.J.; FUERST, P.A.; BOOTON, G.; VISVESVARA, G.S. Infections caused by pathogenic free-living amebas (*Balamuthia mandrillaris* and *Acanthamoeba* sp.) in Horses. *Journal of Veterinary Diagnostic Investigation*, v. 19,n.3, p.317–322,2007.

234 WALOCHNIK, J.; SCHEIKL, U.; HALLER-SCHOBER, E.M. Twenty years of *Acanthamoeba* diagnostics in Austria. *Journal of Eukaryotic Microbiology*.v. 62, n.1, p.3–11, 2015.

235 BENTERKI, M.S.; AYACHI, A.; BENNOUNE, O.; RÉGOUDIS, E.; PÉLANDAKIS, M.

Meningoencephalitis due to the amoeboflagellate *Naegleria fowleri* in ruminants in Algeria. *Parasite*, v.23,n.11,p. 1-4,2016.

236 HEBBAR, S.; BAIRY, I.; BHASKARANAND, N.; UPADHYAYA, S.; SARMA, M. SEN; SHETTY, A.K. Fatal case of *Naegleria fowleri* meningo-encephalitis in an infant: case report. *Annals of Tropical Paediatrics*,v.25,n.3 p.223–226,2005.

237 EL-SAYED, N.M.; HIKAL, W.M. Several staining techniques to enhance the visibility of *Acanthamoeba* cysts. *Parasitology Research*, v.114, p.823–830,2015.DOI 10.1007/s00436-014-4190-4.

238 JAMERSON, M.; DA ROCHA-AZEVEDO, B.; CABRAL, G.A.; MARCIANO-CABRAL, F. Pathogenic *Naegleria fowleri* and non-pathogenic *Naegleria lovaniensis* exhibit differential adhesion to, and invasion of, extracellular matrix proteins. *Microbiology*, v.158, pt.3,p. 791–803,2012.

239 FOUQUE, E.; TROUILHÉ, M.C.; THOMAS, V.; HARTEMANN, P.; RODIER, M.H.; HÉCHARDA, Y. Cellular, biochemical, and molecular changes during encystment of free-living amoebae. *Eukaryotic Cell,* v.11,n.4,p. 382–387,2012.

240 DYKOVÁ, I.; KYSELOVÁ, I.; PECKOVÁ, H.; OBORNÍK, M.; LUKEŠ, J. Identity of *Naegleria* strains isolated from organs of freshwater fishes. *Diseases of Aquatics Organisms*, v. 46, n.2,p.115–121,2001.

241 FOUQUE, E.; YEFIMOVA, M.; TROUILHÉ, M.C.; QUELLARD, N.; FERNANDEZ, B.; RODIER, M.H.; THOMAS, V.; HUMEAU, P.; HÉCHARD, Y. Morphological study of the encystment and excystment of *Vermamoeba vermiformis* revealed original traits. *The Journal of Eukaryotic Microbiology*, v. 62, n.3,p.327–337,2015.

242 FOUQUE, E.; TROUILHÉ, M.C.; THOMAS, V.; HUMEAU, P.; HÉCHARD, Y. Encystment of *Vermamoeba* (*Hartmannella*) vermiformis: effects of environmental conditions and cell concentration. *Experimental Parasitology*, v. 145, p.S62–S68, 2014.DOI 10.1016/j.exppva2014.03.029.

243 SIFAOUI, I.; REYES-BATLLE, M.; LÓPEZ-ARENCIBIA, A.; CHIBOUB, O.; BETHENCOURT-ESTRELLA, C.J.; SAN NICOLÁS-HERNÁNDEZ, D.; RODRÍGUEZ EXPÓSITO, R.L.; RIZO-LIENDO, A.; PIÑERO, J.E.; LORENZO-MORALES, J. Screening of the pathogen box for the identification of anti-*Acanthamoeba* agents. *Experimental Parasitology*,v.201,p.90–92,2019.DOI 10.1016/exppara.2019.04.016.

244 BAQUERO, R.A.; REYES-BATLLE, M.; NICOLA, G.G.; MARTÍN-NAVARRO, C.M.; LÓPEZ-ARENCIBIA, A.; GUILLERMO ESTEBAN, J.; VALLADARES, B.; MARTÍNEZ-CARRETERO, E.; PIÑERO, J.E.; LORENZO-MORALES, J. Presence of potentially pathogenic free-living amoebae strains from well water samples in Guinea-Bissau. *Pathogen Global Health*, v.108, n.4, p. 206–11,2014.

245 SOHN, H.; KANG, H.; SEO, G.; KIM, J.; JUNG, S.; SHIN, H. Efficient liquid media for

encystation of pathogenic free-living amoebae. *The Korean Journal of Parasitology*, v.55, n.3, p.233–238,2017.

246 DE JONCKHEERE, J.F. Characterization of Naegleria species by restriction endonuclease digestion of whole-cell DNA. *Molecular Biochemical Parasitology*, v.24, n.1,p.55–66,1987.

247 MORENO, Y.; MORENO-MESONERO, L.; AMORÓS, I.; PÉREZ, R.; MORILLO, J.A.; ALONSO, J.L. Multiple identification of most important waterborne protozoa in surface water used for irrigation purposes by 18S rRNA amplicon-based metagenomics. *International of Journal Hygiene Environmental Healt*h , v.221,n.1, p.102–111,2018.

248 BOOTON, G.C.; VISVESVARA, G.S.; BYERS, T.J.; KELLY, D.J.; FUERST, P.A. Identification and distribution of *Acanthamoeba* species genotypes associated with nonkeratitis infections. *Journal of Clinical Microbiology,* v.43,n.4, p.1689–1693,2005.

249 STOTHARD, D.R.; SCHROEDER-DIEDRICH, J.M.; AWWAD, M.H.; GAST, R.J.; LEDEE, D.R.; RODRIGUEZ-ZARAGOZA, S.; DEAN, C.L.; FUERST, P.A.; BYERS, T.J. The evolutionary history of the genus *Acanthamoeba* and the identification of eight new 18S rRNA gene sequence types. *Journal of Eukaryotic Microbiology*, v. 45,n.1, p.45–54,1998.

250 BOOTON, G.C., *et al*. Molecular and physiological evaluation of subtropical environmental isolates of *Acanthamoeba* spp., causal agent of *Acanthamoeba* keratitis. *Journal of Eukaryotic Microbiology*. v.51, n.2, p. 192–200, 2004.

251 PÉLANDAKIS, M.; SERRE, S.; PERNIN, P. Analysis of the 5.8S rRNA gene and the internal transcribed spacers in *Naegleria* spp. and in *N. fowleri*. *Journal of Eukaryotic Microbiology*, v. 47, n.2, p.116–21,2000.

252 GREEN, R.; ROGERS, E.J. Transformation of chemically competent *E. coli*. *Methods in Enzymology*. v.529, p.329-336. 2013.

253 CAMARA, G,; CARTAXO, R.; SOUZA, M. DE; CARLOS, J.; GARRIDO, P. SPRING : Integrating remote sensing and GIS by object-oriented data modelling. *Computers & Graphics*, v.20, n.3, p.395,1996.

254 SCHINDELIN, J. *et al*. Fiji: An open-source platform for biological-image analysis. *Nature Methods*, v. 9, p.676–682,2012.DOI 10.1038/nmeth.2019.

255 CHENNA, R.; SUGAWARA, H.; KOIKE, T.; LOPEZ, R.; GIBSON, T.J.; HIGGINS, D.G.; THOMPSON, J.D. Multiple sequence alignment with the Clustal series of programs. *Nucleic Acids Research* ,v. 31, n.13,p.3497–3500,2003.

256 HALL, B.G. Building phylogenetic trees from molecular data with MEGA. *Molecular Biology Evolution*, v.30, n.5, p.1229–1235,2013.

257 BARRILLI, G.H.C.; ROCHA, O.; FELIX NEGREIROS, N.; ROBERTO VERANI, J. Influence of environmental quality of the tributaries of the Monjolinho River on the relative

condition factor (Kn) of the local ichthyofauna. *Biota Neotropica*.v. 15, n.1,p.1–9,2015.

258 CAMPAGNA, A.F.; FRACÁCIO, R.; RODRIGUES, B.K.; ELER, M.N.; VERANI, N.F.; ESPÍNDOLA, E.L.G. Analyses of the sediment toxicity of Monjolinho River, São Carlos, São Paulo state, Brazil, using survey, growth and gill morphology of two fish species (*Danio rerio* and *Poecilia reticulata*). *Brazilian Archives of Biology and Technology*, v.51,n.1, p.193–201,2008.

259 LEVLIN, E. *Conductivity measurements for controlling municipal wastewater treatment.* 2014. Available from: thttp://www.energiomiljo.org/kth/Polishproject/rep15/ConductV15.pdf. Accessible at: Sept.17,2020.

260 VENTUROTI, G.P.; VERONEZ, A.C.; SALLA, R. V.; GOMES, L.C. Variation of limnological parameters in a tropical lake used for tilapia cage farming. *Aquaculture Reports* ,v. 2, p.152–157,2015.DOI 10.1016/aqrep20.159.006.

261 YANG, X.; WU, X.; HAO, H.; HE, Z. Mechanisms and assessment of water eutrophication. *Journal of Zhejiang University Science* B , v.9,n.3, p.197–209,2008.

262 ALVES, M.T.R.; MACHADO, K.B.; FERREIRA, M.E.; VIEIRA, L.C.G.; NABOUT, J.C. A snapshot of the limnological features in tropical floodplain lakes: the relative influence of climate and land use. *Acta Limnologica Brasiliensia*, v.31, n.10, p.229,2019.

263 ZHANG, L.; CHENG, Y.; GAO, G.; JIANG, J. Spatial-temporal variation of bacterial communities in sediments in lake chaohu, a large, shallow eutrophic lake in China. *International Journal of Environmental Research Public Health*, v.16.n.20, p.3966,2019

264 KONZEN, G.; FIGUEIREDO, J.; QUEVEDO, D. History of water quality parameters – a study on the Sinos River/Brazil. *Brazilian Journal of Biology*,v.75,n.2, p.1–10,2015.

265 JANEIRO, D. *et al*. Detection of ts carbapenemase genes in aquatic environmenin Rio de Janeiro, Brazil. *Antimicrobial Agents and Chemotherapy,* v. 60, n.7,p.4380–4383, 2016.

266 BRASIL. Ministerio da Saude. *Portaria no 2.914, de 12 de dezembro de 2011*. Dispõe sobre os procedimentos de controle e de vigilância da qualidade da água para consumo humano e seu padrão de potabilidade. Available from: https://bvsms.saude.gov.br/bvs/saudelegis/gm/2011/prt2914_12_12_2011.html.Accessible at: Sept.18,2020.

267 WAGNER, C. *et al*. Genotyping of clinical isolates of *Acanthamoeba* genus in Venezuela. *Acta Parasitology*, v.61, n,4,p.796–801,2016.

268 GRACE, E.; ASBILL, S.; VIRGA, K. *Naegleria fowleri*: pathogenesis, diagnosis, and treatment options. *Antimicrobioal Agents and Chemotherapy*,v. 59,n.11,p. 6677–6681,2015.

269 SCHEID, P.L. Amoebophagous fungi as predators and parasites of potentially pathogenic free-living amoebae. *Open Parasitology Journal*, v. 6, p.75–86,2018.DOI

102174/18744.21401806010075.

270 BUI, X.T.; WINDING, A.; QVORTRUP, K.; WOLFF, A.; BANG, D.D.; CREUZENET, C. Survival of *Campylobacter jejuni* in co-culture with *Acanthamoeba castellanii*: role of amoeba-mediated depletion of dissolved oxygen. *Environmental Microbiology*, v.14, n.8,p.2034–2047, 2012.

271 LORENZO-MORALES, J.; CORONADO-ÁLVAREZ, N.; MARTÍNEZ-CARRETERO, E.; water-isolated strains of *Acanthamoeba* in the Canary Islands, Spain. *American Journal of Tropical Medicine and Hygiene*,v. 77, n.4,p.753–756,2007.

272 REYES, M.; AITOR, B.; LIENDO, R.; VIERA, R.A.; SARA, S.; MORALES, A. Isolation and molecular identification of *Naegleria australiensis* in irrigation water of fuerteventura island , Spain. *Acta Parasitologica*, v.64, p.331-335, 2019.DOI 10.2478/s11686-019-0046-8

273 CHAVATTE, N.; LAMBRECHT, E.; VAN DAMME, I.; SABBE, K.; HOUF, K. Free-living protozoa in the gastrointestinal tract and feces of pigs: Exploration of an unknown world and towards a protocol for the recovery of free-living protozoa. *Veterinary Parasitology,*v. 225,p. 91–98,2016.DOI 10+1016/j.volpor2016.06002.

274 CHELKHA, N.; JARDOT, P.; MOUSSAOUI, I.; LEVASSEUR, A.; LA SCOLA, B.; COLSON, P. Core gene-based molecular detection and identification of *Acanthamoeba* species. *Science Reports*, v. 10,p. 19–21,2020.DOI 10.1038/s41598-020-57998-5.

275 REYES-BATLLE, M. *et al*. Isolation and molecular identification of *Vermamoeba* vermiformis strains from soil sources in El Hierro Island, Canary Islands, Spain. *Current Microbiology*, v.73, n.1,p.104–107,2016.

276 CAVALIER-SMITH, T.; FIORE-DONNO, A.M.; CHAO, E.; KUDRYAVTSEV, A.; BERNEY, C.; SNELL, E.A.; LEWIS, R. Multigene phylogeny resolves deep branching of Amoebozoa. *Molecular Phylogenetic Evolution*, v.83, p.293–304.2015.DOI 10.1016/j.ympev.2014.08.011.

277 ADL, S.M. *et al*. Revisions to the classification, nomenclature, and diversity of eukaryotes. *Journal of Eukaryotic Microbiology*, v.66, p.293-304,2019.

278 GEISEN, S.; WEINERT, J.; KUDRYAVTSEV, A.; GLOTOVA, A. Two new species of the genus *Stenamoeba* (Discosea , Longamoebia): Cytoplasmic MTOC in one more amoebae lineage.*European Journal of Protistology*, v.50, n.2,p.13-165,2014.

279 ALEJANDRO, M.; FERNANDO, L.; RODRIGUEZ-ANAYA, L.Z.; GONZALEZ-GALAVIZ, J.R.; FUERST, P.A.; LARES-VILLA, F. *Stenamoeba dejonckheerei* sp. nov., a free-living amoeba isolated from a thermal spring. *Pathogens*, v.9,n.7,p.588,2020.

280 PECKOVA, H.; FIALA, I. Filamoeba sinensis sp . n ., a second species of the genus *Filamoeba page* , 1967 , isolated from gills of *Carassius gibelio* (Bloch , 1782). *Acta Protozoologica*, v.44, n.1, p.75-80,2005.

281 ALEXEY, S. Amoebas , Lobose. *In*: ALEXEY, S. *Eukaryotic microbes*. 2nd. Amsterdan*:* Academic Press, 2012, p.191-211.

282 DYKOVÁ, I.; BOHÁČOVÁ, L.; FIALA, I.; MACHÁČKOVÁ, B.; PECKOVÁ, H.; DVOŘÁKOVÁ, H. Amoebae of the genera *Vannella* Bovee, 1965 and *Platyamoeba* Page, 1969 isolated from fish and their phylogeny inferred from SSU rRNA gene and ITS sequences. *European Journal Protistology*,v. 41,n.3, p.219–230, 2005.

283 MATIN, A.; SIDDIQUI, R.; JAYASEKERA, S.; KHAN, N.A. Increasing Importance of *Balamuthia mandrillaris*.*Clinical Microbiology Reviews*, v. 21,n.3,p 435–448,2008.

284 DYKOVÁ, I.; PINDOVÁ, Z.; FIALA, I.; DVO, H.; MACHÁ, B. Fish-isolated strains of *Hartmannella vermiformis* page , 1967 : morphology , phylogeny and molecular diagnosis of the species in tissue lesions. *Folia Parasitologica*, v.52,n.4, p.295–303,2005.

285 SCHEID, P. Mechanism of intrusion of a microspordian-like organism into the nucleus of host amoebae (Vannella sp .) isolated from a keratitis patient. *Parasitology Research*, v.101, p.1097–1102,2007.

286 TAYLOR, S.J.; AHONEN, L.J.; LEIJ, F.A.A.M. DE; DALE, J.W. Infection of *Acanthamoeba castellanii* with *Mycobacterium bovis* and *M . bovis* BCG and Survival of M . bovis within the Amoebae. *Applied and Environmental Microbiology*, v.69, n. 7,p.4316–4319, 2003.

287 SHIN, H.; CHO, M.; JUNG, S.; KIM, H.; PARK, S.U.N.; SEO, J.; YOO, J.; IM, K. Cytopathic changes in rat microglial cells induced by pathogenic *Acanthamoeba culbertsoni* : morphology and cytokine release. *Clinical and Diagnostic Laboratory Immunology*, v.8,n.4,p. 837–840,2001.

288 OMAÑA-MOLINA, M.; GONZÁLEZ-ROBLES, A.; SALAZAR-VILLATORO, L.I.; LORENZO-MORALES, J.; CRISTÓBAL-RAMOS, A.R.; HERNÁNDEZ-RAMÍREZ, V.I.; TALAMÁS-ROHANA, P.; RENÉ, A.; CRUZ, M.; MARTÍNEZ-PALOMO, A. Reevaluating the mechanisms role of *Acanthamoeba* proteases in tissue invasion : observation of cytopathogenic on mdck cell monolayers and hamster corneal cells. *Immunology and Cell Biology of Parasitic Diseases.* v.2013, p.461329,2013.

289 FONTES, M., SALTON, J., CAUMO, K., BROETTO, L., ROTT, M.B.. Isolation and genotyping of free-living environmental isolates of *Acanthamoeba* spp . from bromeliads in Southern Brazil. *Experimental Parasitology.* v.134, n.3, p.290–4, 2013.

290 YAMANOUCHI, K.; TAKEUCHI, M.; ARIMA, H.; TSUJIGUCHI, T. Development of a method to extract protozoan DNA from black soil. *Parasite Epidemiomology and Control*,v. 4, p.0–6, 2019.

291 TUNG, M.C.; HSU, B.M.; TAO, C.W.; LIN, W.C.; TSAI, H.F.; JI, D. DER; SHEN, S.M.; CHEN, J.S.; SHIH, F.C.; HUANG, Y.L. Identification and significance of *Naegleria fowleri*

isolated from the hot spring which related to the first primary amebic meningoencephalitis (PAM) patient in Taiwan. *International Journal of Parasitology*. v.43, n.9,p.691–696, 2013.

292 YOUSUF,F. A. *et al*. Status of free-living amoebae (*Acanthamoeba* spp ., *Naegleria fowleri* , *Balamuthia mandrillaris*) in drinking water supplies in Karachi , Pakistan. *Journal of Water and Health*, v.11, n.2, p.371–375, 2013.

293 HIKAL, W.M.; DKHIL, M.A. Nested PCR assay for the rapid detection of *Naegleria fowleri* from swimming pools in Egypt.*Acta Ecologica Sinica*, v.38,n.2, p. 102–107,2018.

294 DAINA, P.; MAKAROVA, S.; VALCIN, O. Co-Occurrence of free-living amoeba and *Legionella* in drinking water supply systems. *Medicina (Kaunas)*, v.55 ,n.8, p.492,2019.

295 JONCKHEERE, J.F.D.E. Isolation and molecular identification of *Vahlkampfiid* amoebae from an Island(Tenerife, Spain). *Acta Protozoologica*, v.45, n.1, p.91-96,2006.

296 GIANINAZZI, C.*et al*. Screening swiss water bodies for potentially pathogenic free-living amoebae. *Research in Microbiology*, v.160, n.6,p.367-374,2009.

297 AL-HERRAWY, A.Z.; GAD, M.A. Isolation and molecular identification of *Naegleria fowleri* from Nile river, Egypt. *Journal. Egyptian Public Health Association*, v.90, n.4, p. 161–5,2015.

298 ZHOU, L.; SRIRAM, R.; VISVESVARA, G.S.; XIAO. L. Genetic variations in the internal transcribed spacer and mitochondria1 small subunit rRNA gene of *Naegleria* spp. *Jornal of Eukaryotic Microbiological*; v.50, p.522–6, 2003.

299 DE JONCKHEERE, J.F. A century of research on the amoeboflagellate genus *Naegleria*. *Acta Protozoologica*, v.41, p.309–342,2002.

300 KUIPER, M.W.; WULLINGS, B.A.; AKKERMANS, A.D.L.; BEUMER, R.R.; VAN DER KOOIJ, D. Intracellular proliferation of *Legionella pneumophila* in *Hartmannella vermiformis* in aquatic biofilms grown on plasticized polyvinyl chloride. *Applied Environmental Microbiology.* v.70, n.11,p.6826–6833,2004.

301 DYKOVÁ, I.; KOSTKA, M.; WORTBERG, F.; NARDY, E.; PECKOVÁ, H. New data on aetiology of nodular gill disease in rainbow trout, Oncorhynchus mykiss. *Folia Parasitology (Praha)*. v.57, n.3, p.157–163, 2010.

302 DEĞERLI, S.; DEĞERLI, N.; ÇAMUR, D.; DOĞAN, Ö.; İLTER, H. Genotyping of *Acanthamoeba* and *Naegleria* isolates from the thermal pool distributed throughout by sequencing Turkey. *Acta Parasitologica*, v.65,p.174-186,2020.

303 CAVALIER-SMITH, T.; CHAO, E.E.Y.; OATES, B. Molecular phylogeny of Amoebozoa and the evolutionary significance of the unikont Phalansterium. *European Journal of Protistology.* v.40, p.21–48, 2004.

304 DE JONCKHEERE, J.F. What do we know by now about the genus *Naegleria*? *Experimental Parasitology.* v.145, p.S2–S9, 2014.DOI: 10.1016/j.exppara.2014.07.011.

305 MARCIANO-CABRAL, F. Biology of *Naegleria* spp. *Microbiology Reviews*. v.52, n.1,p.114–133,1988.

306 CARTER, R.F. Primary amoebic meningo-encephalitis: clinical, pathological and epidemiological features of six fatal cases. *The Journal of Pathology and Bacteriology*, v.96, n.1,p.1–25, 1968.

307 KANG, H.; SEONG, G.S.; SOHN, H.J.; KIM, J.H.; LEE, S.E.; PARK, M.Y.; LEE, W.J.; SHIN, H.J. Effective PCR-based detection of *Naegleria fowleri* from cultured sample and PAM-developed mouse. *European Journal of Protistology*, v.51,n.5, p.401–408, 2015.

308 FØRDE, I.S.; GAUSTAD, K.; STUBHAUG, T.T.; REIAKVAM, O.M.; STENSVOLD, C.R.; ANTAL, E.-A.; HERMANSEN, N.O.; HOLBERG-PETERSEN, M.; HEGER, B. Fatal primary amoebic meningoencephalitis in a Norwegian tourist returning from Thailand. *JMM Case Reports* ,v.3, n.3,p.e005042,2016.

309 COGO, P.E.; SCAGLIA, M.; GATTI, S.; ROSSETTI, F.; ALAGGIO, R.; LAVERDA, A.M.; ZHOU, L.; XIAO, L.; VISVESVARA, G.S. Fatal *Naegleria fowleri* Meningoencephalitis, Italy. *Emerging Infectious Diseases*, v.10,n.10,p. 1835–1837,2004.

310 MARTI, E.; LORENZO-MORALES, J.; LO, M.; VALLADARES, B. Isolation of potentially pathogenic strains of *Acanthamoeba* in wild squirrels from the Canary Islands and Morocco. *Experimental Parasitology*, v.117, n.1.p.74–79, 2007.

311 BETANZOS, A.; BAÑUELOS, C.; OROZCO, E. Host invasion by pathogenic amoebae: epithelial disruption by parasite proteins. *Genes (Basel).* v.10,n.8,p.618,2019.

312 OMAÑA-MOLINA, M.; VANZZINI-ZAGO, V.; HERNÁNDEZ-MARTÍNEZ, D.; CASTELAN-RAMÍREZ,N.8, I.; HERNÁNDEZ-OLMOS, P.; SALAZAR-, L.; GONZÁLEZ-ROBLES, A.; RAMÍREZ-FLORES, E.; SERVÍN-, C. *Acanthamoeba* keratitis in Mexico: Report of a clinical case and importance of sensitivity assays for a better outcome Maritza. *Experimental Parasitology*,v.196, p.22-27,2019. DOI 10.1016/j.exppara.2018.11005.

313 MARCIANO-CABRAL, F.; JAMERSON, M.; KANESHIRO, E.S. Free-living amoebae , *Legionella* and *Mycobacterium* in tap water supplied by a municipal drinking water utility in the USA. *Journal of Water and Health*, v.8, n.1, p.71–82, 2010.

314 MICHEL, R.; SCHMID, E.N.; BÖKER, T.; HAGER, D.G.; MÜLLER, K.D.; HOFFMANN, R.; SEITZ, H.M. *Vannella* sp. harboring *Microsporidia*-like organisms isolated from the contact lens and inflamed eye of a female keratitis patient. *Parasitology Research.* v. 86, n.6,p.514–520,2000.

315 ANDERSON, O.R.; PEGLAR, M.T.; NERAD, T.A.; ANDERSON, O.R. *Stenamoeba polymorpha* , a new species isolated from domesticated horse equus ferus caballus. *Journal of*

Eukaryotic Microbiology, v.63, n.6, p.698-708,2016.

316 DYKOVÁ,1; KOSTKA, M.; PECKOVÁ,H. Two new species of the Genus *Stenamoeba* Smirnov, Nassonova, Chao et Cavalier-Smith, 2007. *Acta Protozoologica* ,v.49,n.3,p. 245–251,2010.

317 LARES-JIMÉNEZ, L.F.; BORQUEZ-ROMÁN, M.A.; LARES-GARCÍA, C.; OTERO-RUIZ, A.; GONZALEZ-GALAVIZ, J.R.; IBARRA-GÁMEZ, J.C.; LARES-VILLA, F. Experimental parasitology potentially pathogenic genera of free-living amoebae coexisting in a thermal spring. *Experimental Parasitology,*v. 195, p.54–58,2018.DOI 10.1016/j.exppara.2008.10.006.

318 THOMAS, J.M.; ASHBOLT, N.J. Do free-living amoebae in treated drinking water systems present an emerging health risk? *Environmental Science Technology*, v.45, n.3, p.860–869,2011.

APPENDIX

APPENDIX I

Experimental Parasitology 187 (2018) 1–11

Contents lists available at ScienceDirect

Experimental Parasitology

journal homepage: www.elsevier.com/locate/yexpr

The therapeutic strategies against *Naegleria fowleri*

Natália Karla Bellini [a], Thomás Michelena Santos [a], Marco Túlio Alves da Silva [a], Otavio Henrique Thiemann [a, b, *]

[a] Instituto de Física de São Carlos, Universidade de São Paulo, Caixa Postal 369, 13560-590, São Carlos, SP, Brazil
[b] Departamento de Genética e Evolução, Universidade Federal de São Carlos, São Carlos, Brazil

HIGHLIGHTS

- *N. fowleri* is an important human pathogen, causing a disease with high fatality rates.
- The fast development of the patients' clinical condition calls for a prompt diagnosis.
- Identifying sources of *N. fowleri* is critical for prevention and diagnosis.
- Existing therapy shows limitations regarding effectiveness and side effects.
- Studies point to new therapeutic alternatives that reveal promising treatment results.

GRAPHICAL ABSTRACT

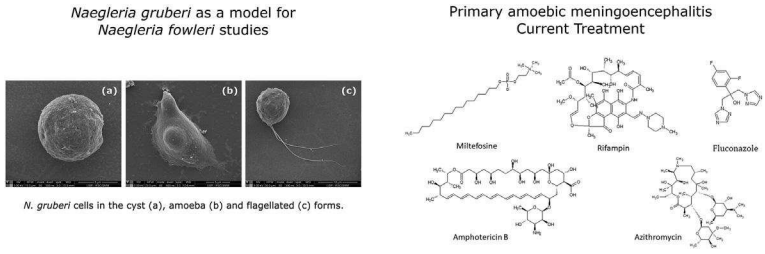

ARTICLE INFO

Article history:
Received 30 July 2017
Received in revised form
7 February 2018
Accepted 28 February 2018
Available online 1 March 2018

Keywords:
Naegleria fowleri
Primary amoebic meningoencephalitis
PAM
Therapeutic agents

ABSTRACT

Naegleria fowleri is a pathogenic amoeboflagellate most prominently known for its role as the etiological agent of the Primary Amoebic Meningoencephalitis (PAM), a disease that afflicts the central nervous system and is fatal in more than 95% of the reported cases. Although being fatal and with potential risks for an increase in the occurrence of the pathogen in populated areas, the organism receives little public health attention. A great underestimation in the number of PAM cases reported is assumed, taking into account the difficulty in obtaining an accurate diagnosis. In this review, we summarize different techniques and methods used in the identification of the protozoan in clinical and environmental samples. Since it remains unclear whether the protozoan infection can be successfully treated with the currently available drugs, we proceed to discuss the current PAM therapeutic strategies and its effectiveness. Finally, novel compounds for potential treatments are discussed as well as research on vaccine development against PAM.

Contents

Abbreviations: DUWL, Dental unit waterlines; DWDS, Drinking water distribution system; Trp, Tritrpticin.

* Corresponding author. Instituto de Física de São Carlos, Universidade de São Paulo, Caixa Postal 369, 13560-590, São Carlos, SP, Brazil.
E-mail address: thiemann@ifsc.usp.br (O.H. Thiemann).

https://doi.org/10.1016/j.exppara.2018.02.010
0014-4894/

1. Introduction

Free-living amoebae (FLA) include amphizoic protists capable of living in a variety of different habitats, not only in freshwater bodies, seawater and sewage systems, soil samples - which are actually expected habitats for amoebas to thrive in - but also in the air, dust samples, drinking water, dialysis units, eyewash solutions, contact lenses and dental treatment equipment (Trabelsi et al., 2012). Furthermore, some FLA species can be involved in both opportunistic as well as non-opportunistic infections in humans resulting in cerebral, skin or corneal infections. Pathogenic FLA belong to five genera, *Balamuthia, Acanthamoeba, Sappinia, Naegleria* and *Vermamoeba* (Abdul Majid et al., 2017; Teide et al., 2015). They share a life cycle that comprises a trophozoite (ameboid), feeding and replicating form, and a dormant cyst stage when faced with adverse environments. (Abdul Majid et al., 2017).

Particularly *Naegleria* is the unique genera of FLA that has both the amoeboid and cyst forms, besides a flagellate, motile, intermediate. (Fritz-Laylin and Cande, 2010; Khan et al., 2015). This ability to differentiate in a flagellate stage is one of the features that places *Naegleria* spp. as a member of the Vahlkampfiidae family, class Heterolobosea, together with Jakobozoa and Euglenozoa, the JEH clade, presently classified at the Excavata supergroup (Parfrey et al., 2006; Rodríguez-Ezpeleta et al., 2007). A previous research, using transcriptome approach, has analysed the enflagellation process of *Naegleria gruberi* showing that it takes about one hour to be completed and requires the transcription of a set of basal body and flagellar apparatus genes (Fritz-Laylin and Cande, 2010).

Similar to other FLA members, *Naegleria* is a free-living organism, feeding primarily on bacteria (De Jonckheere, 2011). To date over 40 different species of *Naegleria* have been identified (Abdul Majid et al., 2017). For the last 40 years attention has been focused on *Naegleria fowleri* (Carter, 1970) named in honour of its discoverers: the French zoologist Mathieu Naegler and the Australian doctor Malcolm Fowler. *N. fowleri* is the etiological agent of Primary Amoebic Meningoencephalitis (PAM), a devastating infection that targets the Central Nervous System (CNS) with high lethality rates (Grace et al., 2015).

N. fowleri is a thermophilic amoeboflagellate that have been isolated as a cyst resistant form, a trophozoite proliferative and feeding form and a motile flagellate form (reviewed by Grace et al., 2015; Baig et al., 2014; Heggie, 2010). All these stages have the ability to establish infection (Martinez and Visvesvara, 1997; Schuster and Visvesvara, 2004). Generally the trophozoite and flagellate forms are inhaled during swimming or diving, migrate through the neuroepithelium and have been found in affected tissue and the cerebrospinal fluid (De Jonckheere, 2002). The trophozoite attaches to human olfactory epithelium, move exuding pseudopodia and pass the cribriform plate to the brain through the olfactory cell axon (Visvesvara, 2010). The flagellate, a biflagellate form, once inside the nasal cavity transforms into a trophozoite taking several hours to complete differentiation (Marciano-Cabral, 1988), in contrast with *N. gruberi* fast differentiation process.

The spherical cysts, 8–12 μm in diameter, are naturally resistant to unfavourable environment, containing a single nucleus and a double-wall with pores through which the amoeba escape when conditions become favourable (Visvesvara, 2010). They are transported by dust and can occasionally enter the nasal mucosa, however they have not been encountered in the brain tissue (Martinez and Visvesvara, 1997). With a broad environment dispersion, the three *N. fowleri* stages have been found from fresh water and soil to airborne dust particles containing cysts (Martinez and Visvesvara, 1997). With the exception of Antarctica, its presence has been identified on all continents (De Jonckheere, 2011). Furthermore, due to its thermophilic nature, *N. fowleri* has been isolated from hot springs and thermally polluted rivers (Schuster and Visvesvara, 2004; Yoder et al., 2012).

Regarding of PAM occurrences, 143 cases have been registered in the USA from 1962 to 2016 (Centers for Disease Control and Prevention (CDC), 2017), and about 440 reported worldwide (Abdul Majid et al., 2017; Coupat-Goutaland et al., 2016). The scarcity of cases seems to indicate a very rare type of infection. However, the number of reported cases appears to be increasing over the last years (Cope et al., 2016, 2015; Grace et al., 2015; Heggie, 2010; Linam et al., 2015; Stowe et al., 2017) and a precise diagnosis is an essential tool to obtain a veritable assessment of its distribution. Interestingly a small number of cases are reported in tropical areas as Africa and South America, probably resulting from a lack of interest in such an occasional disease, while millions of people are affected by other severe infections in those regions (De Jonckheere, 2011).

This leads to the underestimation in the number of cases around the globe, seriously aggravated by other factors such as the difficulty of an accurate diagnosis due to its short incubation period, leading to the patient death in 48 h after the appearance of the first symptoms (Chow and Glaser, 2014). Headache, fever, stiff neck, vomiting and mental confusion illustrate the onset of illness that frequently evolves to seizures, neurological impairment and cerebral haemorrhages, resulting in death (Heggie, 2010; Herwaldt, 2001; Siddiqui and Khan, 2014). When rarely diagnosed, the current therapy to treat PAM includes mainly Amphotericin B combined with several different drugs, as azoles, whose nonspecific treatment results in low survival efficacy (Heggie, 2010; Yoder et al., 2012). Not surprising, PAM high fatality rate has become a serious concern for public health agencies and officials, with an approximate mortality rate of 95%, and affecting mostly children in good health (De Jonckheere, 2011).

In this review we discuss the incidence of *Naegleria fowleri*, its environmental occurrence, the challenges in an accurate and fast diagnosis and how it has evolved. We proceed to present the most conflicting points of the current PAM therapy, related to drug efficacy and its side effects. In conclusion, new potential therapies are presented, including novel molecules with amoebicidal activity and possible vaccination strategies.

2. Environmental occurrence of *Naegleria fowleri*

Several studies have been conducted aiming at identifying *N. fowleri* trophozoites or cysts in the most varied environments, here classified under two categories of natural habitats and urban zones. Among natural habitats are grouped: rivers and freshwater lakes (Farra et al., 2017), ponds (Dobrowsky et al., 2016), hot springs and warm aquatic environments (Farra et al., 2017; Latifi et al., 2017). Under the urban zones category are grouped: recreational fountains (Morgan et al., 2016; Reyes-Batlle et al., 2017), pasteurized and unpasteurized water sources (Dobrowsky et al., 2016), domestic and hotel swimming pools (Farra et al., 2017), hospitals, pipe wall biofilms related to drinking water distribution system (DWDS) (Puzon et al., 2017), geothermal heated water (Streby et al., 2015), tap water used on nasal flooding (Cope et al., 2015; Streby et al., 2015), dental unit waterlines (DUWLs) (Leduc et al., 2012), contaminated drinking water (Morgan et al., 2016) and waterparks (Heggie and Küpper, 2017). Among these sites, those with higher water temperature, above 28 °C, are reported to harbour a greater number of *N. fowleri* (Heggie, 2010).

Furthermore, an occurrence that has been attracting attention is the association with bacteria and other eukaryotic organisms that live in symbioses with *Naegleria* spp. on biofilms of DWDS, known for their low chlorine levels (Miller et al., 2017). It has been shown that the higher the bacterial density the less viable is the coexistence with the amoebae (Morgan et al., 2016). The most common strategy to avoid amoebae associated with other bacteria in these distribution systems is the chlorination. The chlorine concentration usually applied, 0.5 mg/L, is not sufficient to eliminate *Naegleria* since they can differentiate into the resistant cyst form. A recent study outlines that a disinfection regimen consisting on a daily application of 1 mg/L of chlorine during 60 days is efficient against the amoebae (Miller et al., 2017).

This DWDS example reinforces the importance of amoeba genotyping to identify the appropriate elimination strategy, avoiding its re-emergence and decreasing PAM dissemination. Studies describing *N. fowleri* genetic diversity, linking different strains to their geographical occurrences, contribute to better comprehend the environmental reach of the strains (Al-Herrawy and Gad, 2015; Farra et al., 2017; Latifi et al., 2017; Tung et al., 2013). Among the main methods used to isolate and identify *Naegleria* in risk areas are morphological and molecular analyses (Bonilla-Lemus et al., 2014; Kang et al., 2015; Kao et al., 2014; Streby et al., 2015). The morphological approach is undertaken mainly as a complementary analysis by using wet sample mounts and visualizing them under an optical microscope, cultivating the organisms in non-nutrient agar (NNA) plates, conducting differentiation tests that induce enflagellation or encystment (Benterki et al., 2016; Latifi et al., 2017; Reyes-Batlle et al., 2017). Thermotolerance assays are usually carried out assessing their viability contributing to species identification (Abdul Majid et al., 2017).

The main identification approaches are those based in molecular techniques, using conventional and quantitative PCR (Polymerase Chain Reaction) associated with amplicon sequencing to confirm the morphological findings (Benterki et al., 2016; Dobrowsky et al., 2016; Liang et al., 2010; Régoudis and Pélandakis, 2016; Reyes-Batlle et al., 2017). Bioinformatics tools are essential for further data analysis. Table 1 summarizes the different primer sets used for *Naegleria* identification in case reports from the last 5 years, along with other relevant information. This molecular approach is of great importance since it allows not only for the recognition of known species, but also for the identification of new strains. Khwon and Park (2017) used rDNA ITS sequence of 45 *Naegleria* species and 18S rDNA sequence of 27 *Naegleria* species to describe three new species named *N. jejuensis*, *N. neojejuensis* and *N. koreanum*. Quantitative PCR analysis, in addition of been a detection tool, also allows for the quantification of amoebae cells using the number of gene copies and standard curves for calibration (Régoudis and Pélandakis, 2016). Furthermore, the melt curve analyses of the amplicons can be applied as primer specificity verification (Liang et al., 2010) as well as for strain genotyping (Benterki et al., 2016). Furthermore, Régoudis and Pélandakis (2016) used a single copy rDNA gene and applied both PCR techniques. The quantitative approach showed more reliable results when compared to the traditional PCR-based assay (Régoudis and Pélandakis, 2016).

In addition to PCR-based techniques, two new strategies to identify environmental occurrences have been proposed and showed promising results: microsatellites as neutral genetic markers (Coupat-Goutaland et al., 2016) and a metabolomic approach (Yu et al., 2017). The first is based on the fact that the *N. fowleri* specie has several different strains and can be isolated in the most diverse geographical sites. This issue was addressed by using microsatellites as strong population markers. Analyses of 47 *N. fowleri* strains using six microsatellites loci have described seven different genetic groups. Prior to these discoveries, only five were known (EA, WP, SP, CHO and CAT) adding NZ and RA. This new approach could help to better understand the genus population structure, contributing also with a better understanding of its evolutionary history (Coupat-Goutaland et al., 2016). The second strategy, metabolomics, aims to classify characteristic metabolites of each species that allow its rapid identification by using techniques such as ultra-performance liquid chromatography (UPLC) and mass spectrometry (MS). Among 550 metabolites studied, 4 have shown to be specie markers. Thereby, it can be used to examine water samples and on PAM diagnosis of CSF with the possibility to discriminate pathogenic from non-pathogenic *Naegleria* spp. (Yu et al., 2017).

3. Clinical diagnosis of PAM

Even considering PAM as a rare disease due to the scarcity of reported cases, the critical points are its high mortality rate (Coupat-Goutaland et al., 2016; Stubhaug et al., 2016) and the short incubation period (Chow and Glaser, 2014). Regarding its fast evolution, several PAM cases were only diagnosed *post-mortem*, through brain autopsies (Roy et al., 2014; Stubhaug et al., 2016). In this context, an accurate and fast diagnosis is likely to be the bottleneck for a better understanding of the global number of cases. Likewise, the PAM survival rate could be increased by allowing a fast and efficient medical intervention. This section presents the current methods used in PAM diagnosis.

The clinical diagnosis of PAM usually consists of three approaches that are time consuming and technically challenging. These are conducted together as often as possible and consist of: morphological analysis of cerebrospinal fluid (CSF) wet mount, molecular identification using the PCR, and differentiation tests with the organisms found on the CSF (e.g., enflagellation, encystment or thermotolerance tests) (Abdul Majid et al., 2017; Benterki et al., 2016; Streby et al., 2015; Stubhaug et al., 2016). In order to assess the clinical manifestations of the disease, the patients are primarily submitted to body temperature and blood pressure measurements, since any discrepancy from normal in these values can indicate an ongoing infection. The primary PAM symptoms are: headaches, fever, nausea, vomiting, exhaustion and lethargy (Heggie and Küpper, 2017; Linam et al., 2015; Stowe et al., 2017). This first phase of the infection is analogous to bacterial or viral meningitis. It has been shown that an in-depth CSF examination is required to distinguish a naegleriasis from a pneumococcal meningitis (Zahid et al., 2016). However, with the evolution of the

Table 1
Comprehensive primer set used for detecting *Naegleria* upon environmental (E), clinical (C) and *in vitro* (V) contexts. All primers are designed to search regions on ribosomal DNA of *Naegleria*, as the most recent papers have reported. Each target amplicon 18S_1 to 18S_3, ITS_1 to ITS_8 and 5.8S can be found in KT375442 strain, except ITS_4 found in M18732 strain both used as models to determine size and region of the amplicons.

Accession number/ PCR for	Target/Size (pb)	FW primer name/Sequence (5′ → 3′)	RV primer name/Sequence (5′ → 3′)	Context	Location	Reference
KT375442/*N. fowleri*	18S_1/153	NaeglF192/ GTGCTGAAACCTAGCTATTGTAACTCAGT	NaeglR344/ CACTAGAAAAAGCAAACCTGAAAGG	E	South Africa	(Dobrowsky et al., 2016)
				E	Georgia and U.S.	(Streby et al., 2015)
				C	Texas	(Barnett et al., 1996)
				C	California	(Johnson et al., 2016)
				C	Thailand	(Stubhaug et al., 2016)
				E	Louisiana (U.S.)	(Cope et al., 2015)
KT375442/*Naegleria*	18S_2/577	NF-ITS-F1/GACTTCATTCGTTCTTGTAGA	NF-ITSR1/CTCTTGCGAGGTCCAGAC	E	Louisiana (U.S.)	(Cope et al., 2015)
KT375442/*Naegleria*	18S_3/256	Nae3-For/CAAACACCGTTATGACAGGG	NII/AAATGATCCCTACGCAGGTT	E	Austria	(Scheikl et al., 2014)
KT375442/*N. fowleri*	18S_4/183	Nae3-For/CAAACACCGTTATGACAGGG	Nae3-R/CTGGTTTCCCTCACCTTACG	*V*	Republic of Korea	(Kang et al., 2015)
				E	Taiwan	(Kao et al., 2013)
				C	Taiwan	(Su et al., 2013)
				E	Taiwan	(Tung et al., 2013)
M18732/*Naegleria*	18S_4/183	Nae3-For/CAAACACCGTTATGACAGGG	51 R/CTGGTTTCCCTTACCTTGCG	E	Egypt	(Al-Herrawy and Gad, 2015)
KT375442/*N. fowleri*	ITSr_1/404	NGITSF/AACCTGCGTAGGGATCATTT	ITSRV/TTTCCTCCCCTTATTAATAT	E	Georgia and Florida	(Streby et al., 2015)
KT375442/*Naegleria*	ITSr_2/410	Veer.gs fw/GAACCTGCGTAGGGATCATTT	Veer.gs rv/TTTCTTTTCCTCCCCTTATTA	E	Northern Iran	(Latifi et al., 2017)
				V	Republic of Korea	(Kang et al., 2015)
				E	Taiwan	(Kao et al., 2014)
				E	Rural Western Australia	(Morgan et al., 2016)
				E	Rural Western Australia	(Miller et al., 2017)
KT375442/*Naegleria*	ITSr_3/405	Veer.gs fw/GAACCTGCGTAGGGATCATTT	ITSRV/TTTCCTCCCCTTATTAATAT	E	Central African Republic	(Farra et al., 2017)
KT375442/*N. fowleri*	ITSr_4/377	FWS/GTGAAAACCTTTTTTCCATTT	Veer.gs rv/TTTCTTTTCCTCCCCTTATTA	E	Western Australia	(Miller et al., 2017)
				E	Georgia and U.S.	(Streby et al., 2015)
				E	Rural Western Australia	(Morgan et al., 2016)
KT375442/*N. fowleri*	ITSr_5/311	Veer.ss fw/ TGAAAACCTTTTTTCCATTTACA	Veer.ss rv/ AAATAAAAGATTGACCATTTGAAA	E	Northern Iran	(Latifi et al., 2017)
				E	Taiwan	(Kao et al., 2014)
				E	Taiwan	(Tung et al., 2013)
				E	Egypt	(Al-Herrawy and Gad, 2015)
KT375442/*N. fowleri*	ITSr_6/311	FWS/GTGAAAACCTTTTTTCCATTT	Veer.ss rv/ AAATAAAAGATTGACCATTTGAAA	E	Rural Western Australia	(Morgan et al., 2016)
				E	Taiwan	(Kao et al., 2014)
KT375442/*N. fowleri*	ITSr_7/309	NFITSFW/TGAAAACCTTTTTTCCATTTACA	NFITSRV/ AATAAAAGATTGACCATTTGAAA	E	Central African Republic	(Farra et al., 2017)
				E	Southeast Asian	(Abdul Majid et al., 2017)
KT375442/*N. fowleri*	ITSr_8/125	JBVF/AGGTACTTACGTTAGAGTGCTAG	JBVR/ATGGGACAATCCGGTTTTCTCA	E	Georgia and U.S.	(Streby et al., 2015)
				E	Georgia	(Mull et al., 2013)
KT375442/*Naegleria*	5.8S/109	ITS-F/CAAAAAGCGATATGTAATGA	ITS-R2/ TTGATATAAAACTAGCACTCTAA	E	Taiwan	(Kao et al., 2014)

clinical condition of a PAM patient other complications may occur, such as bleeding and brain dysfunction (Benterki et al., 2016; Su et al., 2013).

With the identification of the primary encephalitis symptoms, a lumbar puncture is performed, collecting CSF to quantify glucose and protein levels, leukocyte count, fluid turbidity, among other parameters (Stowe et al., 2017; Su et al., 2013). Patients with positive results for PAM tend to present CSF with low glucose levels, high C-reactive protein concentration (around 260 mg/L) and leukocyte count (roughly 2100 cells/mm^3) (Stubhaug et al., 2016). The fresh CSF is also microscopically inspected for the presence of trophozoites. Once detected, further analyses must be performed investigating the quantity and granularity of the cytoplasmic vacuoles (Su et al., 2013), the amoebae length and width, the cysts diameter and number of pores (Khwon and Park, 2017). Moreover, by the CSF examination it is possible to verify the movement, size, pseudopod morphology and motility of the amoebas, contributing to species identification (Benterki et al., 2016).

Several staining methods have been suggested to aid in the amoebas identification (Abdul Majid et al., 2017; Heggie and Küpper, 2017). Table 2 summarizes the different histological techniques used for PAM diagnosis in case reports from the last 5 years. These morphological analyses are usually combined with immunochemical assays and radiological approaches, also indicated on Table 2. Imaging techniques such as contrast-enhanced computer tomography (CT) and magnetic resonance (MR) show a variety of CNS alterations as diffuse cerebral edema (Stowe et al., 2017), cortical sulci effacement and hydrocephalus herniation (Stubhaug et al., 2016). These conditions can evolve, worsening dramatically towards more advanced stages and possibly becoming necrotic areas, stenosis and aneurysms that lead to death (Stubhaug et al., 2016).

The aforementioned histopathological analyses are of extreme importance for a correct diagnosis. However, they allow the identification of amoebae only at the genus level (Abdul Majid et al., 2017). Therefore, molecular approaches, mainly PCR-based assays, have been developed. A growing improvement on the available molecular techniques over the past few decades such as sequencing, quantitative PCR, and the use of microsatellites gene markers, resulted in a more accurate identification of the target

Table 2
Clinical strategies used for PAM diagnosis (2013–2017). Regarding the staining information Ziehl-Neelsen is also known as acid-fast stain, H&E as hematoxylin and eosin stain, and PAS as Periodic acid–Schiff. The immunohistochemical (HI) methods groups IFF (indirect immunofluorescence staining), IHC (immune alkaline phosphatase staining), CD45 (pan-leukocyte marker) and CD68 (macrophage marker). The central nervous system analyses include cerebrospinal fluid (CSF) measurements, contrast enhanced computed tomography (CT), magnetic resonance (MR) and electroencephalogram (EEG).

Case Reports Gender (Year)	Staining Methods	IH	CSN Analysis	Culture assays	Molecular trials (PCR)	Reference
F (21)	–	–	CSF measurements	x	x	(Johnson et al., 2016)
M (11)	–	–		x	x	(Abrahams-Sandí et al., 2015)
M (42)	India ink preparation. Acid fast smear	–	CSF measurements, EEG	x	x	(Shariq et al., 2014)
M (6)	Ziehl Neelsen, India ink	–	CSF measurements	x		(Sood et al., 2014)
M (75)	Liu's stain, acidfast stain	–	CT, CSF measurements, MR	–	x	(Su et al., 2013)
M (4)	–	–	CT, EEG, MR, CSF measurements	–	x	(Cope et al., 2015; Stowe et al., 2017)
M(14)	–	IFF, IHC	CT, EEG	–	x	(Roy et al., 2014; Stowe et al., 2017)
F (71)	Mucicarmine stain, PAS, periodic acid staining	CD45, CD68	CSF measurements, CT	–	x	(Stubhaug et al., 2016)
F (12)	Giemsa, H&E, Wright	–	CSF measurements, CT	–	x	(Cope et al., 2016; Dunn et al., 2016; Heggie and Küpper, 2017; Linam et al., 2015)
M(8)	Wright	–	CSF measurements, CT	–	x	(Cope et al., 2016; Roy et al., 2014)
M (10)	H&E	IFF, IHC	CT	–	x	(Roy et al., 2014)
M (22)	–	–	–	–	x	
F (16)	–	–	–	–	x	
M (9)	Wright	–	–	–	x	

species. In most cases, total DNA is extracted from the cells found on the CSF and PCR is conducted using *Naegleria* specific primers (Fig. 1), frequently the 18S rDNA region. The internal transcribed sequence (ITS) regions (Benterki et al., 2016; Streby et al., 2015; Su et al., 2013) as well as the 5.8S and the 28S regions (Kao et al., 2014; Stubhaug et al., 2016) are targets also used for the identification, as illustrated in Fig. 1. The significance of using the rDNA as a PCR target is due to its inner variable regions allowing for individual genotype recognition (Pélandakis and Pernin, 2002; Tavares et al., 2006). Once the amplicons are obtained, sequencing is conducted, combined with bioinformatics tools to determine the species (Farra et al., 2017).

The current state of the art in the diagnosis of naegleriasis is the combination of the morphological and molecular approaches just discussed. For instance, it was reported in 2013 a diagnostic of combined techniques which has been considereda successful pipeline in PAM diagnosis (Linam et al., 2015). This case describes a real-time PCR assay that testing positive for *N. fowleri* was of critical importance for the successful treatment, saving a young patient's life (Dunn et al., 2016; Heggie and Küpper, 2017). The analysis of the CSF showed a higher than normal white blood cells count (3675 cells/μL), glucose levels near 20 mg/dL and protein concentration around 370 mg/dL. In addition, microscope inspection of Giemsa-Wright stained CSF samples identified the presence of *Naegleria* trophozoites. Moreover the radiological images revealed blood in the brain frontal lobes and restricted diffusion in the

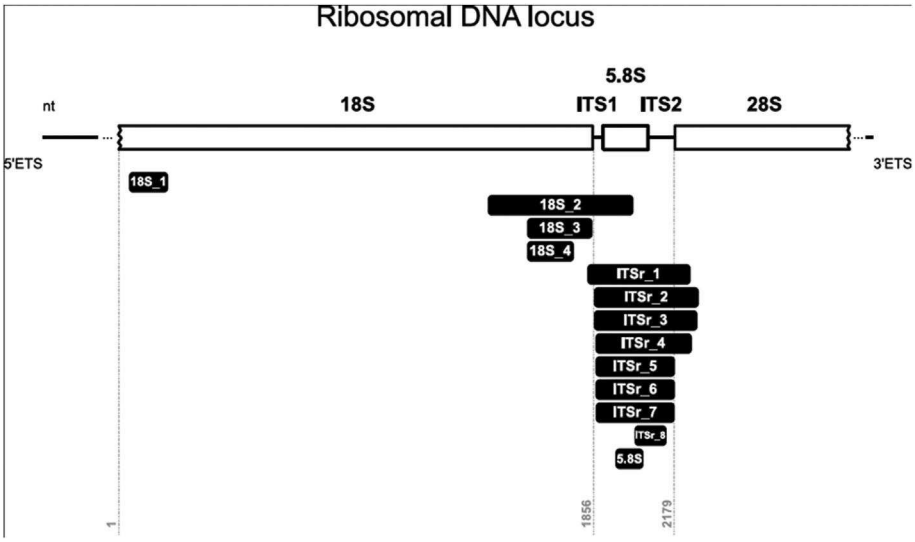

Fig. 1. Scheme of *Naegleria's* ribosomal DNA locus showing the set of primers used as a molecular approach to perform environmental and clinical investigations. The external transcribed spacers (5′ETS and 3′ETS) and internal transcribed spacers (ITS1 and ITS2) are also exhibited. The black boxes display the relative lengths of ampilicons and indicate the position chosen to perform the PCR. The forward and reverse set of primers used to amplify these amplicons are reported on Table 2.

cerebellum and multiple brain areas (Linam et al., 2015). The history of the patient, specially recent contacts with freshwater bodies, is relevant to further confirm a thorough diagnosis (Dunn et al., 2016). For instance, in the case reported by Linam et al. (2015), the patient was described as having swum in a water park right before the onset of the first symptoms (Linam et al., 2015). Other studies have also pointed out this correlation among PAM manifestations: recent use of water for recreational practices and the discovery of *N. fowleri* in the vicinities (Gyori, 2003; Morgan et al., 2016; Okuda et al., 2004; Yoder et al., 2010).

Simultaneously to the clinical aspects described, an improved environmental detection of *N. fowleri,* as described in the previous section, resulting in the characterization of its geographical dispersion, will render the implementation of prophylactic measures more effective.

4. The current therapy against PAM

Although some drugs commonly employed in PAM treatment show positive results (e.g., amphotericin B and miltefosine), it is actually unclear whether the disease can be successfully cured using a determined combination of them. Such combined therapy has been commonly applied in the last five years. Even when treated under similar therapeutic approaches, the fatality rate is still about 95% of the cases (Capewell et al., 2015). This section briefly describes the current treatment options for PAM (Grace et al., 2015; Pugh and Levy, 2016). Recently reported cases of PAM are summarized on Table 3, including their treatment strategy and its outcomes.

Amphotericin B (AmB) has been the most used drug for the treatment of PAM. All recent cases reporting treatment success have administered this compound either intravenously or intrathecally in combination with other drugs (Capewell et al., 2015). Best known for its antifungal activity, AmB is also indicated as an antiviral and antiprotozoal drug, with a minimal inhibitory concentration (MIC) of 0.075 μg/mL against *Naegleria* sp. (Carter, 1969). However, AmB administration is restricted by toxicity effects, generally accompanied by a series of severe side effects ranging from nausea and vomiting to acute kidneys damage (Sau et al., 2003). The conventional therapy consists on AmB deoxycholate administration, which increases the compound solubility.

Rifampin is an antibiotic commonly associated with AmB to potentiate the effects of the treatment. It has been proved to yield satisfactory results when used on bacterial and protozoan infections while at higher concentrations (Conti and Parenti, 1983; Vargas-Zepeda et al., 2005; Yoder et al., 2012). Therefore, it is widely present among the ensemble of drugs administered to PAM diagnosed patients (Capewell et al., 2015). Monotherapy with rifampin is normally discouraged due to the very rapid development of resistance during the treatment (Wehrli, 1983).

Another set of drugs employed on the treatment of PAM are the Azoles. They are prominently known as potent antifungals although their application is not restricted to it (Ghannoum and Rice, 1999). There is strong evidence of Azoles' activity against protozoa (De Macedo-Silva et al., 2013; Raether and Seidenath, 1984), and their use in this context is common (Kappagoda et al., 2011) with Miconazole, Fluconazole and Ketoconazole most frequently used in PAM treatment (Capewell et al., 2015).

Miltefosine is a breast cancer and anti-leishmanial drug that has shown good results when tested against FLA *in vitro* (Kim et al., 2008b; Schuster et al., 2006). In 2013 the drug was successfully administered to two patients diagnosed with PAM that have survived the infection (Cope et al., 2016; Linam et al., 2015). Even though it is an investigational drug, the CDC has expanded its access to clinicians for the treatment of FLA infections (Capewell et al., 2015; Centers for Disease Control and Prevention (CDC), 2013). The availability of Miltefosine and its apparent success has made the drug a potential option of the current therapeutic strategies against PAM. However, the latest case reports have not shown consistent results (Table 3).

Drug delivery is a key problem for the treatment of the central nervous system (CNS) amoebic infections. Reaching the site of infection at the effective concentrations is hampered by the blood-brain barrier. On the other hand, the transport to brain parenchyma through blood vessels presents a minor problem. Being able to successfully reach the brain parenchyma is a very important factor influencing the treatment efficacy. Therefore, the search for molecules that present these characteristics and with attractive amoebicidal effects can improve the therapeutic arsenal against *N. fowleri* (Schuster et al., 2006).

AmB, as previously stated, has been the most commonly used drug to treat PAM. However, alternatives such as lipid formulations (i.e., liposomal, lipid complex, colloidal suspension) (Botero et al., 2014) and nanoencapsulation (Diaz et al., 2015) have been proposed, showing promising results (Falci et al., 2015). A published study also proposes that a single dose of liposomal AmB could have the same efficacy as the conventional alternate day infusions of AmB deoxycholate for the treatment of visceral leishmaniasis, a

Table 3
Cases of PAM found in recent literature (2013–2017). IT – intrathecal; IV - intravenous.

Gender	Age	Outcome	Treatment	Location	Year of the Incident	Year of Publication	Reference
M	4	Death	Amphotericin B IV, fluconazole, rifampin, azithromycin, miltefosine	USA	2015	2017	(Stowe et al., 2017)
M	14	Death	Amphotericin B IV/IT, fluconazole, rifampin, azithromycin, miltefosine	USA	2015	2017	
M	12	Death	Amphotericin B IV, fluconazole, rifampin, azithromycin, miltefosine	USA	2013	2016	(Cope et al., 2016)
M	8	Survival	Amphotericin B IV, fluconazole, rifampin, azithromycin, miltefosine	USA	2013	2016	
F	21	Death	Dead before accurate diagnosis	USA	2015	2016	(Johnson et al., 2016)
F	12	Survival	Amphotericin B IV/IT, fluconazole, rifampin, azithromycin, miltefosine	USA	2013	2015	(Linam et al., 2015)
M	11	Death	Dead before accurate diagnosis	USA	2014	2015	(Abrahams-Sandí et al., 2015)
M	4	Death	Dead before accurate diagnosis	USA	2013	2015	(Cope et al., 2015)
M	42	Death	Amphotericin B IV/IT	Pakistan	Not reported	2014	(Shariq et al., 2014)
M	6	Survival	Amphotericin B, rifampin, fluconazole	India	Not reported	2014	(Sood et al., 2014)
M	10	Death	Rifampin, and vancomycin	USA	2009	2014	(Roy et al., 2014)
M	22	Death	Not reported	USA	2009	2014	
F	16	Death	Amphotericin B, azithromycin, fluconazole, rifampin	USA	2011	2014	
M	75	Death	Amphotericin B IV	Taiwan	Not reported	2013	(Su et al., 2013)

dose reduction which could drastically decrease the side effects of the treatment (Sundar et al., 2010). It is possible that a similar effect is observed for *N. fowleri.*

The Azoles are a set of drugs also commonly used as therapeutic agents against amoebic infections, but showing some drawbacks. For instance, the characteristic water insolubility of this group of molecules leads to drug processing in the liver and can induce drug interactions, or even toxicity, when taken in combination with other drugs. Voriconazole is a triazole generally used to treat invasive fungal infections. An *in vitro* study demonstrated its effects against different *N. fowleri* strains at concentrations as low as 1 μg/mL. Adding the drug to the culture medium at a concentration from 10 μg/mL up to 40 μg/mL, the amoebae still appeared viable after one week of incubation, but did not proliferate after transferring to a drug-free medium. Extensive lysis of amoebas was observed at concentrations higher than 1 μM. At those concentrations, Voriconazole showed no inhibitory effect on monolayers of monkey kidney cells, thus giving indications of reduced or no toxic effects on healthy mammalian cells. This characteristic, together with the molecule ability to penetrate the CSF and brain tissue, makes it a promising drug for further investigations towards developing new treatment for PAM (Schuster et al., 2006).

Chlorpromazine is primarily known as an antipsychotic compound while it is also used regularly in other contexts, such as an antiemetic agent. It can be further used for attenuating the replication of adenovirus as well as for the treatment of patients in shock. The drug showed promising amoebicidal properties in *N. fowleri*-infected mice compared to AmB treated animals. Additionally, marginal levels of liver and kidneys toxicity were found. The mechanism of action of Chlorpromazine may be connected to its lipophilic interactions with the plasma membrane of the amoebae or to the changes on proteins regulating the calcium metabolism. The fact that Chlorpromazine accumulates well in the CNS raises some interest regarding this drug as a potential useful agent on the treatment of PAM in humans (Kim et al., 2008a).

Antimicrobial peptides (AMPs) are recognized as an important component of the nonspecific host immune system against invading pathogens. The characteristics of AMPs include having small molecular size and cationic affinity, usually non-immunogenic and a short half-life. Their activities comprise membrane targeting, disrupting protein-protein interactions and the ability to penetrate tissues. Tiewcharoen et al. (2014) tested the effects of different AMPs against *N. fowleri* trophozoites and described that Tritrpticin (Trp) reduced the viability of the amoeba at concentrations as low as 100 μg/mL (Tiewcharoen et al., 2014). These findings are consistent with other reports in which Trp decreased the viability of *Trichomonas vaginalis* when tested at the same concentration (Infante et al., 2011). A combination of Chlorpromazine and AmB resulted in damage to *N. fowleri* trophozoites, causing bleb formation and disappearance of suckers and pseudopodia. Trp activity is comparable to this AmB-Chlorpromazine combination, with the advantage of not presenting human neuroblastoma SK-N-MC cells damage. These findings suggest Trp as an additional candidate drug against *N. fowleri* trophozoites (Tiewcharoen et al., 2014).

In a previous study (Kim et al., 2008b), seven different antibiotics were tested against *N. fowleri* (i.e., Roxithromycin, Hygromycin B, Zeocin, Clarithromycin, Erythromycin, Neomycin and Rokitamycin). Hygromycin B and Rokitamycin were the most effective *in vitro* drugs of this group, showing 100% of growth inhibition after 6 days. Roxithromycin also showed constant positive results along the same experimental time, maintaining a high rate of trophozoites growth inhibition. Other antibiotics such as Clarithromycin, Erythromycin, Neomycin and Zeocin did not have similar effects. During the *in vivo* tests, Rokitamycin exhibited a survival rate of 80% of the infected mice compared to 25% for Roxithromycin. Altogether, of the seven compounds tested, Rokitamycin has the greatest potential (Kim et al., 2008b).

Another study, Baig et al. (2014) tested compounds targeting vital biochemical pathways and receptors. Some of the compounds are currently used for treating disorders of the nervous system. Amlodipine reduced the viability of amoebas to about 19% compared to the control group. Other compounds revealed good results as well, with Haloperidiol and Apomorphine reducing the trophozoites viability to approximately 22% and 33%, respectively. Amiodarone and Loperamide exhibited less significant reductions in viability, both to values higher than 50%. Procyclidine, another tested compound, showed potential for amoebicidal activity while, similarly, Digoxin presented interesting lytic capabilities. However, future investigation is still necessary to validate their mechanism of action on *Naegleria*, both *in vivo* and *in vitro* (Baig et al., 2014).

Diamidines have shown interesting amoebicidal capabilities, including FLA, as well as antitrypanosomal, antileishmanial and antimalarial agents (Werbovetz, 2006). These molecules have the capability of crossing the blood-brain barrier, therefore being effective against CNS protozoan infections, representing an important class of compounds in the search for new therapeutic approaches. A recently published study (Rice et al., 2015) validated two new assays for high-throughput screening of molecules for new alternatives to treat PAM. Two compounds potentially suitable at the nanomolar range were identified among 150 amidino derivatives tested. From these, DB173 presented the best results. The authors concluded that the class of molecules derived from amidinos offer a very promising scenario in the development of new treatments for CSN infections (Rice et al., 2015).

The most commonly used methods for the discovery of new compounds with interesting amoebicidal effects are not generally cost and time effective when it comes to *Naegleria* infections. Aiming to find new alternatives to tackle this problem, a new high-throughput screening assay was proposed by Debnath and co-workers, directed towards accessing *Naegleria* viability (Debnath et al., 2012). Using *N. gruberi* as a model to comprehend *N. fowleri,* for safety reasons inhibitors to five kinases and an NK kappa B were identified as good hits during primary screens. Also, a recently identified compound belonging to the same antifungal class as AmB, namely Corifungin, was tested to determine its efficiency, yielding favourable results. Both *in vitro* and *in vivo* tests of Corifungin showed lower toxicity when compared to AmB, and a survival rate of 100% of *N. fowleri* infected mice compared to a 60% survival for mice treated with AmB (Debnath et al., 2012). A more recent study corroborated these results with *in vitro* testing of Corifungin against *Acanthamoeba castellanii*. Analysis of transmission electron microscopy showed several alterations on the cells when incubated with Corifungin, including swollen mitochondria, disordered nuclear chromatin and degeneration of cytoplasm architecture. It was also observed that the drug induced the cell encystment process while also lysing the cysts after long periods of incubation (Debnath et al., 2014).

Considering the results here described, several compounds with potential for treatment of PAM are been investigated, requiring validation and further confirmation. In summary, the current direction towards the reduction of PAM mortality rates comprises the development and availability of new treatments using these compounds, along with more rapid diagnostic techniques, and a careful environmental evaluation of incidence of *N. fowleri.*

5. Potential vaccination strategies against *N. fowleri*

Vaccination strategies are always an important part of the therapeutic arsenal against a pathogenic agent, and some studies

here discussed have shown potential for the development of a vaccine against *N. fowleri*, which would represent a welcome achievement.

John et al. (1977) demonstrated that the immunization of mice with different preparations of *N. fowleri* protected the animal from lethal parasitemia doses. Mice immunized with living or formalinized *N. fowleri* or living *N. gruberi* presented a significant increase in their protection to successive challenges with *N. fowleri*. In general, intravenous inoculation conferred higher protection when compared to other administration routes; intact cells showed better results than cell fragments; and *N. gruberi* extracts seem a better immunogen than *N. fowleri* extracts (John et al., 1977). In a later study, Thong et al. (1983) noted that mice could be protected against *N. fowleri* after being immunized with the culture medium used for the amoebae growth, whose protection occurred in the nasal mucosa.

Other reports describe the use of the *Bacillus thuringiensis* Cry1Ac protoxin coadministered with amoebal lysate, increasing *N. fowleri* challenged mice survival compared to amoebal lysate alone. Mice humoral response was activated and IgG and IgA mucosal levels were increased, however, only IgG response persisted after a two months period (Saúl Rojas-Hernández et al., 2004). The interaction between trophozoites and IgA antibody in the nasal lumen was also observed. In comparison, in non immunized mice the trophozoites were able to invade the nasal mucosa (Jarillo-Luna et al., 2008).

A deeper investigation about the Cry1Ac as an adjuvant showed a 100% survival rate in STAT6+/+ mice co-administrating amoebic lysates and Cry1Ac with subsequent challenging with intranasal *N. fowleri* amoebae. On the other hand, STAT6−/− mice did not survive the same treatment, which suggest a Th2-biased immune response, related to the presence of the STAT6 protein. Other markers of Th2 response were observed, such as elevated levels of IgG1 and IL-4, while the STAT6−/− mice presented higher levels of IL-12, IFN-γ and Th1-associated IgG2a (Carrasco-Yepez et al., 2010).

In vitro experiments revealed that the inoculation of *N. fowleri* induces the activation of Neutrophil Extracellular Traps (NET), together with the release of other characteristic components, but the trophozoites were still able to evade the killing process. When the *N. fowleri* were opsonized with human IgG, the trophozoites were susceptible to neutrophil activity, suggesting a significant role of polymorphonuclear cells (PMNs), allowing NET formation in response to *N. fowleri* infection (Contis-Montes de Oca et al., 2016). Together, IgA and IgG up-regulation mentioned above with the PMN induction to liberate NET reduces trophozoite attachment to the olfactory mucosa (Rojas-Hernández et al., 2004).

By immunoscreening with sera obtained from both infected and immune mice, new antigenic molecules were identified (e.g., the nfa1 gene). Western blot experiments demonstrated that Nfa1 protein reacted strongly with infected and immune sera. Immunofluorescence experiments were able to identify the antigen to a pseudopodium-specific localization, suggesting a potential role in amoeba motility. Highly virulent amoebae presented faster movement in comparison to less virulent variants (Cho et al., 2003). Immunization with recombinant Nfa1, with or without adjuvant (i.e., Freund's complete), stimulated an immune response in mice exhibiting high levels of specific IgGs - including isotypes IgG2b, IgG2a and IgG3 - and IgA antibodies. The immunized mice were challenged with a lethal dose of *N. fowleri* trophozoites and a survival rate of 100% was observed after 9–10 days post infection (Lee et al., 2011).

In another study, inoculation of mice with recombinant Nfa1 protein and cholera toxin B subunit (CTB) or *Escherichia coli* heat-labile enterotoxin B subunit (LTB) activated the secretion of INF-γ (Th1 response), IL-4 (Th-2 response), IL-2 and IL-10 (T regulatory response) cytokines. Recombinant Nfa1 administration associated with CTB and LTB triggered Th1/Th2/Treg responses and the mice survival rates were 100% and 80%, respectively (Lee et al., 2015). Nfa1 was also used in a potential DNA vaccination strategy using a lentiviral vector (pCDH). Among the effects of this vaccine, increased IgG levels (IgG1 and IgG2a) and higher expression of IL-4 and IFN- γ were observed, suggesting a Th1/Th2 mixed response. The mice vaccinated with nfa1 DNA vaccine exhibited survival rates around 90% after a challenge with *N. fowleri* trophozoites with humoral and cellular immune responses activation (Kim et al., 2013).

Returning to some problems presented before as the diagnosis difficulties, i. e., the current drug arsenal with low efficacy and unreported cases mainly in tropical areas, this possible vaccination strategies calls attention. Assuming its large availability after validation, they could become an attractive method against increasing PAM deaths.

6. Conclusions

Potential risk factors for an increase in the number of PAM cases range from poor basic sanitation conditions, recreational activities on warm waters to nasal irrigations with contaminated water and other seemingly harmless factors. The current trend of global warming also pose a new factor in the rise of reported PAM cases as well as the development of drug resistance (Siddiqui and Khan, 2014). Solutions to these problems are as diverse as the factors leading to potential exposure to *N. fowleri* and include avoiding swimming in, or inhaling, warm contaminated water. Swimming should be forbidden whenever *N. fowleri* has been identified in the nearby environment, regardless its concentration (De Jonckheere, 2012) and the use of physical barriers to *N. fowleri* entry, such as nose clips, could be enforced. While taking baths, the water can be sterilized by boiling or filtering to be properly disinfected (Siddiqui and Khan, 2014). These recommendations, although seemingly simple to follow, are extremely difficult to be implemented at a large scale, especially in low-income areas, and sometimes are quite unpopular.

Prevention of infection with *N. fowleri* is dependent on two pillars: a rapid and accurate diagnosis for effective treatment, and the prevention of environmental contamination. Moreover, environmental surveys aid to chart the potential risk areas and pathogen sources. As described, *N. fowleri* occurrence has a worldwide distribution and it has been encountered from lakes, warm water and pools to hospitals and mineral water. The knowledge about population structure and its presence in public environmental allow the implementation of the elimination methods. An accurate and fast diagnosis method is of vital importance for treatment success. After identification of the initial symptoms, a combined investigation including histological analysis, neuroimaging showing necrotic process and immunoassays should be applied. Among these, histopathological studies are widely used and cost effective tools for the diagnosis of PAM. However, one of its drawbacks is the requirement of technical skill in the identification of the amoebae and is time consuming to yield conclusive results. The clinical diagnosis and environmental survey of *N. fowleri* have gained momentum with the popularization of molecular biology techniques, becoming affordable in research and clinical laboratories. A favourable horizon is envisioned as the development of this branch of science is still progressing as new techniques are developed and applied. The main molecular approach resulting in sensitive and precise identifications amplifies the rDNA conserved regions to genotype the species, with a preference for the 18S subunit. Therefore, investigating suspected cases of PAM by both histopathological and molecular approaches becomes a great

strategy to diagnosis.

The fundamental PAM therapy in the last five years have employed amphotericin B combined with miltefosine. However, the survival outputs remain around 5% and the drug arsenal is commonly associated with a variety of side effects. It is undeniable that urgent improvement in the therapeutic arsenal against *N. fowleri* is necessary. Strategies include tests with drugs with known mechanisms of action that possess the ability to cross the blood–brain barrier. This initiative, also known as a "piggy-back" approach, decreases the cost and time required for development of new molecules and marketing approval of the drugs. In this article we presented several cases where these strategies were applied, such as for chlorpromazine, azoles and other classes of drugs, with promising results. Conversely, the search for new molecules is imperative on the long run and can contribute in the development of more effective drugs, with reduced side effects including drug resistance. High-throughput screening initiatives were able to detect new mono and diamidino derivatives with activity against *N. fowleri* and identified a promising drug, corifungin, as a candidate for PAM therapy.

Although not currently available, vaccination can represent an important strategy to cope with the potentially imminent surge in *N. fowleri* infections. Despite having many satisfactory different candidates to vaccination against *N. fowleri*, its practical application remains to be validated. Thereby more research around this topic is needed and if immunization is to be made available, it would surely represent an important contribution to areas where PAM might become a serious public health issue.

Conflict of interest

There is no conflict of interest regarding this paper.

Acknowledgements

This work was supported by the Coordination for the Improvement of Higher Education Personnel (CAPES), the National Council for Scientific and Technological Development (CNPq) grant #134534/2015-8, and São Paulo Research Foundation (FAPESP), grant #2011/24017-4. We also would like to thank the members of the Protein Crystallography and Structural Biology Group (IFSC-USP) for helpful discussions, Dr. Susana A. S. Beozzo for technical assistance and Douglas Cedrim for assistance in the text formatting.

Appendix A. Supplementary data

Supplementary data related to this article can be found at https://doi.org/10.1016/j.exppara.2018.02.010.

References

Abdul Majid, M.A., Mahboob, T., Mong, B.G.J., Jaturas, N., Richard, R.L., Tian-Chye, T., Phimphila, A., Mahaphonh, P., Aye, K.N., Aung, W.L., Chuah, J., Ziegler, A.D., Yasiri, A., Sawangjaroen, N., Lim, Y.A.L., Nissapatorn, V., 2017. Pathogenic waterborne free-living amoebae: an update from selected Southeast Asian countries. PLoS One 12, e0169448. https://doi.org/10.1371/journal.pone.0169448.

Abrahams-Sandí, E., Retana-Moreira, L., Castro-Castillo, A., Reyes-Batlle, M., Lorenzo-Morales, J., 2015. Fatal meningoencephalitis in child and isolation of Naegleria fowleri from Hot Springs in Costa Rica. Emerg. Infect. Dis. 21, 382–384. https://doi.org/10.3201/eid2102.141576.

Al-Herrawy, A.Z., Gad, M.A., 2015. Isolation and molecular identification of Naegleria fowleri from Nile river, Egypt. J. Egypt. Public Health Assoc. 90, 161–165. https://doi.org/10.1097/01.EPX.0000475937.97216.03.

Baig, A.M., Kulsoom, H., Khan, N.A., 2014. Primary amoebic meningoencephalitis: amoebicidal effects of clinically approved drugs against Naegleria fowleri. J. Med. Microbiol. 63, 760–762. https://doi.org/10.1099/jmm.0.072306-0.

Barnett, N.D.P., Kaplan, A.M., Hopkin, R.J., Saubolle, M.a., Rudinsky, M.F., 1996. Primary amoebic meningoencephalitis with Naegleria fowleri: clinical review. Pediatr. Neurol. 15, 230–234. https://doi.org/10.1016/S0887-8994(96)00173-7.

Benterki, M.S., Ayachi, A., Bennoune, O., Régoudis, E., Pélandakis, M., 2016. Meningoencephalitis due to the amoeboflagellate Naegleria fowleri in ruminants in Algeria. Parasite 23, 11. https://doi.org/10.1051/parasite/2016011.

Bonilla-Lemus, P., Caballero Villegas, A.S., Carmona Jiménez, J., Lugo Vázquez, A., 2014. Occurrence of free-living amoebae in streams of the Mexico Basin. Exp. Parasitol. 145, S28–S33. https://doi.org/10.1016/j.exppara.2014.07.001.

Botero, M.C., Puentes-Herrera, M., Cortés, J.A., 2014. Formas lipídicas de anfotericina. Rev. Chil. infectol. 31, 518–527. https://doi.org/10.4067/S0716-10182014000500002.

Capewell, L.G., Harris, A.M., Yoder, J.S., Cope, J.R., Eddy, B.A., Roy, S.L., Visvesvara, G.S., Fox, L.A.M., Beach, M.J., 2015. Diagnosis, clinical course, and treatment of primary amoebic meningoencephalitis in the United States, 1937-2013. J. Pediatric Infect. Dis. Soc. 4, e68–e75. https://doi.org/10.1093/jpids/piu103.

Carrasco-Yepez, M., Rojas-Hernandez, S., Rodriguez-Monroy, M.A., Terrazas, L.I., Moreno-Fierros, L., 2010. Protection against Naegleria fowleri infection in mice immunized with Cry1Ac plus amoebic lysates is dependent on the STAT6 Th2 response. Parasite Immunol. 32, 664–670. https://doi.org/10.1111/j.1365-3024.2010.01222.x.

Carter, R.F., 1970. Description of a Naegleria sp. isolated from two cases of primary amoebic meningo-encephalitis, and of the experimental pathological changes induced by it. J. Pathol. 100, 217–244. https://doi.org/10.1002/path.1711000402.

Carter, R.F., 1969. Sensitivity to amphotericin B of a Naegleria sp. isolated from a case of primary amoebic meningoencephalitis. J. Clin. Pathol. 22, 470–474. https://doi.org/10.1136/jcp.22.4.470.

Centers for Disease Control and Prevention (CDC), 2017. Case Report Data & Graphs [www document]. https://www.cdc.gov/parasites/naegleria/graphs.html. (Accessed 17 July 2017).

Centers for Disease Control and Prevention (CDC), 2013. Investigational drug available directly from CDC for the treatment of infections with free-living amebae. MMWR Morb. Mortal. Wkly. Rep. 62, 666.

Cho, M., Jung, S., Park, S., Kim, K.H., Kim, H.-I., Sohn, S., Kim, H.-J., Im, K., Shin, H., 2003. Immunological characterizations of a cloned 13.1-kilodalton protein from pathogenic Naegleria fowleri. Clin. Diagn. Lab. Immunol. 10, 954–959. https://doi.org/10.1128/CDLI.10.5.954.

Chow, F.C., Glaser, C.A., 2014. Emerging and reemerging neurologic infections. The Neurohospitalist 4, 173–184. https://doi.org/10.1177/1941874414540685.

Conti, R., Parenti, F., 1983. Rifampin therapy for brucellosis, flavobacterium meningitis, and cutaneous leishmaniasis. Rev. Infect. Dis. 5, S600–S605. https://doi.org/10.1093/clinids/5.Supplement_3.S600.

Contis-Montes de Oca, A., Carrasco-Yépez, M., Campos-Rodríguez, R., Pacheco-Yépez, J., Bonilla-Lemus, P., Pérez-López, J., Rojas-Hernández, S., 2016. Neutrophils extracellular traps damage Naegleria fowleri trophozoites opsonized with human IgG. Parasite Immunol. 38, 481–495. https://doi.org/10.1111/pim.12337.

Cope, J.R., Conrad, D.A., Cohen, N., Cotilla, M., DaSilva, A., Jackson, J., Visvesvara, G.S., 2016. Use of the novel therapeutic agent miltefosine for the treatment of primary amebic meningoencephalitis: report of one fatal and one surviving case. Clin. Infect. Dis. 62, 774–776. https://doi.org/10.1093/cid/civ1021.

Cope, J.R., Ratard, R.C., Hill, V.R., Sokol, T., Causey, J.J., Yoder, J.S., Mirani, G., Mull, B., Mukerjee, K.A., Narayanan, J., Doucet, M., Qvarnstrom, Y., Poole, C.N., Akingbola, O.A., Ritter, J.M., Xiong, Z., Da Silva, A.J., Roellig, D., Van Dyke, R.B., Stern, H., Xiao, L., Beach, M.J., 2015. The first association of a primary amebic meningoencephalitis death with culturable naegleria fowleri in tap water from a US treated public drinking water system. Clin. Infect. Dis. 60, e36–e42. https://doi.org/10.1093/cid/civ017.

Coupat-Goutaland, B., Régoudis, E., Besseyrias, M., Mularoni, A., Binet, M., Herbelin, P., Pélandakis, M., 2016. Population structure in Naegleria fowleri as revealed by microsatellite markers. PLoS One 11, 1–14. https://doi.org/10.1371/journal.pone.0152434.

De Jonckheere, J.F., 2012. The impact of man on the occurrence of the pathogenic free-living amoeboflagellate. Future Microbiol. 7, 5–7. https://doi.org/10.2217/fmb.11.141.

De Jonckheere, J.F., 2011. Origin and evolution of the worldwide distributed pathogenic amoeboflagellate Naegleria fowleri. Infect. Genet. Evol. 11, 1520–1528. https://doi.org/10.1016/j.meegid.2011.07.023.

De Jonckheere, J.F., 2002. A century of research on the amoeboflagellate genus Naegleria. Acta Protozool. 41, 309–342.

De Macedo-Silva, S.T., Urbina, J.A., De Souza, W., Rodrigues, J.C.F., 2013. In vitro activity of the antifungal azoles itraconazole and posaconazole against Leishmania amazonensis. PLoS One 8. https://doi.org/10.1371/journal.pone.0083247.

Debnath, A., Tunac, J.B., Galindo-Gómez, S., Silva-Olivares, A., Shibayama, M., McKerrow, J.H., 2012. Corifungin, a new drug lead against Naegleria, identified from a high-throughput screen. Antimicrob. Agents Chemother. 56, 5450–5457. https://doi.org/10.1128/AAC.00643-12.

Debnath, A., Tunac, J.B., Silva-Olivares, A., Galindo-Gomez, S., Shibayama, M., McKerrow, J.H., 2014. In vitro efficacy of corifungin against Acanthamoeba castellanii trophozoites and cysts. Antimicrob. Agents Chemother. 58, 1523–1528. https://doi.org/10.1128/AAC.02254-13.

Diaz, I.L., Parra, C., Linarez, M., Perez, L.D., 2015. Design of micelle nanocontainers based on PDMAEMA-b-PCL-b-PDMAEMA triblock copolymers for the encapsulation of amphotericin B. AAPS PharmSciTech 16, 1069–1078. https://doi.org/10.1208/s12249-015-0298-9.

Dobrowsky, P.H., Khan, S., Cloete, T.E., Khan, W., 2016. Molecular detection of Acanthamoeba spp., Naegleria fowleri and Vermamoeba (Hartmannella)

vermiformis as vectors for Legionella spp. in untreated and solar pasteurized harvested rainwater. Parasites Vectors 9. https://doi.org/10.1186/s13071-016-1829-2, 539.
Dunn, A.L., Reed, T., Stewart, C., Levy, R.A., 2016. Naegleria fowleri that induces primary amoebic meningoencephalitis: rapid diagnosis and rare case of survival in a 12-year-old Caucasian girl. Lab. Med. 47, 149–154. https://doi.org/10.1093/labmed/lmw008.
Falci, D.R., Da Rosa, F.B., Pasqualotto, A.C., 2015. Comparison of nephrotoxicity associated to different lipid formulations of amphotericin B: a real-life study. Mycoses 58, 104–112. https://doi.org/10.1111/myc.12283.
Farra, A., Bekondi, C., Tricou, V., Mbecko, J.R., Talarmin, A., Access, O., 2017. Free-living amoebae isolated in the Central African Republic: epidemiological and molecular aspects. Pan Afr. Med. J. 26, 1–10. https://doi.org/10.11604/pamj.2017.26.57.9021.
Fritz-Laylin, L.K., Cande, W.Z., 2010. Ancestral centriole and flagella proteins identified by analysis of *Naegleria* differentiation. J. Cell Sci. 123, 4024–4031. https://doi.org/10.1242/jcs.077453.
Ghannoum, M.A., Rice, L.B., 1999. Antifungal agents: mode of action, mechanisms of resistance, and correlation of these mechanisms with bacterial resistance. Clin. Microbiol. Rev. 12, 501–517 doi:10.1.1.322-6182.
Grace, E., Asbill, S., Virga, K., 2015. Naegleria fowleri: pathogenesis, diagnosis, and treatment options. Antimicrob. Agents Chemother. 59, 6677–6681. https://doi.org/10.1128/AAC.01293-15.
Gyori, E., 2003. December 2002: 19-year old male with febrile illness after jet ski accident. Brain Pathol. 13, 237–239.
Heggie, T.W., 2010. Swimming with death: Naegleria fowleri infections in recreational waters. Trav. Med. Infect. Dis. 8, 201–206. https://doi.org/10.1016/j.tmaid.2010.06.001.
Heggie, T.W., Küpper, T., 2017. Surviving Naegleria fowleri infections: a successful case report and novel therapeutic approach. Trav. Med. Infect. Dis. 16, 49–51. https://doi.org/10.1016/j.tmaid.2016.12.005.
Herwaldt, B.L., 2001. Laboratory-acquired parasitic infections from accidental exposures laboratory-acquired parasitic infections from accidental exposures. Clin. Microbiol. Rev. 14, 659–688. https://doi.org/10.1128/CMR.14.3.659.
Infante, V.V., Miranda-Olvera, A.D., De Leon-Rodriguez, L.M., Anaya-Velazquez, F., Rodriguez, M.C., Avila, E.E., 2011. Effect of the antimicrobial peptide tritrpticin on the in vitro viability and growth of trichomonas vaginalis. Curr. Microbiol. 62, 301–306. https://doi.org/10.1007/s00284-010-9709-z.
Jarillo-Luna, A., Moreno-Fierros, L., Campos-Rodríguez, R., Rodríguez-Monroy, M.A., Lara-Padilla, E., Rojas-Hernández, S., 2008. Intranasal immunization with Naegleria fowleri lysates and Cry1Ac induces metaplasia in the olfactory epithelium and increases IgA secretion. Parasite Immunol. 30, 31–38. https://doi.org/10.1111/j.1365-3024.2007.00999.x.
John, D.T., Weik, R.R., Adams, A.C., 1977. Immunization of mice against Naegleria fowleri infection. Infect. Immun. 16, 817–820.
Johnson, R.O., Cope, J.R., Moskowitz, M., Kahler, A., Hill, V., Behrendt, K., Molina, L., Fullerton, K.E., Beach, M.J., 2016. Notes from the field: primary amebic meningoencephalitis associated with exposure to swimming pool water supplied by an overland pipe - Inyo county, California, 2015. MMWR Morb. Mortal. Wkly. Rep. 65, 424. https://doi.org/10.15585/mmwr.mm6516a4.
Kang, H., Seong, G.S., Sohn, H.J., Kim, J.H., Lee, S.E., Park, M.Y., Lee, W.J., Shin, H.J., 2015. Effective PCR-based detection of Naegleria fowleri from cultured sample and PAM-developed mouse. Eur. J. Protistol. 51, 401–408. https://doi.org/10.1016/j.ejop.2015.07.003.
Kao, P., Tung, M., Hsu, B., Chou, M.-Y., Yang, H.-W., She, C.-Y., Shen, S.-M., 2013. Quantitative detection and identification of Naegleria spp. in various environmental water samples using real-time quantitative PCR assay. Parasitol. Res. 112, 1467–1474. https://doi.org/10.1007/s00436-013-3290-x.
Kao, P.M., Hsu, B.M., Hsu, T.K., Chiu, Y.C., Chang, C.L., Ji, W.T., Huang, S.W., Fan, C.W., 2014. Application of TaqMan qPCR for the detection and monitoring of Naegleria species in reservoirs used as a source for drinking water. Parasitol. Res. 113, 3765–3771. https://doi.org/10.1007/s00436-014-4042-2.
Kappagoda, S., Singh, U., Blackburn, B.G., 2011. Antiparasitic therapy. Mayo Clin. Proc. 86, 561–583. https://doi.org/10.4065/mcp.2011.0203.
Khan, N.A., Baqir, H., Siddiqui, R., 2015. The immortal amoeba: a useful model to study cellular differentiation processes? Pathog. Glob. Health 109, 305–306. https://doi.org/10.1080/20477724.2015.1103504.
Khwon, W.J., Park, J.S., 2017. Morphology and phylogenetic analyses of three novel Naegleria isolated from freshwaters on Jeju Island, Korea, during the winter period. J. Eukaryot. Microbiol. 0–1. https://doi.org/10.1111/jeu.12434.
Kim, J.-H., Jung, S.Y., Lee, Y.J., Song, K.J., Kwon, D., Kim, K., Park, S., Im, K.I., Shin, H.J., 2008a. Effect of therapeutic chemical agents in vitro and on experimental meningoencephalitis due to Naegleria fowleri. Antimicrob. Agents Chemother. 52, 4010–4016. https://doi.org/10.1128/AAC.00197-08.
Kim, J.-H., Lee, Y.-J., Sohn, H.-J., Song, K.-J., Kwon, D., Kwon, M.-H., Im, K.-I., Shin, H.-J., 2008b. Therapeutic effect of rokitamycin in vitro and on experimental meningoencephalitis due to Naegleria fowleri. Int. J. Antimicrob. Agents 32, 411–417. https://doi.org/10.1016/j.ijantimicag.2008.05.018.
Kim, J.H., Sohn, H.J., Lee, J., Yang, H.J., Chwae, Y.J., Kim, K., Park, S., Shin, H.J., 2013. Vaccination with lentiviral vector expressing the nfa1 gene confers a protective immune response to mice infected with Naegleria fowleri. Clin. Vaccine Immunol. 20, 1055–1060. https://doi.org/10.1128/CVI.00210-13.
Latifi, A.R., Niyyati, M., Lorenzo-Morales, J., Haghighi, A., Javad, S., Tabaei, S.J.S., Lasjerdi, Z., Azargashb, E., 2017. Occurrence of Naegleria species in therapeutic geothermal water sources, Northern Iran. Acta Parasitol. 62, 104–109. https://doi.org/10.1515/ap-2017-0012.
Leduc, A., Gravel, S., Abikhzer, J., Roy, S., Barbeau, J., 2012. Polymerase chain reaction detection of potentially pathogenic free-living amoebae in dental units. Can. J. Microbiol. 58, 884–886. https://doi.org/10.1139/w2012-071.
Lee, J., Yoo, J.-K., Sohn, H.-J., Kang, H., Kim, D., Shin, H.-J., Kim, J.-H., 2015. Protective immunity against Naegleria fowleri infection on mice immunized with the rNfa1 protein using mucosal adjuvants. Parasitol. Res. 114, 1377–1385. https://doi.org/10.1007/s00436-015-4316-3.
Lee, Y.J., Kim, J.H., Sohn, H.J., Lee, J., Jung, S.Y., Chwae, Y.J., Kim, K., Park, S., Shin, H.J., 2011. Effects of immunization with the rNfa1 protein on experimental Naegleria fowleri-PAM mice. Parasite Immunol. 33, 382–389. https://doi.org/10.1111/j.1365-3024.2011.01296.x.
Liang, S.Y., Ji, D.R., Hsia, K.T., Hung, C.C., Sheng, W.H., Hsu, B.M., Chen, J.S., Wu, M.H., Lai, C.H., Ji, D.D., 2010. Isolation and identification of Acanthamoeba species related to amoebic encephalitis and nonpathogenic free-living amoeba species from the rice field. J. Appl. Microbiol. 109, 1422–1429. https://doi.org/10.1111/j.1365-2672.2010.04779.x.
Linam, W.M., Ahmed, M., Cope, J.R., Chu, C., Visvesvara, G.S., da Silva, A.J., Qvarnstrom, Y., Green, J., 2015. Successful treatment of an adolescent with Naegleria fowleri primary amebic meningoencephalitis. Pediatrics 135, e744–e748. https://doi.org/10.1542/peds.2014-2292.
Marciano-Cabral, F., 1988. Biology of Naegleria spp. Microbiol. Rev. 52, 114–133.
Martinez, A.J., Visvesvara, G.S., 1997. Free-living, amphizoic and opportunistic amebas. Brain Pathol. 7, 583–598. https://doi.org/10.1111/j.1750-3639.1997.tb01076.x.
Miller, H.C., Morgan, M.J., Wylie, J.T., Kaksonen, A.H., Sutton, D., Braun, K., Puzon, G.J., 2017. Elimination of Naegleria fowleri from bulk water and biofilm in an operational drinking water distribution system. Water Res. 110, 15–26. https://doi.org/10.1016/j.watres.2016.11.061.
Morgan, M.J., Halstrom, S., Wylie, J.T., Walsh, T., Kaksonen, A.H., Sutton, D., Braun, K., Puzon, G.J., 2016. Characterization of a drinking water distribution pipeline terminally colonized by Naegleria fowleri. Environ. Sci. Technol. 50, 2890–2898. https://doi.org/10.1021/acs.est.5b05657.
Mull, B.J., Narayanan, J., Hill, V.R., 2013. Improved method for the detection and quantification of Naegleria fowleri in water and sediment using immunomagnetic separation and real-time PCR. J. Parasitol. Res. 2013, 1–8. https://doi.org/10.1155/2013/608367.
Okuda, D.T., Hanna, H.J., Coons, S.W., Bodensteiner, J.B., 2004. Naegleria fowleri hemorrhagic meningoencephalitis: report of two fatalities in children. J. Child Neurol. 19, 231–233.
Parfrey, L.W., Barbero, E., Lasser, E., Dunthorn, M., Bhattacharya, D., Patterson, D.J., Katz, L.A., 2006. Evaluating support for the current classification of eukaryotic diversity. PLoS Genet. 2, 2062–2073. https://doi.org/10.1371/journal.pgen.0020220.
Pélandakis, M., Pernin, P., 2002. Use of multiplex PCR and PCR restriction enzyme analysis for detection and exploration of the variability in the free-living amoeba Naegleria in the environment. Appl. Environ. Microbiol. 68, 2061–2065. https://doi.org/10.1128/AEM.68.4.2061-2065.2002.
Pugh, J.J., Levy, R.A., 2016. Naegleria fowleri : diagnosis, pathophysiology of brain inflammation, and antimicrobial treatments. ACS Chem. Neurosci. 7, 1178–1179. https://doi.org/10.1021/acschemneuro.6b00232.
Puzon, G.J., Wylie, J.T., Walsh, T., Braun, K., Morgan, M.J., 2017. Comparison of biofilm ecology supporting growth of individual Naegleria species in a drinking water distribution system. FEMS Microbiol. Ecol. 93, 1–8. https://doi.org/10.1093/femsec/fix017.
Raether, W., Seidenath, H., 1984. Ketoconazole and other potent antimycotic azoles exhibit pronounced activity against Trypanosoma cruzi, Plasmodium berghei and Entamoeba histolytica in vivo. Zeitschrift für Parasitenkd. 70, 135–138. https://doi.org/10.1007/BF00929583. Parasitol. Res.
Régoudis, E., Pélandakis, M., 2016. Detection of the free living amoeba Naegleria fowleri by using conventional and real-time PCR based on a single copy DNA sequence. Exp. Parasitol. 161, 35–39. https://doi.org/10.1016/j.exppara.2015.12.007.
Reyes-Batlle, M., Wagner, C., López-Arencibia, A., Sifaoui, I., Martínez-Carretero, E., Valladares, B., Piñero, J.E., Lorenzo-Morales, J., 2017. Isolation and molecular characterization of a Naegleria strain from a recreational water fountain in Tenerife, Canary Islands, Spain. Acta Parasitol. 62, 265–268. https://doi.org/10.1515/ap-2017-0033.
Rice, C.a., Colon, B.L., Alp, M., Göker, H., Boykin, D.W., Kyle, D.E., 2015. Bis-benzimidazole hits against Naegleria fowleri discovered with New high-throughput screens. Antimicrob. Agents Chemother. 59, 2037–2044. https://doi.org/10.1128/AAC.05122-14.
Rodríguez-Ezpeleta, N., Brinkmann, H., Burger, G., Roger, A.J., Gray, M.W., Philippe, H., Lang, B.F., 2007. Toward resolving the eukaryotic tree: the phylogenetic positions of jakobids and cercozoans. Curr. Biol. 17, 1420–1425. https://doi.org/10.1016/j.cub.2007.07.036.
Rojas-Hernández, S., Jarillo-Luna, A., Rodríguez-Monroy, M., Moreno-Fierros, L., Campos-Rodríguez, R., 2004. Immunohistochemical characterization of the initial stages of Naegleria fowleri meningoencephalitis in mice. Parasitol. Res. 94, 31–36. https://doi.org/10.1007/s00436-004-1177-6.
Rojas-Hernández, S., Rodríguez-Monroy, M.A., López-Revilla, R., Reséndiz-Albor, A.A., Moreno-Fierros, L., 2004. Intranasal coadministration of the Cry1Ac protoxin with amoebal lysates increases protection against Naegleria fowleri meningoencephalitis. Infect. Immun. 72, 4368–4375. https://doi.org/10.1128/IAI.72.8.4368-4375.2004.

Roy, S.L., Metzger, R., Chen, J.G., Laham, F.R., Martin, M., Kipper, S.W., Smith, L.E., Lyon, G.M., Haffner, J., Ross, J.E., Rye, A.K., Johnson, W., Bodager, D., Friedman, M., Walsh, D.J., Collins, C., Inman, B., Davis, B.J., Robinson, T., Paddock, C., Zaki, S.R., Kuehnert, M., Dasilva, A., Qvarnstrom, Y., Sriram, R., Visvesvara, G.S., 2014. Risk for transmission of naegleria fowleri from solid organ transplantation. Am. J. Transplant. 14, 163–171. https://doi.org/10.1111/ajt.12536.

Sau, K., Mambula, S.S., Latz, E., Henneke, P., Golenbock, D.T., Levitz, S.M., 2003. The antifungal drug amphotericin B promotes inflammatory cytokine release by a Toll-like receptor- and CD14-dependent mechanism. J. Biol. Chem. 278, 37561–37568. https://doi.org/10.1074/jbc.M306137200.

Scheikl, U., Sommer, R., Kirschner, A., Rameder, A., Schrammel, B., Zweimüller, I., Wesner, W., Hinker, M., Walochnik, J., 2014. Free-living amoebae (FLA) co-occurring with legionellae in industrial waters. Eur. J. Protistol. 50, 422–429. https://doi.org/10.1016/j.ejop.2014.04.002.

Schuster, F.L., Guglielmo, B.J., Visvesvara, G.S., 2006. In-vitro activity of miltefosine and voriconazole on clinical isolates of free-living amebas: Balamuthia mandrillaris, Acanthamoeba spp., and Naegleria fowleri. J. Eukaryot. Microbiol. 53, 121–126. https://doi.org/10.1111/j.1550-7408.2005.00082.x.

Schuster, F.L., Visvesvara, G.S., 2004. Opportunistic amoebae: challenges in prophylaxis and treatment. Drug Resist. Updates 7, 41–51. https://doi.org/10.1016/j.drup.2004.01.002.

Shariq, A., Afridi, F.I., Farooqi, B.J., Ahmed, S., Hussain, A., 2014. Fatal primary meningoencephalitis caused by Naegleria fowleri. J. Coll. Physicians Surg. Pakistan 24, 523–525, 07.2014/JCPSP.523525.

Siddiqui, R., Khan, N.A., 2014. Primary amoebic meningoencephalitis caused by naegleria fowleri: an old enemy presenting new challenges. PLoS Neglected Trop. Dis. 8, e3017 https://doi.org/10.1371/journal.pntd.0003017.

Sood, A., Chauhan, S., Chandel, L., Jaryal, S.C., 2014. Prompt diagnosis and extraordinary survival from Naegleria fowleri meningitis: a rare case report. Indian J. Med. Microbiol. 32, 193–196. https://doi.org/10.4103/0255-0857.129834.

Stowe, R.C., Pehlivan, D., Friederich, K.E., Lopez, M.A., DiCarlo, S.M., Boerwinkle, V.L., 2017. Primary amebic meningoencephalitis in children: a report of two fatal cases and review of the literature. Pediatr. Neurol. 70, 75–79. https://doi.org/10.1016/j.pediatrneurol.2017.02.004.

Streby, A., Mull, B.J., Levy, K., Hill, V.R., 2015. Comparison of real-time PCR methods for the detection of Naegleria fowleri in surface water and sediment. Parasitol. Res. 114, 1739–1746. https://doi.org/10.1007/s00436-015-4359-5.

Stubhaug, T.T., Reiakvam, O.M., Stensvold, C.R., Hermansen, N.O., Holberg-Petersen, M., Antal, E., Gaustad, K., Førde, I.S., Heger, B., 2016. Fatal primary amoebic meningoencephalitis in a Norwegian tourist returning from Thailand. JMM Case Rep. 3, 1–5. https://doi.org/10.1099/jmmcr.0.005042.

Su, M.Y., Lee, M.S., Shyu, L.Y., Lin, W.C., Hsiao, P.C., Wang, C.P., Ji, D., Der, Chen, K.M., Lai, S.C., 2013. A fatal case of Naegleria fowleri meningoencephalitis in Taiwan. Kor. J. Parasitol. 51, 203–206. https://doi.org/10.3347/kjp.2013.51.2.203.

Sundar, S., Chakravarty, J., Agarwal, D., Rai, M., Murray, H.W., 2010. Single-dose liposomal amphotericin B for visceral leishmaniasis in India. N. Engl. J. Med. 362, 504–512. https://doi.org/10.1056/NEJMoa0903627.

Tavares, M., Da Costa, J.M.C., Carpenter, S.S., Santos, L.A., Afonso, C., Aguiar, Á., Pereira, J., Cardoso, A.I., Schuster, F.L., Yagi, S., Sriram, R., Visvesvara, G.S., 2006. Diagnosis of first case of Balamuthia amoebic encephalitis in Portugal by immunofluorescence and PCR. J. Clin. Microbiol. 44, 2660–2663. https://doi.org/10.1128/JCM.00479-06.

Teide, M., Islands, C., Reyes-batlle, M., Niyyati, M., Martín-navarro, C.M., López-arencibia, A., 2015. Unusual Vermamoeba Vermiformis Strain Isolated from Snow in upon Observation of the Snow Samples Cultured in 189–192.

Thong, Y.H., Carter, R.F., Ferrante, A., Rowan-Kelly, B., 1983. Site of expression of immunity to Naegleria fowleri in immunized mice. Parasite Immunol. 5, 67–76. https://doi.org/10.1111/j.1365-3024.1983.tb00724.x.

Tiewcharoen, S., Phurttikul, W., Rabablert, J., Auewarakul, P., Roytrakul, S., Chetanachan, P., Atithep, T., Junnu, V., 2014. Effect of synthetic antimicrobial peptides on Naegleria fowleri trophozoites. Southeast Asian J. Trop. Med. Publ. Health 45, 537–546.

Trabelsi, H., Dendana, F., Sellami, a, Sellami, H., Cheikhrouhou, F., Neji, S., Makni, F., Ayadi, a, 2012. Pathogenic free-living amoebae: epidemiology and clinical review. Pathol. Biol. 60, 399–405. https://doi.org/10.1016/j.patbio.2012.03.002.

Tung, M.C., Hsu, B.M., Tao, C.W., Lin, W.C., Tsai, H.F., Ji, D., Der, Shen, S.M., Chen, J.S., Shih, F.C., Huang, Y.L., 2013. Identification and significance of Naegleria fowleri isolated from the hot spring which related to the first primary amebic meningoencephalitis (PAM) patient in Taiwan. Int. J. Parasitol. 43, 691–696. https://doi.org/10.1016/j.ijpara.2013.01.012.

Vargas-Zepeda, J., Gómez-Alcalá, A.V., Vázquez-Morales, J.A., Licea-Amaya, L., De Jonckheere, J.F., Lares-Villa, F., 2005. Successful treatment of Naegleria fowleri meningoencephalitis by using intravenous amphotericin B, fluconazole and rifampicin. Arch. Med. Res. 36, 83–86. https://doi.org/10.1016/j.arcmed.2004.11.003.

Visvesvara, G.S., 2010. Free-living amebae as opportunistic agents of human disease. J. Neuroparasitol. 1, 1–13. https://doi.org/10.4303/jnp/N100802.

Wehrli, W., 1983. Rifampin: mechanisms of action and resistance. Rev. Infect. Dis. 5 (Suppl. 3), S407–S411.

Werbovetz, K., 2006. Diamidines as antitrypanosomal, antileishmanial and antimalarial agents. Curr. Opin. Invest. Drugs 7, 147–157.

Yoder, J.S., Eddy, B. a, Visvesvara, G.S., Capewell, L., Beach, M.J., 2010. The epidemiology of primary amoebic meningoencephalitis in the USA, 1962-2008. Epidemiol. Infect. 138, 968–975. https://doi.org/10.1017/S0950268809991014.

Yoder, J.S., Straif-Bourgeois, S., Roy, S.L., Moore, T.A., Visvesvara, G.S., Ratard, R.C., Hill, V.R., Wilson, J.D., Linscott, A.J., Crager, R., Kozak, N.A., Sriram, R., Narayanan, J., Mull, B., Kahler, A.M., Schneeberger, C., Da Silva, A.J., Poudel, M., Baumgarten, K.L., Xiao, L., Beach, M.J., 2012. Primary amebic meningoencephalitis deaths associated with sinus irrigation using contaminated tap water. Clin. Infect. Dis. 55, 79–85. https://doi.org/10.1093/cid/cis626.

Yu, Z., Miller, H.C., Puzon, G.J., Clowers, B.H., 2017. Development of untargeted metabolomics methods for the rapid detection of pathogenic Naegleria fowleri. Environ. Sci. Technol. 51, 4210–4219. https://doi.org/10.1021/acs.est.6b05969.

Zahid, M.F., Saad Shaukat, M.H., Ahmed, B., Beg, M.A., Kadir, M.M., Mahmood, S.F., 2016. Comparison of the clinical presentations of Naegleria fowleri primary amoebic meningoencephalitis with pneumococcal meningitis: a case–control study. Infection 44, 505–511. https://doi.org/10.1007/s15010-016-0878-y.

APPENDIX II (a)

pathogens

MDPI

Article

Isolation of *Naegleria* spp. from a Brazilian Water Source

Natália Karla Bellini [1,2], Ana Letícia Moreira da Fonseca [1], María Reyes-Batlle [2], Jacob Lorenzo-Morales [2], Odete Rocha [3] and Otavio Henrique Thiemann [1,4,*]

[1] Instituto de Física de São Carlos, Universidade de São Paulo, Caixa Postal 369, São Carlos 13560-590, SP, Brazil; nataliabellini@ifsc.usp.br (N.K.B.); mfanaleticia@gmail.com (A.L.M.d.F.)
[2] Instituto Universitario de Enfermedades Tropicales y Salud Pública de Canarias, Universidad de La Laguna, Avda. Astrofísico Fco. Sánchez, S/N, 38203 La Laguna, Tenerife, Canary Islands, Spain; mreyesbatlle@gmail.com (M.R.-B.); jmlorenz@ull.edu.es (J.L.-M.)
[3] Departamento de Ecologia e Biologia Evolutiva, Universidade Federal de São Carlos, Rodovia Washington Luis, km 235, CEP, São Carlos 13565-905, SP, Brazil ; doro@ufscar.br
[4] Departamento de Genética e Evolução, Universidade Federal de São Carlos, São Carlos 13560-590, Brazil
* Correspondence: thiemann@ifsc.usp.br; Tel.: +55-16-3373-8089

Received: 2 December 2019; Accepted: 28 January 2020; Published: 31 January 2020

Abstract: The genus *Naegleria*, of the free-living amoeba (FLA) group, has been investigated mainly due to its human health impact, resulting in deadly infections and their worldwide distribution on freshwater systems. *Naegleria fowleri*, colloquially known as the "brain-eating amoeba," is the most studied *Naegleria* species because it causes primary amoebic meningoencephalitis (PAM) of high lethality. The assessment of FLA biodiversity is fundamental to evaluate the presence of pathogenic species and the possibility of human contamination. However, the knowledge of FLA distribution in Brazil is unknown, and to rectify this situation, we present research on identifying *Naegleria* spp. in the Monjolinho River as a model study. The river is a public Brazilian freshwater source that crosses the city of São Carlos, in São Paulo state, Brazil. Five distinct sampling sites were examined through limnological features, trophozoites culturing, and PCR against internal transcribed spacer (ITS) regions and 5.8S rRNA sequences. The results identified *N. philippinensis, N. canariensisi, N. australiensis, N. gruberi, N. dobsoni* sequences, as well as a *Hartmannella* sequence. The methodology delineated here represents the first Brazilian *Naegleria* spp. study on a freshwater system. Our results stress the urgency of a large scale evaluation of the presence of free-living amoebas in Brazil.

Keywords: *Naegleria* spp.; free-living amoeba; PCR; Monjolinho River; Brazil

1. Introduction

Naegleria is a genus that comprises single-celled, heterotrophic protists that are widely distributed in natural environments [1–3]. The 47 species identified up to now exist as free-living amoebas (FLAs) with a bacteria-based feeding habit and binary fission division [4]. In unfavorable environmental conditions, they transform from trophozoites to the cyst stage as a resting form [5]. Additionally, a third stage, commonly biflagellate, can be formed to seek a better surrounding [6]. The known exceptions are *Naegleria indonesiensis, N. chilensis, N. paradobsoni* and *N. neochilensis* for which a flagellate form has never been identified [4].

Naegleria is described as an amphizoic genus, as four species are able to thrive not only as free living organisms but also as parasites: *Naegleria fowleri, Naegleria australiensis, Naegleria philippinensis* and *Naegleria italica* [7–9]. Since *N. fowleri* withstands higher temperatures, as found in geothermal sources and heated recreational aquatic systems, the species has been classified as thermophilic [3,10] with the ability to grow in temperatures ranging from 30 to 46 °C [11,12]. Other species, like *N.*

australiensis, *N. italica*, *N. lovaniensis* and *N. philippinensis*, have been recognized as thermo tolerant as well [4,13].

Naegleria is phylogenetically grouped with another amphizoic genus, *Vahlkampfia*, within the Vahlkampfiidae family, the clade Discoba, and the super group Excavata [5,14–16]. In addition, the *Acanthamoeba, Balamuthia, Sappinia* and *Vermamoeba* genera are pathogenic FLA groups whose main threats to humans are granulomatous amoebic encephalitis (GAE) and amoebic keratitis (AK) [17–19]. GAE is caused by *Acanthamoeba* spp., *Balamuthia mandrillaris and Sappinia pedata,* with several cases in immunocompromised persons, whereas AK is caused mainly by *Acanthamoeba* spp. with prevalence in contact lens wearers [19–21]. More recently, *Vermamoeba vermiforms,* a common free-living amoebae, was identified in one corneal scraping from an AK case [22].

Primary amoebic meningoencephalitis (PAM) is a fatal infection caused by *Naegleria fowleri,* whose trophozoite can reach the central nervous system (CNS) through the olfactory neuroepithelial pathway [23]. In 95% of the reported cases, death results from seven to fourteen days after the appearance of symptoms [18,24–27]. This alarmingly low survival rate has been correlated with the difficulty in diagnosis and the low efficacy of the available therapy, commonly based on antifungal and antibacterial drugs [28,29]. Additionally *N. australiensis, N. philippinensis* and *N. italica* are potentially pathogenic species because they have presented infectivity in mice models [7–9]. Considering that the amoeba infects the host by direct contact and that most PAM patients have a history of water contact (e.g., bathing in freshwater) [23] prior the outcome of encephalitis, the investigation on the environmental distribution of these species is of great public health importance to prevent new cases and is critical to deepen the knowledge on *Naegleria* diversity.

South American countries have faced a scarcity of information on *Naegleria* distribution throughout the world [25]. In Brazil, the first occurrence of *N. fowleri* was reported in an artificial lake from the city of Rio de Janeiro [30]. Later, the presence of *Naegleria* genus was linked to dust and biofilm from hospitals in the cities of Presidente Prudente [31] and Porto Alegre [32]. The cyst capability of resisting to desiccation enables PAM infections via the dry infection route [33]. In 2009, *N. fowleri* was correlated to dust in two campuses of a university in the city of Santos [34]. Regarding Brazilian PAM cases, a 1985 report diagnosed the infection through an immunological analysis of the cerebral tissue of a deceased patient [30], and two reports identified *N. fowleri* infection in cattle, based on histological and immunohistochemical analysis [35,36]. These reports lacked molecular techniques to confirm the findings as a complementary strategy to combine with the morphological and physiological characterization of the isolated organism. Currently, the ribosomal RNA gene, particularly the region of the internal transcribed spacers (ITS1 and ITS2), and the 5.8S ribosomal gene have been used in the newest studies of *Naegleria* [37–41].

Accentuating the lack of reports, Brazil is one of the most promising countries for *Naegleria* dispersion because it harbors about twenty percent of the global freshwater [42], the most prevalent habitat in which *Naegleria* has been found. Taking into account this fact when considering the biodiversity of *Naegleria* species, pathogenic or non pathogenic, in Brazilian freshwater courses, we undertook this initiative by investigating a river in the city of São Carlos, São Paulo state, as a model system. The Monjolinho River belongs to a basin that covers São Carlos city and neighboring districts in the state of São Paulo, and it reaches a watershed dimension of 275 km^2. The area belonging to São Carlos city is under intense anthropogenic activity and is highly impacted with domestic and industrial sewage, in addition to agricultural runoff [43,44]. Therefore, the present research examined five distinct sampling sites in which *Naegleria* spp. were isolated and characterized by the PCR amplification and DNA sequencing of the ITS1, 5.8S, and ITS2 regions of the total DNA from each site. This characterization, when combined with the morphological investigation after culturing and the limnological characterization of the water, allowed us to identify the presence of five *Naegleria* spp . in a Brazilian freshwater course.

2. Results

2.1. Limnologic Characterization

The DO (dissolved oxygen), conductivity, pH and temperature measurements that were acquired in situ along the Monjolinho River are summarized in Figure 1.

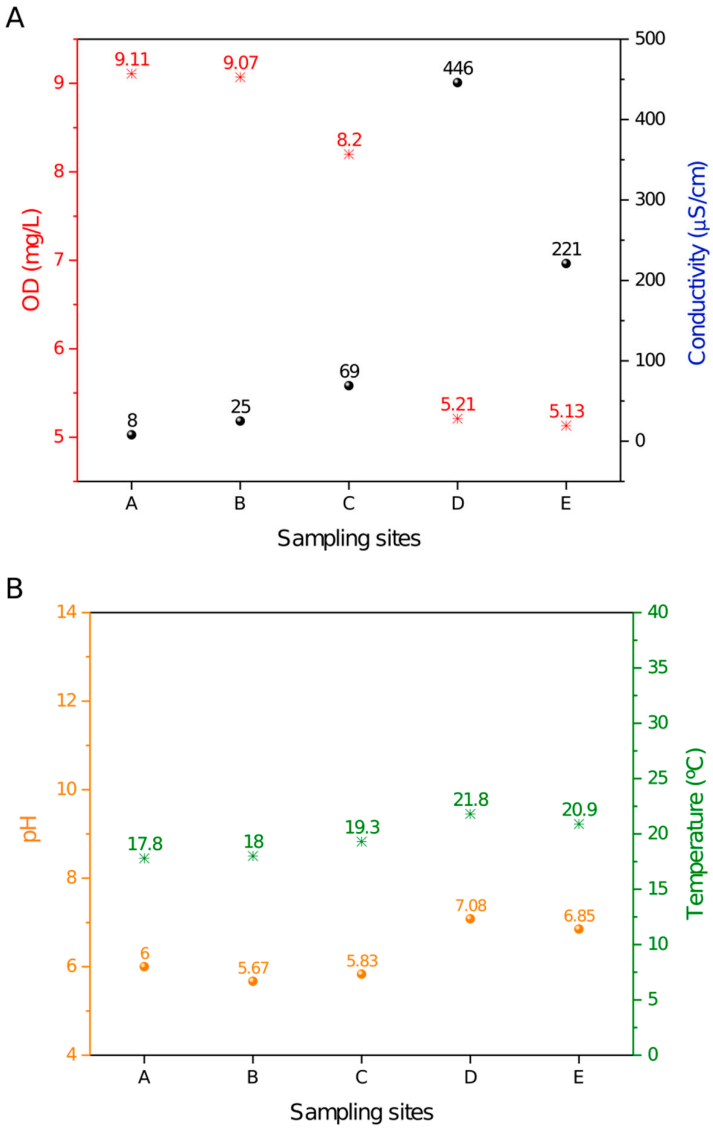

Figure 1. Limnological profile throughout the sampling sites in the Monjolinho River. (A) DO (dissolved oxygen) and conductivity values plotted along the river samples. (B) Temperature and pH values plotted along the river samples.

Samples A–E along the river displayed a decrease in the dissolved oxygen that was concomitant with the increase in the conductivity values. The D position was striking, as it showed an abrupt accentuation in both data (Figure 1A). This result correlated well with site D being located at a domestic sewage discharge area where organic compounds are dissolved in the water, leading to a high ionic concentration that is consistent with a decrease in DO. The temperature and pH values were relatively constant from sites A to E (Figure 1B) and apparently were not influenced by the domestic sewage discharge. A small increase in temperature was observed, most likely due to daily variations in ambient temperature. As shown in Figure 1B, the recorded pH values ranged from 5.67

to 7.08, and temperatures ranged from 17.8 to 21.8 °C. Thus, pH and temperature exhibited a smaller variation among sites as compared to the DO and conductivity values along the five sampling sites.

2.2. Light Microscopy

The daily microscopic examination of non-nutrient agar (NNA) plates allowed for the identification of amoeba growth in 100% of the sampling sites that were covered in this study. According the amoeba cell morphologic profile defined by Page'S Key [45], two life cycle stages, trophozoite and cyst, were observed (Figure 2).

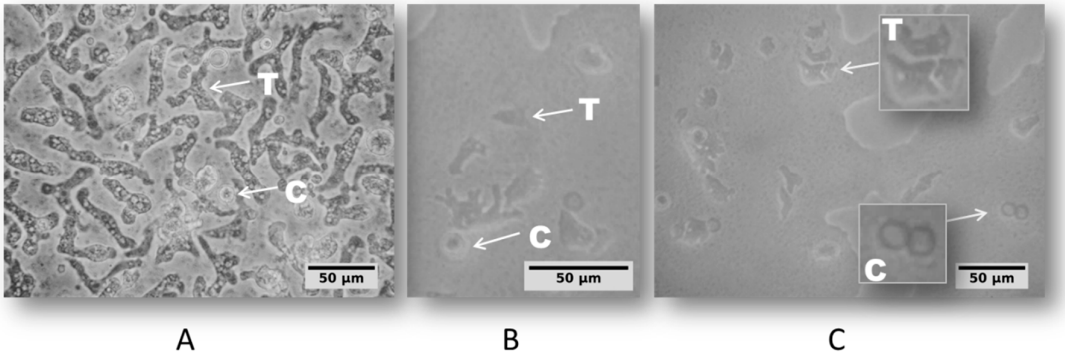

Figure 2. Light microscopy images of amoeba cells on non-nutrient agar (NNA) plates from sampling site D that were cultivated at 26 °C (A), 37 °C (B), and 44 °C (C). Arrows indicate trophozoite (T) and cyst (C) cells that were observed with an inverted microscope (Nikon TS 100) at x400 magnification.

The appearance of trophozoites and cystic forms was regularly inspected until the cultures reached 14 days outgrowth and the correspondence between culture findings (Figure 2) and their respective species was addressed by the molecular approach, detailed next.

2.3. PCR amplification and sequence analysis

By using the Ng.spp_FW and Ng.spp_RV primers, the PCR products obtained ranged from 395bp to 502bp, corresponding to the expected size of *Naegleria* spp amplicon (N1 to N5). An amplicon of about 750bp was obtained in one sample, consistent with the expected fragment size of *Hartmannella* spp (H1), as shown in Figure 3.

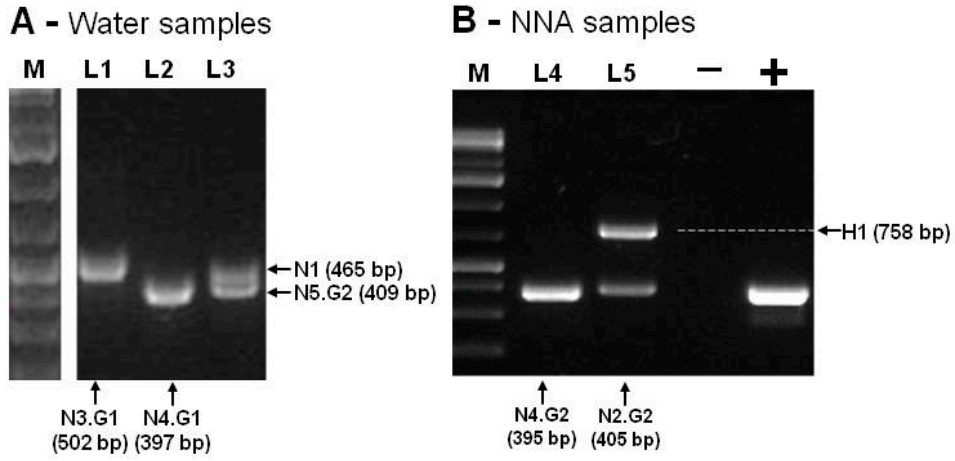

Figure 3. PCR amplification of *Naegleria* internal transcribed spacer (ITS) rDNA region. In (A), the lanes L1 and L2 correspond to the isolates of sampling site C, and L3 corresponds to the isolates of sampling site E. In (B), the lanes L4 and L5 correspond to sampling site D cultivated at 37 and 44 °C, respectively. The arrows indicate the amplified products that correspond to *Naegleria* ITS genes (N1–

N5) and the *Hartmannella* (H1) gene. The molecular marker (M, Gene Ruler 1 kb Plus DNA Ladder, Thermo Fisher Scientific), positive (+) control, and negative (-) control are also displayed.

Figure 3 summarizes the amplification results that were obtained by using Ng.spp_FW and Ng.spp_RV primers. The negative control was performed with DNA-free water, and the positive control was performed with DNA of *Naegleria gruberi* ATCC (American Type Culture Collection) 30224. All these amplicons (Figure 3A,B) were isolated from the agarose gel, sequenced, and compared with each corresponding species through BLASTn searches. Table 1 summarizes the results for all the sampling sites.

Table 1. *Naegleria* and *Hartmannella* isolates from NNA cultures (1) and directly from the water (2) through sampling sites of the Monjolinho River (A–E) in São Carlos, São Paulo state.

Sample Sites	Culture Temperature	1-Isolates from NNA Cultures		2-Isolates Directly from Water Samples	
		Code	BLASTn /Accession [1]	Code	BLASTn /Accession [1]
A	26 °C	N2.G2	*N. philippinensis/ LC191904.1*	N1	*N. canariensis/ FJ475124.1*
	37 °C	N1	*N. canariensis/ FJ475124.1*		
B	26 °C	N1	*N. canariensis/ FJ475124.1*	N2.G1	*N. philippinensis;*
	26 °C	N1	*N. canariensis/ FJ475124.1*	N1	*N. canariensis/ FJ475124.1*
				N4.G1	*N. australiensis*/AB128053.1;
C	37 °C	N1	*N. canariensis/ FJ475124.1*	N3.G1	*N. dobsoni/ KU380484.1*
				N3.G2	*N. dobsoni/ KU380484.1*
D	26 °C	N4.G2	*N. australiensis / AB128052.1*		
	37 °C	N2.G2	*N. philippinensis/ LC191904.1*	N2.G1	*N. philippinensis*/AY033618.1;
		H1	*Hartmannella*/HE617186.1	N5.G1	*N. gruberi* / MG699123.1
	44 °C	N4.G1	*N. australiensis/* AB128053.1		
E	26 °C	N5.G2	*N. gruberi/* MG699123.1	N5.G2	*N. gruberi*/MG699123.1;
	37 °C	N1	*N. canariensis/ FJ475124.1*	N1	*N. canariensis/ FJ475124.1*

[1] Gene-Bank accession numbers.

Our findings were 95%–100% identical with GenBank *Naegleria* spp. reference sequences, with a query coverage of 98%–100% at BLASTn alignment, and the variants ".G1" and ".G2" mean that differences were detected on the nucleotide composition within the same species. The number of substitutions per site from averaging over all sequence pairs of the *Naegleria* reference sequences was 0.06, with a standard error estimate of 0.01, revealing a high sequence conservations among *Naegleria* species. However, this internal variability on the rDNA sequences that were detected within the *Naegleria* species DNA was not significant enough to suggest the identification of new species.

The sequencing results from the NNA plate samples (Table 1) revealed the presence of four distinct *Naegleria* species, *N. philippinensis, N. canariensis*, *N. australiensis* and *N. gruberi*, as well as one *Hartmannella* species. According to the D site findings, *N. australiensis* was capable of growing at 44 °C. Additionally, *N. dobsoni* could be isolated when taking into account the identifications directly from water (Table 1).

2.4. Phylogeny

The neighbor joining (NJ) tree of the aligned ITS and 5.8S rDNA sequences (Figure S1) clearly show the N5 (G1 and G2 variants) branching with the *Naegleria gruberi* species. The N4 sequence belonged to the *N. australiensis* group, N2 belonged to *N. philippinensis*, N1 belonged to *N. canariensis*, and N3 belonged to the *N. dobsoni* clades. The sequence resulting from the 758bp amplicon (H1) was identified as belonging to the *Hartmannella* and *Acanthamoeba* clades (Figure 4) with good bootstrap support.

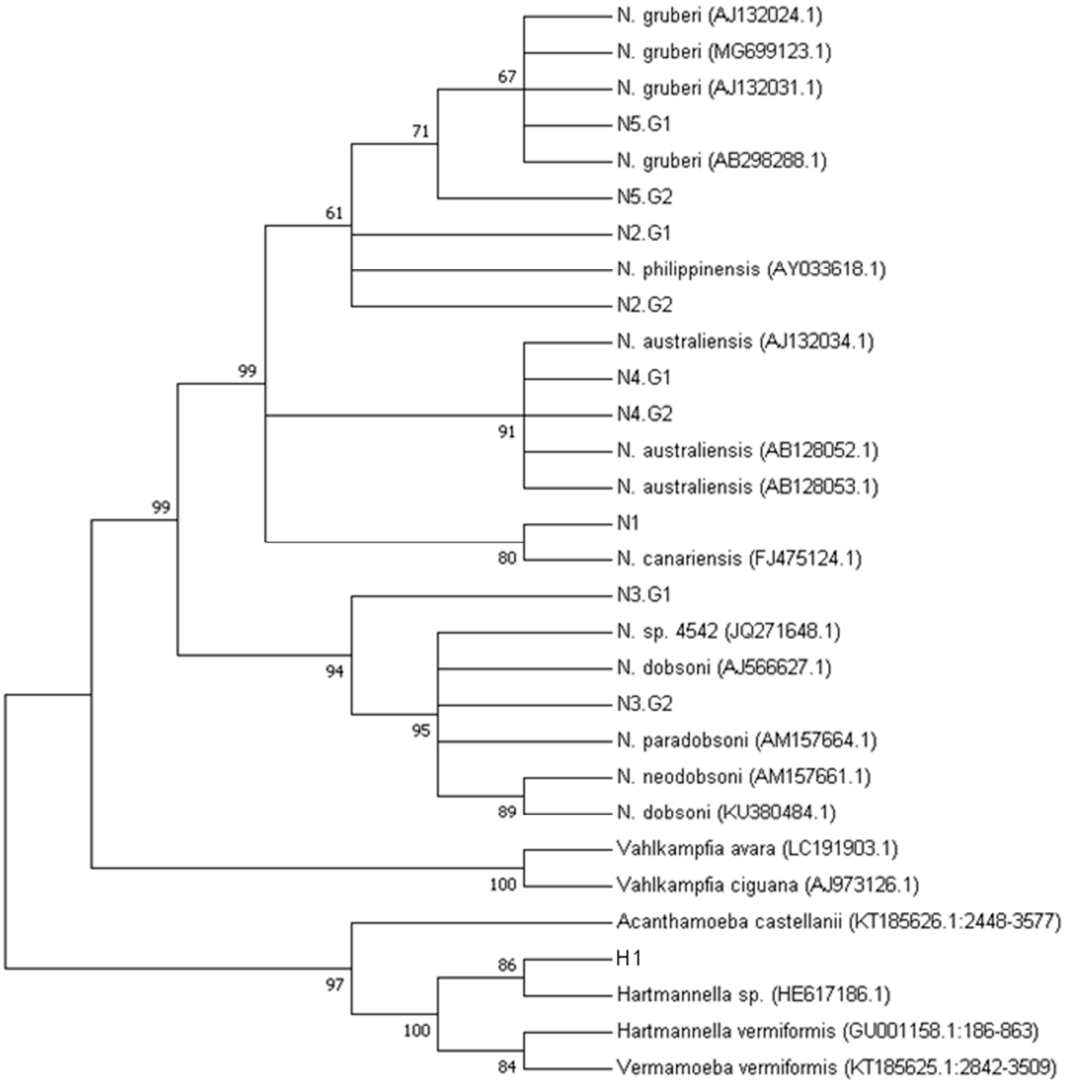

Figure 4. Evolutionary relationship among *Naegleria* spp., *Hartmannella* spp. and *Vahlkampfia* spp. based on internal transcribed sequences (ITS1 and ITS2 regions) and 5.8S sequence. The bootstrap consensus tree was inferred from 1000 replicates. Branches corresponding to partitions reproduced in less than 50% of the bootstrap replicates are collapsed. *Hartmannella vermiformis* and *Acanthamoeba pearcei* were used as outgroups for the *Vahlkampfia* and *Naegleria* clades.

3. Discussion

3.1. Eutrophication along the Monjolinho River

The samples were collected along the Monjolinho river, which passes through the city of São Carlos in the São Paulo state, Brazil. Five sampling sites were selected. Site A represented the river

headwaters and the catchment area [43]. The subsequent sampling sites were located within (B and C) and nearby (D) the urban area where the population can use the water for agricultural, domestic or recreational purposes. According the limnological measurements shown in Figure 2, the dissolved oxygen and conductivity results revealed the degree of eutrophication of the Monjolinho River basin, as these are the known parameters that are to evaluate levels of organic material contaminating the water [46]. From the headwater towards the two subsequent sampling sites, a gradual increase in conductivity values is observed, together with a decrease of dissolved oxygen. However, the severe reduction of the electrical conductivity of sites D to E was likely due to the sewage treatment plant located between sites D and E. Increment of the electrical conductivity of water are closely related to organic matter decomposition, anthropogenic activities, and soil flushing, as these activities elevate potassium, magnesium, calcium, carbonate and sulphate concentrations [47]. The lowest DO values that were found in the D and E sampling sites were below the recommendations from the Brazilian Council of Environmental Regulations, which has determined that DO values should not be lower than 6.0 mg.L-1 as an environmental parameter of water quality [48]. The slight increase of the temperature from headwater to the last meander was likely due to the daily temperature change once the sampling followed the longitudinal course of the river (A–E), and it took an interval of five hours from the first to the last site. The gentle increase in the pH value was probably a consequence of the presence of alkaline compounds, such as carbonates and calcium, that could increase the pH and were also responsible for the increase of the electrical conductivity. Additionally, detergents that are commonly encountered in domestic wastewater have the potential to increase the pH to levels that were consistent with the recorded values compared to the upstream sampling sites [49]. Nevertheless, all physical and chemical features registered in the Monjolinho River could harbor *Naegleria,* as described in this paper.

3.2. Presence of Naegleria *Thermophilic Species in Brazil*

Our cultivation results, particularly the trophozoite growth observed at 44 °C, indicated the presence of species with pathogenic potential, as it has been discussed in earlier studies that all pathogenic species of *Naegleria* have the capability of tolerating temperature of up to 40 °C [16]. The observed capability of *N. australiensis* to grow and sustain its growth at 44 °C broadens the thermotolerance that has thus far been associated with this species, because no earlier studies have demonstrated its tolerance to 44 °C, either from environmental samples or in laboratorial conditions [4]. To date, the highest temperatures tolerated by *N. australiensis* have been reported to be in the range of 40–43 °C [2,11,37,50,51]. On the other hand, *N. philippinensis* has been reported to grow at 40 °C [4], which is consistent with our results, which confirmed its inability to withstand a temperature of 44 °C.

The identification of *N. australiensis* and *N. philippinensis* (Table 1) brings an important issue to be explored due to their capability to cause encephalitis in experimental animals [52,53], and their presence in the river water represents a threat not only to the ichthyofauna but also to domestic mammals that use the river as water supply. Moreover, just because the causative agent of PAM in humans, *N. fowleri*, was not recovered in this collection does not mean that there is no need for the frequent evaluation of this and other river streams. These assessment are becoming urgent with the rising temperatures that are being experienced due to global warming effects [11,29,54].

3.3. Naegleria *spp. Diversity in Brazil*

Besides the identification of *N. australiensis* and *N. philippinensis*, this study also identified *N. canariensis*, *N. gruberi,* and a *Harmannella* spp. through the same morphological approach combined with sequencing analysis, as shown by the bootstrap supported phylogenetic tree (Figure 4), although the short length of the ITS-5.8S sequences did not resolve the polytomy within each species. The potential of the selected primers to amplify two distinct free-living amoeba genera has been recently reported in two studies from the Nile River, Egypt [38] and from regions of Malaysia [39]. By analyzing the DNA sequences that were directly extracted from the river water (Tables 1 and 2), one additional *Naegleria* species could be identified: *N. dobsoni*. Similarly, some species were not isolated

in the direct approach, but, after enriching the trophozoites presence by culturing, we could obtain them. Thus, we highlight the importance on performing both complementary PCR analyses when using the DNA extracted directly from the river and the DNA after culturing.

To the best of our knowledge, this is the first report of *N. philippineneis*, *N. australiensis*, *N dobsoni* and *N. gruberi* in South America environmental samples. To date, reports of the presence of *Naegleria* from South American countries have relied on the identification of *N. fowleri* from suspected PAM victims. For instance, two Venezuelan [55] and five Brazilian [30] PAM cases have been registered. One additional *Naegleria* species has been identified in the public swimming pools of Santiago, Chile [56]. Thus, our findings represent a significant improvement on our knowledge on the presence and diversity of *Naegleria* in South America.

4. Materials and Methods

4.1. Description of the Geographical Area and Sample Collection

Five water samples (A–E) were collected from the Monjolinho river, which runs through the city of São Carlos, São Paulo, Brazil. Different levels of human intervention along the Monjolinho River basin were considered when selecting the five sampling sites that are described in the present study. To insert each sampling site (Universal Transverse Mercator, UTM) coordinates in the Monjolinho River basin image, a geographic information system (GIS) named the Georeferenced Information Processing System (SPRING 5.5.5, http://www.dpi.inpe.br/spring/english/index.html) was used. The resulting cadastral map (Figure 5) revealed the basin limit and the respective geographic positions of each sampling site along the main stream of the Monjolinho as follows: headwater (A: 22° 0' 2.87'' S, 47° 50' 8.96'' W), peri-urban stream (B: 21° 58' 40.6884'' S, 47° 52' 25.50'' W), urban stream (C: 21° 59' 45.40'' S, 47° 54' 6.32'' W), domestic sewage discharge (D: 22° 0' 52.41'' S, 47° 55' 26.65'' W), and after a sewage treatment plant (E: 22° 1' 34.92'' S, 47° 57' 26.29'' W). The samples were collected in October, 2017 in the dry season by using one liter sterile glass flasks in a range of 10-15 cm of the water surface, following a literature recommendation [57].

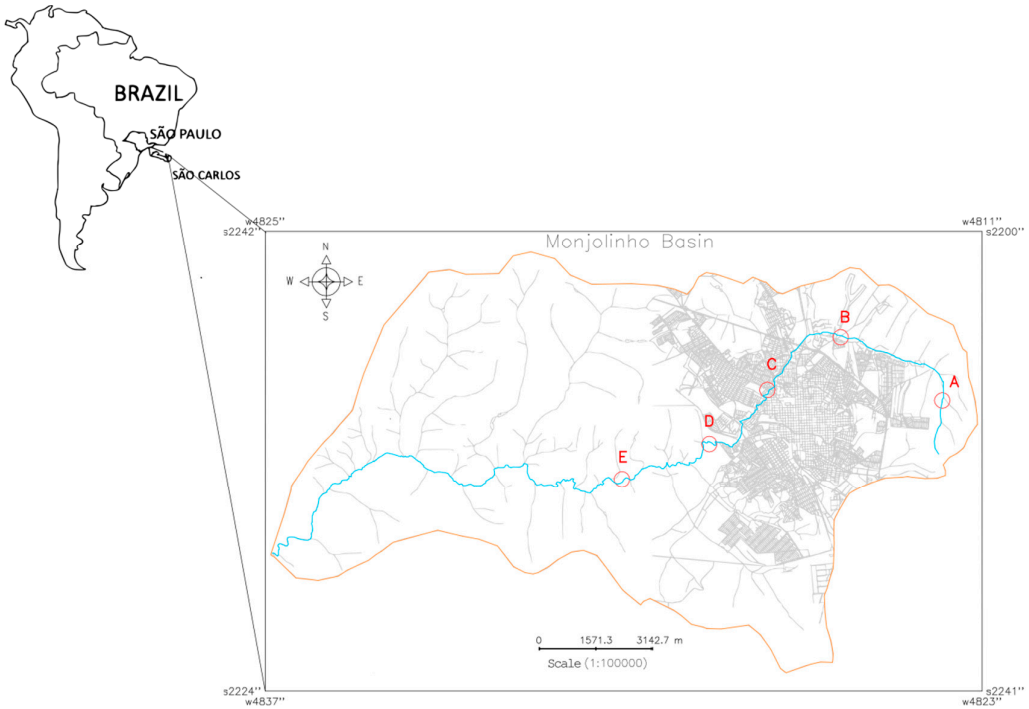

Figure 5. Cadastral map of the Monjolinho River Basin, São Carlos, São Paulo (Brazil) that shows the Monjolinho river (blue line) and sampling sites A–E (in red letters and circles) that were investigated in this study.

4.2. Limnology and Sampling Process

The global positioning system (GPS) coordinates of each sampling site were registered. The limnological data of the sampling sites, such as dissolved oxygen (DO), hydrogen ionic potential (pH), and temperature, were recorded by a portable water quality analyzer (Horiba U-10). Within 12 hours after collection, the samples were homogenized and filtered through a granulometric sieve (BERTEL-MESH 120, pore diameter of 0,125 mm). Five hundred milliliters of the sieved samples were used for culturing, and the remaining 500 ml were used for the PCR amplification of the target DNA and the DNA sequencing.

4.3. Amoeba Isolation and Culturing

The water samples were filtered in a 0.45 μm cellulose nitrate membrane (Nalgene®) and cut in nine pieces, and each piece was placed in a 2% agar NNA plate [58] for each sampling site. They were then overlaid with heat-inactivated *Escherichia coli* (60 °C for 30 minutes) [53]. Three of each sealed plates were incubated at 26, 37, and 44 °C [39,40].

4.4. Morphological Characterization

The cultures were examined daily for the presence of amoeba growth and the trophozoites identified were sub-cultured onto new NNA plates and their growth was inspected in an inverted Nikon Eclipse TS 100 microscope. To infer the taxonomic identity based on the Page´s classification key, the photomicrographs were screened for amoeba-related morphological characters [45]. The trophozoites were harvested in 2 ml Page´s saline solution (PAS) [58], centrifuged (800 x g, 10 min), suspended in a freezing solution (9:1, heat inactivated fetal bovine serum:DMSO), and then stored in liquid nitrogen vapor.

4.5. DNA Extraction, Amplification and Sequencing

To perform the molecular identification directly from the water samples, 500 ml of filtered water was centrifuged at 3000 x g for 15 min at room temperature and washed once in phosphate-buffered saline (PBS). The final pellet was used for DNA extraction. Likewise, the NNA-cultured trophozoites were washed once with 5 ml PAS on the agar surface to homogenization in a plate shaker (60 rpm, 10 min). The suspended cells were poured into a canonical 15 ml tube and centrifuged at 1000 x g for 10 min at RT, and the pellet was solubilized with 50 μl of ultrapure water (MiliQ) prior to DNA extraction. The commercial extraction kit DNeasyPowerSoil® Kit (QIAGEN) was used to achieve high DNA purity and yield for both input materials—the water samples and the NNA-cultured trophozoites. The DNA concentration was quantified in a Nanodrop 2000 Spectrophotometer (Thermo Scientific), analyzed by agarose-gel electrophoresis, and amplified by the polymerase chain reaction (PCR).

The DNA was amplified with *Naegleria* genus-specific primers, Ng.spp_FW 5′-GAACCTGCGTAGGGATCATTT-3′ and Ng.spp_RV 5′-TTTCTTTTCCTCCCCTTATTA-3′, to the internal transcribed spacer regions (ITS1 and 2) that comprise the 5.8S rDNA gene that was previously adopted in phylogenetic studies [37–41]. The PCR reactions contained Taq High Fidelity Pol Master Mix 2x (Red, Cellco Biotec), 100 ng of the DNA template, and 200 nmoles of each primer. The reactions were incubated in a T100 Thermal Cycler (BIO-RAD) under a cycling condition of 95 °C for 3 min followed by 35 cycles at 95 °C for 30 s, 50 °C for 30 s, 72 °C for 1 min, and a final extension at 72 °C for 2 min. Amplified fragments were examined in SYBR Safe-stained 2% agarose gels. The amplified DNA bands were purified by using the Agarose Gel Extraction Kit (Cellco Biotec), cloned into a pJET 1.2/blunt cloning vector (Thermo-Scientific) and transformed into *E. coli* TOP 10 competent cells. The plasmid DNA was isolated with Fast-n-Easy Plasmid Mini-Prep Kit (Cellco Biotec) and sequenced in triplicate in both directions in a 3130 Genetic Analyzer (Thermo Scientific); therefore, each base was independently sequenced six times. The chromatograms were carefully examined with DNA analysis software (SnapGene Viewer), and the nucleotide homology was

investigated through Basic Local Alignment Search Tool (BLAST) at the National Centre for Biotechnology Information (NCBI) blasting with Eukarya Domain sequences.

4.6. Phylogenetic Inferences

The phylogenetic analysis was based on the ITS and 5.8 S sequences from this work. The consensus sequences were aligned with the *Naegleria* rDNA reference sequences that were already deposited in the GenBank database by using ClustalW software with the following gap penalties: 20/0.1 and 15/6.66 to gap opening/extension for the pairwise and multiple alignments, respectively. The final alignment was used for the phylogenetic analysis with Molecular Evolutionary Genetics Analysis (MEGA7) to build a phylogenetic tree based on neighbor joining (NJ) inference method with the Tamura–Nei statistic model [59]. In order to determine the statistical reliability of each node, 1000 bootstrap replicates were performed.

5. Conclusions

In this study, we describe the identification of *Naegleria* along the Monjolinho River Basin with morphological and molecular approaches. Although not exhaustive, the combination of both morphological and molecular methodologies allowed for a more complete understanding of the amoebas that were present. Because earlier Brazilian studies focused the *Naegleria* environmental investigations based on morphological analyses, they reported their information at genera level. In this context, the present research was the first Brazilian study to perform a molecular approach to detect *Naegleria* in an environmental sample and in which the findings could change the scenario by revealing the presence of *Naegleria* at the species level. Thus, this study increases knowledge on diversity due the identification of five distinct *Naegleria* species and one *Harmannella* gene. The limnological characterization that was accomplished by this study allowed for the assessment of eutrophication, as the D sampling site was found to be the most eutrophic compared to the remaining four sites. Additionally, this site was the most diverse regarding the species that were, identified as it had three of the five *Naegleria* spp. and the *Hartmannella* species that were found in the river. Although *N. fowleri* was not recovered in this survey, the presence of *N. australiensis* and *N. philippinensis*, distributed from the headwater to the fourth sampling site, indicates that potentially pathogenic species could grow in the Monjolinho River. Even if they have never been reported in human infections, their potential to cause encephalitis in laboratory conditions renders these species worthy of a more careful investigation. Since both species were found in the most eutrophic sampling site, there is a need to investigate the surrounding freshwater systems with similar limnological conditions that could favor their presence and dispersion. Our findings strengthen the importance of combining morphological approaches with molecular investigations in order to reach a deeper investigation of *Naegleria* spp. in environmental samples. This study highlights the need to perform further investigations that address the presence and distribution of potentially pathogenic FLA genera in Brazil.

Supplementary Materials: The following are available online at www.mdpi.com/xxx/s1, Figure S1: Aligned ITS and 5.8S rDNA sequences.

Author Contributions: All authors have read and agree to the published version of the manuscript. Conceptualization, O.H.T.; Data curation, N.K.B.; Funding acquisition, O.H.T.; Investigation, N.K.B., A.L.M.d.F. and O.R.; Methodology, N.K.B, A.L.M.d.F., M.R.-B. and J.L.-M; Project administration, O.H.T.

Funding: NKB was supported by the Coordination for the Improvement of Higher Education Personnel (CAPES) fellowship. This work was funded by BIOTA São Paulo Research Foundation (FAPESP) program, #2018/20693-4 to OHT. J.L.M. and M.R.B. were funded by PI18/01380 from Instituto de Salud Carlos III, Spain and RICET [RD16/0027/0001 project, from Programa Redes Temáticasde Investigación Cooperativa, FIS (Ministerio Español de Salud, Madrid, Spain), FEDER.

Acknowledgments: We would like to thank the members of the Structural Biology Laboratory (IFSC-USP) and of the Free Living Amoeba Laboratory (ULL) for helpful discussions in the course of this work. We thank

specially to José Valdecir de Lucca for the assistance in the water sample collection. We would like to thank also Dr. Susana Andrea Sculaccio Beozzo for technical assistance.

Conflicts of Interest: The authors declare no conflict of interest.

References

1. Kilvington, S.; Beeching, J. Identification and epidemiological typing of Naegleria fowleri with DNA probes. *Appl. Environ. Microbiol.* **1995**, *61*, 2071–2078.
2. Latifi, A.R.; Niyyati, M.; Lorenzo-Morales, J.; Haghighi, A.; Tabaei, S.J.S.; Lasjerdi, Z.; Azargashb, E. Occurrence of Naegleria species in therapeutic geothermal water sources, Northern Iran. *Acta Parasitol.* **2017**, *62*, 104–109.
3. Trabelsi, H.; Dendana, F.; Sellami, A.; Sellami, H.; Cheikhrouhou, F.; Neji, S.; Makni, F.; Ayadi, A. Pathogenic free-living amoebae: Epidemiology and clinical review. *Pathol. Boil.* **2012**, *60*, 399–405.
4. De Jonckheere, J.F. What do we know by now about the genus Naegleria? Exp. Parasitol. **2014**, *145*, doi:10.1016/j.exppara.2014.07.011.
5. Opperdoes, F.R.; De Jonckheere, J.F.; Tielens, A.G. Naegleria gruberi metabolism. *Int. J. Parasitol.* **2011**, *41*, 915–924.
6. 6. Fritz-Laylin, L.K.; Prochnik, S.E.; Ginger, M.L.; Dacks, J.B.; Carpenter, M.L.; Field, M.C.; Kuo, A.; Paredez, A.; Chapman, J.; Pham, J.; et al. The Genome of Naegleria gruberi Illuminates Early Eukaryotic Versatility. *Cell* **2010**, *140*, 631–642.
7. Cogo, P.E.; Scaglia, M.; Gatti, S.; Rossetti, F.; Alaggio, R.; Laverda, A.M.; Zhou, L.; Xiao, L.; Visvesvara, G.S. Fatal Naegleria fowleri Meningoencephalitis, Italy. *Emerg. Infect. Dis.* **2004**, *10*, 1835–1837.
8. Majid, M.A.A.; Mahboob, T.; Mong, B.G.J.; Jaturas, N.; Richard, R.L.; Tian-Chye, T.; Phimphila, A.; Mahaphonh, P.; Aye, K.N.; Aung, W.L.; et al. Pathogenic waterborne free-living amoebae: An update from selected Southeast Asian countries. *PLoS One* **2017**, *12*, 1–17.
9. Tung, M.-C.; Hsu, B.-M.; Tao, C.-W.; Lin, W.-C.; Tsai, H.-F.; Ji, D.-D.; Shen, S.-M.; Chen, J.-S.; Shih, F.-C.; Huang, Y.-L. Identification and significance of Naegleria fowleri isolated from the hot spring which related to the first primary amebic meningoencephalitis (PAM) patient in Taiwan. *Int. J. Parasitol.* **2013**, *43*, 691–696.
10. Sukthana, Y.; Lekkla, A.; Sutthikornchai, C.; Wanapongse, P.; Vejjajiva, A.; Bovornkitti, S. Spa, springs and safety. *Southeast Asian J. Trop. Med. Public Heal.* 2005, *36*.
11. De Jonckheere, J.F. The impact of man on the occurrence of the pathogenic free-living amoeboflagellateNaegleria fowleri. *Futur. Microbiol.* **2012**, *7*, 5–7.
12. Tiewcharoen, S.; Phurttikul, W.; Rabablert, J.; Auewarakul, P.; Roytrakul, S.; Chetanachan, P.; Atithep, T.; Junnu, V. Effect of synthetic antimicrobial peptides on Naegleria fowleri trophozoites. *Southeast Asian J. Trop. Med. Public Heal.* 2014, *45*, 537–46.
13. Schuster, F. Opportunistic amoebae: challenges in prophylaxis and treatment. *Drug Resist. Updat.* **2004**, *7*, 41–51.
14. Adl, S.M.; Simpson, A.G.B.; Farmer, M.A.; Andersen, R.A.; Anderson, O.R.; Barta, J.R.; Bowser, S.S.; Brugerolle, G.; Fensome, R.A.; Fredericq, S.; et al. The New Higher Level Classification of Eukaryotes with Emphasis on the Taxonomy of Protists. *J. Eukaryot. Microbiol.* **2005**, *52*, 399–451.
15. Mann, D.G.; Hoppenrath, M.; Cárdenas, P.; Lukeš, J.; Powell, M.J.; Shimano, S.; Bass, D.; Shadwick, L.; del Campo, J.; James, T.Y.; et al. Revisions to the Classification, Nomenclature, and Diversity of Eukaryotes. *J. Eukaryot. Microbiol*. **2019,** *66, 4–119.*
16. De Jonckheere, J.F. A century of research on the amoeboflagellate genus Naegleria. *Acta Protozool.* **2002**, *41*, 309–342.
17. Delafont, V.; Rodier, M.-H.; Maisonneuve, E.; Cateau, E. Vermamoeba vermiformis: a Free-Living Amoeba of Interest. *Microb. Ecol.* **2018**, *76*, 991–1001.
18. Biswal, D.S.R.S.D.A.K.A. Role of Acanthamoeba in Granulomatous Encephalitis: A Review. *J. Infect. Dis. Immune Ther.* **2017**, *1*, 1–12.
19. Visvesvara, G.S. Amebic meningoencephalitides and keratitis: challenges in diagnosis and treatment*. *Curr. Opin. Infect. Dis.* **2010**, *23*, 590–594.
20. Qvarnstrom, Y.; Silva, A.J.; Schuster, F.L.; Gelman, B.B.; Visvesvara, G.S. Molecular Confirmation of Sappinia pedata as a Causative Agent of Amoebic Encephalitis. *J. Infect Dis.* **2018**, *199*, 1139–1142.

21. Khan, N.A.; Ong, T.Y.Y.; Siddiqui, R. Targeting Brain-Eating Amoebae Infections. *ACS Chem. Neurosci.* **2017**, *8*, 687–688.
22. Di Filippo, M.M.; Berrilli, F.; Di Cave, D.; Novelletto, A. Novel data from Italian Vermamoeba vermiformis isolates from multiple sources add to genetic diversity within the genus. *Parasitol. Res.* **2019**, *118*, 1751–1759.
23. Ong, T.Y.Y.; Khan, N.A.; Siddiqui, R. Brain-Eating Amoebae: Predilection Sites in the Brain and Disease Outcome. *J. Clin. Microbiol.* **2017**, *55*, 1989–1997.
24. Niyyati, M.; Dodangeh, S.; Lorenzo-Morales, J. A Review of the Current Research Trends in the Application of Medicinal Plants as a Source for Novel Therapeutic Agents Against Acanthamoeba Infections. *Heal. Serv. Iran. J. Pharm. Res.* **2016**, *15*, 893–900.
25. De Jonckheere, J.F. Origin and evolution of the worldwide distributed pathogenic amoeboflagellate Naegleria fowleri. *Infect. Genet. Evol.* **2011**, *11*, 1520–1528.
26. Debnath, A.; Tunac, J.B.; Galindo-Gómez, S.; Silva-Olivares, A.; Shibayama, M.; McKerrow, J.H. Corifungin, a New Drug Lead against Naegleria, Identified from a High-Throughput Screen. *Antimicrob. Agents Chemother.* **2012**, *56*, 5450–5457.
27. Yoder, J.S.; Eddy, B. a; Visvesvara, G.S.; Capewell, L.; Beach, M.J. The epidemiology of primary amoebic meningoencephalitis in the USA, 1962-2008. *Epidemiol. Infect.* **2010**, *138*, 968–975.
28. Visvesvara, G.S. Free-Living Amebae as Opportunistic Agents of Human Disease. *J. Neuroparasitology* **2010**, *1*, 1–13.
29. Bellini, N.K.; Santos, T.M.; Da Silva, M.T.A.; Thiemann, O.H. The therapeutic strategies against Naegleria fowleri. *Exp. Parasitol.* **2018**, *187*, 1–11.
30. 30. Salazar, H.; Moura, H.; Fernandes, O.; Peralta, J. Isolation of Naegleria fowleri from a lake in the city of Rio de Janeiro, Brazil. *Trans. R. Soc. Trop. Med. Hyg.* **1986**, *80*, 348–349.
31. Aparecida, M.; Aristeu, J. Isolation of potencially pathogenic free-living amoebas in hospital dust. *Rev Saude Publ.* **2003**, *37*, 242–246.
32. Carlesso, A.M.; Simonetti, A.B.; Artuso, G.L.; Rott, M.B. [Isolation and identification of potentially pathogenic free-living amoebae in samples from environments in a public hospital in the city of Porto Alegre, Rio Grande do Sul]. *Rev. da Soc. Bras. de Med. Trop.* 2007, *40*, 316–320.
33. Maciver, S.K.; Piñero, J.E.; Lorenzo-Morales, J. Is Naegleria fowleri an Emerging Parasite? *Trends Parasitol.* **2020**, *36*, 19–28.
34. Teixeira, L.H.; Rocha, S.; Pinto, R.M.F.; Caseiro, M.M.; Costa, S.O.P. Prevalence of potentially pathogenic free-living amoebae from Acanthamoeba and Naegleria genera in non-hospital, public, internal environments from the city of Santos, Brazil. *Braz. J. Infect. Dis.* **2009**, *13*, *395-397.*
35. Pimentel, L.A.; Dantas, A.F.M.; Uzal, F.; Riet-Correa, F. Meningoencephalitis caused by Naegleria fowleri in cattle of northeast Brazil. *Res. Veter- Sci.* **2012**, *93*, 811–812.
36. Henker, L.C.; Da Cruz, R.A.S.; Da Silva, F.S.; Driemeier, D.; Sonne, L.; Uzal, F.A.; Pavarini, S.P. Meningoencephalitis due to Naegleria fowleri in cattle in southern Brazil. *Revista Brasileira de Parasitologia Veterinária* **2019**, *28*, 514–517.
37. Edagawa, A.; Kimura, A.; Kawabuchi-Kurata, T.; Kusuhara, Y.; Karanis, P. Isolation and genotyping of potentially pathogenic Acanthamoeba and Naegleria species from tap-water sources in Osaka, Japan. *Parasitol. Res.* **2009**, *105*, 1109–1117.
38. El-Badry, A.A.; Aufy, S.M.; El-Wakil, E.S.; Rizk, E.M.; Mahmoud, S.S.; Taha, N.Y. First identification of Naegleria species and Vahlkampfia ciguana in Nile water, Cairo, Egypt: Seasonal morphology and phylogenetic analysis. *J. Microbiol. Immunol. Infect.* **2018**.
39. Ithoi, I.; Ahmad, A.F.; Nissapatorn, V.; Lau, Y.L.; Mahmud, R.; Mak, J.W. Detection of Naegleria Species in Environmental Samples from Peninsular Malaysia. *PLOS ONE* **2011**, *6*, e24327.
40. Pélandakis, M.; Pernin, P. Use of Multiplex PCR and PCR Restriction Enzyme Analysis for Detection and Exploration of the Variability in the Free-Living Amoeba Naegleria in the Environment. *Appl. Environ. Microbiol.* **2002**, *68*, 2061–2065.
41. Pelandakis, M.; Serre, S.; Pernin, P. Analysis of the 5.8S rRNA gene and the internal transcribed spacers in Naegleria spp. and in N. fowleri. *J. Eukaryot. Microbiol.* **2000**, *47*, 116–121.
42. Junk, W.J.; Piedade, M.T.F.; Lourival, R.; Wittmann, F.; Kandus, P.; Lacerda, L.D.; Bozelli, R.L.; Esteves, F.A.; Nunes da Cunha, C.; Maltchik, L.; et al. Brazilian wetlands: Their definition, delineation, and classification for research, sustainable management, and protection. *Aquat. Conserv. Mar. Freshw. Ecosyst.* **2014**, *24*, 5–22.

43. Barrilli, G.H.C.; Rocha, O.; Negreiros, N.F.; Verani, J.R. Influence of environmental quality of the tributaries of the Monjolinho River on the relative condition factor (Kn) of the local ichthyofauna. *Biota Neotropica* **2015**, *15*, 1–9.
44. Campagna, A.F.; Fracácio, R.; Rodrigues, B.K.; Eler, M.N.; Verani, N.F.; Espíndola, E.L.G. Analyses of the sediment toxicity of Monjolinho River, São Carlos, São Paulo State, Brazil, using survey, growth and gill morphology of two fish species (Danio rerio and Poecilia reticulata). *Braz. Arch. Boil. Technol.* **2008**, *51*, 193–201.
45. Buhse, H.E.; Page, F.C. A New Key to Freshwater and Soil Gymnamoeba. *Trans. Am. Microsc. Soc.* **1988**, *107*, 379.
46. Yang, X.-E.; Wu, X.; Hao, H.-L.; He, Z.-L. Mechanisms and assessment of water eutrophication*. *J. Zhejiang Univ. Sci. B* **2008**, *9*, 197–209.
47. Baird, C.; Cann, M. Environmental Chemistry; Fifth edit.; W. H. Freeman, Macmillan: New York, USA, 2012
48. Brasil. Conselho Nacional do Meio Aambiente Resolução CONAMA n 357; Brazilian Ministry of the Environment; Brasilia, Brazil, 2005.
49. Patterson, R.A. A Resident ' s Role in Minimising Nitrogen , Phosphorus and Salt in Domestic Wastewater. In Proceedings of the Tenth National Symposium on Individual and Small Community Sewage Systems Proceedings; Mankin, K.R., Ed.; Sacramento, USA, 21–24 March, 2004, pp. 740–749.
50. De Jonckheere, J.F.; Pernin, P.; Scaglia, M.; Michel, R. A comparative study of 14 strains of Naegleria australiensis demonstrates the existence of a highly virulent subspecies: N. australiensis italica n. spp. *J. Protozool.* 1984, *31*, 324–331.
51. Scaglia, M.; Strosselli, M.; Grazioli, V.; Gatti, S.; Bernuzzi, A.M.; de Jonckheere, J.F. Isolation and identification of pathogenic Naegleria australiensis (Amoebida, Vahlkampfidae) from a spa in northern Italy. *Appl. Environ. Microbiol.* **1983**, *46*, 1282–1285.
52. Dyková, I.; Kyselová, I.; Pecková, H.; Oborník, M.; Lukes, J. Identity of Naegleria strains isolated from organs of freshwater fishes. *Dis. Aquat. Org.* **2001**, *46*, 115–121.
53. Visvesvara, G.S.; Moura, H.; Schuster, F.L. Pathogenic and opportunistic free-living amoebae: Acanthamoeba spp., Balamuthia mandrillaris , Naegleria fowleri , and Sappinia diploidea. *FEMS Immunol. Med. Microbiol.* **2007**, *50*, 1–26.
54. Schuster, F.L.; Visvesvara, G.S. Free-living amoebae as opportunistic and non-opportunistic pathogens of humans and animals. *Int. J. Parasitol.* **2004**, *34*, 1001–1027.
55. Petit, F.; Vilchez, V.; Torres, G.; Molina, O.; Dorfman, S.; Mora, E.; Cardozo, J. Meningoencefalitis amebiana primaria: comunicacion de dos nuevos casos Venezolanos. *Arq. de Neuro-Psiquiatria* **2006**, *64*, 1043–1046.
56. Muñoz, V.; Reyes, H.; Toche, P.; Carcamo, C.; Gottlieb, B. Aislamiento de amebas de vida libre en piscinas públicas de Santiago de Chile. *Parasitología latinoamericana* **2003**, *58*, 106–111.
57. Kao, P.-M.; Hsu, B.-M.; Hsu, T.-K.; Chiu, Y.-C.; Chang, C.-L.; Ji, W.-T.; Huang, S.-W.; Fan, C.-W. Application of TaqMan qPCR for the detection and monitoring of Naegleria species in reservoirs used as a source for drinking water. *Parasitol. Res.* **2014**, *113*, 3765–3771.
58. Reyes-Batlle, M.; Hernández-Piñero, I.; Rizo-Liendo, A.; López-Arencibia, A.; Sifaoui, I.; Bethencourt-Estrella, C.J.; Chiboub, O.; Valladares, B.; Piñero, J.E.; Lorenzo-Morales, J. Isolation and molecular identification of free-living amoebae from dishcloths in Tenerife, Canary Islands, Spain. *Parasitol. Res.* **2019**, *118*, 927–933.
59. Kumar, S.; Stecher, G.; Tamura, K. MEGA7: Molecular Evolutionary Genetics Analysis Version 7.0 for Bigger Datasets. *Mol. Biol. Evol.* **2016**, *33*, 1870-1874.

APPENDIX II (b)

Supplementary figure

Multiple sequence alignment of the ITS and 5.8S rDNA sequences, excluding sites with alignment gaps. Yellow highlighting displays the conserved nucleotides among the sequences. The ITS1, 5.8S, ITS2 and LSU markings were based on the *Naegleria* genes alignment to delimited regions.

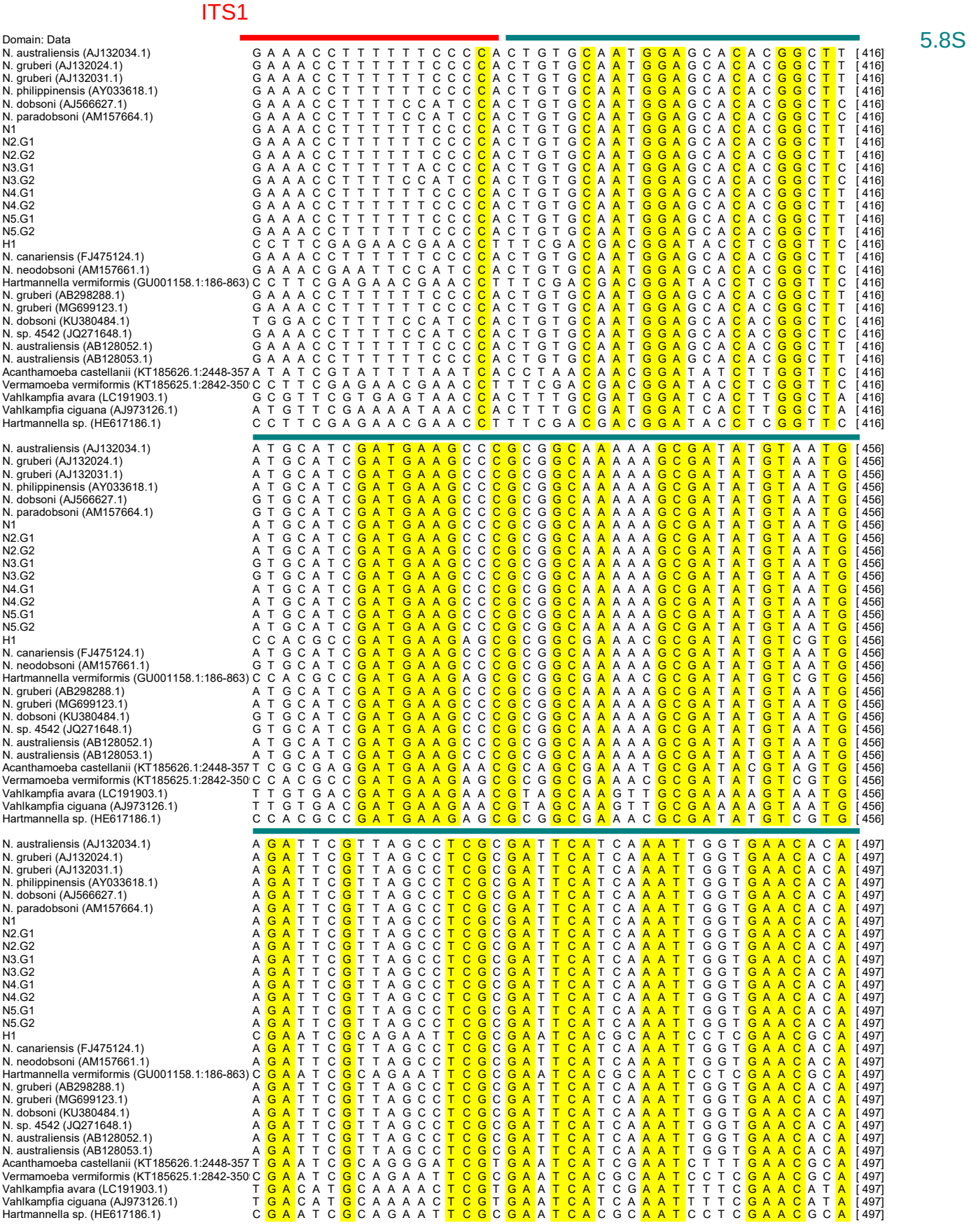

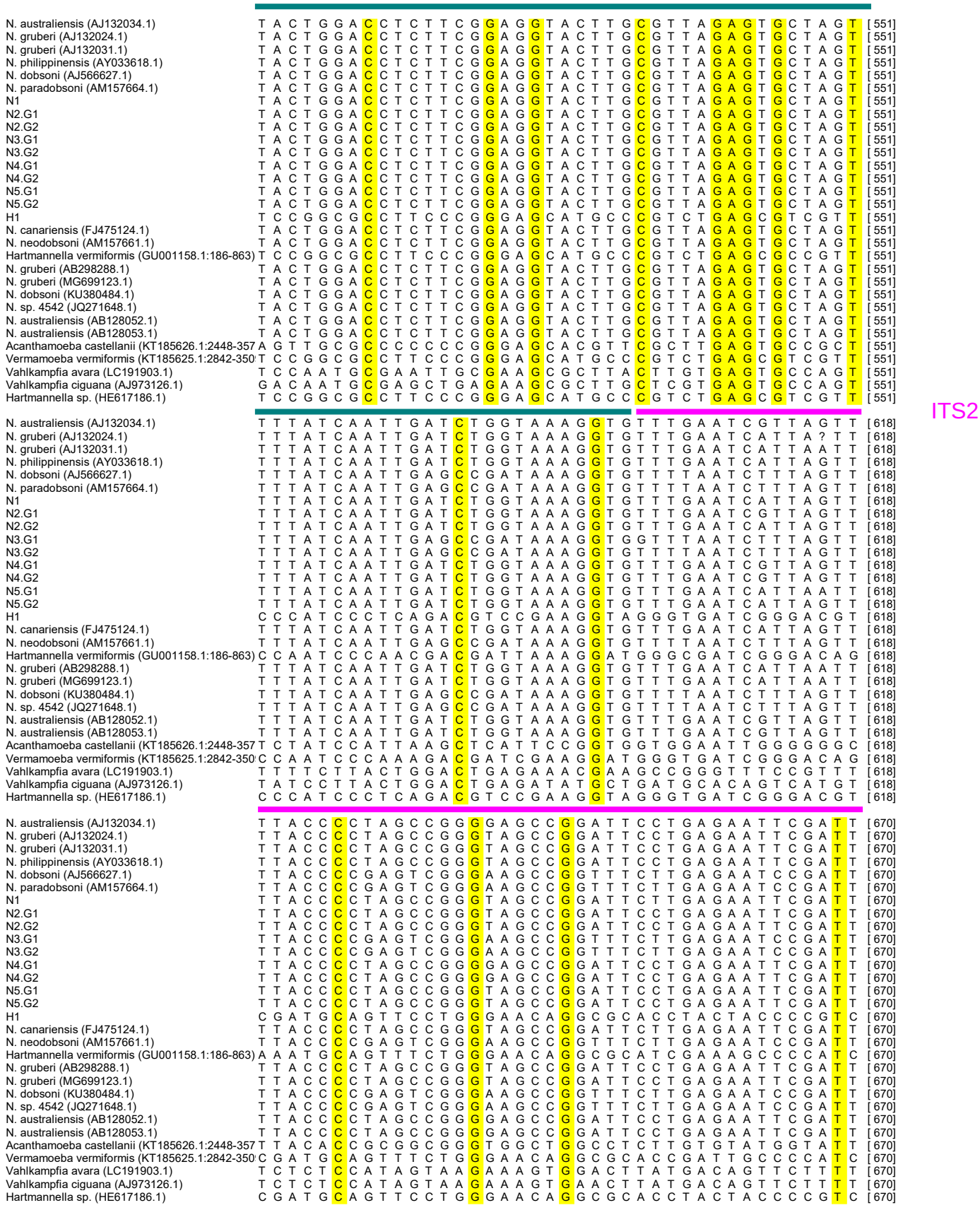
N. australiensis (AJ132034.1) [551]
N. gruberi (AJ132024.1) [551]
N. gruberi (AJ132031.1) [551]
N. philippinensis (AY033618.1) [551]
N. dobsoni (AJ566627.1) [551]
N. paradobsoni (AM157664.1) [551]
N1 [551]
N2.G1 [551]
N2.G2 [551]
N3.G1 [551]
N3.G2 [551]
N4.G1 [551]
N4.G2 [551]
N5.G1 [551]
N5.G2 [551]
H1 [551]
N. canariensis (FJ475124.1) [551]
N. neodobsoni (AM157661.1) [551]
Hartmannella vermiformis (GU001158.1:186-863) [551]
N. gruberi (AB298288.1) [551]
N. gruberi (MG699123.1) [551]
N. dobsoni (KU380484.1) [551]
N. sp. 4542 (JQ271648.1) [551]
N. australiensis (AB128052.1) [551]
N. australiensis (AB128053.1) [551]
Acanthamoeba castellanii (KT185626.1:2448-357 [551]
Vermamoeba vermiformis (KT185625.1:2842-350 [551]
Vahlkampfia avara (LC191903.1) [551]
Vahlkampfia ciguana (AJ973126.1) [551]
Hartmannella sp. (HE617186.1) [551]
ITS2
N. australiensis (AJ132034.1) [618]
N. gruberi (AJ132024.1) [618]
N. gruberi (AJ132031.1) [618]
N. philippinensis (AY033618.1) [618]
N. dobsoni (AJ566627.1) [618]
N. paradobsoni (AM157664.1) [618]
N1 [618]
N2.G1 [618]
N2.G2 [618]
N3.G1 [618]
N3.G2 [618]
N4.G1 [618]
N4.G2 [618]
N5.G1 [618]
N5.G2 [618]
H1 [618]
N. canariensis (FJ475124.1) [618]
N. neodobsoni (AM157661.1) [618]
Hartmannella vermiformis (GU001158.1:186-863) [618]
N. gruberi (AB298288.1) [618]
N. gruberi (MG699123.1) [618]
N. dobsoni (KU380484.1) [618]
N. sp. 4542 (JQ271648.1) [618]
N. australiensis (AB128052.1) [618]
N. australiensis (AB128053.1) [618]
Acanthamoeba castellanii (KT185626.1:2448-357 [618]
Vermamoeba vermiformis (KT185625.1:2842-350 [618]
Vahlkampfia avara (LC191903.1) [618]
Vahlkampfia ciguana (AJ973126.1) [618]
Hartmannella sp. (HE617186.1) [618]
N. australiensis (AJ132034.1) [670]
N. gruberi (AJ132024.1) [670]
N. gruberi (AJ132031.1) [670]
N. philippinensis (AY033618.1) [670]
N. dobsoni (AJ566627.1) [670]
N. paradobsoni (AM157664.1) [670]
N1 [670]
N2.G1 [670]
N2.G2 [670]
N3.G1 [670]
N3.G2 [670]
N4.G1 [670]
N4.G2 [670]
N5.G1 [670]
N5.G2 [670]
H1 [670]
N. canariensis (FJ475124.1) [670]
N. neodobsoni (AM157661.1) [670]
Hartmannella vermiformis (GU001158.1:186-863) [670]
N. gruberi (AB298288.1) [670]
N. gruberi (MG699123.1) [670]
N. dobsoni (KU380484.1) [670]
N. sp. 4542 (JQ271648.1) [670]
N. australiensis (AB128052.1) [670]
N. australiensis (AB128053.1) [670]
Acanthamoeba castellanii (KT185626.1:2448-357 [670]
Vermamoeba vermiformis (KT185625.1:2842-350 [670]
Vahlkampfia avara (LC191903.1) [670]
Vahlkampfia ciguana (AJ973126.1) [670]
Hartmannella sp. (HE617186.1) [670]

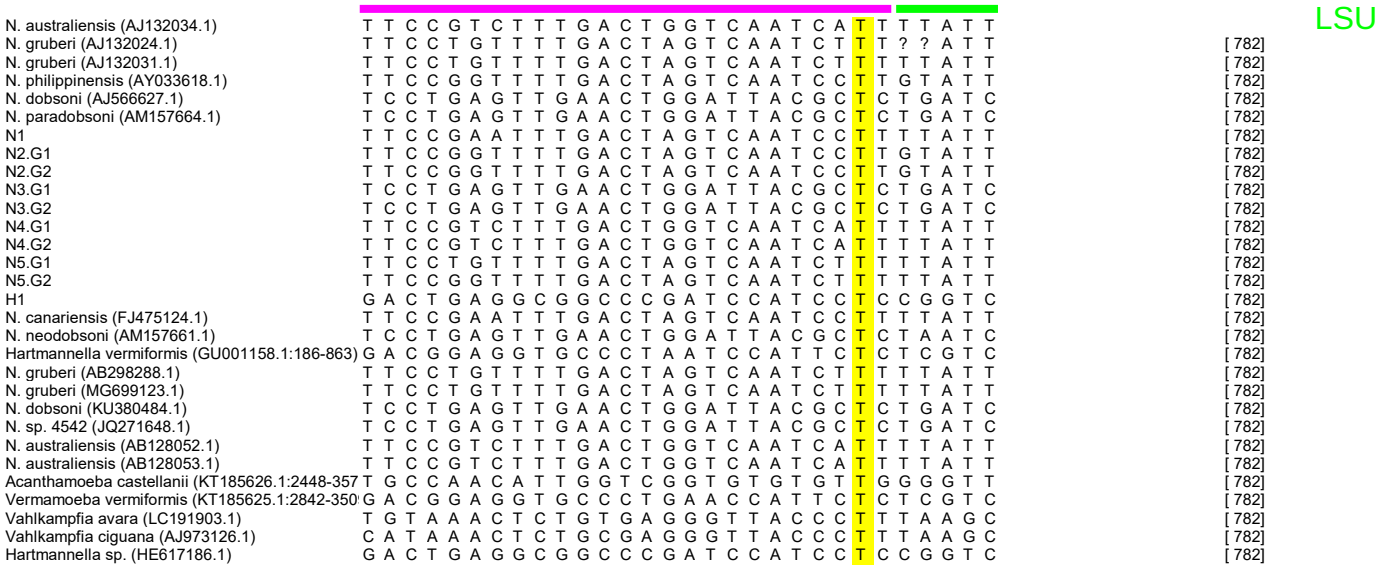
LSU
N. australiensis (AJ132034.1) T T C C G T C T T T G A C T G G T C A A T C A T T T A T T
N. gruberi (AJ132024.1) T T C C T G T T T T G A C T A G T C A A T C T T ? ? A T T [782]
N. gruberi (AJ132031.1) T T C C T G T T T T G A C T A G T C A A T C T T T T A T T [782]
N. philippinensis (AY033618.1) T T C C G G T T T T G A C T A G T C A A T C C T T G T A T T [782]
N. dobsoni (AJ566627.1) T C C T G A G T T G A A C T G G A T T A C G C T C T G A T C [782]
N. paradobsoni (AM157664.1) T C C T G A G T T G A A C T G G A T T A C G C T C T G A T C [782]
N1 T T C C G A A T T T G A C T A G T C A A T C C T T T T A T T [782]
N2.G1 T T C C G G T T T T G A C T A G T C A A T C C T T G T A T T [782]
N2.G2 T T C C G G T T T T G A C T A G T C A A T C C T T G T A T T [782]
N3.G1 T C C T G A G T T G A A C T G G A T T A C G C T C T G A T C [782]
N3.G2 T C C T G A G T T G A A C T G G A T T A C G C T C T G A T C [782]
N4.G1 T T C C G T C T T T G A C T G G T C A A T C A T T T A T T [782]
N4.G2 T T C C G T C T T T G A C T G G T C A A T C A T T T A T T [782]
N5.G1 T T C C T G T T T T G A C T A G T C A A T C T T T T A T T [782]
N5.G2 T T C C G G T T T T G A C T A G T C A A T C T T T T A T T [782]
H1 G A C T G A G G C G G C C C G A T C C A T C C T C C G G T C [782]
N. canariensis (FJ475124.1) T T C C G A A T T T G A C T A G T C A A T C C T T T T A T T [782]
N. neodobsoni (AM157661.1) T C C T G A G T T G A A C T G G A T T A C G C T C T A A T C [782]
Hartmannella vermiformis (GU001158.1:186-863) G A C G G A G G T G C C C T A A T C C A T T C T C T C G T C [782]
N. gruberi (AB298288.1) T T C C T G T T T T G A C T A G T C A A T C T T T T A T T [782]
N. gruberi (MG699123.1) T T C C T G T T T T G A C T A G T C A A T C T T T T A T T [782]
N. dobsoni (KU380484.1) T C C T G A G T T G A A C T G G A T T A C G C T C T G A T C [782]
N. sp. 4542 (JQ271648.1) T C C T G A G T T G A A C T G G A T T A C G C T C T G A T C [782]
N. australiensis (AB128052.1) T T C C G T C T T T G A C T G G T C A A T C A T T T A T T [782]
N. australiensis (AB128053.1) T T C C G T C T T T G A C T G G T C A A T C A T T T A T T [782]
Acanthamoeba castellanii (KT185626.1:2448-357 T G C C A A C A T T G G T C G G T G T G T G T T G G G G T T [782]
Vermamoeba vermiformis (KT185625.1:2842-350 G A C G G A G G T G C C C T G A A C C A T T C T C T C G T C [782]
Vahlkampfia avara (LC191903.1) T G T A A A C T C T G T G A G G G T T A C C C T T T A A G C [782]
Vahlkampfia ciguana (AJ973126.1) C A T A A A C T C T G C G A G G G T T A C C C T T T A A G C [782]
Hartmannella sp. (HE617186.1) G A C T G A G G C G G C C C G A T C C A T C C T C C G G T C [782]